UNIVERSIDAD DE GRANADA

FACULTAD DE FARMACIA

Departamento de Farmacología

Programa de Doctorado en Medicina Clínica y Salud Pública

Role of intestinal microbiota in obesity-associated colorectal cancer development: a novel target for pharmacological treatment

Tesis doctoral para aspirar al Grado de Doctor presentada por

Antonio Jesús Ruiz Malagón

Bajo la dirección de los Doctores:

Julio Juan Gálvez Peralta

Alba Rodríguez Nogales

Granada, 2023

Editor: Universidad de Granada. Tesis Doctorales
Autor: Antonio Jesús Ruíz Malagón
ISBN: 978-84-1195-502-7
URI: https://hdl.handle.net/10481/96718

A mi madre…

“Del lodo crecen
las flores más altas”

Xoel López

Index

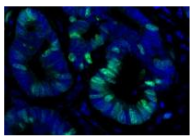

RESUMEN

RESUMEN

El cáncer colorrectal (CRC) es uno de los cánceres con mayor incidencia, siendo el tercer cáncer más común y la segunda causa de muerte relacionada con el cáncer en el mundo. La etiología del CRC es multifactorial, combinando un componente genético heredado influenciado por numerosas condiciones ambientales como el sedentarismo, una dieta rica en carnes procesadas, consumo de alcohol, tabaquismo y varias enfermedades como las enfermedades inflamatorias intestinales (colitis ulcerosa y enfermedad de Crohn) u obesidad. Entre estos factores de riesgo, el consumo de una dieta rica en grasas se ha relacionado estrechamente con el desarrollo de un estado de obesidad, lo que aumenta el riesgo de desarrollar CRC en casi un 10%. Las vías moleculares que intervienen en el desarrollo del CRC en personas obesas no están completamente descritas; sin embargo, se sabe que la desregulación del metabolismo, así como el estado inflamatorio crónico y la situación de disbiosis intestinal pueden contribuir a la aparición de CRC. De hecho, muchos estudios han descrito el papel de los metabolitos derivados de una microbiota alterada o disbiosis asociada a la obesidad en la promoción del CRC. Entonces, la comprensión de los mecanismos moleculares involucrados en la relación obesidad y el CRC, especialmente aquellos asociados con la microbiota alterada, tiene un valor traslacional potencial para la terapia y el manejo del CRC, así como para prevenir el desarrollo de esta enfermedad en pacientes obesos.

La modulación del microbioma es una de las estrategias más innovadoras de la medicina personalizada actual. De hecho, se ha descrito que pueden en un futuro mejorar la salud de las personas y reducir el riesgo de diferentes afecciones, entre ellas el cáncer, enfermedades metabólicas, inmunitarias, inflamatorias y degenerativas.

En este escenario, los extractos de plantas obtenidos de las partes aéreas de *Thymus serpyllum* L. o de las hojas de *Morus alba* L. han demostrado ejercer propiedades prebióticas que se han asociado con actividades antiinflamatorias y antioxidantes. En consecuencia, han sido ampliamente utilizados en la medicina tradicional contra varias enfermedades relacionadas con la inflamación. Adicionalmente, las tetraciclinas son fármacos con demostradas propiedades antibióticas e inmunomoduladoras que han mostrado actividad citotóxica frente a diferentes tipos de cáncer. Estas terapias se han caracterizado por modular la disbiosis intestinal característica de ambas patologías, la obesidad y el CRC. A pesar de que se han logrado numerosos avances en la terapia de la obesidad y el CRC, los tratamientos actuales no siempre son bien tolerados o su eficacia es baja en una gran parte de grupos de pacientes. Todo lo anterior justifica la necesidad de más investigación centrada en la capacidad

de los nuevos agentes para dirigirse a las vías celulares y moleculares alteradas en la obesidad y el CRC, especialmente en la disbiosis intestinal que comparten ambos trastornos. Para abordar esto, se propusieron los siguientes objetivos:

1. Evaluar estrategias terapéuticas capaces de modular la microbiota intestinal en el manejo de la obesidad.
2. Determinar dianas terapéuticas que impactan en la composición de la microbiota intestinal en el manejo del CRC.
3. Caracterizar el impacto de la obesidad en el desarrollo de CRC, estableciendo el papel de la microbiota intestinal como potencial diana terapéutica.

Con estos objetivos, en primer lugar, se evaluó el impacto de dos extractos, de partes aéreas de *Thymus serpyllum* y hojas de *Morus alba,* en un modelo murino experimental de obesidad inducida por una ingesta de una dieta rica en grasa (HFD). Además, se estudió la actividad de estos extractos de plantas sobre los trastornos metabólicos asociados a la obesidad, el estado inflamatorio y redox, la disfunción endotelial y las alteraciones de la microbiota intestinal. Los hallazgos mostraron que ambos extractos mostraron un efecto positivo en el aumento de peso corporal inducido por la suplementación con HFD, que se asoció con una mejora de los perfiles de lípidos y glucémicos en plasma, así como con una reducción de los depósitos de grasa. Además, los extractos de *Thymus serpyllum* y *Morus alba* lograron mejorar significativamente la inflamación crónica que caracteriza al fenotipo obeso. En este sentido, los tratamientos regularon a la baja varios mediadores proinflamatorios como la expresión de IL-6, TNFα y ciclooxigenasa 2. Este efecto podría estar relacionado con la capacidad de los extractos para modular la microbiota intestinal y mejorar la función de barrera intestinal alterada, reduciendo así el acceso de los lipopolisacáridos (LPS) bacterianos intestinales a la corriente sistémica, y resultando en una menor endotoxemia metabólica en ratones obesos tratados. Además, la presencia de compuestos fenólicos en ambos extractos de plantas fue responsable de una mejora del estado de estrés oxidativo asociado con la obesidad.

Por otro lado, se investigó el efecto de la tigeciclina, una tetraciclina de tercera generación, en modelos experimentales de CRC. Inicialmente, se estudió el impacto de este antibiótico sobre las líneas celulares de cáncer de colon, HCT116, Caco2 y CMT93, y se comparó con la actividad del 5-fluorouracilo, que constituye el fármaco estándar en la terapia del CRC. Posteriormente, y tras evidenciar los efectos antiproliferativos y proapoptóticos que la tigeciclina ejerció sobre las células tumorales, se profundizó en el estudio de los mecanismos moleculares implicados en estas acciones. Se observó que la tigeciclina dificultaba la activación de las vías proliferativas Wnt/β-catenina y JAK/STAT3, así como la activación de marcadores implicados en las diferentes vías de apoptosis estudiadas: extrínseca, intrínseca y mediada por retículo endoplásmico. Además, la tigeciclina ejerció un efecto beneficioso sobre las

células madre del cáncer de colon (CSC), las cuales se relacionan con el inicio del proceso tumoral y una mayor malignidad de los cánceres debido a sus propiedades invasivas y metastásicas. Esta acción puede estar relacionada con la capacidad de la tigeciclina de interferir en la transición epitelio-mesenquimatosa, principalmente asociada con una inhibición del factor de transcripción SNAI1. Todos estos efectos se relacionaron con una mejora significativa de la tumorigénesis *in vivo* en un modelo de xenotransplante tumoral y en el modelo de CRC asociado a colitis (CAC) en ratones. La administración de tigeciclina a ratones xenotrasplantados con CSC HCT116 resultó en una reducción del volumen tumoral y los niveles de CTNNB1 (β-catenina), un factor clave en la proliferación de células tumorales. Este efecto antiproliferativo de la tigeciclina también se observó en ratones CAC tratados con el antibiótico, y se asoció con una reducción del proceso inflamatorio y un aumento de las células T citotóxicas en los ganglios linfáticos mesentéricos de estos ratones. Además, la mitigación de la tumorigénesis observada con el tratamiento con tigeciclina se relacionó con un efecto proapoptótico *in vivo*, como lo demuestra el aumento de los niveles de caspasa 7. Finalmente, el antibiótico fue capaz de modular la microbiota intestinal, al promover el enriquecimiento en taxones bacterianos beneficiosos asociados con propiedades antiinflamatorias y antitumorales como *Parabacteroides distasonis* y *Akkermansia sp.*

Finalmente, se estudió la asociación entre obesidad y CRC en un modelo murino de CRC asociado a obesidad mediante la administración de HFD a ratones, seguido de inducción de CAC con azoximetano (AOM) y dextrano sulfato de sodio (DSS). Se observó un agravamiento de la tumorigénesis en los ratones no tratados alimentados con HFD en comparación con los que recibieron una dieta estándar (SD), caracterizada por un aumento de la malignidad del tumor y la invasión a los tejidos submucosos. Además, los ratones alimentados con HFD no tratados exhibieron una regulación positiva de las citocinas derivadas del tejido adiposo, como la IL-6, que puede contribuir a la tumorigénesis. Asimismo, también se informaron cambios en la microbiota intestinal en estos ratones cuando se analizó la diversidad beta. Curiosamente, se observó un aumento significativo del género *Alistipes* en ratones alimentados con HFD no tratados con CAC en comparación con los alimentados con SD. Finalmente, también se estudió el efecto de la tigeciclina en este modelo de CRC asociado a obesidad y se encontró que ejercía un impacto similar al obtenido en el estudio previo realizado en ratones CAC. En resumen, la tigeciclina pudo interferir con las vías moleculares implicadas en la proliferación celular y modular la respuesta inmunitaria hacia una respuesta antiinflamatoria con actividad linfoide mejorada. Con respecto al impacto del tratamiento de la tigeciclina en la microbiota intestinal de ratones alimentados con HFD, el tratamiento pudo aumentar significativamente los niveles de *Parabacteroides goldsteinii* y *Akkermansia*

mucinifiphila, estando ambas especies bacterianas asociadas con una mejora de la enfermedad del cáncer.

En resumen, en la presente Tesis se ha realizado un análisis detallado de las terapias moduladoras de la microbiota intestinal basadas en el uso de los prebióticos *Thymus serpyllum* o *Morus alba*, así como del antibiótico tigeciclina, describiendo su impacto en modelos de obesidad, CRC y CRC asociado a obesidad. Además, la evidencia de los mecanismos moleculares implicados en los efectos beneficiosos que ejercen estos compuestos ha sido ampliamente descrita, prestando especial atención a aquellos cambios inducidos en la microbiota intestinal. Por tanto, el desarrollo de esta Tesis Doctoral tiene como objetivo proporcionar una mejor comprensión de la asociación obesidad-CRC, así como la búsqueda de nuevas terapias basadas en la modulación de la microbiota intestinal que contribuyan a la mejora de las terapias existentes para la obesidad y el CRC.

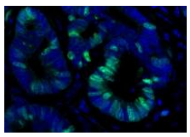

SUMMARY

SUMMARY

Colorectal cancer (CRC) is one of the cancers with the highest incidence, being the third most common cancer and the second leading cause of cancer-related deaths in the world. The etiology of CRC relies on the combination of multiple factors, including an inherited genetic component influenced by numerous environmental conditions such as sedentarism, a diet rich in processed meats, alcohol consumption, tobacco use and several diseases such as inflammatory bowel diseases (ulcerative colitis and Crohn's disease) or obesity. Among these risk factors, the consumption of a high-fat diet (HFD) has been closely linked to the development of an obesity status, which increases the risk of CRC development by almost 10%. The molecular pathways that are involved in the development of CRC in obese individuals are not fully described; however, it is known that the deregulation of metabolism as well as the chronic inflammatory state and the gut dysbiosis situation can contribute to CRC occurrence. In fact, many studies have reported the role of metabolites derived from an obesity-associated dysbiotic microbiota in CRC promotion. Then, the understanding of the molecular mechanisms involved in the crosstalk between obesity and CRC, especially those associated with the altered microbiota, has a potential translational value for CRC therapy and management, as well as for preventing the development of this disease in obese patients.

Microbiome modulation is one of the novel strategies in medicine with the greatest future to improve the health of individuals and reduce the risk of different conditions, including cancer, metabolic, immune, inflammatory and degenerative diseases. In this scenario, plant extracts obtained from the aerial parts of *Thymus serpyllum* L. or the leaves of *Morus alba* L. have been shown to exert prebiotic properties that have been associated with antiinflammatory and antioxidant activities. Consequently, they have been widely used in traditional medicine against several inflammatory-related diseases. Additionally, tetracyclines are drugs with proven antibiotic and immunomodulatory properties that have demonstrated cytotoxic activity against different types of cancer. These therapies have been characterized by modulating the gut microbiota, which is altered in both pathologies, obesity and CRC. Despite numerous advances have been achieved in the therapy of obesity and CRC, the current treatments are not always well tolerated and/or lack efficacy can occur in certain population groups. All the above justifies the necessity of further research focusing on the capacity of new agents to target the cellular and molecular pathways altered in obesity and CRC, especially in the gut dysbiosis that isd shared in both disorders. In order to address this, the following objectives were proposed:

1. To evaluate therapeutic strategies able to modulate the gut microbiota in the management of obesity.
2. To assess therapeutic strategies able to modulate the gut microbiota in the management of CRC.
3. To characterize the impact of obesity in the development of CRC, establishing the role of the intestinal microbiota as potential therapeutic target.

With these aims, first, the impact of two extracts, from *Thymus serpyllum* aerial parts and *Morus alba* leaves, were evaluated in an experimental murine model of obesity induced by a HFD intake. Moreover, the activity of these plant extracts on obesity-associated metabolic disorders, inflammatory and redox status, endothelial dysfunction as well as gut microbiota alterations were studied. The findings showed that both extracts showed a positive effect on the body weight gain induced by the HFD-supplementation, which was associated with an amelioration of the plasma glycemic and lipid profiles, as well as with a reduction of the fat deposits. Moreover, *Thymus serpyllum* and *Morus alba* extracts were able to significantly improve the chronic inflammation that characterizes the obese phenotype. In this sense, the treatments downregulated several pro-inflammatory mediators such as IL-6, TNFα and cyclooxygenase 2 expression. This effect could be related with the capacity of the extracts to modulate gut microbiota and ameliorate the altered gut barrier function, thus reducing the access of intestinal bacterial lipopolysaccharide (LPS) to the systemic stream, and resulting in a lower metabolic endotoxemia in obese-treated mice. Additionally, the presence of phenolic compounds in both plant extracts were responsible for an amelioration of the oxidative stress status associated with obesity.

Then, the effect of tigecycline, a third generation tetracycline, was investigated in experimental CRC models. Initially, the impact of this antibiotic on colon cancer cell lines, HCT116, Caco2 and CMT93, was studied and compared with the activity of 5-fluorouracil, which constitutes the standard drug in the therapy of CRC. Subsequently, and after evidencing the antiproliferative and proapoptotic effects exerted by tigecycline on tumor cells, the molecular mechanisms involved in these actions were further studied. It was observed that tigecycline hindered the activation of the Wnt/β-catenin and JAK/STAT3 proliferative pathways, and also the activated markers involved in the different programmed death pathways studied: extrinsic, intrinsic and endoplasmic reticulum-mediated apoptosis. Moreover, tigecycline exerted a beneficial effect against colon cancer stem cells (CSCs), which are related to the initiation of the tumor process and a greater malignancy of cancers due to their invasive and metastatic properties. This action may be related to the capacity of tigecycline to interfere with the epithelial-

mesenchymal transition, mainly related with an inhibition of the transcription factor SNAI1. All these effects were associated with a significant amelioration of the tumorigenesis *in vivo* in a tumor xenograft model and in the colitis-associated CRC (CAC) model in mice. Tigecycline administration to mice xenotransplanted with HCT116 CSCs resulted in a reduction of tumor volume and CTNNB1 (β-catenin) levels, a key player in tumor cell proliferation. This anti-proliferative effect of tigecycline was also observed in CAC mice treated with the antibiotic and was associated with a reduction of the inflammatory process and an increase in cytotoxic T cells in mesenteric lymph nodes in these mice. Moreover, the mitigation of the tumorigenesis observed with tigecycline treatment was linked to a proapoptotic effect *in vivo*, as evidenced by increased levels of caspase 7. Finally, the antibiotic was able to modulate the intestinal microbiota, by promoting enrichment in beneficial bacterial taxa associated with antiinflammatory and antitumor properties such as *Parabacteroides distasonis* and *Akkermansia* sp.

Finally, the association between obesity and CRC was studied in a murine model of obesity-associated CRC through the administration of a HFD to mice, followed by CAC induction with azoxymethane (AOM) and dextran sulfate sodium (DSS). An aggravation of tumorigenesis was observed in those untreated mice fed a HFD in comparison with those that received a standard diet (SD), characterized by increased malignancy of tumor and invasiveness of submucosal tissues. Moreover, untreated HFD-fed mice exhibited an upregulation of cytokines derived from adipose tissue such as IL-6 that can contribute to tumorigenesis. Additionally, changes in gut microbiota were also reported in these mice when beta diversity was analyzed. Interestingly, a significant increase of *Alistipes* genus was observed in untreated HFD-fed mice with CAC compared to those fed a SD. Finally, the effect of tigecycline was also studied in this model of obesity-associated CRC and it was found to exert a similar impact to that obtained in the previous study carried out in CAC mice. Briefly, tigecycline was able to interfere with the molecular pathways involved in cell proliferation and modulate the immune response towards an antiinflammatory response with enhanced lymphoid activity. Regarding the effect of tigecycline in gut microbiota of HFD-fed mice, the treatment was able to significantly increase the levels of *Parabacteroides goldsteinii* and *Akkermansia mucinifiphila,* being both bacterial species associated with an amelioration of the cancer disease.

In summary, a detailed analysis of intestinal microbiota modulating therapies based on the use of the prebiotics *Thymus serpyllum* or *Morus alba,* as well as the antibiotic tigecycline, has been carried out in the present Thesis, describing their impact on models of obesity, CRC and obesity-associated CRC. Furthermore, evidence of the molecular mechanisms involved in the beneficial effects exerted by these compounds has been

widely described, paying particular attention to those changes induced in the gut microbiota. Therefore, the development of this Doctoral Thesis aims to provide a better understanding of the obesity-CRC association, as well as the search for new therapies based on the modulation of the intestinal microbiota that contribute to the improvement of existing therapies for obesity and CRC.

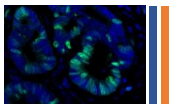

INTRODUCTION

INTRODUCTION

1. CANCER.

1.1. Definition and origin.

The word “cancer” comes from the ancient Greek “καρκίνος”, which means “crab” and “tumor” being this term applied to cancerous tumors in which the spreading projections and large vascularity represented the legs of a crab. The origin of the word is attributed to the Greek physician Hippocrates (460 - 370 BC) who used the terms “carcinos” and “carcinoma” to describe non-ulcer and ulcerative tumors respectively. Later, the Greek term was translated by the Roman physician Celsus (25 BC - 50 AD) to “cancer”, the latin term for crab. However, the disease is more ancient than the word that describes it, being the earliest evidence of cancer found in human mummies in ancient Egypt (1).

To give a proper definition to the term cancer, we first have to define what is neoplasm. The oncologist Willis (1837 - 1894) defined the term “neoplasm” as an abnormal mass of tissue whose growth exceeds and is uncoordinated with that of the normal tissues persisting even in the absence of external stimulus which evoked the change (2). Neoplasms are the result of an increase in cell number and some essential features such as the presence of living cells whose cell cycle is uncontrolled, the partial or total loss of special functions and the acquisition of new functions such as invasion. The term neoplasm refers to the tumor mass itself and it may be benign or malignant depending on their ability to spread into the organism. Benign tumors are those with proliferation capacity but do not invade the surrounding tissues nor metastasize, whereas malignant tumors, commonly known as cancer, are those able to invade and/or metastasize, thus causing secondary tumors in other tissues.

The World Health Organization (WHO) defines cancer as “a large group of diseases that can start in almost any organ or tissue of the body when abnormal cells grow uncontrollably, go beyond their usual boundaries to invade adjoining parts of the body and/or spread to other organs” (3). Many cancers form solid tumors but there are also liquid cancers such as leukemias.

1.2. Evolving models of tumor origin and progression

Cancer initiation and progression is a complex multistep process, which depends on the interactions between the tumor cells with tumor microenvironment and in which genotypic

and phenotypic changes occur. Due to the complexity of the process, some theories or models have been developed, thus allowing a better understanding of the cancer system.

1.2.1. Initial models. Cancer from a humoral to an organ disease.

Throughout the history of medicine several theories have been proposed to explain the root cause of cancer. For long centuries the humoral theory of Hippocrates and Galen became the most common to explain human diseases including cancer. According to this theory, diseases resulted from an excess or deficiency of one of the four basic substances called humors: blood (sanguis), yellow bile (chole), black bile (melan cole) and phlegm (phlegm). It was thought that the origin of cancer was the result of an excess of black bile (4). In the sixteenth century, Paracelsus suggested that the origin of tumors was in harmful chemical substances present in the blood (5). The Italian anatomist Giovanni Battista Morgagni was the first to state in its treatise *De Sedibus et Causis Morborum per Anatomem Indagatis* published in 1761 that the cause of a disease was found in pathological lesions present in a certain organ (6).

1.2.2. Cancer from the microscopic point of view. Emergence of cell disease concept.

Advances in microscopic pathology led to the belief that cancer was a parasitic disease and that the development of tumors might be caused by foreign organisms (6). Histological advances allowed a more precise description of tumor structures; in this sense, Schleiden and Müller (in 1838) as well as Schwann (in 1839) reported that neoplastic tumors were integrated by a mass of cells with different morphology (7). These advances, together with those postulated by Rudolf Virchow in its cell theory, resulted in a further description of tumor characteristics such as the presence of an abnormal number of cells in division with big nuclei, anomalous mitosis and loss of differentiation features. The presence of a tumor stroma, extensive vascularity and apoptotic areas were also described as features of the tumor in the nineteenth century (6). Since then, cancer began to be considered as a disease in which cells divide abnormally (6).

Metastasis was explained by the “seed and soil” and the “mechanical mechanisms” hypothesis proposed by Stephen Paget and James Ewing, respectively. The seed and soil hypothesis states that malignant cells (“seed”) are detached from the tumor mass and reach a suitable place (“soil”) in the body where the microenvironment is favorable for their continued growth causing a secondary tumor (8). James Ewing, in 1928, proposed that the place of metastasis is determined by mechanical forces and circulatory patterns between the primary and the secondary site of tumor development (8, 9).

Despite the great advances made, the origin of neoplastic cells was unknown. Julius Cohnheim postulated in 1877 his theory of the embryonic origin of cancer cells, in which he stated that tumor development was the result of the existence in the body of "embryonic rests", being these tumor cells really embryonic cells that were not removed during the ontogenesis (10). This theory was formulated on the basis that it had previously been said that tumor cells were morphologically similar to embryonic cells (Johannes Müller, 1838) (11).

1.2.3. Cancer as a genetic disease: focus on the cell nucleus.

In 1890, David Paul von Hansemann proposed a theory about the pathogenesis of cancer, which was focused on a specific part of the cell, the genetic material, known at that time as "hereditary material". According to this theory, the first change that occurs in cancer is an alteration of the hereditary material of a normal cell. Moreover, Hansemann postulated that cancer cells could be cells that suffer a process of "dedifferentiation" or "anaplasia", terms coined to this pathologist (12, 13).

Thanks to technological advances, the genetic material began to be studied in depth and at the beginning of twentieth century (1902), Theodor Boveri described the role of chromosomal abnormalities in the development of cancer and predicted that chromosomal (genomic) instability was a key hallmark of cancer (14). Later on, in 1926, Hermann Joseph Muller demonstrated that exposure to X-rays can cause genetic mutations and cancer development (15). The studies on the structure of DNA made by Watson and Crick in 1953, as well as the emergence of DNA cloning and sequencing techniques, contributed to the development of genetics that had an important impact on the understanding of cancer etiology (16). It was in the 1970s and 1980s when a new model of cancer disease was proposed in which three stages can be distinguished in the tumor development process: initiation, promotion and progression (Figure 1). The first stage, initiation, is an irreversible process that starts with two or more relevant mutations (also transversions, transitions and/or small deletions in DNA) in a single cell due to the action of molecules called *initiators* (carcinogens). Then, in the promotion stage, this cell begins to proliferate under the influence of *promoters*, which are proliferation-stimulating factors such as growth factors and hormones. The subsequent division of this cell gives rise to a population of cell clones. Cancer progression is the result of subsequent mutations, thus leading to the appearance of a malignant neoplasm with heterogeneous cells that acquire independent characteristics such as invasion, metastatic capacity and uncontrolled proliferation (17, 18).

Figure 1. Stages of tumor development: initiation, promotion and progression.

During the second half of the 20th century, cancer research focused on the search for carcinogens responsible for the initiation of carcinogenesis, as well as the genes affected in this process. In the late 1960s, certain carcinogens with the ability to bind DNA were described. These genotoxic compounds were able to damage DNA by forming adducts or causing DNA strand breaks (19). Nowadays, it is also known that there are carcinogens that do not act directly on the DNA, but can induce free radicals or activate signaling pathways that alter the cell cycle. In the 1980s, numerous preclinical studies were carried out to elucidate which genes were altered in the carcinogenesis process. In this way, the involvement of certain genes such as *MYC, TP53* and *KRAS* in the cancer process, as well as their structure and functions were described (20). Then, these genes were classified into proto-oncogenes and suppressor genes (anti-oncogenes) and the involvement of each one will be discussed later.

During the promotion and progression stages that occurred in the tumor development process, some mutations can take place in cells that makes the tumor mass heterogeneous (18). Due to these mutations, the tumor acquires new features such as uncontrolled proliferation in absence of stimulus (growth factors for example), apoptosis evasion, drug resistance, invasion and metastatic capabilities. These changes are comparable to an evolutionary process that increases the aggressiveness of the tumor. Peter Nowell, in 1976, proposed the successive clonal evolution model in which this process was considered and tumor progression was compared with an evolutionary process (21).

1.2.4. The stochastic model of cancer.

Until the end of the last century, the most accepted model to explain the process of tumor initiation and promotion was the stochastic model. This classical model proposed that each tumor cell is biologically homogeneous and has the ability to initiate and promote the tumor origin and evolution. According to this model, tumorigenesis occurs from normal differentiated somatic cells that stochastically/randomly suffer oncogenic mutations, thus leading to genomic instability, hyperplasia, uncontrolled proliferation and expansion, and escaping from the homeostatic mechanisms of the cell compartment.

Moreover, subsequent alterations/mutations drive progression to invasive and more aggressive phenotypes with metastatic characteristics (22-24).

1.2.5. Cancer stem cells and cancer: the hierarchical model and retrodifferentiation concept.

The most recent models of tumorigenesis affirm that the origin of the tumor process lies in an altered stem cell type that is called CSC (25). The CSCs theory was proposed in 1994, when Lapidot T. et al., inoculated acute myeloid leukemia stem cells to severe combined immune-deficient (SCID) mice, and they reported the ability of these cells to reproduce the disease in these mice (26). CSCs share many characteristics with normal stem cells such as capability of cell renewal and differentiation into other cells (27). However, unlike normal stem cells, CSCs, due to genetic and epigenetic alterations, are not subject to the normal controls that limit growth (25). Tumor generation would begin when a normal stem cell located in a stem cell niche suffers genetic and epigenetic alterations that lead to the evasion of the regulatory mechanisms present in a normal stem cell, as well as the regulatory signals from the microenvironment where the stem cell is located (28, 29). Therefore, the cell escapes to any control mechanism, thus resulting in a tumorigenic stem-like cell, a CSC. Next, the promotion of the tumor would be explained due to the self-renewal, replication and differentiation capacity of this CSC that would give rise to a hierarchy of heterogeneous cells that constitute the tumor mass (25, 30). This model is known as the hierarchical model of tumor development, and it assumes that the initiation of the tumor is carried out by a CSC. Therefore, these CSCs are also designated as tumor-initiating cells and they would also be responsible for relapses in cancer patients (24, 25, 30). In this model, a special importance is given to the stem cell niche because it is responsible for the maintenance of the stem-like state (28, 29). Moreover, it has been postulated that CSCs can be originated by the microenvironment through induction of CSC features in differentiated tumor cells in a process called retrodifferentiation (31, 32). This process is characterized by a loss of cell differentiation that reverts to an undifferentiated or stem-like phenotype in a rejuvenation process (33). The phenomenon of retrodifferentiation makes the hierarchical model multidirectional rather than unidirectional, and explains the formation of CSCs from normal tumor cells (24).

1.3. Genetic alterations occurred in cancer.

Cancer is a genetic disease and it means that it is caused by mutations occurring in genes that are involved in the maintenance of cell functions, especially cell growth and

division (34). These cancer-causing DNA changes may be due to errors that take place during cell division, DNA damage caused by mutagenic environmental agents such as tobacco carcinogens and/or DNA mutations inherited from our parents (34). These genetic alterations are known as “divers" lesions (35), and generally affect three different types of genes that are classified under the name of proto-oncogenes, tumor suppressor genes and DNA repair genes. Proto-oncogenes are genes involved in normal cell division and proliferation, and when these mutations take place, they become into oncogenes (cancer-causing genes). Some examples of oncogene are *MYC* or *CCND1* that produce transcription factors involved in cell proliferation (36). Tumor suppressor genes are involved in the control of cell growth and division, and mutations in these genes contribute to uncontrolled cell division. *TP53* is the most known tumor suppressor gene, being also known as the guardian of the genome since it induces apoptosis when gene mutations appear (37). Lastly, alterations in DNA repair genes alter mechanisms involved in fixing damaged DNA. *BRCA1* and *BRCA2* are some of the most well-known DNA-repair genes that can be mutated in cancer (38). Therefore, mutations in all these types of genes contribute to the initiation and progression of cancer (34, 39). Moreover, the mismatch repair system has an important role in the repair of erroneous insertion, deletion, and base-base mismatches generated during DNA replication and recombination. Alteration of this system is also linked to a large number of cancers (40).

These genetic alterations lead to disruption of the cell normal cycle causing an abnormal proliferation of a single cell. The cell uncontrolled proliferation results in the outgrowth of a population of clonally derived tumor cells creating a tumor (41). This uncontrollable and high speed division favors the appearance of new mutations in these cells, thus contributing to tumor progression. Additional mutations confer a selective advantage to the cell, and the descendant cells that are generated from this one become the dominant ones in the tumor mass. This process is called clonal selection and results in a clone of tumor cells with malignant properties, such as uncontrolled proliferation, apoptosis evasion, survival, angiogenesis induction, immune evasion, genome instability and mutations, deregulation of cellular energetics, invasion or metastasis (42). Therefore, cancers are the result of a reiterative process of clonal expansion, genetic diversification and clonal selection with the ability of environmental adaptation (35).

During the course of the disease, cancers generally become more heterogeneous. It means that the tumor mass harbors a diverse collection of cells with different molecular signatures, which would make the tumor more or less sensitive to antitumor therapies (43). Genetic and epigenetic alterations, as well as changes in the tumor microenvironment, are the most important factors that contribute to the heterogeneity of

the tumor mass (43). In fact, a tumor is not only composed of a group of cancer cells, but it is also made up of resident host cells, secreted factors and extracellular matrix that form the tumor microenvironment (44). The composition of tumor microenvironment varies between different tumor types, but it includes immune cells, stroma cells, blood vessels and extracellular matrix (44). Independently from the composition of the tumor microenvironment, its function is to support tumor growth and progression (45).

2. COLORECTAL CANCER

2.1. Epidemiology.

According to the WHO, cancer is a leading cause of death worldwide with almost 10 millions of deaths in 2020 (46). CRC is the third most frequent cancer in the world, and the second leading cause of cancer-related death worldwide according to the Global Cancer Observatory 2020 data (Figure 2). In fact, there were more than 1.9 million cases and almost one million deaths in 2020 (47). Although the rate of people diagnosed with colon or rectal cancer since the 1980s has dropped due to increased screening and lifestyle changes, since 2012 the incidence of CRC has increased every year by 2% in people younger than 50, and 1% in people from 50 to 64 years of age (48).

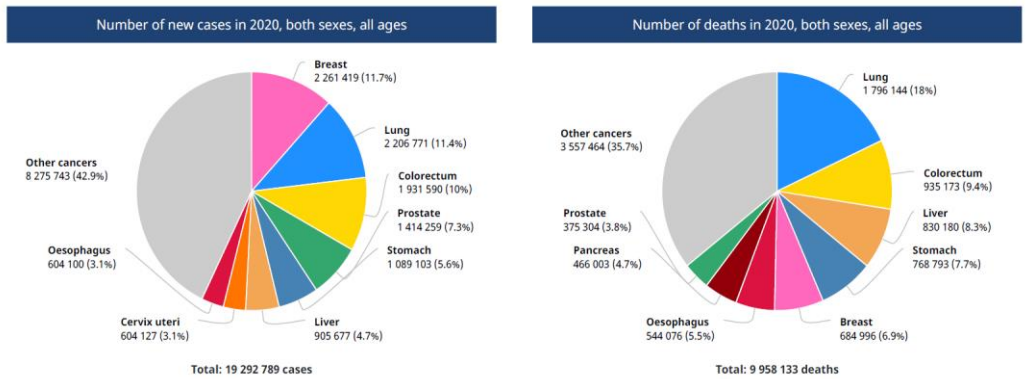

Figure 2. Pie charts present the number of new cases and number of deaths for the most common cancers in 2020 for both sexes. *Source: GLOBOCAN, 2020.* (Accessed on 18.01.23. Available online: https://gco.iarc.fr/today/data/factsheets/cancers/8-Colon-fact-sheet.pdf)

CRC is the second most common cancer diagnosed in women and the third most in men. However, the number of diagnosed cases and deaths is higher in men than in women (GLOBOCAN, 2020). These rates also vary geographically, being CRC most common in

developed countries, most probably associated with the lifestyle of its inhabitants. Due to the continuous development of the countries, the global burden of CRC is expected to increase to more than 2.2 million new cases and 1.1 million deaths by 2030 (49).

2.2. Risk factors.

CRC is a genetic disease with an important hereditary risk to develop this type of cancer. In fact, 10-20% of all patients with CRC have a family history of this disease (50). It means that certain gene alterations involved in tumor development can be transferred from generation to generation, thus making this cancer hereditary. Moreover, the loss of genomic stability leads to CRC progression and some types of genomic instability have been described. Chromosomal instability is the most common type of genomic instability and results from errors in chromosome segregation during mitosis that lead to abnormalities in the chromosome number and structure (51). In fact, this is considered a hallmark of cancer and it causes the loss of wild alleles of tumor suppressor genes such as *TP53* (52, 53). Chromosomal instability is an hereditary process that is involved in initiation, promotion and progression of cancer, being associated with poor prognosis, therapeutic failure and metastasis (51). Mutations and inactivation of DNA repair genes, such as *MSH2, MLH1, MSH6* or *PMS2*, are linked to the so-called microsatellite instability (52). This type of instability, which can be inherited or acquired, is associated with changes in length in regions of repeated DNA. Microsatellite instability occurs in around 15% of all CRC tumors in white populations and this phenomenon is present around 90% of CRC due to Lynch syndrome (54, 55). Lynch syndrome, also known as hereditary non-polyposis CRC, is an inherited disorder linked to mutations in mismatch repair-genes that increases the risk of developing CRC and other cancers (56). In fact, around 3% of new cases of CRC are attributed to the Lynch syndrome (57). In addition to Lynch syndrome, there are other syndromes classified as polyposis syndromes, such as the familial adenomatous polyposis syndrome, which are also hereditary and can result in developing CRC in individuals who suffer from it (58).

Lastly, aberrant DNA methylation can also contribute to genomic instability and increases the risk of cancer (59, 60). CRC is characterized by global DNA hypomethylation and methylation in some gene-specific promoters leading to gene silencing, genomic instability and tumor initiation (61, 62). The *MLH1* gene promoter is susceptible to being aberrantly methylated and silenced in patients with colon cancer, thus leading to mismatch repair system deficiency that is also associated with *BRAF* mutations (62).

Therefore, it cannot be denied that CRC has an important genetic and hereditary factor that increases the risk of suffering from it. In addition to this genetic component, there are

other risk factors such as gender and age that cannot be modified (Figure 3). In fact, it has been shown to have a higher risk of CRC in male (62, 63) and elderly, although the incidence in young people is increasing (64).

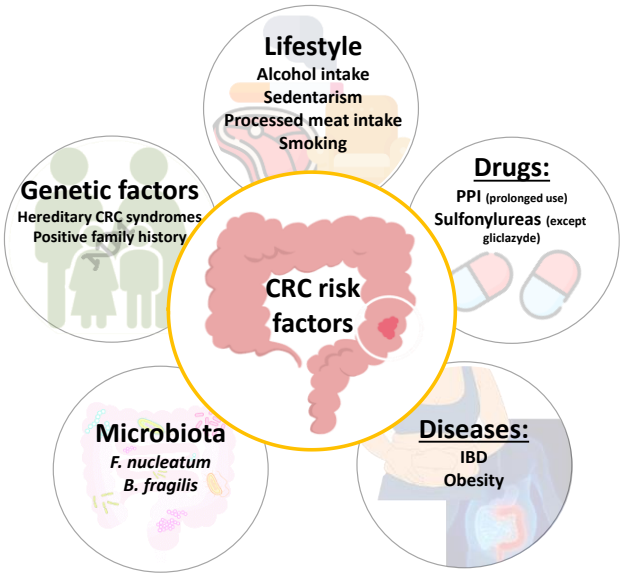

Figure 3. Risk factors for colorectal cancer (CRC). *PPI - Proton-Pump inhibitors.*

On the other hand, several environmental lifestyle factors also contribute to the initiation and development of CRC. Some examples of these environmental factors are smoking (65), physical inactivity (66), alcohol (67) and processed meat intake (68) as well as the consumption of certain drugs (69, 70). Moreover, CRC risk has been reported to be increased by some diseases, typically associated with an inflammatory status, such as inflammatory bowel disease (IBD) (71, 72) and obesity (73, 74) which will be addressed in more detail later in the present Thesis. Another important factor that has been proposed to be more and more relevant in this condition is the colonic microbiota; in fact, an increased risk of CRC has been observed in infections with specific bacterial species such as *Fusobacterium nucleatum (75)* and *Bacteroides fragilis* (76) (Figure 3).

2.3. Pathogenesis.

There are three well-defined mechanisms in the base of CRC carcinogenesis: chromosomal instability, CpG island methylation and microsatellite instability (77, 78) (Figure 4).

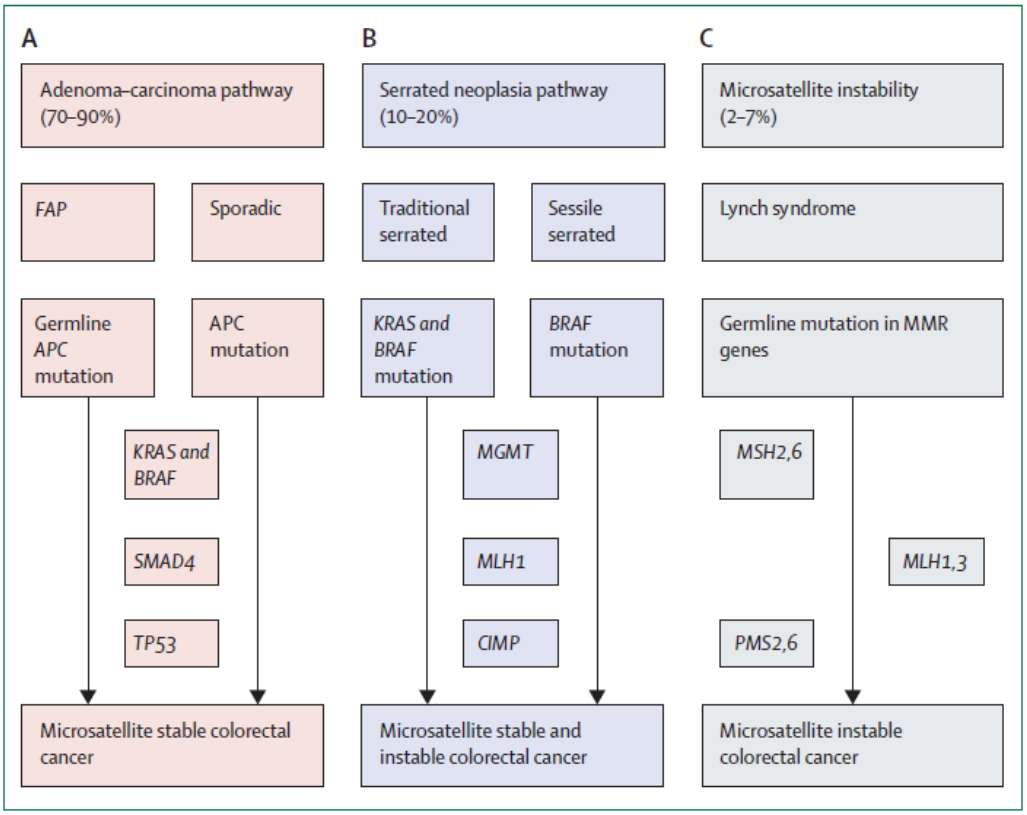

Figure 4. Colorectal cancer development pathways from a genetic point of view. *A) adenoma-carcinoma pathway; B) serrated neoplasia pathway and C) microsatellite instability pathway. Extracted from (79). FAP - familial adenomatous polyposis, MMR - mismatch repair.*

Chromosomal instability occurs in 65-70% of CRC and it refers to the loss of the whole or large portions of chromosomes in tumor cells (80, 81). CRC initiation is a slow and sequential process that occurs in a step-wise manner known as adenoma-carcinoma sequence (82). In this model, initially proposed by Fearon and Volgestein (1990), malignant tumors (carcinomas) with metastatic capacity arise from preexisting benign tumors (adenomas) (82). The process is initiated by the accumulation of genetic and epigenetic alterations, as mentioned above, that result in the activation of oncogenes and the inactivation of tumor suppressor genes. Moreover, certain environmental risk factors contribute and accelerate these gene alterations. Early *APC* (*Adenomatous polyposis coli*) gene mutation occurs in colorectal adenomas, being the location of these mutations correlated with the extent of colorectal polyps and extracolonic manifestations (83). APC protein is a member of the Wnt/β-Catenin pathway and controls colonic epithelial proliferation. *APC* mutation leads to the inactivation of this gene, thus resulting in a

permanent cell division (83). This mutation has been observed in the primary dysplastic lesions that initiate the adenoma-carcinoma sequence, which are called aberrant crypt foci (84, 85). They are microscopic lesions that are considered as precursors of adenomas, which in turn are precursors of adenocarcinomas. *APC* mutation is followed by mutations in other genes such as *KRAS, TP53* and *SMAD4* (86). Some studies carried out in the 1990s showed that at the beginning of the tumor process, not only the accumulation of mutations is important, but also the order in which they occur (84, 85, 87). In this sense, an early mutation is produced in the *APC* gene in most CRCs, and it is followed by other mutations in other genes such as *KRAS, TP53* and *SMAD4*.

A smaller percentage of sporadic CRCs are developed through different molecular pathways that include CpG island methylation or inactivation of the DNA mismatch repair system. Around 10% of CRC are generated through the well-known serrated-neoplasia pathway, thus leading to two possible progression presentations (88). In the first, CRC carcinoma develops from microvesicular hyperplastic polyps through a sessile serrated pathway (89). In the second, in the traditional serrated pathway, adenocarcinoma originates from a serrated adenoma, which in turn originates from a goblet cell-rich hyperplastic polyp (90). In these sessile-serrated lesions, a methylation of CpG island occurs, which results in the CpG island methylator phenotype (CIMP) (91). Depending on the degree of methylation of promoter region CpG islands, CIMP colorectal carcinomas phenotypes are divided into CIMP-H or CIMP-L, when the methylation is higher or intermediate, respectively (92). The aberrant methylation of promoter region CpG is associated with the inactivation of tumor-suppressor genes that leads to neoplasia formation (91, 93). In the serrated subtype of colorectal carcinoma, changes in the methylation pattern of some gene promoters are accompanied by mutations in the mitogen-activated protein kinase (MAPK) pathway components, *BRAF* or *KRAS,* being also frequent microsatellite instability (94).

Lastly, another well-defined subtype of CRC, but with a less incidence (2-7%), is characterized by a deficiency of mismatch repair genes such as *MSH2* and *MSH6* (Mut S homologues), *MLH1* (MutL homologue) or *PMS2* (postmitotic segregation). Microsatellite instability is present in this CRC subtype with some phenotype features that allow its clinical identification: proximal anatomical location, mucinous features, immune infiltration and pushing margins (95). Moreover, this subtype is associated with Lynch Syndrome and is also important from a therapeutic point of view since these tumors are resistant to the standard chemotherapy in CRC, that is, the 5-fluorouracil (5-FU) treatment (95).

2.4. Consensus molecular subtypes.

In 2014, the international CRC Subtyping Consortium created a unified classification of CRC based on the genetic alterations produced in this pathology. Therefore, CRC was classified in four molecular subtypes, termed as Consensus Molecular Subtypes (CMS) 1-4 (96, 97) (Table 1).

Subtype	Characteristics
CMS1 MSI immune subtype	Immune cells infiltration
	MSI
	CIMP
	BRAF mutation
CMS2 Canonical subtype	Epithelial gene-expression signatura
	CIN
	Active Wnt signaling
CMS3 Metabolic subtype	Epithelial component
	Deregulation of metabolic processes
	KRAS mutations
	CIMP low
CMS4 Mesenchymal subtype	Stromal cells
	Epithelial-mesenchymal transition (EMT)
	Angiogenesis.
	Active transforming growth factor-β (TGF-β) signaling
	Matrix remodeling

Table 1. Consensus molecular subtypes (CMS) of CRC and their characteristics.

2.5. Hallmarks of colorectal cancer.

In the normal colon, 4 four layers can be distinguished: mucosa, submucosa, muscle layer and adventitia. The intestinal epithelium is located in the mucosa layer and is composed of a single layer of polarized cells among which the major types include colonocytes, goblet cells, Paneth cells and stem cells. These cells are arranged in cylindrical structures called crypts in which cellular proliferation and migration are regulated. Colonic stem cells reside in the bases of the crypts in the “stem cell niches” and their division and differentiation are regulated by extracellular factors such as growth factors and hormones (98). In normal conditions, these colonic stem cells divide in a regulated manner and give rise to each of the aforementioned specialized cells with specific functions. Genetic and epigenetic changes may occur in any of these stem or differentiated cells, thus resulting in the generation of a tumor cell that acquires autonomy and escapes to regulatory signals that control its cell division. These genetic and epigenetics changes result in some essential alterations in cell physiology that collectively dictate malignant growth and lead to tumor formation. These hallmarks are

common to tumor cells of other cancer types and they are self-sufficiency in growth signals, insensitivity to growth-inhibitory signals, evasion of apoptosis, angiogenesis, tissue invasion and metastasis (99) (Figure 5).

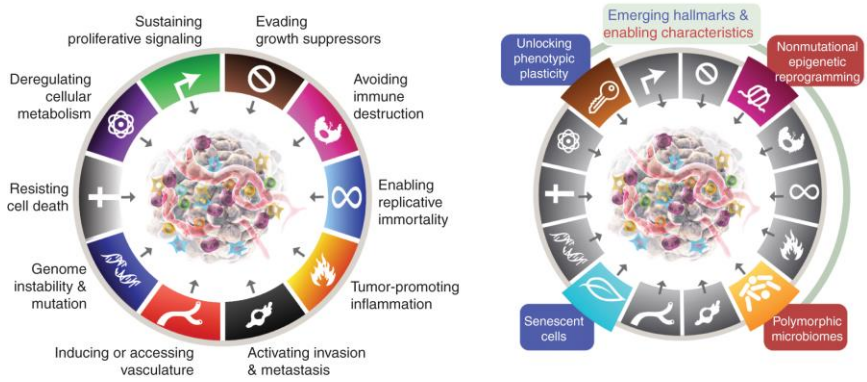

Figure 5. Hallmarks of cancer. *Extracted from (100)*.

2.5.1. Self-sufficiency in growth signals: uncontrolled proliferation.

The activation of the division cycle in normal cells requires mitogenic growth signals that are transmitted by certain molecules such as growth factors; in fact, in absence of these stimulatory signals, normal cells are not able to proliferate. Conversely, tumor cells acquire mutations that make them independent of these exogenous signals and begin to proliferate autonomously. Oncogenes activation and tumor suppressor genes inactivation are responsible for this low response to external signals since the tumor cell generates their own growth signals that allow it to grow independently of its environment (99). Therefore, somatic genetic alterations lead to the overexpression of certain proteins in the tumor cells that activate signaling pathways endowing these cells with a pro-proliferative state. In CRC there is a overstimulation of the main signaling pathways that control cell proliferation such as the Wnt/β-catenin, EGFR/MAPK, phosphoinositide-3-kinase (PI3K)/Akt and the Janus kinase (JAK)/signal transducer and activator of transcription (STAT) pathways.

2.5.1.1. Wnt/β-catenin pathway.

In the adenoma-carcinoma sequence proposed by Fearon and Volgestein in 1990, several driver mutations take place in *APC*, *KRAS*, *SMAD4* and *TP53* genes and the accumulation of these mutations favor the progression of adenoma into CRC (101). *APC* mutations lead to an alteration of the Wnt pathway, being the principal driver of epithelial proliferation, as well as of other functions such as differentiation, migration and stem cell renewal (102). Wnt comprises a diverse family of glycoproteins that act as ligands to

activate the different Wnt pathways: canonical (Wnt 3, 6 and 9b) and non-canonical (Wnt 2b, 4, 5a and 5b). When the canonical pathway is activated, β-catenin is translocated into the nucleus promoting the activation of genes involved in cell proliferation. In this process, Wnt binds to the N-terminal extracellular cysteine rich domain of a Frizzled family receptor, a G-protein-coupled receptor that disrupt the destruction complex of β-catenin, thus favoring its cytoplasm accumulation (102).

The APC protein is a component of this β-catenin destruction complex, together with other proteins such as the Ser/Thr kinases glycogen synthase kinase 3 (GSK-3), casein kinase 1 (CK1), axin, the E3-ubiquitin ligase β-TrCP and the protein phosphatase 2A (PP2A). APC protein is encoded by the *APC* tumor-suppressor gene and it is constituted by 2843 aminoacids consisting of an oligomerization domain and an armadillo region in the N-terminal region, a central portion with 15-20 amino acids repeats and a C-terminal region, which is a binding site for the end-binding 1 (EB1) and human disc large (HDLG) proteins (103). APC, in addition to regulating the Wnt/β-catenin pathway, it also participates in other functions such as cell-cell adhesion and even apoptosis (103, 104). *APC* mutations, which occur in a high percentage of CRC cases, lead to a truncated APC protein that lacks all of the axin binding sites and almost all β-catenin binding sites (103). These mutations prevent the binding of β-catenin to the complex and its phosphorylation and, therefore, they favor the aberrant accumulation of β-catenin in the cytoplasm of the cell.

β-catenin is a structural component of cadherin-based adherens junctions, besides being a core molecule of the Wnt/β-catenin pathway that regulates the cell cycle and proliferation (105). In normal conditions, during the absence of Wnt ligands, β-catenin is targeted by the mentioned protein complex constituted by APC. Then, β-catenin is phosphorylated by CK1 in Ser45 and by GSK3-β in Ser33 and Ser37 leading to its ubiquitination and proteasomal degradation (106). Mutations in *APC* gene also affect to the ubiquitination of β-catenin because the 20R2-CID region of APC has an essential role in promoting β-catenin ubiquitination, which is downstream from β-catenin phosphorylation, and is independent of β-catenin-binding activity of APC (107).

Therefore, *APC* mutations lead to the aberrant activation of β-catenin and its translocation to the nucleus where it binds to members of the Tcf/Lef1 (T-cell factor/Lymphoid enhancer factor 1) family and it promotes the expression of genes involved in cell cycle and proliferation such as *JUN*, *MYC* and *CCND1*, being most of them oncogenes that encode oncoproteins related with cell proliferation activation (108) (Figure 6).

Colon carcinoma cells with mutant *APC* contain large amounts of cytoplasmic and nuclear β-catenin, thus promoting the cell proliferation involved in the initiation of the tumorigenesis process (101, 109, 110).

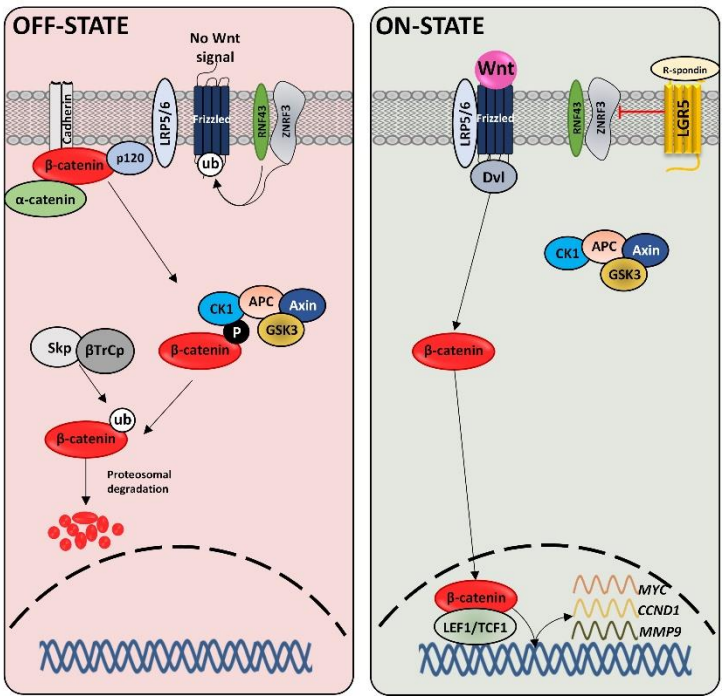

Figure 6. Wnt/β-catenin signaling pathway in off-state (left) and on-state (right).

2.5.1.2. EGFR/MAPK pathway

Epidermal growth factor receptor (EGFR), also known as human epidermal growth factor 1 (HER1) or ErbB-1, is a 170-kDa transmembrane tyrosine kinase receptor that belongs to the ErbB family of receptors. ErbB-2 (HER2), ErbB3 (HER3) and ErbB-4 (HER4) are the other components of this superfamily of receptors, which are characterized by the presence of a cytoplasmic domain with tyrosine kinase activity (111, 112). The EGFR signaling pathway regulates important cellular processes such as cell growth, proliferation and survival, being critical to the normal embryogenesis of vertebrates (113). In normal cells, the pathway is activated by the binding of a ligand, such as the EGF or the insulin-like growth factor 2 (IGF2), to the EGFR, thus inducing its dimerization and activation of the tyrosine kinase function. Then, the intracellular tyrosine kinase residues are autophosphorylated leading to the activation of several signal pathways. Two of the most important pathways activated by the EGFR are the MAPK and the PI3K/AKT pathways that are involved in cell proliferation, migration, differentiation and apoptosis

(114). Some studies have found an association with CRC and EGFR overexpression, which was the basis for in development of cetuximab, an anti-EGFR monoclonal antibody for the treatment of EGFR-positive CRC (115, 116). Moreover, EGFR overexpression is related to an over-activation of MAPK and PI3K/AKT pathways, whose components are usually also mutated in CRC. Indeed, disruption of the EGFR pathway contributes to growth, proliferation, survival and metastasis in neoplastic cells (112).

MAPK is a member of the large family of Ser/Thr kinases. Three major subfamilies of MAPK can be distinguished: the extracellular-signal-regulated kinases (ERK MAPK, Ras/Raf1/MEK/ERK), the c-Jun N-terminal or stress-activated protein kinases (JNK or SAPK), and MAPK14 (117). The ERK MAPK is involved in cell proliferation and the activation and overexpression of this pathway play an important role in the promotion and progression of CRC. Once EGF binds to EGFR, a signaling cascade is triggered, in which different adaptor proteins are involved, such as Shc, Grb2 and the Ras guanine nucleotide exchange factor Sos (118). These adaptor proteins activate $p21^{ras}$ proteins, H-Ras, N-Ras or K-Ras. These proteins are a family of GTPases that can also be activated by the protein kinase C (PKC), a kinase with several isoforms involved in different cellular events, including cell proliferation (119, 120). Ras proteins trigger the activation of Raf1, a cytoplasmic protein with intrinsic serine-threonine kinase activity that phosphorylates MEK1 and MEK2, which in turn phosphorylates and thereby activates ERK proteins (117, 121). ERK comprises a family of proteins (ERK1, 2, 3, 4, 5 and 6) with kinase activity that depend on tyrosine phosphorylation for their activation and activate serine/threonine cascades (122). The MEK1/2-activation of ERK1 ($p44^{MAPK}$) and ERK2 ($p42^{MAPK}$) results in the translocation of activated MAPK into the nucleus, whereby it phosphorylates and activates nuclear transcription factors such as Elk-1, Sap1, c-Jun and ATF2. The activation of these transcription factors lead to the transcription of oncogenes such as *FOS, JUN* and *CCND1* leading to an increase of cell proliferation (117, 123, 124) (Figure 7).

A dysregulation of this pathway occurs in CRC patients leading to malignant transformation and tumor progression through an increase of cell proliferation, angiogenesis and cell survival (125). In fact, mutations in genes that are encoded for components of this pathway, such as Ras (*KRAS* and *NRAS* genes*)* and Raf (*BRAF* gene), occur in a high percentage of CRC patients (126, 127), thus resulting in an increase of ERK activity that contributes to tumorigenesis (128). Therefore, in those tumors in which the EGFR/MAPK is expressed aberrantly, targeting this pathway is considered a therapeutic approach (129).

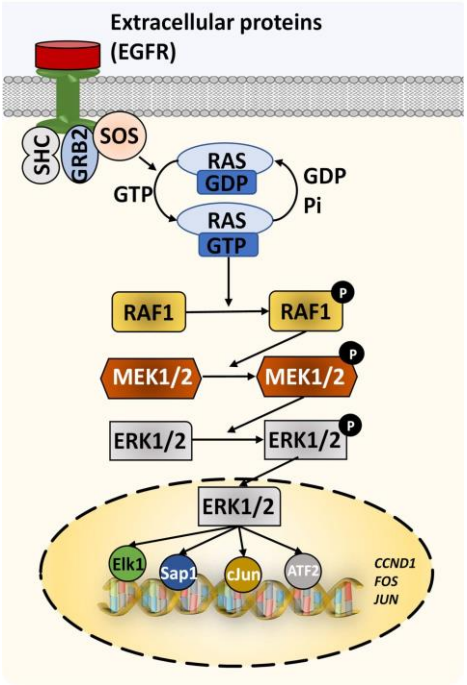

Figure 7. MAPK signaling pathway in CRC. *Adapted from (117).*

2.5.1.3. PI3K/AKT pathway.

The PI3K/Akt pathway is a signaling cascade downstream of EGFR that is overactivated in 60-70% of CRC cases, and the inhibition of its components has been proposed as a CRC therapy approach in several studies (130). EGFR activation by EGF results in the recruitment of PI3K by the adaptor protein Grb2. PI3Ks are a family of kinases that are divided into three classes (I-III). being the class Ia the most implicated type in human cancer (125). Once PI3K is activated, it phosphorylates phosphatidylinositol 4,5 biphosphate (PIP_2), giving rise to phosphatidylinositol 3,4,5 triphosphate (PIP_3). Then PIP_3 binds to the PH domain of AKT and recruits it to the plasma membrane. Akt is then activated by phosphorylation in residues T308 and S473, carried out by phosphoinositide-dependent kinase-1 (PDK1) and the mammalian target of rapamycin complex (mTORC) 2, respectively (131). Akt is a serine/threonine protein kinase (Ser/Thr kinase) also known as protein kinase B (PKB) that, once it is activated, inhibits the tuberous sclerosis complex 2 (TSC2) via phosphorylation. This action leads to the inactivation of the Ras homolog enriched in brain (RHEB) mediator resulting in the activation of mTORC1 (132). In turn, mTORC1 is a kinase that acts as regulator of other proteins such as S6 kinase (S6K), 4E-binding protein 1 (4E-BP1) and the Unc-51-like

kinase 1 (ULK1) that are involved in cell growth and autophagy (132). This pathway is regulated by the phosphatases PTEN and PHLPP1/2 that act by dephosphorylating the substrates PIP3 and Akt, respectively, and thereby balancing pathway activity (133, 134). In a large number of CRC patients, the overstimulation of the PI3K/AKT pathway has been observed, which is associated with mutations in certain components of the pathway. The most common pathway changes are related to mutations in *PI3KCA* and *PTEN* genes, as well as IGF2 overexpression (135). Moreover, *KRAS* and *BRAF* mutations stimulate the Pi3K/AKT pathway because of the existence of a cross-talk at the Raf1 level between the Raf-MEK-ERK and this pathway (136). Therefore, these genetic alterations lead to an overstimulation of the PI3K/AKT pathway that results in reduced apoptosis, cell growth stimulation and increased proliferation in CRC patients (135).

2.5.1.4. JAK/STAT3 pathway

The JAK/STAT pathway is actively involved in cell proliferation, survival, differentiation and apoptosis. Moreover, alterations in this pathway have been associated with tumor progression and poor prognosis in CRC patients (137) (Figure 8).

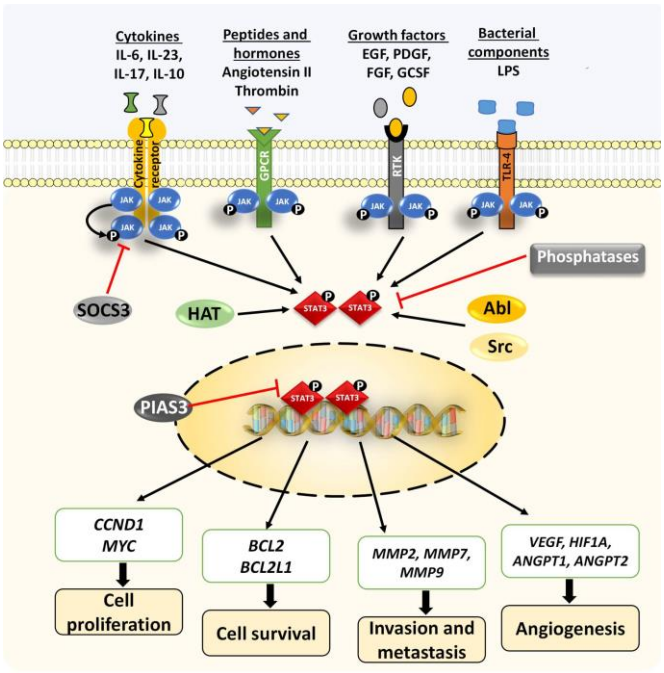

Figure 8. JAK/STAT3 signaling pathway in CRC tumorigenesis. *Adapted from (138, 139).*

The JAK family is composed of four members of non-receptor tyrosine kinases in mammals, JAK1, 2, 3 and the tyrosine kinase 2 (Tyk2). The activation of JAKs proteins

is triggered by the binding of ligands to their receptors, including growth factors (EGF), cytokines (IL-17, IL-6, IL-23), peptides and hormones. In this scenario, the activation of receptor tyrosine kinases (RTK), or cytokine receptors or G-protein-coupled receptors (GPCR) leads to JAK recruitment, which phosphorylates STAT. STAT may also be phosphorylated and activated by non-receptor tyrosine kinases such as Src and Abl. Once phosphorylated, STAT is dissociated from the receptor and forms homodimers or heterodimers able to translocate into the nucleus where they regulate the expression of target genes, usually involved in cell proliferation. STAT acetylation on K685 is an alternative mechanism of the STAT dimer stabilization and activation carried out by Histone acetyltransferases (HAT) (140). On the other hand, this pathway is negatively regulated by tyrosine phosphatases that dephosphorylate STAT leading to its inactivation. Moreover, the suppressor of cytokine signaling 3 (SOCS3) and E3 SUMO-protein ligase (PIAS3) act as inhibitors of STAT at receptor and transcription levels, respectively (138, 140, 141).

STAT3 is a member of the STAT family that has been most associated with CRC initiation and development (142). Moreover, *STAT3* gene is considered as an oncogene because it is involved in several processes that contribute to cancer development such as proliferation, cell survival, angiogenesis, invasion and metastasis (139, 143). STAT3 is overexpressed in this disease, especially when it is associated with intestinal inflammation. Thus, in a model of experimental CAC in mice, the increased levels of IL-6 results in an overstimulation of the JAK/STAT3 pathway, thus linking inflammation and cancer (144). The involvement of the IL-6/STAT3 pathway in CAC tumorigenesis has been also shown *in vivo* in a murine model of Stat3 deletion in intestinal epithelial cells ($Stat3^{\Delta IEC}$ mice). These mice developed more severe colitis but hardly any adenomas were found when CAC was induced on them (144). Therefore, STAT3 is required for the transduction of tumor-promoting signals derived from cytokines such as IL-6. Moreover, a crosstalk between Wnt/β-catenin and STAT3 pathways has been reported, since STAT3 activation has been involved in the nuclear accumulation of β-catenin (145). This action results in the upregulation of β-catenin target genes such as *CCND1* and *MYC* resulting in tumor cell proliferation (146). Moreover, STAT3 promotes cell survival through the increment of the B cell lymphoma (Bcl) 2 and Bcl-extra large (Bcl-xL) expression levels (143, 147). Other processes involved in the malignancy of the tumor such as invasion and angiogenesis are associated with STAT3. In fact, it has been reported that STAT3 induces the expression of metalloproteinases (MMPs), such as MMP-2 (148), MMP-9 (149) and MMP-1 (150), as well as angiogenic factors like *VEGF* and the hypoxia-inducible factor-1α (HIF1α) (151, 152) (Figure 8).

2.5.2. Apoptosis evasion.

The ability of tumors to expand, with the concomitant increase in cell number, is determined not only by the proliferation rate of tumor cells, but also by the cell death rate. Apoptosis, or programmed cell death, is a well-defined regulation mechanism for the elimination of old cells. Apoptosis is a physiologic process that occurs normally during the development and aging, thus maintaining the homeostatic cell balance in the body. Moreover, apoptosis can be induced when cells are damaged by disease or noxious agents (153). In normal conditions, DNA damage caused by a mutagenic agent or an error during cell replication leads to the activation of apoptosis-associated molecular mechanisms that induce cell death.

Apoptosis process triggers a series of morphological changes that starts with cell shrinkage leading to a cytoplasm and chromatin condensation (pyknosis). Cells undergoing apoptosis decrease in size due to this condensation and acquire around shape. Then, the plasma membrane blebbing occurs, followed by a fragmentation of the nucleus (karyorrhexis) and the separation of cell fragments into apoptotic bodies (154). From a molecular point of view, apoptosis is a highly regulated process by several molecular pathways. The molecular machinery that participates in the process of cell apoptosis can be divided into three major signaling pathways: the extrinsic or death receptor pathway, the intrinsic or mitochondrial pathway, and a third less well-known that involves the endoplasmic reticulum (ER).

The extrinsic pathway is initiated by the binding of a death ligand to a death receptor. These death receptors are members of the tumor necrosis factor (TNF) receptors superfamily (155). These receptors are characterized by containing an intracellular domain, termed “death domain”, that transmits the death signal from the cell surface to the intracellular signal pathway (156). The most known examples of ligands and corresponding death receptors are TNFα and its TNFα receptor 1 (TNFR1), or Fas ligand (FasL) and Fas receptor (FasR) (156). This action leads to the activation of the death inducing signaling complex (DISC) that induces the auto-catalysis and activation of pro-caspase 8, which triggers the apoptosis cascade (157).

On the contrary, the intrinsic pathway is initiated inside the cell, particularly in the mitochondria. This pathway is initiated by non-receptor mediated stimuli, such as oxidative stress or hypoxia, that activates a series of events in the mitochondria that involve BCL2 family proteins. These stimuli result in an imbalance between pro-apoptotic (BAX, BAK and BID) and anti-apoptotic (BCL2, BCL-XL) BCL2 family members in favor of the first ones (158). The pro-apoptotic proteins oligomerize and promote a

mitochondrial outer membrane permeabilization (159). Consequently, mitochondrial inter membrane space pro-apoptotic proteins, such as cytochrome C and SMAC/DIABLO (second mitochondria-derived activator of caspase/direct IAP-binding protein with low PI), are released into the cytoplasm (158). Moreover, a second group of pro-apoptotic proteins, including apoptosis inducing factor (AIF), endonuclease G and caspase-activated DNAse (CAD), are released from the mitochondria at this stage. These proteins are directly translocated to the nucleus causing DNA fragmentation (154). Once Cytochrome C is located in the cytoplasm, it binds and activates the apoptosis protease-activating factor-1 (APAF-1) resulting in the formation of "apoptosome", a protein complex that drives the activation of pro-caspase 9 (160). At this point, the intrinsic and the extrinsic pathways converge in the cleavage and activation of the executioner caspases 3 and 7. This activation can be carried out by active caspase 8 and caspase 9. Additionally, SMAC/DIABLO proteins released from the mitochondria contribute to the pro-apoptotic effect by disrupting the interaction between the inhibitor of apoptosis proteins (IAPs) and caspase 3 or 9, a necessary step for their activation (161, 162). As a final step of these pathways, the activation of caspase 3 and caspase 7 leads to the cleavage of poly (ADP-ribose) polymerase (PARP), which is responsible for creating breaks in the DNA to cause cell death (163, 164).

The third and less-known pathway is the ER apoptosis pathway in which the Ca^{2+} ion has an important role. The flux of this cation between the cytosol, the mitochondria and the ER is regulated by different proteins such as the sarco/endoplasmic-reticulum Ca^{2+}-ATPase (SERCA) and the Ca^{2+} release channels: ryanodine receptors (RyRs) and inositol 1,4,5-trisphosphate receptors (IP3Rs) (165). When levels of this cation are increased inside these organelles, the apoptosis process is initiated (165). There are also three ER transmembrane proteins that are involved in the ER-mediated apoptosis, the inositol-requiring enzyme 1 (IRE1), activating transcription factor (ATF) 6 and protein kinase RNA-like ER kinase (PERK) (166). In the presence of a stressful stimulus, the chaperone BIP (immunoglobulin-binding protein), is dissociated from IRE1 and PERK leading to the homo-oligomerization, auto-phosphorylation and activation of these proteins that try to resolve the stressful situation through the unfolded protein response (UPR). However, if the stressful stimulus persists, PERK promotes cell apoptosis through the activation of pro-apoptotic genes such as death-receptor 5 (*DR5*) gene. This mechanism is mediated by the transcription factor C/EBP homologous protein (CHOP), being an ATF4-dependent process (167). Additionally, ER stress induces ATF6 translocation to the Golgi compartment where it is cleaved and activated (168). Then, the cleaved N-terminal ATF6 cytoplasmic domain is translocated to the nucleus where it

interacts with ATF/cAMP response elements (CRE) and ER stress-response elements. This action results in the upregulation of several genes included CHOP, which is involved in the transmission of the apoptotic signal (169-171). Moreover, Nakagawa et al., reported that the ER stress induced the activation of caspase 12, which is involved in the apoptotic response mediated by ER through the activation of the executioner caspase 3 (172, 173).

Therefore, there is a network of interconnected molecular pathways (Figure 9) that, in the presence of an extracellular or intracellular noxious stimulus, are responsible for transmitting cell death signals to the nucleus, where DNA breakage and the subsequent cell death is induced. However, cancer cells undergo molecular changes that allow them to escape from apoptosis signals (174). The first evidence of apoptosis evasion by cancer cells was reported at the end of the last century with the discovery of *BCL2*, an oncogene with antiapoptotic activity (175, 176). According to these studies, the oncogene *BCL2 was* able to promote B cell lymphomas by increasing the tumor cells survival (177). Resistance to apoptosis is a characteristic feature of cancer cells that, together with the uncontrolled proliferation capacity, lead to a limitless replicative potential of tumor cells (99).

This phenomenon of resistance to apoptosis can be acquired by cancer cells through several mechanisms, which include transcriptional, translational and post-translational modifications (174). The most common strategy carried out by cancer cells to evade apoptosis is the mutation of the tumor protein 53 (*TP53*) gene. Mutations in this tumor suppressor gene are present in 50-60% of human cancer and result in a protein with a reduced capacity to bind to a specific DNA sequence that regulates the p53 transcriptional pathway (178). The result of these mutations is the removal of p53 protein, a key component of DNA damage sensor that can induce apoptosis through the upregulation of BAX and BH3-only proteins such as PUMA (p53 upregulated modulator of apoptosis) and NOXA (also called PMAIP1 [Phorbol-12-myristate-13-acetate-induced protein 1]) (179-181). Besides, the altered PI3K/AKT and JAK/STAT3 pathways in cancer also contribute to increased cell survival and apoptosis evasion in the cancer cell through an upregulation of *BCL2* or a downregulation of the pro-apoptotic proteins PUMA and BIM (143, 182).

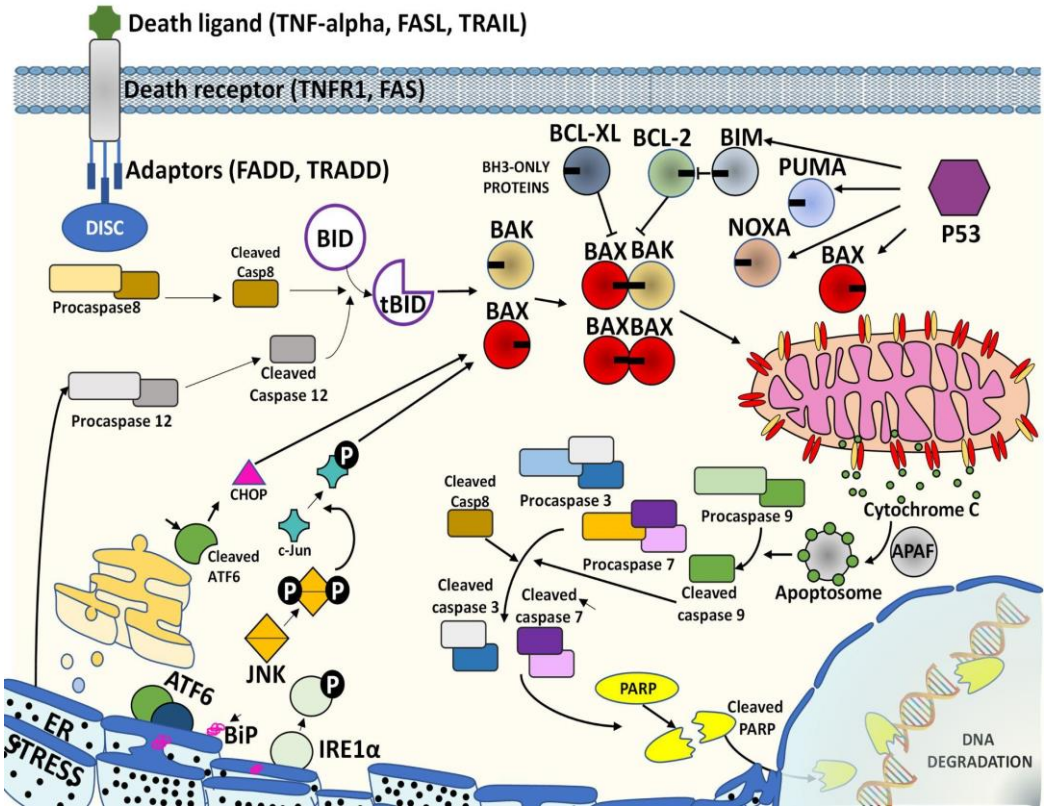

Figure 9. Network of interconnected apoptosis pathways: extrinsic, intrinsic and ER-mediated apoptosis pathways.

2.5.3. Immune response modulation

In addition to uncontrolled cell growth and apoptosis evasion, another characteristic of the colon cancer cells is its ability of escaping the host immune system (183, 184). Initially, the presence of tumor cells activates the immune system involving both the innate and adaptive immune response. These tumor cells have molecular mechanisms that allow them to evade the inflammatory immune response that tries to kill them (184). Therefore, cancer induces a tolerant response characterized by the presence of M2 macrophages and regulatory T (Treg) cells, both of them with an antiinflammatory phenotype that favors the tumor development (185).

The first line of immune defense against tumor cells is the innate immune response, mainly constituted by macrophages, neutrophils, mast cells and natural killer cells (186). The release of chemokines by local cells, as well as other factors released by tumor cells, favor the recruitment of monocytes to the tumor microenvironment. Once there, monocytes are differentiated into macrophages, which phenotypically can be

distinguished as type 1 (M1) or type 2 (M2). These macrophages in the tumor microenvironment are known as tumor-associated macrophages (TAMs) (187). The classically activated macrophages (M1) exert a pro-inflammatory response characterized by the release of nitric oxide (NO), reactive oxygen species (ROS) and pro-inflammatory cytokines such as TNFα (186, 187). On the contrary, alternatively activated macrophages (M2) present an anti-inflammatory phenotype, thus secreting immunosuppressive mediators such as IL-10 and transforming growth factor-β (TGF-β), as well as proteases, like MMP-2 and MMP-9, which promote cancer proliferation, invasion and metastasis (188). Therefore, it has been reported that the M1/M2 ratio could be considered as an indicator of the cancer prognosis (189).

Cancer cells also activate the adaptive response, that is, the second line of immune defense against cancer. Some studies have attributed the tumor infiltration of $CD8^+$ and $CD4^+$ effector T cells to a beneficial prognosis of CRC (190, 191). Moreover, it seems that the presence of Treg cells contribute to tumor immune escape and cancer progression (192, 193). Based on T cell infiltration, Chen and Mellman classified the tumors as “immune-inflamed tumors”, “immune-excluded tumors” and “immune-desert tumors” (194). The first phenotype is characterized by the presence of $CD4^+$ and $CD8^+$ T cell infiltration and it is correlated with a better prognosis. Conversely, the immune-excluded and the immune-desert phenotypes present a lower infiltration of T cells, as well as a worse prognosis (194). In fact, $CD8^+$ cytotoxic T lymphocytes (CTLs) are able to exert a cytotoxic response against tumor cells through the release of the serine proteases granzyme A and granzyme B. This granzyme B cleaves and activates caspase 3 thus inducing the tumor cell apoptosis (195). Moreover, CTLs can induce tumor cell apoptosis via activation of the extrinsic pathway through the FasL/FasR interaction (196). Many strategies can be induced by the tumor to reduce the immunogenicity and the infiltration of immune cells in the tumor microenvironment (184). The secretion of immune-supresive cytokines and mediators by tumor cells, such as TGF-β, prostaglandin E2 (PGE2) or IL-10, promotes the differentiation of monocytes or the subversion of macrophages to a tumor-promoting M2 phenotype, which in turn favors tumor progression and metastasis through the suppression of antitumor response, matrix remodeling and angiogenesis (184).

2.5.4. Angiogenesis.

Nutrients and oxygen supply is crucial for tumor development. To provide these energy demands, new blood vessels are formed through a process called angiogenesis (197). This process is essential for tumor growth and progression because in absence of

vascular support, tumors may become apoptotic or necrotic (198, 199). The growth of new vessels is a carefully regulated process by activating and inhibitory molecules. Among the activators of angiogenesis, vascular endothelial growth factor (VEGF) and angiopoietin (ANGPT) play an important role. In cancer, an imbalance between the stimulatory and inhibitory signals leads to angiogenesis (200). In the early stages of tumor generation, a VEGF subtype, VEGFA, and fibroblast growth factor (FGF) are released in high concentrations to the tumor microenvironment. VEGFA is considered as the initiator of the angiogenesis process and this factor is highly expressed in most types of cancer (201, 202). Some tumor events occurred during the tumor development such as acidification, hypoxia or hypoglycemia, as well as high levels of the oncoprotein MYC contribute to an increase in VEGFA expression (203, 204). In addition to VEGFA, other factors such as ANGPT, FGF and TGF-β contribute to the angiogenesis process (205-207).

Despite being a controlled process, tumor vessels originated during angiogenesis are structurally and functionally abnormal. It leads to a blood flow chaotic and variable that results in hypoxia and acidification in some regions of the tumor. Moreover, these new vessels are characterized by their high permeability that allows a greater flow of nutrients and cells towards the tumor (208). The increase of vascular permeability is also considered a crucial step for tumor cell invasion and metastasis because of the generation of a wide vascular area that allows the intravasation of tumor cells. Moreover, VEGFA also contributes to invasion and metastasis through the upregulation of MMPs and some genes such as *SOX2* and *SNAI2* that are involved in the epithelial-mesenchymal transition (EMT) process (209, 210). Therefore, VEGF is considered an important molecule in the tumor development and this resulted in the search for therapies that target this molecule. In fact, as it will be discussed in more detail later in the present Thesis, Bevacizumab is an approved monoclonal antibody against VEGF that is currently approved for the treatment of metastatic cancer (211).

2.5.5. Tissue invasion and metastasis.

During the development of most types of human cancer, tumor cells acquire the ability to expand and colonize adjacent tissues in a process called invasion (99). Moreover, these cancer cells can detach from the primary tumor, reach blood and lymphatic vessels and travel through them to other organs where they form a secondary tumor. This process is called metastasis and it leads to a worse prognosis of the disease, being responsible for around 90% of cancer deaths (212, 213). Regarding CRC data, metastasis is the major cause of death in the majority of patients being the liver and peritoneum the most

common sites of distant metastasis (214-216). Invasion and metastasis are complex processes that are closely allied to each other. In fact, the process of metastasis is preceded by an invasion process giving rise to a sequence of stages that are included in the CRC invasion-metastasis cascade (217, 218). This process consists of five steps (218): (1) local invasion of tumor cells into the surrounding tumor-associated stroma and thereafter into the adjacent normal tissue parenchyma; (2) intravasation of tumor cells into lymphatic or blood vessels; (3) dissemination of the circulating tumor cells through the circulatory system; (4) extravasation of the tumor cells into parenchyma of distant tissues; and (5) metastatic colonization of a distant tissue and formation of macroscopic secondary tumors.

Submucosal invasion is an important feature of advanced colorectal carcinomas that is considered the beginning of this cascade and implies a worse prognosis, as well as a risk factor for metastasis (219, 220). In tumor invasion, the EMT is a key process in which the epithelial cells lose their cell adherens and tight junctions and acquire mesenchymal properties. This process implies an enhanced mobility and increased production of extracellular matrix components thus conferring invasiveness capacity to tumor cells (221). E-cadherin or cadherin-1 (CDH1) is considered to play an important role in the EMT; in fact, a downregulation of E-cadherin is associated with lymph node metastasis, reduced tumor differentiation and a poor prognosis in CRC patients (222, 223). E-cadherin is a transmembrane protein involved in homotypic cell-cell adhesion, thus being considered a marker of epithelial cells. EMT process is associated with a downregulation of *CDH1,* which is associated with cancer progression, tumor dedifferentiation and metastasis in CRC patients (224, 225). Conversely, vimentin (VIM) has been also associated with the EMT, being considered a marker of mesenchymal cells (226). In fact, *VIM* expression is significantly associated with CRC metastasis and poor prognosis (227).

The EMT is a complex process, which is highly regulated by different transcription factors and signaling pathways (Figure 10). This process is induced by three core groups of transcription factors that suppress the *CDH1* transcription. The first group is constituted by the Snail Family Transcriptional Repressor 1 (SNAI1) and 2 (SNAI2, also called SLUG) (228). The second group of transcription factors that induce the EMT is the zinc-finger E-box-binding homeobox family proteins 1 (ZEB1) and 2 (ZEB2) (229). The last group of EMT inductors is formed by the twist family helix-loop-helix transcription factors 1 (TWIST1) and 2 (TWIST2) (230). A significant correlation has been observed between an upregulation of these transcription factors with a downregulation of *CDH1,* as well as higher expression of *VIM,* thus favoring a mesenchymal phenotype of tumor cells (221).

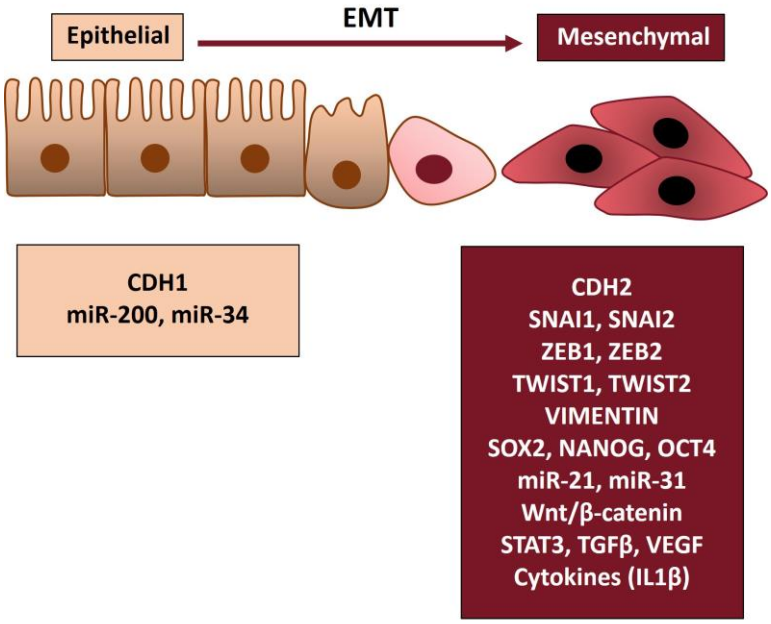

Figure 10. Simplified overview of the epithelial mesenchymal transition and transcription factors and signaling networks that regulate it in CRC. *Adapted from (221, 231)*

Other transcription factors have evolved recently as inductors of the EMT process and some of them are the SRY-box transcription factor 2 (SOX2) (232), POU Class 5 Homeobox 1 (POU5F1, also called OCT4) (233) and Nanog homeobox (NANOG) (232). Moreover, there are some signaling pathways such as Wnt/β-catenin, JAK/STAT3 and PI3K/AKT and TGF-β pathways that induce EMT due to an upregulation of EMT-related transcription factors like *SNAI1, SNAI2* and *ZEB1* (234-236). Additionally, the EMT process is also regulated by small non-coding RNAs or micro-RNAs (miRNAs). Some examples of miRNAs that are involved in the promotion of EMT are miR-21 or miR-31 (237), whereas others such as miR-200 family (238) or miR-34 (239) inhibit this transition process.

Lastly, components of the tumor microenvironment also contribute to the regulation of the EMT process. In this sense, fibroblasts present in the tumor microenvironment can promote the EMT process and the invasiveness of tumor cells through the release of growth factors such as TGF-β, cytokines and MMPs (240). Additionally, as discussed above, endothelial cells formed in the angiogenesis process also promote the EMT through the release of mediators such as VEGF (209). Cytokines released into the tumor environment by immune cells and other stromal cells contribute to the EMT process.

Among these cytokines, IL-1β, IL-6 and IL-8 are reported to promote EMT and, subsequently tumor invasion (241-243).

Epithelial tumor cells that undergo an EMT acquire the appropriate features to develop the invasion process. Then, a single cell or a small cluster of these cells can be detached from the primary tumor in a process called tumor budding (244). It has been reported that tumor cells that are involved in tumor budding have undergone an EMT and they are $ZEB1^+$ $SNAI1^+$ cells with a mesenchymal morphology that contain higher levels of nuclear β-catenin together with a loss of *CDH1* expression (221). CSCs markers such as CD44 and CD133 are also expressed in these cells that spearhead the invasion process (245). Additionally, proteins involved in the extracellular matrix degradation such as MMP9, cathepsin B and matrilysin are overexpressed in tumor buds (246, 247). Acquisition of these properties results in the rupture of the basement membrane, which is a component of the extracellular matrix, and the subsequent invasion of the stroma compartment by these cancer cells (218). Then, tumor cells interact with stroma cells such as fibroblasts, endothelial cells, mesenchymal stem cells and immune cells (248). As previously mentioned, stroma cells are capable of further enhancing the aggressiveness of carcinoma cells by inducing the EMT.

The stroma invasion by tumor cells provides abundant opportunities for intravasation of these cells into systemic circulation (218). Once there, tumor cells can spread and reach distant organs. Despite being able to colonize any organ, cancer cells tend to metastasize with a high frequency in certain organs and this process is known as metastatic tropism (249). Colon cancer cells reach the microvasculature of distant organs, usually liver or lung and are extravasated into the parenchyma of this new organ. Next, the cell or cells causing the metastasis have to adapt to the new environment. Some authors have proposed the establishment of a “pre-metastatic niche” to address this problem (250). According to these studies, primary tumors release systemic signals that will reach the organ where the future metastasis will occur and prepare it for the arrival of metastatic tumor cells. Some cell types such as fibroblast of the metastatic niche are involved in this process, as well as proteins like fibronectin or MMP9 (218). Then, and once the carcinoma cells have reached the metastatic niche, they may remain in a quiescent state or may start to proliferate giving rise to microcolonies that are known as micrometastases. The ability of disseminated tumor cells to escape dormancy and originate a secondary tumor depends on their autonomy and the characteristics of the new environment (218).

2.6. Cancer stem cells and their implications for CRC.

A stem cell is a self-renewing cell that displays totipotency. The base of the colonic crypt is the niche to several multipotent stem cells. These colonic stem cells have the ability to divide and differentiate, thus producing the different cells that form the colonic crypt (251). Stem cells can divide either asymmetrically, to produce one daughter cell and one stem cell, or symmetrically to originate two daughter cells or two stem cells (98). The proliferation and differentiation of stem cells are highly regulated processes that are controlled by signaling factors from cells that are part of the niche (98).

As previously mentioned, among the proposed models to explain the development of cancer, the hierarchical model has been widely accepted (252, 253). According to this model, the cancer process is initiated in a normal stem cell located in the stem cell niche that undergoes genetic and epigenetic alterations giving rise to a CSC with uncontrolled proliferation. The Wnt/β-catenin signaling in these stem cells has an important role in controlling their proliferation and maintaining the stemness state. In fact, alteration of this signaling pathway induced by *APC* mutations is the most frequent event that initiates the transformation of a normal stem cell to a CSC (253). It has been reported that these CSCs, which overexpress markers that are part of the Wnt signaling pathway such as β-catenin and the Leucine-rich repeat-containing G-protein coupled receptor 5 (LGR5), are involved in the origin or early adenomas through the transmission of the mutations in their subsequent divisions (253).

Colon CSCs have been widely characterized and there are several markers that allow its identification. Among them, the aforementioned LGR5, a marker of intestinal stem cells with tumor-initiating capacity in immunodeficient mice, as well as long-term self renewal potential (254). LGR5 (also known as GPR49) is a transmembrane receptor for R-spondin, which potentiates the Wnt/β-catenin signaling pathway (255). *LGR5* is also a β-catenin target gene, which is overexpressed in CRC tumors and distant metastasis (256, 257). Furthermore, $LGR5^+$ cells have shown tumor-initiating capacity (253, 258, 259). LGR5 is expressed in stem cells located at the crypt base whereas its expression is lost as the cells migrate upwards (260). Moreover, LGR5 is involved in self-renewal and differentiation of CSCs whereas $LGR5^-$ cells exhibited higher rates of proliferation, as well as competency to replenish tumor growth through the regeneration of LGR5 expressing cells (261). LGR5 also contributes to EMT through the upregulation of Notch signaling in CRC cells (262).

CD133 or prominin-1 is one of the most common markers used for the identification and isolation of CSCs (263) in numerous solid tumors including colon cancer (264). CD133

is a transmembrane glycoprotein that was initially discovered as a hematopoietic stem cell marker in 1997 (265). The involvement of $CD133^+$ cells in the initiation of colon cancer was reported ten years later, when human colon cancer cells were xenotransplanted in NOD/SCID mice and discovered that human colon cancer-initiating cells were a small population of $CD133^+$ cells, whereas those $CD133^-$ cells were unable to initiate tumor growth (264, 266). Furthermore, it has been reported that CRC cells isolated from colon tumors were able to form CD133-enriched tumor spheroids (267). These $CD133^+$ presented stem capacities, thus being able to self-renew and differentiate into adherent epithelial tumor cells (267). Moreover, CD133 stimulates several pathways that confer a malignant phenotype to those cells that overexpress this marker. In fact, CD133 stimulates the Wnt/β-catenin (268) and PI3K/AKT (269) signaling pathways in CSCs, and leading to proliferation and apoptosis inhibition. CD133 is also involved in angiogenesis and metastasis of these CSCs through the activation of VEGF (270) and the upregulation of EMT markers, such as SNAI2 and N-cadherin, that promote stem properties in the cell (271).

CD44, also known as homing cell adhesion molecule (HCAM), is a cell-surface glycoprotein involved in cell-cell interactions, adhesion and migration. This protein is considered another CSC marker commonly associated with CD133, being involved in CRC metastasis (272). Moreover, it has been reported that $CD44^+$ cells are able to form spheroids with tumorigenic and metastasis ability when injected in immunodeficient mice (273). CD44 upregulates *MYC* and *TWIST1,* thus promoting cell proliferation and EMT (273). Furthermore, CD44 has an important role in cell migration, a crucial process for tumor invasion and metastasis. This action is exerted by forming a complex with the Src-like tyrosine kinase, Lyn, that induces AKT phosphorylation and activation (274).

Increased activity of the aldehyde dehydrogenase 1 (ALDH1) enzyme has been observed in colonic CSCs. In fact, ALDH1 is another marker of these CSCs that is involved in cell proliferation, differentiation, chemotherapy and radiotherapy resistance, as well as in EMT (275). A high activity of ALDH1 has been associated with stimulation of Wnt/β-catenin (276), PI3K/AKT (277) pathways and upregulation of EMT transcription factors such as *ZEB1* and *SNAI2* (278).

In addition to being responsible for the initiation of the tumor process, CSCs also play an important role in drug resistance and cancer recurrence (279). Accumulating evidence suggests that CSCs are responsible for the chemoresistance due to its ability to self-renew and to differentiate into heterogeneous tumor cells (279). Moreover, CSCs may remain in a quiescent state in which they do not divide, thus resisting the effect of most antitumor drugs that act in those tumor cells with an active cell cycle (280). This

quiescence capacity of CSCs is also responsible for cancer relapse. Moreover, CSCs can overexpress multidrug resistance or detoxification proteins such as the enzyme ALDH and ATP binding cassette transporters (ABCG1 and ABCB1) that eliminate dangerous substances for the cell, including drugs (281). Other mechanisms by which CSCs contribute chemoresistance include resistance to DNA damage due to their capacity of promoting DNA repair and enhancing ROS scavenging (279, 282). Lastly, autophagy is also a mechanism that allows CSC to adapt to stressful conditions. During this process, the cell is able to destroy itself to produce the nutrients needed by other cells (283). Due to the involvement of CSCs in drug resistance and cancer relapse, current research is pursuing the search for new therapies that target CSCs.

2.7. Clinical features and diagnosis of CRC.

CRC patients can present with a wide range of signs and symptoms that increase with the disease progression: rectal bleeding, which may frequently remain occult in feces until late stages, abdominal pain and distension, intestinal blockage, asthenia due to anemia, as well as changes in bowel habits (284). Additionally, and depending on the tumor location, the signs, symptoms and even the molecular characteristics and histology are different (285). Thus, tumors in the right-side colon and in the transverse colon are more frequent in women, and they are usually sessile serrated adenomas or mucinous adenocarcinomas. In these right-side tumors the luminal contents are predominantly liquid and the lesions usually bleed. On the other hand, tumors in the left-side are more frequent in men and they usually are tubular, villous adenocarcinomas. Patients with these tumors usually have constipation or diarrhea, and feces with blood and mucus (79, 285).

However, and unfortunately, the disease is usually silent in its early stages, and the symptomatology appears in the advanced phases. For this reason, screening techniques for the early diagnosis of the disease are necessary. Screening methods are one of the most powerful tools to reduce the mortality in these patients (286), since the early diagnosis of small local tumors would prevent the development of advanced cancer (287). Despite its low sensitivity and lack of analytical specificity, the fecal occult blood test for men and women aged 50-74 years is a suitable technique for CRC screening according to the European guidelines for CRC screening (288). A positive result in this test must be followed by an endoscopy, which is one of the most common methods of screening. Other tests, such as fecal immunochemical faecal occult blood test or multitarget stool DNA test, colonoscopy, computed tomographic colonography and flexible sigmoidoscopy are also recommended (289). Moreover, all screening guidelines

mention the necessity of checking carcinoembryonic antigen concentrations in blood, because elevated levels of this marker are associated with a worse prognosis (290).

2.8. Management.

The Tumor/Nodes/Metastasis (TNM) classification of a tumor is a useful tool for its prognostic evaluation and treatment choice. This classification is based on the parameters detailed below (291).

- **T - Tumor:** this parameter takes into account the size of the primary tumor and its invasion into adjacent tumors.
    - T0: no evidence of tumor is present.
    - T1: invasion into the submucosa.
    - T2: invasion of the muscularis propria.
    - T3: invasion into the subserosa.
    - T4: tumor extension through all the layers.
    - Tis: carcinoma in situ
    - Tx: inability to assess the tumor size and invasiveness.
- **N - Nodes**: this parameter is used to determine the involvement of lymph nodes in the tumor process.
    - N0: no regional nodal spread
    - N1: involvement of 1-3 regional nodes.
    - N2: 4-6 regional nodes affected.
    - N3: 7 or more nodes involved.
- **M - Metastasis:** this parameter reports the presence of distant metastasis.
    - M0: no distant metastasis.
    - M1: evidence of distant metastasis.
        - M1b: the tumor is spread to 2+ areas.
        - M1c: the tumor is spread to the peritoneal surface.

According to these parameters the TNM classification is listed on Table 2.

When cancer is diagnosed in an early stage and it is considered a T1 tumor in the TNM classification, an endoscopic resection is usually enough for tumor extirpation. However, the extent of the lesion must be evaluated to see which resection technique must be applied and if any other therapeutic intervention is necessary. The evaluation of the lesion by a pathologist is essential to know the depth of this, i.e., if there is submucosal invasion, differentiation or lymphatic invasion. Depending on the size of the lesion, the resection technique will be different: en-bloc endoscopic mucosal resection, endoscopic submucosal dissection or endoscopic full-thickness resection (292-294).

TNM Stage	Primary Tumor (T)	Lymph Node involvement (N)	Distant metastasis (M)
0	T1s	N0	M0
I	T1 T2	N0 N0	M0 M0
II	T3 T4	N0 N0	M0 M0
IIIA	T1,2	N1	M0
IIIB	T3,4	N1	M0
IIIC	Any T	N2	M0
IV	Any T	Any N	M1

Table 2. CRC staging classification according to the TNM classification.

Surgery is the most effective treatment in CRC and it consists in the removal of the tumor mass, part of the healthy tissue surrounding it and the regional lymph nodes. The extent of resection will vary depending on the tumor size and invasiveness. The main procedures carried out in this surgery are: right hemicolectomy, transverse resection, left hemicolectomy, segmental colonic resection and total colectomy (295).

Radiotherapy is another strategy for CRC management. It consists in the administration of high doses of radiation inducing the formation of free radicals that cause damage in the DNA of tumor cells. It is not common to use radiation to treat CRC because of the adverse effect on adjacent tissues, however it may be used in certain cases. Radiotherapy can be used before surgery to make the tumor easier to remove. Radiation may also be applied during or after surgery to kill tumor cells that have not been removed during the surgical process (296). Radiation therapy can also be combined with chemotherapy resulting in chemoradiotherapy, which is one of the most used therapy in the management of CRC (79).

As mentioned before, TNM classification is essential for the tumor treatment approach. In advanced stages (III and IV or T4 in stage II), the use of chemotherapy is necessary for the CRC management (287). This chemotherapy is usually administered intravenously, although there are also drugs that can be taken orally. Chemotherapy may be used at different times during the disease. In the adjuvant chemotherapy, drugs are administered after surgery in order to kill tumor cells that have not been removed by the

surgical process. On the other hand, neoadjuvant chemotherapy is commonly given in rectal cancer in combination with radiotherapy before surgery to reduce the tumor volume and make the surgical process easier (https://www.cancer.org/cancer/colon-rectal-cancer/treating/chemotherapy.html).

Depending on the specificity of the drug for its target of action, chemotherapy can be divided into two types: cytotoxic chemotherapy or targeted chemotherapy. In the last one, unlike cytotoxic chemotherapy, drugs act on a specific molecule differentially overexpressed in the tumor that drives tumor growth. Therefore, target chemotherapy presents lower levels of adverse reactions and a better tolerance by patients. However, the primary and acquired drug resistance represent one of the major obstacles of cancer therapy and, for this reason, the combination of cytotoxic and targeted therapies represents an improved approach for cancer management (297).

One of the most common chemotherapy drugs used in the treatment of CRC is 5-Fluorouracil (5-FU), which is a pyrimidine analogue that acts inhibiting the thymidylate synthase enzyme. Specifically, 5-FU is a derivative of uracil in which a hydrogen is replaced by a fluorine in 5-position. Once the 5-FU enters the cell, it is metabolized by dihydropyrimidine dehydrogenase and converted into 5-fluorouracil deoxynucleotide. This metabolite inhibits the thymidylate synthase and prevents the methylation of the normal substrate of this enzyme, the deoxyuridine acid to deoxythymidylic acid. Blockade of DNA synthesis occurs due to this molecular mechanism. Moreover, 5-FU can be converted into the fluorouridine triphosphate in vivo, which is incorporated into RNA interfering with the protein synthesis (298). These molecular mechanisms resulted in the inhibition of tumor cell replication, the induction of its apoptosis and the blockade of tumor growth (299). 5-FU is a first-line drug in the chemotherapy against CRC (299). However, the emergence of early resistances to 5-FU implies the concomitant use of other drugs, as well as alternative therapies. In this scenario, capecitabine is an alternative to oral fluoropyrimidine that has shown similar efficacy to 5-FU with even lower adverse reactions (300). In fact, capecitabine is a pro-drug of 5-FU that is used to avoid complications derived from intravenous administration.

The combination of 5-FU with other drugs such as cis-platin and derivatives (oxaliplatin) or irinotecan (a topoisomerase I inhibitor) results in an improvement of survival rates (301-303), as well as in a reduction of drugs resistance and toxicity (299). 5-FU is usually administered in combination with levofolinic acid (leucovorin), which reduces the frequency and severity of adverse effects of 5-FU and optimizes the efficacy of the antimetabolite by increasing its capacity to inhibit the enzyme thymidylate synthase (304,

305). Of note, the simultaneous use of these different drugs has led to the current availability of various combination regimens including FLOX and FOLFOX (5-FU, leucovorin and oxaliplatin), FOLFIRI (irinotecan, 5-FU and leucovorin) and XELOX (capecitabine and oxaliplatin) (287). In fact, the efficacy of these cytotoxic drugs regimens against CRC has been improved with their combination; however, and unfortunately, their side effects are still relevant, becoming disabling and causing therapy suspension in many cases (306, 307). In this scenario, research has given rise to targeted therapies that increase the effectiveness of the cytotoxic drugs, thus reducing their adverse reactions and even reaching significant advances in the management of metastatic CRC in the last decade (287). Among these therapies, monoclonal antibodies against the VEGF and EGFR stand out. Bevacizumab is an humanized monoclonal antibody against VEGF that targets angiogenesis, was the first biologic agent approved for the treatment of metastatic CRC (308). Cetuximab is a monoclonal antibody against EGFR that has been shown to be effective in CRC treatment improving the survival rates and preserving the quality-of-life of patients (116). This drug can be used alone but is frequently used as an adjuvant of other cytotoxic drugs (287).

3. COLITIS-ASSOCIATED COLORECTAL CANCER.

IBD is an important risk factor for the development of CRC. Epidemiologic data estimate that the risk of CRC development in patients with ulcerative colitis or Crhon’s disease is approximately 2- to 3-fold that of the general population (309). It is well known that the chronic inflammation associated with IBD can promote carcinogenesis and the risk of CRC development in IBD patients depends on the persistence and size of the inflammatory process (310). In fact, CAC is a CRC subtype linked to IBD that represents around 2% of all diagnosed CRC cases and usually has poor prognosis and high mortality rates (311). The first evidence of CRC as a complication of IBD was recognised by Crohn and Rosenberg in 1925 (312). Over time the CRC risk associated with IBD has increased and the use of meta-analysis techniques have evidenced that CRC incidence is higher in ulcerative colitis (18%) than Crohn's disease (8.3%) patients, being the risk higher as time passes (71, 313, 314).

The concept of inflammation as a driver of tumorigenesis was first realized in 1863 when Rudolf Virchow hypothesized that the origin of cancer was at sites of chronic inflammation with leukocyte infiltration (310). Nowadays, the causal relationship between inflammation and cancer is widely accepted. Moreover, it is well known that immune cells present in

tumor microenvironment contribute to tumor progression through the secretion of cytokines and other factors (310). In CAC, the inflammatory chronic state promotes carcinogenesis through three main processes: (1) the persistent release of pro-inflammatory mediators and activation of pro-inflammatory pathways; (2) tissue remodeling during remission periods and (3) bacterial components translocation from the gut lumen (315-318).

Inflammatory mediators in the tumor microenvironment, such as TNF-α, can contribute to carcinogenesis by inducing the production of ROS and reactive nitrogen intermediates derived from nitric oxide (NO), able to produce DNA alterations and damage. These mediators may contribute to tumor initiation through the induction of mutations in some oncogenes and tumor suppressor genes such as *TP53* (319). In fact, it has been reported that early mutations in this gene occur in more than 50 % of CAC patients (320, 321). Furthermore, these inflammatory mediators can activate signaling pathways involved in cell proliferation and survival. Indeed, nuclear factor-kappaB (NF-κB) pathway plays a pivotal role in the link between inflammation and carcinogenesis. This pathway can be stimulated by pro-inflammatory cytokines and microbial products, since both components are present in the colon environment of CAC patients (315). Activation of NF-κB results in the translocation of this transcription factor to the nucleus where upregulates the expression of cytokines such as *TNFA* and *IL6.* These cytokines can directly act on the tumor cells and stimulate signaling pathways involved in cell proliferation and survival (315). In fact, soluble IL-6 can bind to its membrane bound IL-6 receptor (IL-6R) and activates the JAK/STAT3 pathway, which is overexpressed in CRC tumor cells (144, 322). Moreover, NF-κB can directly induce the transcription of anti-apoptotic genes such as *BCL2* and *BCL2L1* (323), as well as several genes that encode MMPs, thus promoting tumor invasion (324).

The cyclooxigease-2 (COX-2)/PGE_2 pathway plays a central role in the development of the inflammatory process in IBD patients (325, 326). Overexpressed cytokines found in IBD, mainly TNF-α, in combination with microbial products, like LPS, can upregulate COX-2 expression through the NF-κB pathway (327). It is also known that COX-2 contributes to carcinogenesis through the production of PGE_2, which is a mediator that promotes proliferation, and stimulates angiogenesis and invasion processes. In fact, the importance of COX-2 signaling in CAC development has been confirmed by previous studies that report a lower risk of cancer development in those patients that daily consume non-steroidal anti-inflammatory drugs (NSAIDs) (328). The ability of PGE_2 to increase tumor growth has been supported by studies that report an increase in tumor burden in $Apc^{Min/+}$ mice treated with PGE_2 (329). PGE_2 contributes to CRC development

through different mechanisms that involved an increased tumor cell proliferation by activating Wnt/β-catenin and RAS/ERK pathways in colon cancer cells (330, 331). Moreover, PGE_2 is able to increase cancer cells survival through an upregulation of *BCL2* gene (332). Additionally, PGE_2 promotes cell migration and invasion through the activation of EGFR/PI3K/AKT signaling pathway (333), as well as the induction of MMP2 activity (334). In addition to the direct effects of PGE_2 on tumor cells, this eicosanoid can directly act on immune cells in the tumor microenvironment, thus modulating their immune response towards a response that results in escape of tumor cells from effective immunosurveillance (335).

Immune cells also play an important role in the pathogenesis of CAC. As previously discussed, TAM are one of the most abundant and important cells in the tumor microenvironment. During acute phases of UC, macrophages acquire an inflammatory phenotype (M1 macrophages) and secrete inflammatory cytokines that cause cell damage, thus contributing to cancer initiation. Besides, M2 macrophages are also found in IBD and CAC patients, being these alternatively-activated macrophages involved in colon tumorigenesis in CAC (336). Growth factors (EGF, FGF and VEGF), cytokines (IL-6), PGE_2 and MMPs are mediators secreted by M2 macrophages that promote tumor cell proliferation, invasion and angiogenesis (336). Adaptive immune response has also been implicated in CAC development. Initially, $CD4^+$ and $CD8^+$ T cells promote chronic inflammation in IBD, thus creating a tumor-friendly environment that can lead to cancer initiation (337). Conversely, Treg cells act as suppressors of chronic inflammation and prevent the initiation of the tumor process (337). Once the tumor process is initiated, the role of this adaptive immune response changes being T-helper (Th) 1 cells and $CD8^+$ cytotoxic T cells the main cells involved in the antitumor response (191, 338). On the other hand, it has been consistently shown that Th17 lymphocytes promote inflammation and tumorigenesis in CAC through the release of cytokines such as IL-17a, IL-17F, IL-21 and IL-22 (339, 340). IL-23 is an essential cytokine for the differentiation of Th17 cell and immune responses involving these lymphocytes are closely associated with higher levels of IL-23 (341). The first evidence of the involvement of IL-23 in tumor-promoting pro-inflammatory process was recognized by Langowski et al. (2006). To examine the role of this cytokine in tumorigenesis, Langowski et al. used mice deficient in IL-23 and observed a resistance to tumor induction. Additionally, these mice showed a reduction in MMP9 and IL-17 levels, as well as a high infiltration of $CD8^+$ T cells, events that contribute to an amelioration of the disease (342). Besides, the contribution of IL-23 to tumor development was confirmed by Grivennikov et al. (2012) who associated IL-23 signaling with a high infiltration of myeloid and Th17 cells in CRC that contribute to tumorigenesis.

Moreover, they discovered that IL-23 is mainly produced by tumor-associated myeloid cells that are activated by microbial products, which are in the tumor microenvironment (343). IL-23 overexpression has been associated with a worse prognosis of CRC due to its ability to increase the proliferation of tumor cells, modulate the immune response by reducing the levels of tumoricidal $CD4^+$ and $CD8^+$ cells and increasing the metastatic capacity of the tumor by promoting the production of MMP9 and VEGF (344).

4. COLORECTAL CANCER AND OBESITY.

Epidemiological data suggest that obesity is linked to an increased risk of CRC, mainly in men (345-347); and even high early life body mass index (BMI) increase further CRC risk (348). Since the prevalence of overweight and obesity has risen noticeably worldwide over the last years (7-fold increase for adults in 40 years) (349) the increased risk to develop CRC could be correlated with this situation.

4.1. Molecular links between CRC and obesity.

It is important to note that both obesity and cancer share altered cellular pathways (Figure 11). Thus, obesity has been linked to chronic low grade systemic inflammation that contributes to metabolic dysfunctions, including an altered production of steroid hormones, which in turn can promote cancer development and progression (350, 351). Moreover, the obesity-associated imbalance between the caloric intake and caloric expenditure leads to hyperadiposity, characterized by hyperplasia and hypertrophy of adipocytes, thus resulting in changes in the adipose tissue function relative to the production of steroid hormones and adipokines, as well as the release of proinflammatory mediators. All these alterations have been implicated in carcinogenesis, tumor progression and metastasis (352), as previously commented.

Another common feature in these two conditions is the existence of an altered intestinal microbiome or dysbiosis. It has been described in both diseases a decrease in commensal bacterial species and an enrichment of detrimental bacterial populations. This imbalance in the gut microbiota could hamper their key digestion/metabolic functions and alter the production of different metabolites, including short-chain fatty acids (SCFA), polyphenols, vitamins, tryptophan catabolites and polyamines (353).

4.1.1. Obesity-induced mutagenic DNA lesions in cancer development.

The onset of cancer in obese patients may be associated with a hypermethylation of CpG islands that may account for epigenetic instability. This alteration can promote the

activation of oncogenes, such as *KRAS* and BRAF (354). Additionally, it has been reported an increase in single nucleotide variants, insertions and deletions in obese patients in comparison with non-obese patients with microsatellite stable CRC (355).

In obese patients, lipid peroxidation is abnormally increased, being this associated with the generation of different reactive species, like 4-hydroxy-2-nonenal (4-HNE) and malondialdehyde (MDA) (356). Similarly, CRC patients have shown a significant increase in the levels of these lipid peroxidation products (357). 4-HNE and MDA are well-known mutagenic agents due to its high reactivity with free amino groups of both proteins and nucleic acids (358, 359). Furthermore, 4-HNE and MDA can interfere with different cellular pathways involved in cancer development. 4-HNE is involved in cell proliferation and apoptosis via the activation of ERK1/2 pathway, and the upregulation of AKT (360). Moreover, it has been reported that both 4-HNE and MDA upregulate COX-2 activity (361, 362), and the subsequent production of PGE_2 and other proinflammatory lipid mediators, which promote chronic inflammation and facilitate tumor progression, stem cell expansion and metastasis (335, 363, 364).

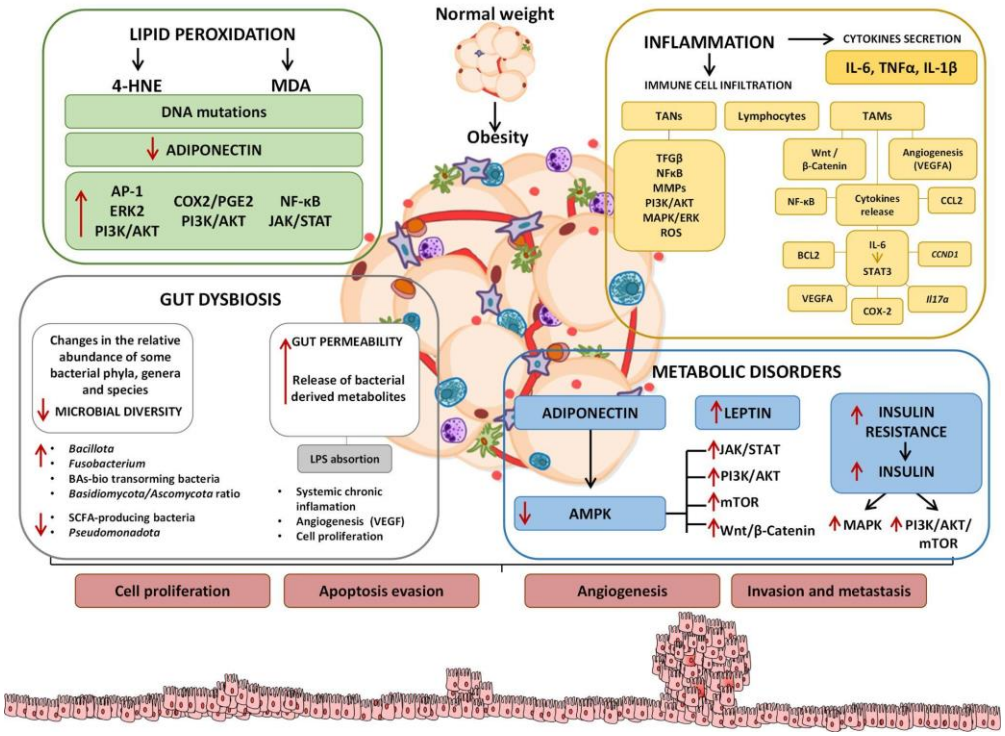

Figure 11. Molecular pathways involved in the obesity-CRC crosstalk. *Lipid peroxidation occurred in obesity leads to the release of mutagenic factors, 4-HNE and MDA, that induce alterations in DNA of colonocytes and promote the initiation and*

progression of CRC through the downregulation of adiponectin. Furthermore, the deregulated metabolism in obese patients results in an imbalance in some hormones such as adiponectin, leptin and insulin. Besides, obesity is characterized by a chronic inflammation that promotes the infiltration of immune cells and the release of harmful cytokines in the tumor microenvironment. Gut dysbiosis is another key event of obesity that increases gut permeability and changes the diversity and composition of microbiota resulting in the release of metabolites such as LPS that contribute to CRC development. All these events induce the activation of molecular pathways involved in cell proliferation, apoptosis evasion, angiogenesis, invasion and metastasis leading to initiation, promotion and progression of CRC.

4.1.2. Obesity promotes CRC through deregulation of the metabolism.

Obesity is associated with several metabolic disorders, which in turn can promote the onset of metabolic syndrome (365, 366) as well as tumor development (367, 368). In obese people, adipocytes suffer hypertrophy and hyperplasia, thus leading to changes in the secretion of several adipokines that may be responsible for the association between obesity and CRC (369, 370). Among these changes, adiponectin levels are reduced in obesity, and it has been reported the existence of an inverse association of total adiponectin with CRC (371); in fact, low circulating total adiponectin is considered a risk factor for CRC development (372). Furthermore, obese people frequently have an altered cellular signaling and insulin response, displaying hyperinsulinemia and insulin resistance, thus exhibiting an altered cellular signaling and insulin response (373). It is well known that the binding of insulin to its receptor can activate the AKT/PI3K/mTOR and MAPK pathways, which subsequently exert downstream metabolic and cellular growth effects (374). Hyperleptinemia is another feature in obese people, and it has also been associated with tumor progression in CRC (375). Leptin exerts its action through the leptin receptor (Ob-R), mainly the Ob-Rb isoform, thus activating the JAK/STAT pathway, which promotes cellular growth, migration and invasion (376).

4.1.3. Inflammation in obesity contributes to CRC development.

Obesity is also associated with a chronic inflammatory status that increases the risk of developing several diseases, including cancer (351) This chronic inflammation has an important role in tumor progression favoring the development of CRC. Indeed, obesity has been associated with an increased risk of IBD and CAC (377-380). Adipose tissue in

obese people is progressively infiltrated by macrophages and other immune cells that secrete pro-inflammatory cytokines like TNFα, IL-1β and IL-6, facilitating chronic inflammation (381). Moreover, these immune cells and cytokines play an important role in the tumor microenvironment, participating in the neoplastic process, proliferation, survival, migration and angiogenesis (310). Wunderlich et al., (2018) demonstrated that obesity-induced IL-6 promoted M2 macrophage polarization resulting in an up-regulation of CCL-20 chemokine, which recruits CCR-6 expressing lymphocytes (B cells, γδ T cells and Treg cells) to the tumor microenvironment and participate in the tumorigenesis (382).

5. GUT DYSBIOSIS IN CRC AND ITS IMPLICATION ON CRC-ASSOCIATED OBESITY.

In a healthy host, the colonic microbiome is typically dominated, at the phyla level, by Gram-negative *Bacteroidota* and Gram-positive *Bacillota* (representing >90% of all phylogenetic types), with a smaller, but sizable, abundance of *Pseudomonadota, Actinobacteria* and *Verrucomicrobia* (383). The healthy microbiota plays a prominent role in maintaining body homeostasis as well as in the development and regulation of the mucosal immune system, but also in the production of essential nutrients, the control of pathogenic microorganisms, the modulation of gastrointestinal epithelial cell proliferation and differentiation, or the management of bioactive foods and chemical components (384).

5.1. Gut microbiota in obesity

The homeostasis of the gut microbiota is altered in obese patients (385) showing an inverse relationship between gut alpha microbial diversity and BMI (385, 386). Additionally, a shift in the Firmicutes (*Bacillota*)/Bacteroidetes (*Bacteroidota*) (F/B) ratio is observed in obesity due to a decrease in the relative abundance of *Bacteroidota* and an increase of *Bacillota*, thus resulting in a microbiome with an enhanced ability to harvest dietary energy (387-389). In obesity this dysbiosis is related to an increase in *Bacillota* phylum and some bacterial genera such as *Clostridium* and the species *Eubacterium rectale*, *Clostridium coccoides, Lactobacillus reuteri, Akkermansia muciniphila, Clostridium histolyticum* and *Staphylococcus aureus* (390) . On the other hand, the relative abundance of *Bacteroidetes, Actinobacteria, Bacteroides, Bifidobacterium*, *Bacteroides fragilis, Faecalibacterium prausnitzii, Butyrivibrio fibrisolvens* and *Lactobacillus plantarum* is reduced in obesity (390, 391). This situation of dysbiosis in obese patients can be accompanied by gut barrier function impairments, including

decreased tight junction proteins gene expression that leads to higher plasma levels of LPS, a component of the outer membrane of Gram-negative bacteria (392, 393). The LPS absorption leads to a metabolic endotoxemia, which is proposed as the main responsible for the systemic chronic inflammation that takes place in obesity (394, 395). In consequence, obesity-induced modifications in the gut microbiota community are associated with the onset of an inflammatory state that becomes chronic and significantly increases the risk for CRC (396, 397).

5.2. Gut microbiota in CRC.

Similarly, CRC has been associated with gut dysbiosis (398). Thus, lifestyle risk factors for CRC, such as obesity and diet, can promote changes in microbiota composition, thus inducing dysbiosis, which causes an increase of the so-called pathobionts (microorganisms with pathogenic potential). In this situation, the dysbiosis is characterized by a reduction of the *Bacillota*/*Bacteroidota* ratio in comparison with healthy individuals (399, 400). CRC patients show a less diversity in its microbial community (401). Moreover it seems that the microbiota composition in individuals with CRC changes along the colorectal-adenoma-carcinoma sequence (402). An increase in the levels of *Bacillota* and *Fusobacteria,* as well as, a reduction of *Pseudomonadota* occurs in CRC patients (403). Additionally, a depletion of some bacteria genera considered "beneficial" such as, *Bifidobacterium, Faecalibacterium,* and *Blautia,* has been described in CRC subjects (404). On the other hand, there are some bacteria genera such as *Bacteroides, Fusobacterium, Atopobium, Parvimonas, Peptostreptococcus* and *Porphyromonas* that are positively correlated with tumor burden (405). In this scenario, there is also a negative correlation between tumor number and the SCFA production and the abundance of SCFA-producing bacteria (406). To sum up, an alteration of the microbe community structure occurs in CRC and it is associated with the onset of an inflammatory state that becomes chronic and increases the risk for develop this disease (396, 397).

Microbial species linked to CRC include certain strains of *Bacteroides fragilis*, *Escherichia coli*, *Streptococcus gallolyticus*, *Enterococcus faecalis*, *Fusobacterium nucleatum*, *Atopobium parvulum* and *Actinomyces odontolyticus*. Yachida et al., reported that changes in the microbiome and metabolome in CRC patients occur in very early cancer stages, discovering two patterns of microbiome changes during CRC development: initially, an increase of *Fusobacterium nucleatum* colonization takes place becoming the bacteria with the highest elevation; and in a second stage, *Atopovium parvulum* and *Actinomyces odontolyticus* are the main involved (407).

Tjaslma et al., proposed a bacterial counterpart of the genetic driver–passenger model for CRC. According to this model, some indigenous intestinal bacteria drive the epithelial DNA damage that contributes to the initiation of CRC (termed bacterial drivers). Once these bacterial drivers initiate tumorigenesis, it induces intestinal niche alterations that favor the proliferation of opportunistic bacteria (termed bacterial passengers) colonization. These bacterial drivers act as pro-oncogenic and capable of promoting CRC whereas bacterial passengers act as tumor-promoting or tumor-suppressing (408). *Fusobacterium* spp. appears to be the most common passenger bacteria to colonize CRC tissue (75), although others have been also proposed, including *Streptococcus gallolyticus* subsp. *Gallolyticus* (409), *Clostridium perfringens* and *Granulicatella morbillorum* (76) or even gut commensals of the family *Coriobacteriaceae* (*Slackia* and *Collinsella* spp.), the genus *Roseburia* and the genus *Faecalibacterium*, some of them reported as probiotics, which, in certain circumstances may also contribute to the tumor formation (410).These bacteria have been reported to display the ability to generate a proinflammatory microenvironment by enhancing the production of different pro-inflammatory cytokines (such as TNF-α, IL-1β, IL-6, and IL-8) or by recruiting myeloid-derived immune cells, which in turn promote tumor development (75, 411).

Fusobacterium is a genus of gram-negative anaerobic bacteria that have been proposed as a risk factor for CRC development and progression (412). Species of this genus, mainly *Fusobacterium nucleatum,* can activate the E-cadherin/β-catenin signaling pathway, being associated with microsatellite instability and CpG island methylation phenotype (412). *Fusobacterium* has a surface adhesion molecule called FadA which binds to E-cadherin in epithelial cells surface leading to E-cadherin phosphorylation, thus activating β-catenin signaling pathway (413). Mouse xenografts of primary colorectal tumors were found to retain viable *Fusobacterium,* which was also detected in liver metastases suggesting that this bacterium has an important role in tumor microenvironment being implicated in cell proliferation, invasiveness and metastasis (414). In the *Apc*$^{min/+}$ mouse model of CRC, the exposition to *Fusobacterium nucleatum* increased the tumor-infiltrating myeloid-derived suppressor cells such as macrophages, dendritic cells and granulocytes that play an important role in promoting tumor progression and angiogenesis (75). *B. fragilis* is another bacterial species increased in patients with CRC and obesity (415, 416).In fact, enterotoxigenic *B. fragilis* is considered a bacterial driver according to Tjaslma et al., model (408). *B. fragilis* produces a chronic inflammation that induces colitis and carcinogenesis. In these processes, IL-17 released by Th17 cells and PGE2 produced by COX-2 plays an important role (417).

5.3. Gut microbiota in individuals with both comorbidities: obesity and CRC.

Data from a case-control study conducted by Campisciano G. et al., (2020) with fecal samples from obese individuals and CRC patients showed a similar microbiome pattern in CRC and obese subjects, and some bacterial species including *Hafnia alvei, Akkermansia muciniphila, Blautia wexlerae*, *Eubacterium rectale*, *Lactobacillus rogosae* and *Ruminococcus faecis* showed a similar relative abundance between obese individuals and those with CRC (418). Moreover, in subjects with the two comorbidities, obesity and CRC, it has been reported a reduction of the gut microbial richness (Chao and Shannon indexes) (Sánchez-Alcoholado et al., (2020) (419).

Of note, Sánchez-Alcoholado observed the microbiota profile of obese people with CRC were similar to that of non-obese individuals with CRC, with an increase of *Fusobacteriaceae, Prevolotellaceae, Clostridiaceae, Barnesiellaceae, Porphyromonodaceae* and *Desulfovibrionaceae* in comparison with healthy people. However, significantly higher levels of *Firmicutes* and *Proteobacteria* phylum, as well as of *Enterobacteraceae* and *Streptococcaceae* families, were found in obese cancer patients when compared with non-obese with cancer (419).

At genus level, an increase of *Prevotella, Clostridium, Desulfovibrio* and *Enterococcus,* together with a significant decrease in *Bacteroides, Butyricimonas, Roseburia and Ruminococcus* were reported in CRC patients, regardless BMI. When considering the differences between non-obese and obese patients with CRC, the richness of *Enterobacter, Escherichia, Fusobacterium* and *Streptococcus* was increased in obesity whereas *Blautia* and *Faecalibacterium* was reduced. These changes at genus level were correlated with an increase of *Fusobacterium nucleatum, Eschrerichia coli, Streptococcus bovis, Clostridium septicum* and *Enterobacter cloacae* in obese-CRC patients and a reduction of *Faecalibacterium prausnitzii* when compared with lean-CRC subjects (419). This microbiota imbalance was associated with lower levels of SCFAs in gut lumen, as well as an increase of pro-inflammatory mediators such as IL-1β and the metabolite trimethylamine N-oxide (TMAO) (419), which is involved in the activation of the NOD-like receptor family pyrin domain containing 3 (NLRP3) inflammasome, implicated in tumor growth and metastasis (420).

The association between CRC and obesity has also been studied in experimental models of obesity-associated CRC. At this level, Yang et al., (2022) have shown that HFD contributes to CRC tumorigenesis through gut dysbiosis accompanied by metabolomic

dysregulation and an alteration of the intestinal barrier (421). Indeed, several studies reported that obesity promotes CRC development in both chemically induced or spontaneously generated cancer models, as well as in subcutaneous tumor models (422-431). Moreover, this obesity-CRC association is dependent on gut microbiota changes, since antibiotic-induced depletion of gut microbiota reduces tumor burden (421). Additionally, the causal link between obesity and CRC through the microbiota was confirmed by performing fecal microbiota transplantation (FMT) of HFD-mice to germ-free mice with CRC resulting in higher levels of tumorigenesis in comparison to CRC-mice treated with phosphate buffered saline (PBS) (421, 423). Some microorganisms from genus *Alistipes* and *Marseille* have been singled out as responsible for an aggravation of the tumor process, also favored by a reduction of *Parabacteroides* abundance (421). Increased levels of *Verrucomicrobia, Coprobacillus, Prevotella, Biophila, S24-7, Akkermansia muciniphila* as well as bile salt hydrolase (BSH)-producing bacteria (such as *Mucispirillum, Blautia* or *Streptococcus*) were also reported in obese and CRC-mice in comparison with those fed with a low-fat diet (421, 422, 424). As it will be discussed below, the dysbiosis occurred in obesity-associated CRC results in the release of microbial metabolites that may be involved in the increase of tumorigenesis (421, 424).

6. GUT MICROBIOTA MODULATION AS A THERAPEUTIC STRATEGY IN OBESITY-ASSOCIATED CRC.

Considering all the above, it is clear that the microbiome plays a relevant role in the progression and even the initiation of the tumor process. Although the molecules that mediate the crosstalk between microbiota and CRC are not fully described, it is well known that some bacteria-derived metabolites contribute to cancer development. Among these metabolites, LPS (432), bile acids (433) and glycerophospholipids (421) have an important role in CRC progression and metastasis. On the other hand, it seems that SCFAs are associated with an antitumor effect (434). Therefore, microbiota modulation, with the use of prebiotics, probiotics, postbiotics, antibiotics or FMT, has been postulated as adjuvant therapies for CRC and there are several investigations in this field (435-437).

6.1. PREBIOTICS IN THE TREATMENT OF INFLAMMATORY DISEASES: OBESITY AND CAC.

In 2008, the 6th Meeting of the International Scientific association of Probiotics and Prebiotics (ISAPP) defined “dietary prebiotics” as “a selectively fermented ingredient that

results in specific changes in the composition and/or activity of the gastrointestinal microbiota, thus conferring benefit(s) upon host health" (438). To consider a compound as prebiotic it must be resistant to pH of stomach, it cannot be hydrolyzed by mammalian enzymes and it should be fermented by intestinal bacteria stimulating their growth and/or activity (438).

Accumulating evidence suggests that prebiotics exert beneficial effects against inflammatory diseases such as obesity (439-441), IBD (442-444), and cancer (445, 446). Of note, prebiotics are a source of energy for gut microbiota, thus modulating its composition and function. Moreover, the result of digestion and fermentation of prebiotics is usually the production of new compounds that, on the one hand, can be subsequently absorbed and exert a beneficial effect on the body, or on the other hand, can be used by other microorganisms from this microbiota, hereby affecting its composition and/or function. Additionally, prebiotics can cause changes in the environment, e.g. decreasing the pH (447); which can also increase the growth of bacterial species, such as *Bacteroidetes*, facilitating SCFAs production, including butyrate (448). In fact, SCFAs are associated with beneficial effects against obesity and cancer (449). Supporting this, it has been reported that SCFAs suppress HFD-induced weight gain through a decrease in the release of gut hormones, peptide YY and glucagon-like peptide GLP-1, as well as by modulating the expression of GPR43 and GPR41 in fat and colon tissues. Moreover, SCFAs supplementation restored the altered microbiota by increasing the biodiversity indexes and reducing the F/B ratio (449). Furthermore, SCFAs also present immunomodulatory properties. Butyrate inhibits LPS-induced NF-κB activation in colonic cell lines and in mouse colon (8). Also, SCFAs (mainly butyrate) have inhibitory effect over histone deacetylase (HDACs) activity promoting histone acetylation, affecting gene regulation of cell proliferation, differentiation, and inflammatory response, contributing to intestinal homeostasis and cancer protection (450, 451). Furthermore, a decrease in pH levels induced by prebiotic degradation result in modulation of gut microbiota composition leading to a reduction in levels of "pathogenic bacteria" such as *Fusobacterium* that is involved in the pathogenesis of CRC (447). Indeed, the transplantation of the butyrate-rich feces from HFD mice treated with metformin into MC38 tumor allograft mice resulted in a reduction of tumor growth (423).

Although the plant extracts were not initially considered as prebiotics, more recently they have been included in this concept, given their well-known ability to interact with gut microbiota, thus modulating its composition and/or activity, which has been associated with some of the beneficial effects classically attributed to these products. Among these plant extracts, accumulating scientific evidence has attributed beneficial pharmacological

properties to those extracts obtained from species of the genus *Thymus* and *Morus* due to their high content in bioactive compounds (452-454). Widely used in traditional medicine, the extracts obtained from *Thymus serpyllum* L. and *Morus alba* L. have proven to be effective against numerous affections, including obesity, cancer, irritable bowel syndrome, microorganisms infections, diabetes and other conditions with a high inflammatory and oxidative component (455-461).

6.1.1. Thymus serpyllum.

Thymus serpyllum, also known as thyme, is an aromatic plant of Mediterranean flora commonly used in the culinary and medicinal field. *Thymus serpyllum* is rich in active ingredients such as rosmarinic acid, tannins, basically polymers of proanthocyanidins, gallotannins, flavonoids, flavonones and triterpenes (462). This composition in bioactive compounds makes this plant traditionally used in various conditions such as headaches, colds, respiratory infections and digestive diseases (463). Additionally, several beneficial properties have been reported for thyme extract including antimicrobial, antiinflammatory and antioxidant activities (464, 465). Indeed, dry powder extract from thyme has been used in recent research against inflammatory diseases such as irritable bowel syndrome (IBS) (459) and ulcerative colitis (465). An amelioration of the inflammatory profile and gut barrier has been achieved with thyme treatment in both diseases. Moreover, the modulation of gut microbiota is a key component in the beneficial activity exerted by this extract, which is able to restore the microbial diversity under pathological conditions (459). Besides, *Thymus serpyllum* has demonstrated to exert a selective cytotoxicity activity against MCF-7 and MDA-MB-231 breast cancer cell lines (460). Thyme extract was able to induce tumor cell apoptosis through an increase of caspase 3 and caspase 7 enzymes activity. Moreover, thyme inhibited the activity of HDAC enzyme, which is overexpressed in tumor cells (460).

6.1.2. Morus alba

Morus alba also known as white mulberry, is a medium-size tree to which numerous nutritional and medicinal properties have been attributed, especially in the Asian continent, where it is native (466). Since ancient times, the leaves of *Morus alba* have been widely used as functional foods and phytotherapy in traditional Chinese medicine against fever, constipation and diabetes (467-469). Accumulating evidence shows an increase in the pharmacological properties associated with mulberry leaves, which are rich in bioactive compounds, including flavonoid, alkaloid and phenolic acids (470). Quercetin, rutin, apigenin, as well as ferulic, chlorogenic and protocatechuic acids are

some of the major compounds present in *Morus alba* leaves. These compounds are responsible for their pharmacological properties, among which antioxidant, antiinflammatory, antidiabetic, antiobesity and antimicrobial properties stand out (455, 469, 470). Moreover, cytotoxic activity against human cancer cells has been also reported for the root and leaves of *Morus alba* (471, 472). Among the molecular mechanisms involved in the anticancer activity described for this plant it is necessary to mention the induction of apoptosis via upregulation of caspase 3 and ATF6 (471, 473), the cell proliferation inhibition via suppression of Wnt/β-catenin pathway (474) and its capacity to modulate the immune response that results in the inhibition of NF-κB signaling pathway and the modulation of the TAM response in the tumor microenvironment (471, 475).

6.2. TETRACYCLINES: A PROMISING TOOL IN THE THERAPY OF COMPLEX DISEASES.

Tetracyclines are a family of broad-spectrum antibiotics used in the treatment of a variety of infectious diseases. Discovered as natural products from a mix of natural compounds produced by species of *Streptomyces,* tetracyclines were first reported in the scientific literature in 1948. The discovery of this family of antibiotics is attributed to Benjamin M. Duggar et al., who identified the soil bacterium *Streptomyces aureofaciens* as a source of chlortetracycline, the first tetracycline brought to light and named as Aureomycin (476). Since then, three generations of tetracyclines have been developed as semisynthetic analogues with improved pharmacokinetic and chemical properties and higher efficacy against resistant bacteria. Throughout history, it has been seen that the activity of these interesting molecules is not limited solely to combating infectious diseases, but has also proven to be an effective tool in the treatment of inflammatory and neurodegenerative diseases, and even cancer (477-479). Therefore, tetracyclines can be considered a promising tool for the treatment of complex diseases with an inflammatory component in which conventional therapies are not effective enough.

6.2.1. Pharmacodynamics properties of tetracyclines.

Tetracyclines were born as drugs with antibiotic activity. Their extensive use led to the appearance of bacterial resistance, which drove the development of new tetracyclines that improved the pharmacological properties of the existing ones (480).

6.2.1.1. Antibiotic activity.

Tetracyclines are broad-spectrum bacteriostatic antibiotics, active against a wide range of aerobic and anaerobic bacteria, as well as other microorganisms. The antibiotic activity of tetracyclines is due to their ability to inhibit protein translation in the bacterial cell. Tetracyclines bind to the acceptor site at the 30S ribosomal subunit of the bacteria and prevent the binding of amino-acyl tRNA to this site leading to an interruption of the protein biosynthesis. In general, tetracyclines are used in a wide range of infectious diseases such as skin infections, rickettsial and chlamydial infections, cholera, Lyme disease, syphilis and periodontal infections (481). New tetracyclines, omadacycline, eravacycline and sarecycline, have been developed to face the main problems of bacterial resistance and they have shown efficacy against Gram-positive, Gram-negative, anaerobic and aerobic bacteria (482).

6.2.1.2. Non-antibiotic properties.

Nowadays, the potential of tetracyclines is not restrained to their use as antibiotics. Several pharmacological activities have been attributed to this family of drugs, highlighting their ability to inhibit enzymes such as MMPs (483) and the inducible NO synthase (iNOS) (484), as well as their immunomodulatory properties (477, 485). Moreover, it has been described anticancer properties to tetracyclines due to their action of different events that contribute to the development of this disease, such as angiogenesis, metastasis, EMT and uncontrolled proliferation (479, 486-488).

The interest of tetracyclines in the field of cancer has been in continuous rise since the discovery of their potential to inhibit MMP activity, followed by reports of additional antitumoral properties (479, 489-492). Among tetracyclines with antitumor activities, tigecycline, doxycycline and CMT-3 are the most promising candidates for cancer treatment being the authors of several papers. Tigecycline has exerted an antitumor effect on pancreatic ductal adenocarcinoma and multiple myeloma through the inhibition of cell proliferation, migration and invasion (491, 493). Doxycycline has shown efficacy in the management of head and neck lymphangiomas in children (494), as well as in prostate cancer where it inhibits cell proliferation and metastasis (495, 496). Mechanisms by which tetracyclines are considered promising agents in the treatment of cancer are encompassed within their antiproliferative (497, 498), proapoptotic (499, 500), antimetastatic (501, 502) and antiangiogenic effects (503, 504).

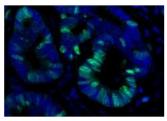

OBJECTIVES

OBJECTIVES

The symbiotic relationship between gut microbiota and host is a crucial component of human homeostasis, participating in metabolic, immunological and protective functions. In fact, it is well known that the host immune system can be modulated through intestinal microbiota in order to balance and resolve inflammation. Moreover, the restoration of gut microbiota composition when a dysbiosis situation occurs can result in the enhancement of gut barrier function and prevention of pathogen colonization, which can also contribute to the prevention and treatment of inflammatory-associated diseases, including obesity-associated CRC. The modulation of the gut microbiota can be achieved by different interventional approaches, including the administration of prebiotics, probiotics or antibiotics. Consequently, a thorough study of how the modulation of gut microbiota influences the host response, inflammatory status and tumor development in obesity-associated CRC can establish the basis for new therapies and innovative biomarkers in this important condition. Subsequently, the hypothesis proposed in this thesis have been:

H1: Intestinal dysbiosis constitutes a risk factor in obesity-associated colorectal cancer.

H2: The modulation of gut microbiota could be considered as an optimal therapeutic approach in obesity-associated colorectal cancer.

Obesity is one of the main health problems worldwide that is considered as a risk factor of several diseases, including CRC. Both diseases, obesity and CRC share altered cellular pathways and gut dysbiosis associated with the release of metabolites that promote the tumorigenesis process. Thus, intestinal microbiota could be considered as a target of action for the search of new effective and safe drugs against obesity and CRC. For that reason, the following objectives were established:

1. **To evaluate therapeutic strategies able to modulate the gut microbiota in the management of obesity.**

Since obesity constitutes a central process in the development of different conditions, the treatment of obesity could be considered a valid therapeutic strategy in the prevention of its associated diseases, including CRC, which are mainly responsible for the high morbidity and mortality in obese patients.

In this scenario, plant extracts like those obtained from the leaves of *Thymus serpyllum* and *Morus alba* are considered prebiotics, which exert beneficial effects in the treatment

of diseases with an inflammatory component, being also characterized by a good safety profile given their traditional use since ancient times.

To address the first objective of this Thesis, the antiobesity effects of leaves extracts from *Thymus serpyllum* and *Morus alba* were evaluated in a murine model of diet-induced obesity with special attention to the modulation of the microbiota activity exerted by both extracts. The following studies were carried out:

- Evaluation and characterization of the effect of an extract of *Thymus serpyllum* leaves in a murine model of diet-induced obesity.
- Evaluation and characterization of the effect of an extract of *Morus alba* leaves in a murine model of diet-induced obesity.

2. To evaluate therapeutic strategies able to modulate the gut microbiota in the management of colorectal cancer.

The antibiotic effect of tetracyclines can cause a crucial impact on gut microorganisms that are involved in CRC development, thus modulating the microbiota towards healthier profiles. Besides, tetracyclines have shown a wide range of pharmacological activities, including immunomodulatory properties, anti-metastatic and anti-angiogenic effects, as well as ability to modulate apoptosis and cell proliferation, that can reinforce their activity against CRC. Among tetracyclines, tigecycline is a third generation tetracycline and one of the most promising drugs due to its pharmacological features, including a broader antibiotic spectrum, a higher capacity to inhibit mitochondrial translation and to activate the integrated stress response in tumor cells, inducing their death, as well as a greater capacity to inhibit their migration.

Therefore, the antibiotic properties of tigecycline together with the rest of properties described above, make this drug a good candidate to address the second objective of this thesis.

To assess the ability of tigecycline to influence CRC, we studied the impact of the drug on the different hallmarks of the disease, including the gut dysbiosis. Firstly, we want to evaluate the anti-proliferative and proapoptotic capacities of tigecycline *in vitro* in colon cancer cell lines. Then, we aimed to characterize the effect of tigecycline in stemness properties of CRC *in vitro* and *in vivo* in a mouse xenograft tumor model. Lastly, the antitumor effect of tigecycline was evaluated *in vivo* in a murine model of CAC allowing us to approach the complexity of the disease from several points, including the role of the microbiota and immune response. In all cases, molecular mechanisms involved in

tigecycline effects were compared with those exerted by 5-FU, the drug of choice in CRC chemotherapy. The following studies were performed:

- Evaluation and characterization of the antiproliferative and apoptotic effects of tigecycline *in vitro*
- Evaluation tigecycline effect on colonospheres *in vitro* and *in vivo* in a mouse model xenotransplanted with colon CSCs.
- Evaluation of the antitumor effect of tigecycline in an experimental model of CAC.

3. To characterize the impact of obesity in the development of colorectal cancer: role of the intestinal microbiota as potential therapeutic target.

It is well known that obesity is a risk factor for CRC development and that dysbiosis occurred in these pathologies could act as a link between both diseases. Therefore, the use of therapies that modulate the microbiota in obese individuals could be considered an optimal strategy for cancer prevention and treatment, once both comorbidities are present. In this sense, prebiotics such as *Thymus serpyllum* or *Morus alba* or antibiotics like tigecycline may be promising candidates for the treatment of obesity and obesity-associated CRC.

To address the third objective of the present Thesis, we first evaluated the direct impact of adipocytes and adipose tissue-derived stem cells (ADSCs) on colon cancer cells proliferation in order to know the main mediators involved in the crosstalk between adipose tissue and tumor. Next, we studied the complex influence of obesity in CRC development *in vivo,* in a murine model of CAC-associated to obesity. Additionally, we tried to determine whether the antitumor effect observed for tigecycline in previous assays could also be extrapolated to this model and how this treatment interfered in the crosstalk between obesity and cancer. Briefly, the following studies were carried out:

- *In vitro* evaluation of the impact of adipose cells-derived metabolites on colon cancer cells malignancy in a coculture model of HCT116 cells and adipocytes or ADSCs.
- *In vivo* characterization of the effect of obesity on the CRC development, in a murine model of CAC-associated obesity, and evaluation of the impact of tigecycline on this association.

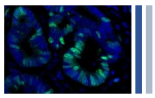

MATERIALS AND METHODS

MATERIALS AND METHODS

1. REAGENTS.

All chemicals were obtained from Sigma-Aldrich (Madrid, Spain), unless otherwise stated.

1.1. *Thymus serpyllum* plant extract

The dried flower aerial parts of wild thyme (*Thymus serpyllum*), registered in the European Pharmacopoeia as *Serpylli herba,* was produced under good manufacturing conditions and provided by Finzelberg GmbH & Co KG (Andernach, Germany). The patented manufacturing process (EP2858655B1) is based on the complete removal of volatile oil substances, an exhaustive aqueous extraction and a gentle spray-drying process with the functional excipient Dextrin. The resulting extract is characterized by its standardization on 70% native extract (DER native 4-8:1) and 30% Dextrin. The chemical analysis revealed that it contains rosmarinic acid (1.8%, HPLC) and no essential oil < 0.1% v/w (Destillation Ph.Eur.), as well as other polyphenols, mainly Luteolin derivatives (505). Moreover, the extract was free of common contaminants (pesticides, aflatoxins or heavy metals).

1.2. Morus alba plant extract

The *Morus alba* BGMU 050 10009 genotype, corresponding to the variety *Italy,* was provided by the Germplasm Bank of the Sericulture Program at the Instituto Murciano de Investigación y Desarrollo Agrario y Alimentario (IMIDA) (Murcia, Spain). The leaves were collected and used for the obtention of a dry extract that was chemically characterized as previously described by Ruiz-Malagón AJ. et al., (2020) (455).

1.3. Tigecycline and 5-fluorouracil.

Tigecycline (Tygacil®, Pfizer, New York, USA) and 5-FU (Accord Farma, Polanco, Mexico) were kindly provided by the pharmaceutical service of the Hospital Virgen de las Nieves (Granada, Spain). The doses of tigecycline used *in vitro* and in the animals models were chosen according to previous results of our group in colitis murine models whereas the doses of 5-FU for *in vitro* and *in vivo* assays were chosen based on previously published studies of efficacy and toxicity (506, 507).

2. *IN VITRO* EXPERIMENTS.

2.1. DPPH Scavenging activity.

The 1,1-diphenyl-2-picrylhydrazyl (DPPH) test was performed to evaluate the free radical scavenging activity of the thyme extract (508). Briefly, *Thymus serpyllum* extract and the positive control ascorbic acid were dissolved in methanol to reach a range of concentrations 1.56-100 µg/mL. Then, 10 µL of each methanolic dilution was mixed with 90 µL of phosphate buffer at pH = 7 and a 200 µL of a DPPH solution at 100 µM. The plate was protected for light and incubated for 30 min at 25 °C. After incubation, the scavenging activity of each compound was measured at 515 nm in a Magellan® Tecan Infinite F50 spectrophotometer. The percentage of radical DPPH scavenging activity (% RSA) was calculated for each concentration using the following equation (1):

$$(1) \quad RSA\ (\%) = [Abs\ Blank - Abs\ Sample)/Abs\ Blank] \times 100$$

where Abs Blank and Abs Sample are the absorbance values at 515 nm of the blank and samples, respectively. The blank absorbance value is the maximum and corresponds with the highest levels of DPPH radical. Then, the half maximal inhibitory concentration (IC50) value was calculated for each compound tested.

2.2. Colon cell lines and culture.

The human colon cancer cell lines HCT116 and Caco2 and the murine CMT93 cell line were obtained from the Cell Culture Unit of the University of Granada (Granada, Spain) whereas de NCM356 human colonic epithelial cells were kindly provided by Laura Medrano González and Ezra Aksoy (William Harvey Research Institute, Queen Mary University of London, London, UK). The HCT116 cell line consists of an adherent epithelial cell line from a male adult with colorectal carcinoma that is widely used in research due to its tumorigenic capacity. These cells have a mutation in *KRAS* oncogene and they are positive for TGFβ1 and TGFβ2. Moreover, they have active proliferation signaling pathways such as Wnt/β-catenin and are able to generate tumors in nude mice after being xenotransplanted (HCT116 ATCC®. Accessed on 16.2.2023. Available online: https://www.atcc.org/products/ccl-247) (509). Caco2 are epithelial adherents cells isolated from an adult male with colorectal adenocarcinoma able to generate tumors in nude mice. These cells express EGF and have the ability to form monolayers of differentiated cells (Caco2 ATCC®. Accessed on 16.2.2023. Available online: https://www.atcc.org/products/htb-37). CMT93 is an adherent cell line with epithelial

morphology that was isolated from the rectum of a C57BL/icrf mouse with polyploid carcinoma. Moreover, CMT93 cells are able to generate spheroids and tumors in nude mice inoculated subcutaneously (CMT93 ATCC®. Accessed on 16.2.2023. Available online: https://www.atcc.org/products/ccl-223). The NCM356 cell line is an adherent epithelial cell line obtained from the normal colon mucosa of a 65-year-old male. These cells are non-tumorigenic and express cytokeratins, villin and other colonic epithelial markers (510).

All colon cell lines were maintained in Dulbecco's modified Eagle's medium (DMEM) High Glucose supplemented with 10% of heat inactivated fetal bovine serum (FBS), 1% L-glutamine, 1% penicillin/streptomycin and 1% amphotericin B (called 10% supplemented DMEM) at 37 ºC in a humidified atmosphere of 5% CO_2. Culture media were changed every 48-72 h and once the cultured cells reached a maximum of 80-90% of confluence were divided or cryopreserved in freezing media (95% FBS, 5% DMSO). For these purposes, cells were washed with PBS 1x and detached from the flask surface with TrypLE (Cat.# 12604021). After 5 min at 37ºC, cells in suspension were neutralized with FBS containing media and centrifuged at 300 x g for 5 minutes at room temperature. Then, cells were counted with trypan blue and resuspended in culture media or freezing media at the desired concentration. All cell culture reagents were purchased from Gibco®-Invitrogen (Thermo Fisher Scientific, Waltham, MA, USA) unless otherwise indicated.

For the evaluation of the impact of tigecycline on the Wnt/β-catenin pathway, HCT116 were cultured for 24h in the presence of 100 ng/mL of Wnt3a and, simultaneously, with 50 µM tigecycline or 50 µM 5-FU. Then, RNA and cytoplasmic and nuclear proteins were isolated for Taqman qPCR and Western blot, respectively, as will be described later.

2.3. Adipose-derived cell lines and coculture.

Human adipose-derived stem cells (ADSCs) were kindly provided by Francisco Javier Ruiz-Ojeda (University of Granada, Centre for Biomedical Research, E-18016, Granada, Spain). For adipogenic differentiation, 4000 cells/cm^2 were seeded into 6-well plates. Cellular differentiation was induced using 10% supplemented DMEM plus 10 µg/mL insulin, 0.2 mM indomethacin, 2 µM dexamethasone and 50 µM 3-Isobutyl-1-methylxanthine (IBMX). In parallel, cells maintained in 10% supplemented DMEM were used as negative differentiation controls. Culture medium was replaced every 3-4 days. After 4 weeks, cellular differentiation was assessed via morphological examination of the cellular accumulation of lipid droplets.

In order to investigate the effect of adipose-derived cells in the progression of colon cancer, HCT116 cells were cultured in a cell coculture model, in which $1x10^5$ HCT116 cells were cultured on transwell (ThinCerts™-6 well, Greiner bio-one, Madrid, Spain Cat.# 657641) of 0.4 µm pore size membrane (up chamber) and confluent ADSCs undifferentiated or differentiated (adipocytes) were cultured on the bottom chamber of the culturing well. Also, a negative control was included that consisted in HCT116 cells cultured on the surface of the transwell with no cells in the bottom chamber. Moreover, 10% supplemented DMEM was used in this coculture system. After 48 h of incubation at 37 ºC in a humidified atmosphere of 5% CO_2, HCT116 cells were harvested, washed and used for protein extraction, as will be described later.

2.4. Generating Colonospheres.

The cell lines HCT116 and CMT93 were used to generate colonospheres following the patented protocol WO2016020572A1 (511). Primary colonospheres were maintained in DMEM/F-12 nutrient mixture without FBS and supplemented with 1 x B-27 (B-27™ Supplement (50x) Minus Vitamin A; Invitrogen), 4 ng/mL heparin, 10 µg/mL insulin (Insulin-Transferrin-Selenium [100x], Invtitrogen), 1 µg/mL hydrocortisone, 10 ng/mL of epidermal growth factor, 10 ng/mL fibroblast growth factor, 10 ng/mL interleukin 6 (Miltenyi Biotec, Bergisch Gladbach, Germany, Cat.# 130-095-365) and 10 ng/mL hepatocellular growth factor (Miltenyi Biotec, Auburn, CA, USA, Cat.# 130-093-872). Secondary colonospheres were generated from the primary colonospheres. For this purpose, primary colonospheres were left with this enriched culture medium in Corning® Costar® ultra-low attachment plates for 72 h. Then, they were washed with PBS 1x and disaggregated with TrypLE for 5 minutes at 37°C. Next, FBS containing media was used to neutralize the TrypLE enzyme activity and the cell suspension was washed to remove traces of the serum. Finally, single cells were resuspended in new low-attachment plates with the conditioned medium to generate the secondary colonospheres.

2.5. Colonosphere-forming efficiency.

Sphere forming efficiency (SFE) was evaluated as previously described by Cruz-Lozano, M. et al., (2018) (512). Briefly, primary spheres obtained after seeding 1000 cells/well in a 96-well ultra low attachment plate were maintained in DMEM/F-12 supplemented medium without FBS and treated with tigecycline at 25 µM or 50 µM for 48 h. Then, these primary spheres were washed with PBS 1x, dissociated with TrypLE and re-plated in a new 96-well ultra-low attachment plate at a density of 500 cells/well in DMEM/F-12 supplemented medium without FBS. After 72 h of incubation at 37ºC and 5% CO_2,

secondary colonospheres with a diameter greater than 50 µM were counted under an Olympus-CKX41 inverted microscope (Olympus Europa SE & Co. KG, Germany). SFE was calculated by dividing the number of secondary colonospheres by the number of cells seeded to obtain these secondary spheres.

2.6. Cell proliferation assay

HCT116 and NCM356 attached cells were treated with different doses of tigecycline (1 µM - 75 µM) or 5-FU (5 µM - 100 µM) for 48 h (n=8). After that, cell viability was measured using a MTS assay according to the manufacturer's instructions (CellTiter 96® AQueous One Solution Cell Proliferation Assay, Promega, Madison, USA, Cat.#G3582)

To evaluate the proliferation rates of CSCs, secondary spheres derived from HCT116 and CMT93 were treated with tigecycline (1 µM - 50 µM) for 48h (n=6). Then, cell viability was measured using the Cell Counting Kit-8 following the manufacturer protocol.

2.7. Migration assay

A wound healing assay was carried out in HCT116 cells in order to evaluate the impact of the tigecycline on cell migration. For this purpose, HCT116 were seeded in a 6-well plate and once they reached confluence, monolayers were scraped with a 200 µL pipette tip coupled to a vacuum system in order to generate a straight line wound. Then, cells were treated with tigecycline (25 µM and 50 µM) and photos of the scratches were taken at 0, 12, 24 and 48 h with an Olympus-CKX41 inverted microscope. The migration index was calculated based on the percentage of wound regeneration and considering 100% of migration the regeneration of the controls at 24 h.

2.8. Colony formation assay

HCT116, Caco2 and NCM356 cells were plated into 6-well plates at 200 cells/well for HCT116 and 400 cells/well for Caco-2 and NCM356. From the following day, fresh media supplemented with different doses of tigecycline (1 µM - 50 µM) or 5-FU (1 µM - 50 µM), were added every 48 h for 1 week. Then, culture medium was removed, the cells were fixed with absolute ethanol and the colonies were stained with 2.3% crystal violet and counted with Image J software after taking the images.

To evaluate the impact of tigecycline on the clonogenicity of CSCs, a colony formation assay in soft agar was carried out as previously described by Griñán-Lisón C. et al., (2020) (513). Briefly, secondary colonospheres were treated with tigecycline at 25 µM or 50 µM for 48h and then washed and disaggregated with TrypLE. The surface of a 6-well plate was covered with 1mL of 0.4% agar base layer diluted in supplemented DMEM

mixed with PBS (1:1 dilution). Then, $1x10^4$ cells were seeded on top of 1 mL of 0.8% agar base layer. Cells were incubated for 28 days at 37ºC and 5% CO_2 with supplemented DMEM and culture media were changed every 48 h. After this period, colonies were stained with 1 mg/mL of iodonitrotetrazolium chloride in PBS at 37ºC and 5 % of CO_2 overnight. Next, colonies were counted using a Leica DM5500 B fluorescence microscope equipped with Leica CW4000 software.

Similarly, in an independent assay, cells were seeded in a 0.8% agar base layer as commented above and, after 24 h at 37ºC and 5 % of CO_2 they started to be treated with tigecycline at 25 µM or 50 µM. The culture medium and the treatments were restored every 48 h. Also, after this period, colonies were stained and counted. The assays were conducted by duplicate in three independent experiments.

In order to study the impact of the metabolites released by ADSCs and adipocytes on the proliferation of the HCT116 tumor cell line, conditioned media from these adipose cells were prepared. For this purpose, ADSCs and adipocytes were seeded in 6-well plates and once they reached confluence, the medium was replaced with fresh 10% supplemented DMEM and incubated for 24 h at 37ºC and 5% of CO_2. Then, the conditioned medium was harvested, centrifuged at 500 x g and stored at -20 ºC in aliquots until use. These conditioned media were used for performing a colony forming assay in HCT116 tumor cell line. For this purpose, HCT116 cells were seeded in 6-well plates (200 cells/well) and left in the incubator for 24 h at 37ºC and 5% of CO_2 to adhere to the plate surface. Then, cells were cultured in control or conditioned media from ADSCs or adipocytes, both diluted 1:1 with fresh basal medium. The culture media were changed every 48 h for 2 weeks and then, cells were washed, fixed with absolute ethanol and the colonies were stained with 2.3% crystal violet and counted with Image J software after taking the images.

2.9. Annexin V (ANXV) and propidium iodide (PI) assay.

Apoptosis and necrosis were evaluated by flow cytometry using FITC ANXV apoptosis detection kit with PI (Immunostep, Salamanca, Spain, Cat.# ANXVF-200T). For this purpose, HCT116 attached cells were treated with different concentrations of tigecycline (1 µM - 50 µM) for 48 h (n=5). Then, attached cells and those present in the supernatant were collected, washed with cold PBS and stained with FITC-ANXV and PI. Labeled cells were acquired on a BD FACsAria Illu cell CAC sorter (BD Biosciences, Becton, Dickinson and Company, Franklin Lakes, NY, USA) and data were analyzed using the FlowJo v10.6.2 software (FlowJo LLC, Ashland, OR, USA).

To study the impact of tigecycline on CSCs, secondary colonospheres derived from HCT116 and CMT93 were treated with tigecycline at 25 µM or 50 µM for 72 h (n = 4) and then they were harvested, washed dissociated with TrypLE, stained with FITC-ANXV and PI and analyzed with FACsAria Illu Cell CAC sorter, as commented above.

2.10. TUNEL assay.

In order to confirm the apoptotic capacity of the treatments, the Terminal deoxynucleotidyl transferase dUTP nick end labeling (TUNEL) assay was carried out in HCT116 cells treated with tigecycline (25 µM and 50 µM) or 5-FU (50 µM) for 48 h (n = 3). After the treatment, attached cells and those present in the supernatant were collected, washed and fixed in PFA 4%. Fixed cells were subjected to cytospin for being attached in slides. The TUNEL assay kit - HRP DAB was used for the staining following the manufacturer's protocol (Abcam, Cambridge, UK, Cat.# ab206386). Images were taken from three random sites on the same slide and ImageJ software was used for counting positive nuclei.

2.11. CSCs characterization by FACS.

ALDH1 activity was analyzed with the ALDFLUOR™ kit assay following the manufacturer's instructions (StemCell Technologies, Vancouver, Canada. Cat.# 01700) and cells were acquired on a BD FACsAria Illu cell CAC sorter (BD Biosciences, Becton, Dickinson and Company, Franklin Lakes, NY, USA). This assay is based on BODIPY-aminoacetaldehy reaction, which is a fluorescent substrate converted into BODIPY-aminoacetate by ALDH1 enzyme and then retained inside the cell. N,N-diethylaminobenzaldehyde (DEAB), a specific inhibitor of ALDH1, was used as control. To perform the assay, $1x10^6$ HCT116 and CMT93 cells derived from secondary colonospheres were treated with tigecycline 25 µM and 50 µM for 72 h, resuspended in the ALDEFLUOR™ kit buffer and incubated with ALDH1 substrate for 60 min in the dark at 37ºC and 5% of CO_2 (n = 4). Negative controls were simultaneously treated with DEAB. Next, cells were centrifuged at 1500 rpm 5 minutes at 4ºC, resuspended in a cold buffer and analyzed by FACS.

To further characterize the impact of tigecycline on CSC populations, HCT116 and CMT93 secondary colonospheres were treated with tigecycline at 25 µM and 50 µM for 72 h at 37ºC and 5 % of CO_2. Then, these spheres were harvested, washed and dissociated with TrypLE for 5 min at 37ºC and 5 % of CO_2. Next, cells were counted and $5x10^5$ cells were stained for 30 min at 4ºC with anti-human CD133-FITC (Miltenyi Biotec, Auburn, CA, USA, Cat.# 130-113-673) and anti-human CD44-APC (Miltenyi Biotec,

Auburn, CA, USA, Cat.# 130-113-893) antibodies for HCT116; and anti-mouse CD133-BV421 (BioLegend, San Diego, CA, USA. Cat.# 141213), anti-mouse CD44-PECy7 (BioLegend, San Diego, CA, USA. Cat.# 103029) and anti-mouse LGR5-PE (Miltenyi Biotec, Auburn, CA, USA. Cat.# 130-111-201) antibodies for CMT93 cells. Antibodies were diluted in the FACS buffer (0.1% Bovine Serum Albumin (BSA) and 2 mM EDTA) and fluorescence minus one (FMO) controls were also stained. Compensation controls were prepared using OneComp eBeads™ (eBioscience, San Diego, CA, USA). Data were acquired using either the BD FACSCantoTM II flow cytometer or BD FACSAriaTM IIIu cell sorter (BD Biosciences, San Diego, CA, USA) and analyzed using the Flowjo v10.6.2 software (FlowJo LLC, Ashland, OR, USA).

2.12. Immunocytochemistry.

HCT116 cells were seeded in a sterile slide with a removable 8 well silicone chamber for cell culture and immunofluorescence staining (Ibidi GmbH, Gräfelfing, Germany). When cells reached a 60-70% confluence the medium was removed and they were treated with tigecycline at 25 µM and 5-FU at 50 µM for 48h at 37ºC and 5% of CO_2. Then, the medium was removed, cells were washed with cold PBS and fixed with 4% paraformaldehyde (PFA) in PBS at pH 7.4 and washed three times with PBS. Permeabilization and blocking were carried out for 1 h at room temperature with saponin solution (0,1% saponin, 0,05% sodium azide in PBS) and 1% of BSA. Then cells were incubated with the primary conjugated anti-Ki67-AlexaFluor488 antibody (ThermoFisher Scientific, Waltham, MA, USA. Cat.# 11-5698-82. 1:100 dilution in blocking buffer) at 4ºC overnight. Nuclei were stained with Hoechst 33342 (Invitrogen, ThermoFisher Scientific). Images were acquired with a fluorescence microscope Leica DM5500B (Centre for Scientific Instrumentation, University of Granada) and then analyzed with ImageJ Software that allows the counting of Ki67 positive nuclei and measuring the fluorescence intensity of the labeling with Ki67 antibody. Images were taken from three random sites on the same slide and the experiment was conducted in triplicate.

2.13. Analysis of gene expression profile in HCT116 cell monolayer and secondary spheroids.

To evaluate the impact of the treatments on the gene expression of several mediators involved in apoptosis, proliferation, stemness and angiogenesis, total RNA was isolated from attached HCT116 cells after being treated with 25 µM of tigecycline and 50 µM of 5-FU for 24h. For total RNA isolation Maxwell® 16 Total RNA Purification Kit (Promega,

Madison, Wisconsin, United States) with DNase treatment was used following the manufacturer's recommendations. RNA was then quantified using NanoDrop™2000 (ThermoFisher Scientific, Waltham, MA, USA) and reverse transcribed using the High-Capacity cDNA reverse Transcription Kit (Applied Biosystems, Waltham, MA, USA; Thermo Fisher Scientific) following the manufacturer's instructions. 12.5 ng/mL of cDNA was used for qPCR analysis. qPCR was performed using FAST qPCR Master Mix and predesigned TaqMan assays (ThermoFisher Scientific, Waltham, MA, USA): human *MYC* (Hs00153408_m1), human *AXIN2* (Hs00610344_m1) and Glyceraldehyde-3-phosphate dehydrogenase (*GAPDH)* (4326317E).

Secondary colonospheres derived from HCT116 were treated with tigecycline 25 µM or 50 µM for 6 h and total RNA was then extracted using cold NucleoZOL (Macherey-Nagel, Düren, Germany, Cat.#740404.200) following the manufacturer's indications, followed by standard phenol/chloroform isolation. Then, RNA was quantified in a NanoDrop™2000 and 3 µg of total RNA was reverse transcribed into complementary DNA (cDNA) using the M-MLV reverse transcriptase (Cat.# M1705), oligo (dT) primers (Cat.# C110A), RNasin® ribonuclease inhibitor (Cat.# N2511) and a 10 mM dNTP mix (all from Promega, Madison, WI, USA) following the manufacturer's indications. Next, cDNA samples were stored at -20ºC until further use. MasterMix qPCR SyGreen kit (PCR Biosystems Ltd, London, UK) was used for carrying out qPCRs of different genes. This MasterMix employs SYBR green as reported. Each reaction was performed in optical-grade 48-well plates, employing an Eco™ Real-Time PCR thermocycler (Illumina, San Diego, CA, USA). Results were normalized to the expression of *GAPDH* transcripts. Relative expression levels were calculated according to the 2–ΔΔCt method, and samples were measured in triplicate. Specific primer sequences are presented in Table 3.

2.1. Analysis of protein expression in HCT116 and CMT93 cell lines.

For evaluating the levels of selected proteins in attached HCT116 cells, these were treated with tigecycline (25 µM or 50 µM) and 5-FU (50 µM) for 48 h (n=3). Similarly, secondary spheroids obtained from HCT116 and CMT93 cell lines were treated with tigecycline at 25 µM or 50 µM for 48 h (n=3). In both cases, cells in the supernatant and

Gene name	Primer sequence 5'→3'	Species	Annealing T (ºC)	RefSeq accesion number
Gapdh	FW 5'- CCATCACCATCTTCCAGGAG RV 5'- CCTGCTTCACCACCTTCTTG	Mouse/Human	60	NM_001289726.1
CDH1	FW 5'-TACATCTCCCTTCACAGC RV 5'-ATAGATTCTTGGGTTGGGTC	Human	55	NM_004360.5
SNAI1	FW 5'-TGCCCTCAAGATGCACATCCGA RV 5'-GGGACAGGAGAAGGGCTTCTC	Human	55	NM_005985.4
CD44	FW 5'- GTGATGGCACCCGCTATGTC RV 5'- AACCTCCTGAAGTGCTGCTCC	Human	55	NM_001202555.2
NOTCH2	FW 5'-GGGACCCTGTCATACCCTCT RV 5'-GAGCCATGCTTACGCTTTCG	Human	55	NM_024408.4
SOX2	FW 5'- GCTACAGCATGATGCAGGACCA RV 5'- TCTGAGAGCTGGTCATGGAGTT	Human	55	NG_101211.1
NANOG	FW 5'-TCCTGAACCTCAGCTACAAAC RV 5'-GCGTCACACCATTGCTATTC	Human	55	NM_001355281.2
CDH2	FW 5'- GTTTTATGGTGAAGTTCCTGAG RV 5'- TATGGGGTTGATCCTTATCG	Human	55	NM_001792.5
CTNNB1	FW 5'- CTTGGAATGAGACTGCTG- RV 5'- AGAGTGAAAAGAACGATAGC	Human	55	XM_047447477.1
Tnfa	FW 5'- AACTAGTGGTGCCAGCCGAT RV 5'- CTTCACAGAGCAATGACTCC	Mouse	56	NM_001278601.1
Il6	FW 5'- TAGTCCTTCCTACCCCAATTTCC RV 5'- TTGGTCCTTAGCCACTCCTTC	Mouse	60	NM_031168.2
Il17a	FW 5'- TCCAGAAGGCCCTCAGACTA RV 5'- AGCATCTTCTCGACCCTGAA	Mouse	59	NM_010552.3
Il23a	FW 5'- AATCTCTGCATGCTAGCCTG RV 5'- AGTTGGCTGAGTCCTAGTAG	Mouse	55	NM_031252.2
Ccnd1	FW 5'- AACACTTCCTCTCCAAAATG RV 5'- GAACTTCACATCTGTGGC	Mouse	55	NM_001379248.1
Angpt2	FW 5'- CAACTACAGGATTCACCTTAC RV 5'- GTACTGTGCATTCAAGTTGG	Mouse	55	NM_007426.4
Mmp9	FW 5'- TGGGGGGCAACTCGGC RV 5'- GGAATGATCTAAGCCCAG	Mouse	59	NM_013599

Table 3. RT-qPCR primer sequences and associated RefSeq accession numbers

those attached were subjected to protein extraction with RIPA buffer (Cat.# R0278) mixed with a cocktail of proteases and phosphatases inhibitors (aprotinin, leupeptin, dithiothreitol, sodium orthovanadate, phenylmethanesulfonyl fluoride, iodoacetamide, sodium fluoride and sodium molybdate) (Sigma-Aldrich, Madrid, Spain) following the manufacturer's instructions.

For nucleus fractionation, Abcam protocol (Accessed 17/02/2023. Available online: https://www.abcam.com/ps/pdf/protocols/Nuclear%20fractionation%20protocol.pdf) was followed. Briefly, after 48 h of treatment, supernatant was removed and cells were scratched in the presence of NP-40 lysis buffer composed of HEPES, $MgCl_2$, KCl, 1,4-Dithiothreitol (DTT) and NP-40. Then, cells were rested on ice for 30 minutes and centrifuged at 3000 rpm for 10 min at 4 ºC. Cytoplasmic proteins remained in the supernatant and the pellet was lysed with a buffer composed of HEPES, $MgCl_2$, EDTA, DTT, glycerol and NaCl. Sonicator was used for proper homogenization and samples were centrifuged at 17000 G after being rested on ice for 30 minutes. The lysate contained the nuclear fraction.

Once the proteins were extracted, the total amount of these were quantified by bicinchoninic acid (BCA) (Cat.# D8284) method described by Smith et al., (1985) (514). Then, 40-60 µg of protein were heated at 96 °C for 5 minutes in a 4x Laemmli sample buffer (Bio-Rad, California, USA) mixed with 10% of β-mercaptoethanol. Proteins were separated on sodium dodecyl sulphate-polyacrylamide gel electrophoresis (SDS-PAGE, 6-12% polyacrylamide under reducing conditions) and electro-transferred to a PVDF membrane (Cat.# IPVH00010). Membranes were blocked with 3% BSA or 5% non-fat dry milk in PBS plus 0.1% Tween 20 according to the manufacturer instructions for each antibody. The utilized primary antibodies were incubated at 4°C overnight and are included in Table 4. We also used anti-mouse IgG (1:3000 dilution, Cat.# 7076 [Cell signaling]) and anti-rabbit IgG (1:5000 dilution, Cat.#A9169) HRP-conjugated secondary antibodies for 1 h of incubation at room temperature. Finally, selected proteins were detected with the Western Lightning™ Chemiluminescence Reagent Plus (PerkinElmer Spain SL). Signal acquisition was performed using a LAS-4000 image system (Fujifilm, Life Science, Cambridge, MA, USA) or a ChemiDoc image system (Bio-Rad). Control of protein loading and transfer was conducted by detection of β-actin (ACTB) levels for cytoplasmic proteins, and β1-laminin (LMNB1) for nuclear proteins. The quantification of bands was performed by densitometric analysis using ImageJ software (Free Software Foundation Inc). Antibodies were used following the manufacturer's indications and are presented in Table 4.

Antibody	Reference	Company
Anti-phospho AMPKα	4188	Cell signaling
Anti-AMPKα	2532	Cell signaling
Anti-phospho MAPK(p38)	9211	Cell signaling
Anti-MAPK(p38)	9212	Cell signaling
Anti-UCP1	sc-293418	Santa Cruz
Anti-COX2	12282	Cell signaling
Anti-phospho-AKT	9271	Cell signaling
Anti-AKT	9272	Cell signaling
Anti-IL6	12912	Cell signaling
Anti-CTNNB1	9587S	Cell signaling
Anti-phospho-CTNNB1	9566S	Cell signaling
Anti-MYC	sc-40	Santa Cruz
Anti-LMNB1	12586S	Cell signaling
Anti-ACTB	sc-47778	Santa Cruz
Anti-STAT3	9139	Cell signaling
Anti-phospho-STAT3	9131	Cell signaling
Anti-CASP8	sc-81656	Santa Cruz
Anti-BID	2002	Cell signaling
Anti-CASP9	sc-56076	Santa Cruz
Anti-CASP7	9492	Cell signaling
Anti-CASP3	9661S	Cell signaling
Anti-PARP1	9542S	Cell signaling
Anti-BAX	sc-7480	Santa Cruz
Anti-BCL2	sc-7382	Santa Cruz
Anti-Cytocrhome C oxidase	4280	Cell signaling
Anti-TP53	sc-126	Santa Cruz
Anti-BIM	2933s	Cell signaling
Anti-ATF6	IMG-273	LuBioScience
Anti-HSPA5	3177S	Cell signaling
Anti-DDTI3	2895S	Cell signaling
Anti-phospho-JNK/SAPK	9251S	Cell signaling
Anti-JNK/SAPK	9252S	Cell signaling
Anti-phospho-JUN	2361S	Cell signaling
Anti-JUN	9165S	Cell signaling
Anti-SNAI1	sc-271977	Santa Cruz
Anti-CDH1	sc-21791	Santa Cruz

Table 4. Primary antibodies used in Western Blot assays.

3. *IN VIVO* STUDIES

All studies were carried out in accordance with the "Guide for the Care and Use of Laboratory Animals" as promulgated by the National Institute of Health and the protocols approved by the Ethic Committee of Laboratory Animals of the University of Granada (Spain) (Ref. No. 28/03/2016/030 and 23/10/2019/174). The experimental procedures were performed in accordance with the ARRIVE guidelines (515, 516). All the animals were housed in makrolon cages, maintained in an air-conditioned atmosphere with a 12 hour light-dark cycle and provided with free access to tap water and food.

3.1. High fat diet induced obesity model

Male C57BL/6J mice (7–9 weeks old) were obtained from Charles River Laboratories (Lyon, France) and fed with either a standard chow diet (13% calories from fat, 20% calories from protein, and 67 % calories from carbohydrates) (Global diet 2014; Harlan Laboratories, Barcelona, Spain) or a HFD with 60 % of its caloric content derived from fat (Purified diet 230 HF; Scientific Animal Food & Engineering, Augy, France). Then, two independent assays were performed to separately evaluate the activity of both plant extracts *Thymus serpyllum* and *Morus alba.*

In the first one, mice were randomly assigned to different groups (n = 10): control SD, control diet treated with thyme extract (150 mg/kg), obese (HFD) and three obese groups treated with different doses of the thyme extract (50, 100 and 150 mg/kg). The selection of these extract doses were made based on previous results obtained in our research group (465).

In the second one, mice were randomly divided into four groups (n = 10): control SD, control obese (HFD) and two obese groups treated with metformin (250 mg/kg) or *Morus alba* leaf extract (10 mg/kg). The selection of this extract dose and metformin dose were made based on previous results obtained in our research group (455, 517).

The administration of the extracts and metformin (dissolved in 0.1 mL of sterile water) was performed daily by oral gavage from the beginning of the experiment. The control groups received daily the same volume of the vehicle used to administer the extract. The treatments were followed for 10 weeks and animal body weight as well as food and water intakes were regularly measured twice a week. Energy efficiency was calculated as the ratio of weight gain (g) to caloric intake (Kcal). After mice were sacrificed by cervical dislocation, liver and abdominal, epididymal and scapular brown fat were collected, cleaned, and weighed. Liver and fat weight indices were calculated by dividing their

weights (g) by tibia length (cm). The samples were then frozen in liquid nitrogen and stored at -80 ºC until further analysis.

3.2. Colitis-associated colorectal cancer model

Female C57BL/6 mice (7–9 weeks old) (Charles River Laboratories, Lyon, France) were subjected to a process of CAC induction by administering one intraperitoneal initial dose of AOM at 10 mg/kg followed by three cycles of DSS (36-50 KDa, MP Biomedicals, Illkirch Cedex, France) added in the drinking water. Each DSS cycle consisted of 2% DSS for 1 week followed by a recovery period of 2 weeks with normal drinking water. Mice were divided into five groups (n = 10): healthy control, CAC control, and three CAC groups treated daily with tigecycline 25 mg/kg or tigecycline 50 mg/kg by oral gavage or every three days with 5-FU 15 mg/kg intraperitoneally. The treatment started 50 days after the beginning of the assay, on the day of initiation of the third cycle of DSS, and lasted for 7 weeks. The control groups received PBS following the same protocol.

On the day of the mice sacrifice, spleen, mesenteric lymph nodes (MLNs) and colon were aseptically excised, rinsed with PBS and weighed. The colon length was also measured under a constant load (2 g). Then, bowels were open longitudinally along the antimesenteric border, trying to avoid cutting through the tumor. Macroscopic tumors were counted, and images were acquired for measuring the size of each tumor with the ImageJ software (Free Software Foundation Inc). Colon samples were taken for RT-qPCR, Western blot, flow cytometry and fixed for histological studies.

3.3. Tumor xenograft model.

HCT116 secondary colonospheres-derived cells were xenotransplanted into 8-week-old NOD scid mice gamma (NSG). Two different assays were performed. In the first one, secondary colonospheres were treated with tigecycline 50 µM for 48 h, counted and then subcutaneously inoculated in the left flank of NSG mice (n = 8). The same number of untreated cells (60.000 cells) derived from these secondary colonospheres were injected into the right flank of the same mice to compare the tumor evolution in both conditions. In the second assay, untreated cells derived from secondary colonospheres (60.000 cells) were subcutaneously injected in the right flank of NSG mice and then randomly divided into three different experimental groups (n = 8): a control untreated group and two groups of mice treated with two doses of tigecycline (25 mg/kg/day and 50 mg/kg/day). Mice started to be treated 2 weeks after cell injection and they were treated for 3 weeks by oral gavage. Cells were injected in both assays in 0.05 mL matrigel and

0.05 mL supplemented DMEM without FBS. Moreover, tumor growth was assessed twice weekly using a caliper and the tumor volume was calculated by the following formula (2):

$$(2) \quad V = length^2 \times width \times \pi/6$$

At the end of the assay, control mice and those orally treated with tigecycline 50 mg/kg (n = 3-4) were intravenously injected with 100 µL of 2-deoxyglucose marked with a fluorescent probe (Xenolight, PerkinElmer, Waltham, Massachusetts, USA, Cat.# 760561) and after 3 hours, animals were observed under the image *in vivo* system IVIS Spectrum (Caliper Life Sciences, Perkinelmer, Waltham, Massachusetts, USA) (Excitation: 745 nm and Emission: 820 nm). Images were taken and the intensity of fluorescence was measured with the IVIS software.

After mice sacrifice, tumors were weighed and samples were taken and stored for further expression, Western blot and histological analysis.

3.4. Obesity-associated colorectal cancer model.

Eight-week-old female C57BL/6 mice (Charles River Laboratories, Lyon, France) were fed using SD and HFD described above (section 3.1) for 10 weeks. Then, CAC was induced in all mice as commented above, in section 3.2. At the beginning of the third cycle of DSS, HFD-fed mice were randomly divided into two groups, one of them was used as HFD control and the other was treated with tigecycline at 25 mg/kg. Therefore, the following groups of mice were used in this study (n = 7): control SD with CAC, control HFD with CAC and a group of HFD mice with CAC and treated daily with tigecycline (25 mg/kg) for 7 weeks. The control groups received PBS following the same protocol.

On the day of the mice sacrifice, colons were harvested, rinsed with PBS, and the weight and length were measured. As commented in section 3.2., colons were open longitudinally and the number and size of tumors were analyzed with ImageJ software (Free Software Foundation Inc). Additionally, samples of inguinal fat were taken from each mice and together with colon specimens were stored until further analysis.

3.5. Disease activity index evaluation in AOM/DSS models.

The severity of the colitis in both AOM/DSS models was macroscopically evaluated by the disease activity index (DAI) score in each DSS cycle by a blind observer. The DAI (scale 0-4) was determined by considering the weight loss, stool consistency and the presence of fecal blood according to the criteria previously described (477) and indicated in Table 5.

Score	Weight loss	Stool consistency	Rectal bleeding
0	None	Normal	None
1	1-5%	Mucous traces	Perianal blood traces
2	5-10%	Loose stools	Blood traces on stools
3	10-20%	Diarrhoea	Bleeding
4	>20%	Gross diarrhoea	Gross bleeding

Table 5. DAI value is the media of weight loss, stool consistency and bleeding scores

3.6. Colonoscopy

Day before the euthanasia in the AOM/DSS study, both tumor number and size was assessed via colonoscopy. Moreover, the tumor score was obtained according to the size of the tumor as previously described by Becker C et al., (518) by a blind observer. For the colonoscopy, mice were fasted for 12 hours and anesthetized with isoflurane (IsoVet, BBraun, Barcelona, Spain). Then, the Coloview Mini Endoscopic System (Karl Storz, Tuttlingen, Germany) connected to an air pump was inserted into the mouse colon and videos were acquired for evaluating the tumor score.

3.7. Glucose tolerance test.

Those mice used to develop the HFD induced obesity model and the obesity-associated CRC model were subjected to a glucose tolerance test one week before the end of the experiment. For this purpose, mice fasted for 6 h and were given a 2 g/kg of body weight glucose solution by intraperitoneal injection. Blood was collected from the tail vein at 0, 15, 30, 60 and 120 min after injection. A handheld glucometer (Contour XT, Ascensia Diabetes Care, S.L., Barcelona, Spain) was used to determine glucose levels.

3.8. Plasma determinations.

At the end of the treatment, mice were fasted overnight and sacrificed under isoflurane anesthesia. Blood samples were collected by cardiac puncture in tubes containing heparin, centrifuged for 20 min at 5000× g at 4 ºC and the plasma frozen at −80 ºC. Plasma glucose, insulin, LDL (low-density lipoprotein)-cholesterol and HDL (high-density lipoprotein)-cholesterol concentrations were measured by colorimetric methods using Spinreact kits (Spinreact, S.A., Girona, Spain). The Insulin Resistance Index was calculated according to the homeostatic model of insulin resistance (HOMA-IR) using the following formula (3):

(3) HOMA-IR = Fasting Glucose (mM) × (Fasting Insulin (µunits/mL)/22.5)

Moreover, plasma levels of LPS were measured using a Pierce™ Chromogenic Endotoxin Quant Kit (Thermo Scientific, Inc.,Waltham, MA, USA, Cat.# PIA39552) following manufacturer's instructions.

3.9. Histological studies.

Histological studies were carried out in different samples: (1) colonic longitudinal sections for swiss roll technique; (2) colon cross sections taken 1 cm from the rectum; (3) liver; (4) epididymal adipose tissue and (4) tumor sections. Regardless of source, these sections were fixed in 4% PFA for 24 h and embedded in paraffin. Depending on the further application, tissues were then dehydrated in distinct solutions.

- Increasing concentrations of ethanol (70%, 85%, 95% and 100%) followed by paraffin embedding and trimming in 5 µm sections for haematoxylin and eosin staining.
- Increasing concentrations of sucrose (15% and 30%) followed by OCT (Tissue-Tek® O.C.T. Compound, Sakura® Finetek, Torence, CA, USA) embedding, frozen with isopentane at -40 ºC and trimming in a cryostat in 8 µm sections for oil red staining and immunofluorescence experiments.

A pathohistological evaluation was performed by an independent pathologist. Thus, the histological index was calculated based on macroscopically visible damage (normal mucosa, adenoma, adenocarcinoma, invasive adenocarcinoma) as previously described by Yang et al., (2022) (421). Moreover, adipocyte size was measured in adipose tissue sections using Fiji imaging software with the Adiposoft v1.16 plugin.

3.9.1. Haematoxylin and eosin staining.

Sectioned paraffin samples (colon, liver, adipose tissue and tumors) were deparaffinized by immersing them two times in xylene (20 minutes/each) and rehydrated with decreasing concentrations of ethanol (100%, 96%, 80%, 70% 50%, dH_2O and tap water) for 10 minutes/each. For colon samples, first, histochemical staining of mucins was performed using 1% of alcian blue and 3% of acetic acid (in 70% ethanol) for 30 minutes. Next, running tap water was used to remove the excess staining and conventional haematoxylin and eosin staining was performed. Briefly, slides were immersed for 1 minute in undiluted Harris Haematoxylin (Casa Álvarez, Cat.# 10-2332) and treated with 3% acetic acid for differentiation and bluing. Then, slides were dipped in 0.5% eosin (Casa Álvarez, Cat.# 10-3002) for 30 seconds, dehydrated in increasing concentrations of ethanol and clarified in xylene before being mounted with DPX media (Casa Álvarez, Cat.# 10-3500). Images were taken from three random sites on the same slide under a

light microscope (Carl Zeiss Primo Star, Oberkochen, Germany) from the Centre for Scientific Instrumentation, University of Granada.

3.9.2. Oil red staining

Cryosections were rinsed with 2-propanol at 60% in distilled water for 20 seconds and stained with freshly prepared Oil Red O working solution (0.5 g Oil Red O powder (Cat.# O0625), 60% 2-propanol in dH_2O, boiled and filtered) for 20 minutes. Then, samples were immersed in 2-propanol 60% for 40 seconds and washed in dH_2O. Finally, slides were mounted with aqueous mounting medium (100 mL dH_2O, 100 g glycerol, 17 g gelatin and 1 g phenol). Images were taken from three random sites on the same slide under a light microscope (Carl Zeiss Primo Star, Oberkochen, Germany) from the Centre for Scientific Instrumentation, University of Granada.

3.9.3. Immunofluorescence.

Cryosections of PFA-fixed OCT-included colonic tissue were used for immunofluorescence assays. For this purpose, slides were brought to room temperature for 10 minutes and then OCT was carefully removed from the tissue surroundings. An hydrophobic pen (Cat.# Z377821) was used to delimit the staining area. These slides were then used for different purposes:

3.9.3.1. Assessment of cell proliferation by Ki67 staining

In order to evaluate the cell proliferation levels in colonic specimens, delimited cryosections were hydrated with PBS 1x for 10 min at room temperature. Then, permeabilization, blocking and staining with anti-Ki67-AlexaFluor488 and Hoechst 33342 steps were achieved as detailed in 2.12. section. Mouse colonic images were taken on a confocal laser microscope ZEISS LSM900 of the Unit of Optical Microscopy and Cellular Imaging of the ibs.GRANADA. Samples were excited with the 405-nm solid-state laser for visualization of Hoeschst labeling and the 488-nm laser for AF488 labeling. Images were captured using a 20x dry objective with a numerical aperture of 0.8 and analyzed with ImageJ Software that allows the counting of Ki-67 (marker of proliferation Ki-67) positive nuclei and measuring the fluorescence intensity of the labeling with anti-KI67 antibody.

3.9.3.2. Assessment of apoptosis by TUNEL assay

Apoptosis in colonic sections was evaluated using the DeadEnd Fluorometric TUNEL system (Promega, Madison, Wisconsin, USA, Cat.# 3250) following the manufacturer's

indications. Briefly, after tissue delimitation with the hydrophobic pen, samples were hydrated with PBS 1x for 10 minutes at room temperature. Then, tissue permeabilization was carried out with proteinase K (20 µg/mL). After 10 minutes, samples were washed and equilibrated for 10 minutes with equilibration buffer (200 mM dimethylarsinic acid, 25 mM Tris-HCl, 0.2 mM DTT, 0.25 mg/ml BSA and 2.5 mM cobalt chloride). Then, slides were incubated with the terminal deoxynucleotidyl transferase (rTdT) enzyme for 1 hour at 37ºC in presence of the equilibration buffer and a nucleotide mix fluorescently labeled. Negative controls were incubated without the rTdT enzyme. Finally, colonic sections were washed with 2x saline sodium citrate buffer and PBS 1x. Hoechst 33342 (Invitrogen, ThermoFisher Scientific, Waltham, MA, USA) was used to stain the nuclei, and the images were acquired with a Leica DM5500B fluorescence microscope (Leica Camera AG, Wetzlar, Germany) (Centre for Scientific Instrumentation, University of Granada). Acquisition of green channel (positive signals) was performed using the 470 nm excitation laser. Images were taken from three random sites on the same slide and ImageJ software (Free Software Foundation Inc) was used for counting positive nuclei.

3.10. Protein extraction and quantification, Western blot analysis and TBARS.

Colonic, liver, adipose tissue and tumor samples were weighed and suspended in a lysis buffer (1:5 w/v) containing 20 mM of HEPES (pH 7.5), 10 mM EGTA, 40 mM β-glycerophosphate, 2.5 mM $MgCl_2$, 1% Igepal®, protease inhibitors – 1mM DTT, 2 µg/mL aprotinin (Cat.# A1153), 5 µg/mL leupeptin (Cat.# L9783), 1 mM phenylmethylsulfonyl Fluoride (PMSF) (Cat.# P7626), 1 µg/mL iodoacetamide (Cat.# I6125) – and phosphatase inhibitors – 2 mM sodium orthovanadate (Cat.# S6508), 5 mM sodium fluoride (Cat.# S1504) and 1 mM sodium molybdate (Cat.# 331058). Lysis was performed for 2 hours in a tube rotator at 4ºC. Next, lysates were stored at -80ºC until further use. Subsequently, samples were defrosted and centrifuged at 10.000xg for 15 minutes at 4ºC. Supernatants were collected and the concentration of protein was measured with the BCA method and used for Western blot analysis as previously described at 2.14. section, using the antibodies presented in Table 4.

Liver and colonic lysates from mice were used to determine the lipid oxidation by measuring the amount of thiobarbituric acid reactive substances (TBARS) (519). Briefly, the malondialdehyde (MDA) resulting from lipid peroxidation reacts with the thiobarbituric acid (TBA) dissolved in dimethyl sulfoxide (DMSO), which was used in the extraction method. The products of the reaction are TBARS, a pink chromogen which was

measured at 535 nm. TBARS levels were expressed as µM/mg protein in liver and colonic tissue.

3.11. Analysis of gene expression by RT-qPCR.

Total RNA from liver, colon and inguinal fat samples from mice was isolated using the RNeasy® Mini Kit (Qiagen, Hilden, Germany) following the manufacturer's instructions. A NanoDropTM2000 (ThermoFisher Scientific, Waltham, MA, USA) was used to measure the total RNA amount and sample purity considering the 260/230 and 260/280 ratios. Then RNA from these tissues was reverse transcribed into cDNA, which was used for qPCR, employing an Eco™ Real-Time PCR system (Illumina, San Diego, CA, USA), as were normalized to the expression of *Gapdh* transcripts and relative expression was calculated using the 2–ΔΔCt method. Samples were measured in triplicate and the specific primer sequences are presented in Table 3.

3.12. Vascular Reactivity Studies and NADPH Oxidase Activity.

The isometric tension measurement was studied using thoracic aortic rings isolated from mice and suspended in the myograph (model 610M, Danish Myo Technology, Aarhus, Denmark) (520) with Krebs solution (mM: NaCl 118, KCl 4.75, $NaHCO_3$ 25, $MgSO_4$ 1.2, $CaCl_2$ 2, KH_2PO_4 1.2 and glucose 11) at 37 ºC and gassed with 95% O_2 and 5% CO_2 (pH 7.4). Length-tension characteristics were obtained via the myograph software (Myodaq 2.01 (Danish Myotechnologies, Hinnerup, Denmark)), and the aortae were loaded to a tension of 5 mN. After a 90 min stabilization period, cumulative concentration-response curves to acetylcholine (10^{-9} M–10^{-5} M) were performed in intact rings that were pre-contracted with U46619 (10^{-8} M). Relaxant responses to acetylcholine were expressed as a percentage of pre-contraction.

Moreover, NADPH oxidase activity in aortic rings was determined by the lucigenin enhanced chemiluminescence assay (521). Aortic rings from all experimental groups were incubated for 30 min at 37 ºC in HEPES-containing physiological salt solution (pH 7.4) of the following composition (in mM): NaCl 119, HEPES 20, KCl 4.6, MgSO4 1, Na_2HPO_4 0.15, KH_2PO_4 0.4, $NaHCO_3$ 1, $CaCl_2$ 1.2 and glucose 5.5. Aortic production of O_2^- was stimulated by the addition of NADPH (100 M). Rings were then placed in tubes containing physiological salt solution, with or without NADPH. Subsequently, lucigenin was injected automatically at a final concentration of 5 mol/L. NADPH oxidase activity was determined by measuring luminescence over 200 s in a scintillation counter (Lumat LB 9507, Berthold, Germany) in 5-s intervals and calculated by subtracting the basal

values from those in the presence of NADPH. Vessels were then dried and dry weight determined. NADPH oxidase activity was expressed as relative luminescence units (RLU)/min/mg dry aortic ring.

3.13. Flow cytometry.

The abundance of immune cell populations in different tissues was analyzed using flow cytometry. More detailed information has been provided below.

3.13.1. Colonic tissue.

Colons from AOM/DSS mice were removed and washed with PBS 1x. Then, cells from the colon were isolated using an enzymatic digestion media composed of DNase I (Cat.# DN25) 50 U/mL, Collagenase XI (Cat.# C7657) 300 U/mL and Dispase II (Roche Applied Systems, Basel, Switzerland, Cat.# 04942078001) 0,08 U/mL for 40 minutes at 37 ºC while shaking. After this time, 2 mM EDTA diluted in PBS was used for neutralizing the enzyme activity. Then, in order to obtain the cell pellet, the samples were filtered with a 70 µm cell strainer and centrifuge at 500 x g for 5 minutes at 4ºC. Lastly, cells were counted and stained as detailed at the end of this section.

3.13.2. Mesenteric lymph nodes

MLNs were harvested from AOM/DSS mice and mashed between two 70 µm filters using a syringe plunger in a precooled plate. Cell suspension was then filtered through a 70 µm filter, counted and incubated with phorbol 12-myristate 13-acetate (PMA) (50 ng/mL) (Cat.# 79346) and ionomycin (1 µg/mL) (Cat.# I0634) in the presence of GolgiPlug™ (1:1000 dilution) (BD Bioscience, Thermo Fisher Scientific, Waltham, MA, USA, Cat.# 555029) for 4 h at 37ºC in order to stimulate the intracellular cytokines production. After this, cells were centrifuged at 400 x g for 5 minutes at 4ºC and stained as detailed at the end of this section

3.13.3. Blood.

Blood samples were collected from anesthetized AOM/DSS mice (xylazine [10 mg/kg] and ketamine [100 mg/kg]) by cardiac puncture with a 25 gauge heparinized needle and transferred to tubes containing heparin. Then, erythrocytes were lysed with a red cells lysis buffer (155 mM NH_4Cl, 12 mM $KHCO_3$ and 0.1 mM EDTA in distilled water at pH 7.25) and blood cells were counted and stained as detailed below.

For staining, colon and MLNs derived cells were first incubated with Fixable Viability Dye eFluor™ 780 (eBioscience™ Thermo fisher Scientific, Waltham, MA, USA, Cat.# 65-0865-14) while Zombie Aqua fixable viability dye (BioLegend, San Diego, CA, USA, Cat.# 423102) was used for blood cells for 20 min at 4ºC. At the same time, samples were incubated with FcR blocking reagent (Miltenyi Biotec, Auburn, CA, USA, Cat.# 130-092-575) and 123 counting eBeads™ (Invitrogen, ThermoFisher Scientific, Cat.# 01-1234-42) previously diluted in PBS 1x. Next, samples and FMO controls were stained with intracellular and surface-staining antibodies for 30 min at 4°C with a different mix of antibodies diluted in FACS buffer (0.1% BSA and 2 mM EDTA) following the manufacturer's indications as detailed in Table 6. Then, samples were washed with PBS 1x to remove excess antibody and fixed with a paraformaldehyde solution (Invitrogen, ThermoFisher Scientific, Cat.# 00-8222). Finally, cells were resuspended in 200 µL of PBS 1x and acquired using a BD FACSymphony™ A5 Cell Analyzer. Results were analyzed with the Flowjo v10.6.2 software (FlowJo LLC) following the different gating strategies (Figure 11-13).

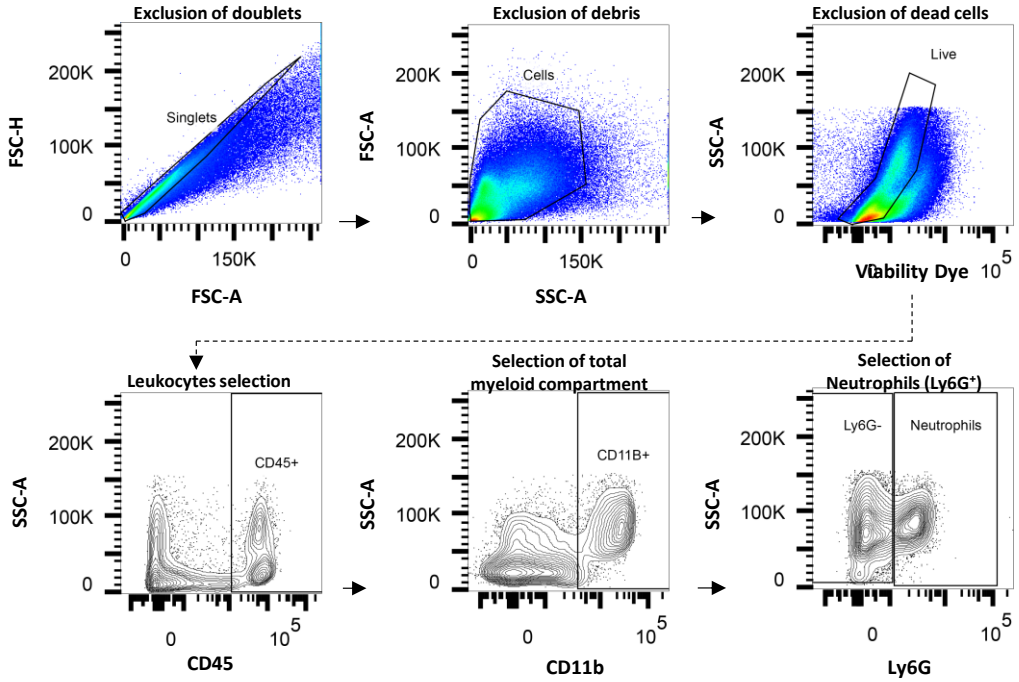

Figure 11. Gating strategy employed for the analysis of colon myeloid populations in AOM/DSS mice.

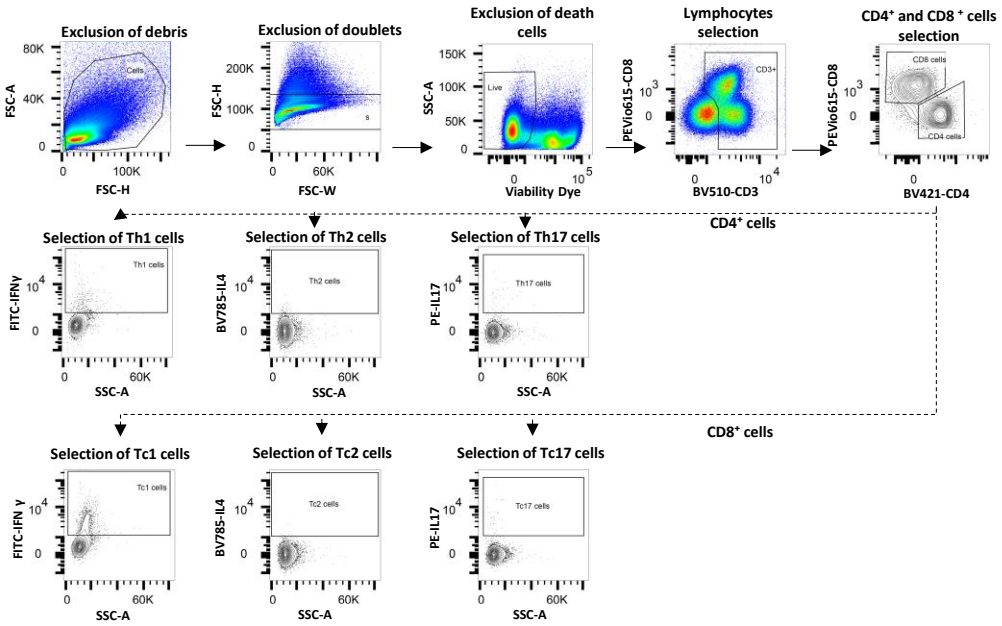

Figure 12. Gating strategy employed for the analysis of MLNs lymphoid populations in AOM/DSS mice.

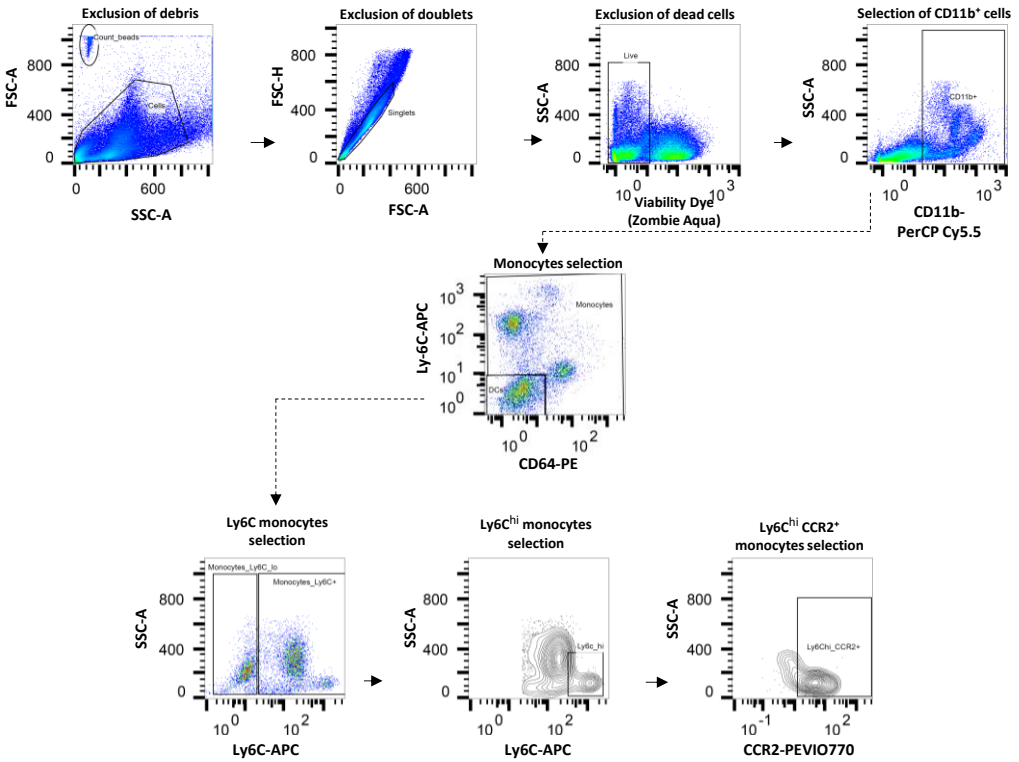

Figure 13. Gating strategy employed for the analysis of blood monocytes populations in AOM/DSS mice.

3.14. Microbiota analysis.

Stool samples from each mouse were aseptically collected on the end-point day of the assay. Faecal DNA was isolated using the QIAamp PowerFecal Pro DNA Kit (Qiagen, Hilden, Germany). Total DNA was amplified and a library for the V3–V4 or V4-V5 region of 16S rRNA was constructed in accordance with the 16S Metagenomic Sequencing Library Preparation Illumina protocol. Sequencing was executed using the MiSeq 2 × 300 platform (Illumina Inc., San Diego, CA, USA) in accordance with the manufacturer's instructions.

4. STATISTICAL AND CORRELATION ANALYSIS

Statistical analysis was performed using the GraphPad Prism version 7 software (GraphPad Software, Inc, San Diego, CA, USA) with statistical significance set at $P<0.05$. All data are represented as mean (SEM) of at least 3 independent experiments/biological replicates unless otherwise stated in the figure legends. The Mann-Whitney U test for nonparametric data was used for the analysis of the DAI. For the rest of the data, multiple comparisons between groups were performed using the one-way ANOVA followed by Tukey's test. In the present Thesis, two different methods were used for indicating statistical significance and the method used is indicated at the bottom of each figure. The system that uses the "*" and "#" symbols, P-values are as follow: *P < 0.05, **P < 0.01, ***P < 0.001, ****P < 0.0001; and $^{\#}$P < 0.05, $^{\#\#}$P < 0.01, $^{\#\#\#}$P < 0.001, $^{\#\#\#\#}$P < 0.0001. Moreover, the letter-based system has been used for *in vivo* assays and in this occasion, when P<0.05, different letters among groups were used and groups that share the same letter do not statistically differ. When no statistical significance among any of the compared groups was obtained, the graph showed any letter or symbol.

In the study that evaluate the effect of a the thyme extract on a murine model of diet-induced obesity, different parameters were intercorrelated with the "R" statistical software package (version 4.0.0; https://www.r-project.org/, accessed on 1 December 2021) using the "rcorr()" function in the "Hmisc" package to compute the significance levels for Pearson's correlations and the function "corrplot()", in the package of the same name to create a correlogram. The correlation matrix was reordered according to the correlation coefficient using the "hclust" method.

Moreover, in the study that evaluate the effect of tigecycline in a murine model of CAC, a heat map depicting the macroscopic parameters, molecular changes and patterns of

microbial abundance of untreated CAC mice and those treated with both doses of tigecycline was constructed within the “R” statistical software using the “Hmisc” and “ggplot2” packages. Spearman’s correlations of each parameter were previously calculated with “R” software.

Bioinformatic analysis of gut microbiota samples were performed using QIIME2 software package (2021.11 version) and “R” statistical software package (version 3.6.0; https://www.r-project.org/). Demultiplexed sequences were loaded into the program and quality control was performed by trimming and filtering, depending on the quality scores of the sequences (522). Sequence data were obtained as FASTQ files, which were further processed using Mothur and DADA2 and Operational Taxonomic Units (OTUs) or amplicons sequence variants (ASVs) were obtained, respectively. Taxonomic assignment was calculated against the RDP (Ribosomal Database Project) (523) or SILVA reference database (524) and they were filtered to discard both Archaea and Eukaryota features. Additionally, those features that had a frequency lower than 10 were also removed from the data.

Alpha diversity and beta diversity were determined by the q2-diversity plugin in QIIME2. Differential abundance analysis was performed using the Wald test implemented DESeq2 v1.30.1 as previously described (525) within the “R” statistical software (version 4.0; https://www.r-project.org/). *EnhancedVolcano* package was used for constructing volcano-plots. Log2-fold-change (Log2FC) normalized values and the adjusted P-value (*Padj)* were used to construct Venn diagrams (Limma package) of differentially microbial communities up-regulated (log2FC>1.5 and *Padj<0.05)* and downregulated (log2FC<1.5 and *Padj<0.05)* among groups.

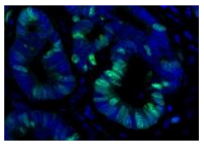

RESULTS

RESULTS

I. EVALUATION OF THE EFFECT OF PLANT EXTRACTS WITH PREBIOTIC PROPERTIES IN HIGH FAT DIET-INDUCED OBESITY: T*HYMUS SERPYLLUM* AND M*ORUS ALBA*.

1. EFFECT OF THE THYME EXTRACT ADMINISTRATION IN HIGH FAT DIET-INDUCED OBESITY.

1.1. Thyme extract reduces body weight gain in HFD-fed mice and improves glucose and lipid metabolic profile.

The administration of a HFD to mice resulted in a significant body weight gain increase compared to mice fed a SD (Figure 14A). Interestingly, the administration of the thyme extract at any of the doses tested (50, 100 and 150 mg/kg/day) ameliorated the body weight gain, leading to a significant reduction of this parameter from day 6 onwards, in comparison to control HFD-fed mice (Figure 14A). On the other hand, the treatment with the highest dose of extract to SD mice did not cause any differences in body weight gain when compared to untreated SD-fed mice (Figure 14A). Furthermore, we observed that this beneficial effect on body weight gain was achieved even though food intake was similar in all groups of mice fed with a HFD (Figure 14A). Consequently, the treatments were able to significantly decrease energy efficiency in comparison with untreated HFD-fed mice (Figure 14A). In concordance with the body weight gain, untreated obese mice exhibited heavier fat deposits (abdominal, epididymal and brown fat) than SD -fed mice and HFD-fed mice treated with thyme extract (Figure 14B). Additionally, liver weight was significantly increased in HFD-fed mice when compared to SD mice and the treatment with thyme extract led to a substantially reduction in the weight of this organ (Figure 14B).

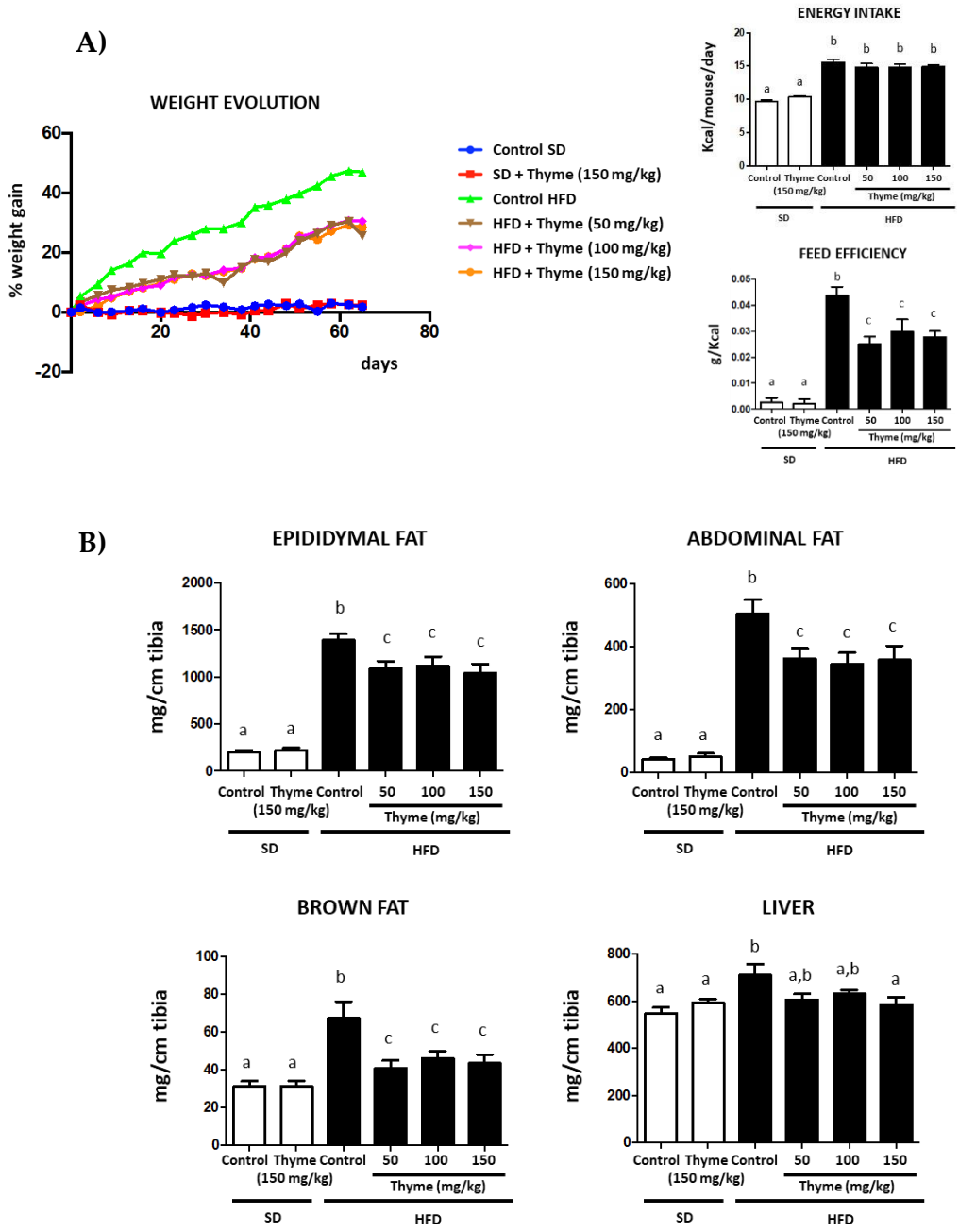

Figure 14. Effects of Thyme extract administration on: *(A) body weight evolution, energy efficiency and energy intake and (B) liver and fat deposits weights. Data are graphed as means ± SEM (n = 10). Groups with different letters statistically differ (p < 0.05).*

Histological studies carried out in the epididymal fat tissue showed that adipocytes of HFD control mice were significantly larger than those derived from the adipose tissue of

SD mice (Figure 15). This effect was evidenced by a substantially increase in the area and perimeter of adipocytes in control obese mice. Conversely, mice treated with thyme extract exhibited a statistically significant reduction in both adipocyte area and perimeter, as well as in immune cell infiltrations (Figure 15).

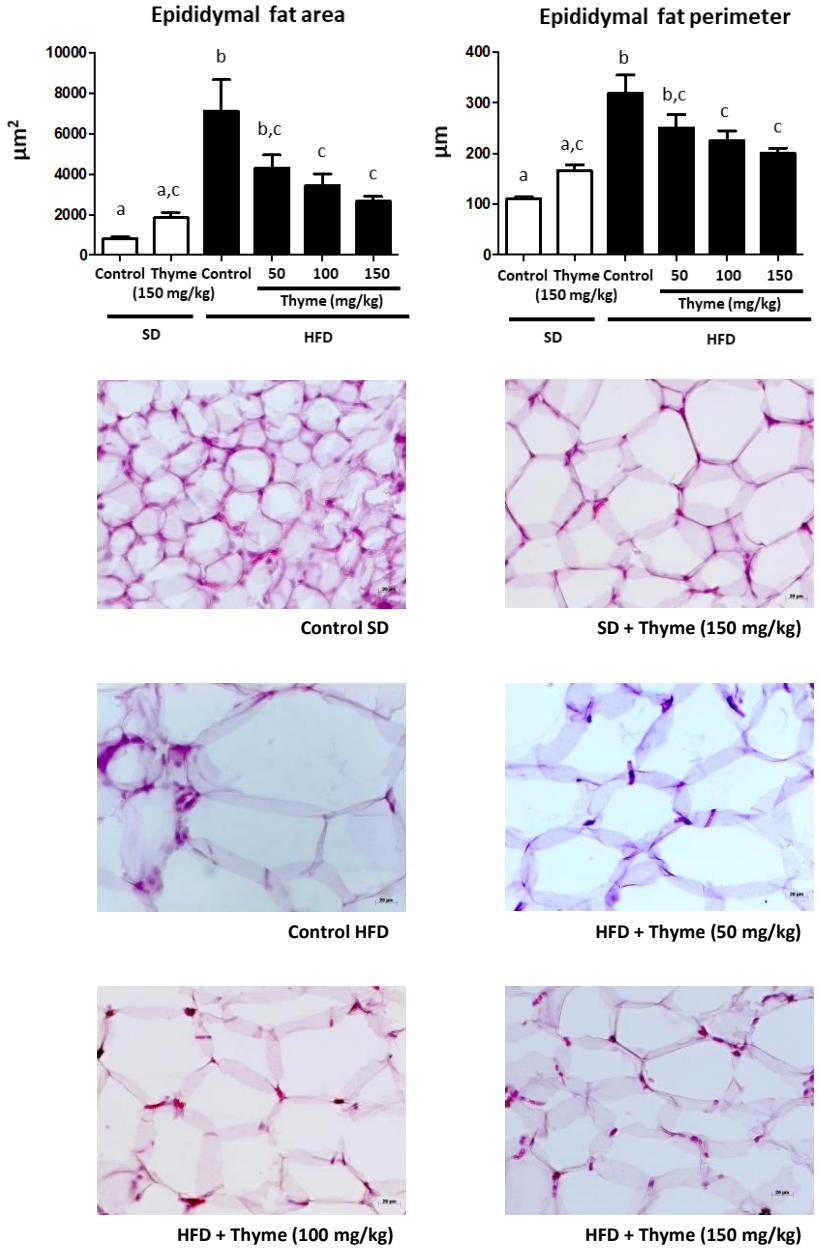

Figure 15. Effects of the treatment with thyme extract on epididymal adipose tissue histology*. (A) Haematoxylin and eosin staining (scale bar = 20 µm) and on area/perimeter of epididymal adipocytes. Data are presented as means ± SEM (n = 10).*

Groups with different letters statistically differ ($p < 0.05$). Red arrows show cell immune infiltrations.

Similarly, the histological study of the liver sections showed important obesity-associated steatosis, mainly characterized by intense fat deposition, as well as the infiltration of inflammatory cells. The oil red staining marked the lipid droplet accumulation in the tissue, and thus, the red coloration was more evident in samples from non-treated obese mice than in non-obese mice (Figure 16A). Conversely, the administration of thyme extract to HFD-fed mice clearly improved hepatic steatosis that was evidenced in the obese mice without treatment (Figure 16A).

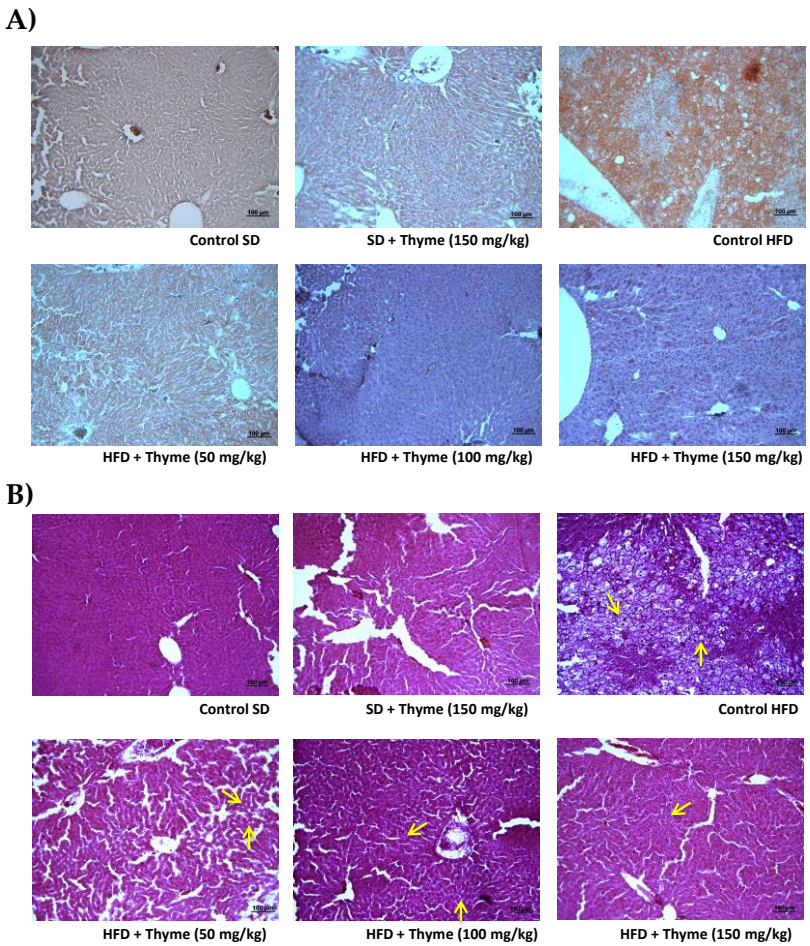

Figure 16. Impact of Thyme extract treatment on fat deposits in liver tissue sections *stained with (A) oil red and haematoxylin and (B) with haematoxylin and eosin. Yellow arrows indicate the presence of lipid vacuoles in the cytoplasm of hepatocytes and red arrows show cell immune infiltrations.*

Correspondingly, hepatic steatosis was evidenced by the increase of both fat deposition and infiltration of cells when these sections were stained with haematoxylin and eosin, since the number of fat drops observed (yellow arrows), the cell infiltration (red arrows), and the ballooning process was higher in the hepatocytes from HFD-fed mice and the administration of thyme extract resulted in a significant reduction of these steatosis markers (Figure 16B)

Also, thyme extract ameliorated the glucose metabolism impairment observed in control obese mice, as evidenced by the glucose tolerance test performed one week before the endpoint of the study. Control obese mice showed significantly higher glucose level peaks than non-obese groups; however, thyme extract treatment to obese mice significantly reduced plasma glucose levels in comparison with the untreated HFD group from 30 min onwards, which resulted in a significant reduction in the area under the curve (AUC) (Figure 17A). At the end of the assay, plasma samples were taken to determine different biochemical parameters, including glycemic levels. Blood glucose levels determined at the end of the assay were significantly higher in control HFD mice when compared to lean groups, and the treatment with thyme reduced them dose-dependently (Figure 17B). Although there were no differences in insulinemia between different groups, thyme extract was able to reduce insulin resistance indicated by HOMA-IR index (Figure 17B).

Glucose transporter type 2 (GLUT2), which is mainly expressed in the liver, has an important role in the glucose uptake by hepatocytes. A downregulation in the expression of this transporter has been reported in obesity-associated insulin resistance (526), which has been confirmed in the present study. However, the treatment with thyme extract significantly upregulated the expression of *Glut2* in hepatocytes (Figure 17C). Similarly, AMP-activated protein kinase (AMPK) is a key component in the regulation of metabolism and it acts suppressing anabolic pathways and stimulating the catabolic ones, thus resulting in the heightening of energy expenditure (527). Accordingly, we observed a statistically significant downregulation of *Ampk* gene expression in the liver from untreated HFD-fed mice compared to those receiving a SD, thus revealing the situation of altered glucose and lipid metabolism in obese mice (Figure 17D). In turn, thyme extract at 150 mg/kg/day significantly restored the expression of *Ampk* in comparison with control obese mice (Figure 17D). These results were supported by Western blot analysis of the phosphorylated and active form of AMPK and total levels of this enzyme. An increase in the pAMPK/AMPK ratio was observed in HFD mice treated with the thyme extract compared to control HFD mice (Figure 17D).

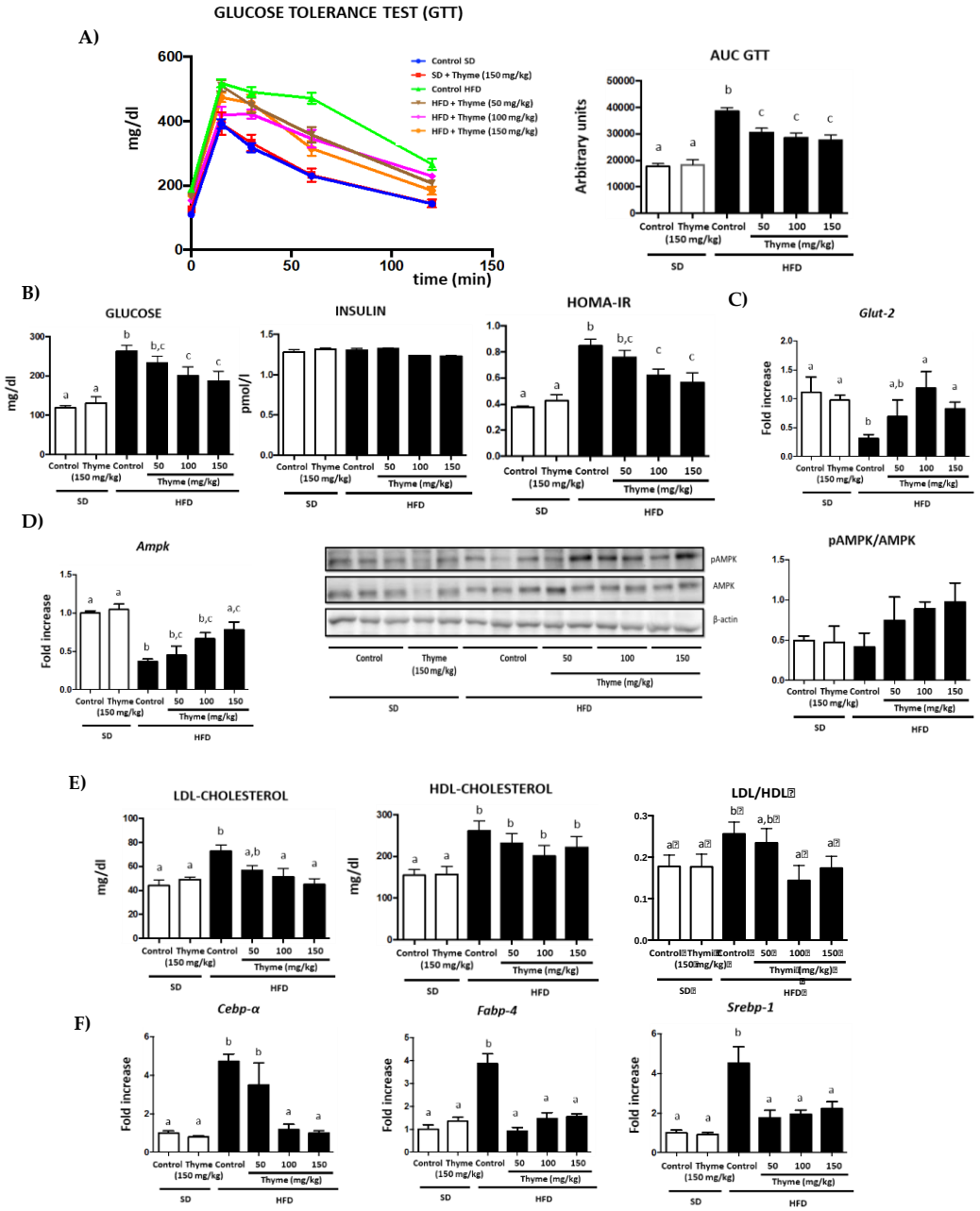

Figure 17. Effects of thyme extract treatment on: *(A) glucose tolerance test (GTT), (B) plasma glucose and insulin levels, as well as on HOMA-IR (C) Glut2 gene expression in liver. (D) Ampk gene expression and pAMPK/AMPK ratio evaluated by Western blot. (E) Plasma LDL- and HDL-cholesterol levels, as well as on LDL/HDL ratio. (F) Expression of genes involved in adipogenesis in epididymal fat (Cebpa, Fabp4 and Srebp1). Data*

are presented as means ± SEM (n = 10). Groups with different letters statistically differ (p < 0.05).

In addition, control HFD-fed mice displayed modifications in lipid metabolism since obesity was associated with hypercholesterolemia in comparison with non-obese mice, and increased levels of both LDL-cholesterol and HDL-cholesterol were observed (Figure 17E). Interestingly, thyme extract administration resulted in significant reductions of LDL-cholesterol and HDL-cholesterol (Figure 17E). In fact, the administration of the extract (100 and 150 mg/kg) significantly ameliorated LDL/HDL ratio in comparison with untreated obese mice (Figure 17E).

Also, we aimed to characterize the impact of the treatment with thyme on adipogenesis markers. Obesity induction was associated with an increase in the expression of the transcription factors CCAT/enhancer binding protein (C/EBPα), fatty acid binding protein 4 (FABP4) and sterol regulatory element-binding protein-1 (SREBP1) (Figure 17F). The administration of thyme resulted in a significant downregulation of these transcription factors (Figure 17F).

1.2. Thyme extract mitigates the chronic inflammation associated with obesity.

Obese phenotype was intimately related to a higher degree of inflammation, highlighted by an increased gene expression of *Tnfa, Il6, Mcp1* in liver and *Tnfa* and *Il6* epididymal fat of control obese mice (Figure 18A). However, the administration of thyme extract to obese mice resulted in a significant reduction in the expression of these proinflammatory mediators in both liver and fat (Figure 18A). Moreover, the expression of JNK proteins was significantly increased in control obese mice, both in the liver (*Jnk2*) and fat (*Jnk1* and *Jnk2*), when compared with non-obese mice, but reduced by the administration of thyme extract (Figure 18B).

LPS plays an important role in the development of chronic inflammation in obesity through the promotion of a metabolic endotoxemia (394), which is correlated with increased expression of Toll-like receptor (TLR) 4 (528). A significant increase in plasma LPS levels in control obese mice was observed and it was correlated with an upregulation of *Tlr4* expression in the liver (Figure 19A). Importantly, thyme administration to obese mice significantly reduced both plasma LPS levels and Tlr-4 expression (Figure 19A).

LPS absorption is associated with an increase of intestinal permeability. This impairment of epithelial barrier integrity was observed in control obese mice that showed a downregulation of the expression of different proteins associated with the intestinal

barrier function, such as zonula occludens 1 (*Zo-1*), Occludin and Mucin (*Muc*) 1 and 3 (Figure 19B). However, the administration of thyme extract to obese mice significantly increased the expression of these proteins (Figure 19B).

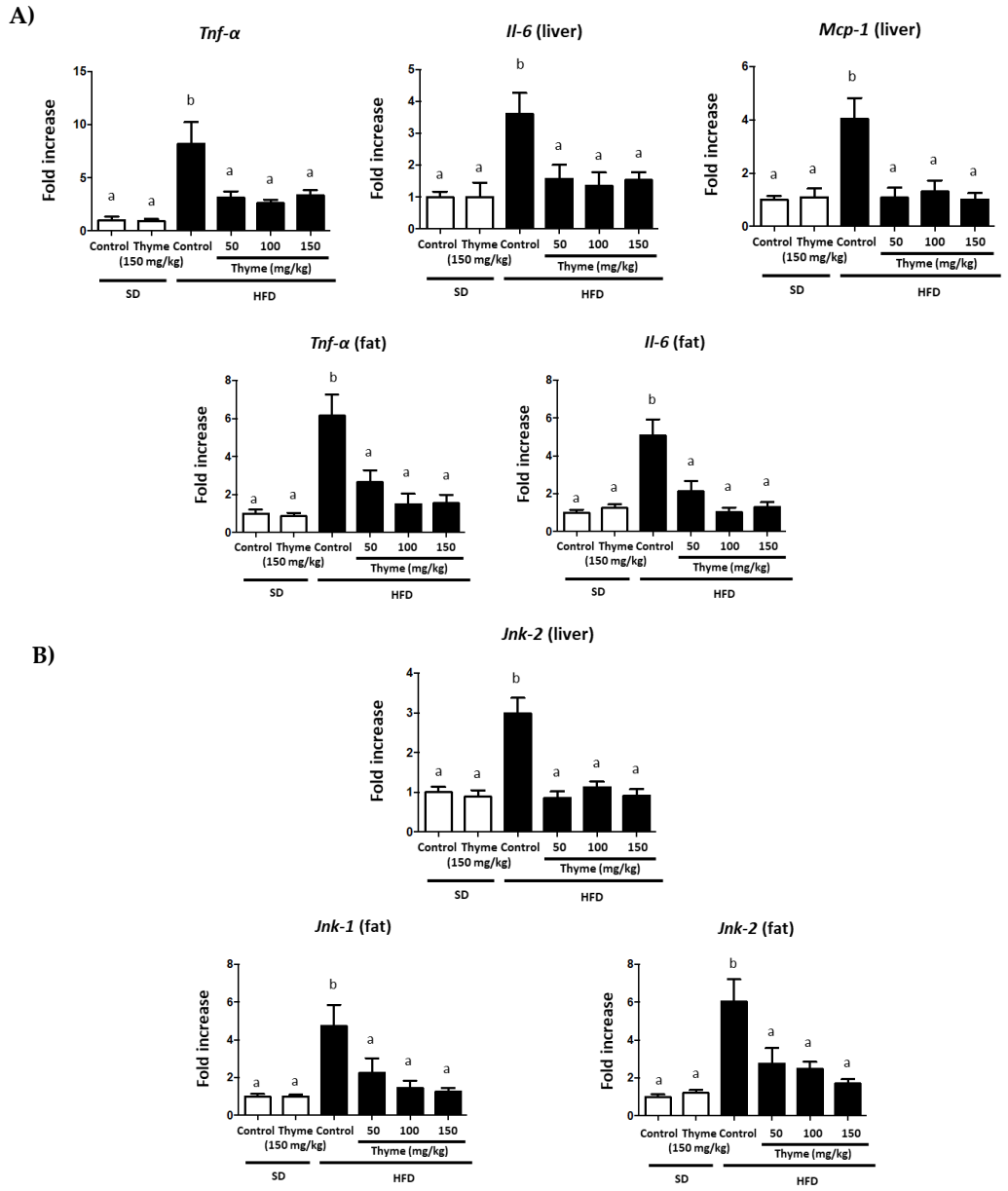

Figure 19. Impact of Thyme extract treatment on: *(A) Tnfa and Il6 gene expression levels in liver and fat, as well as Mcp1 in liver (B) and Jnk1 and Jnk2 in liver and fat. Data are expressed as means ± SEM (n = 10). Groups with different letters statistically differ (p < 0.05).*

A)

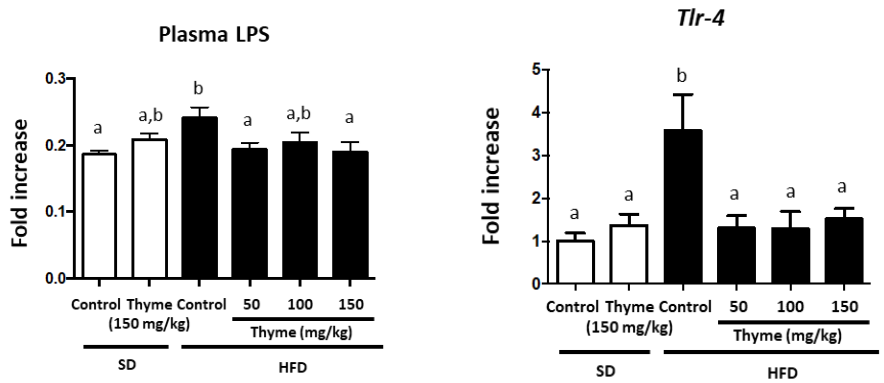

B)

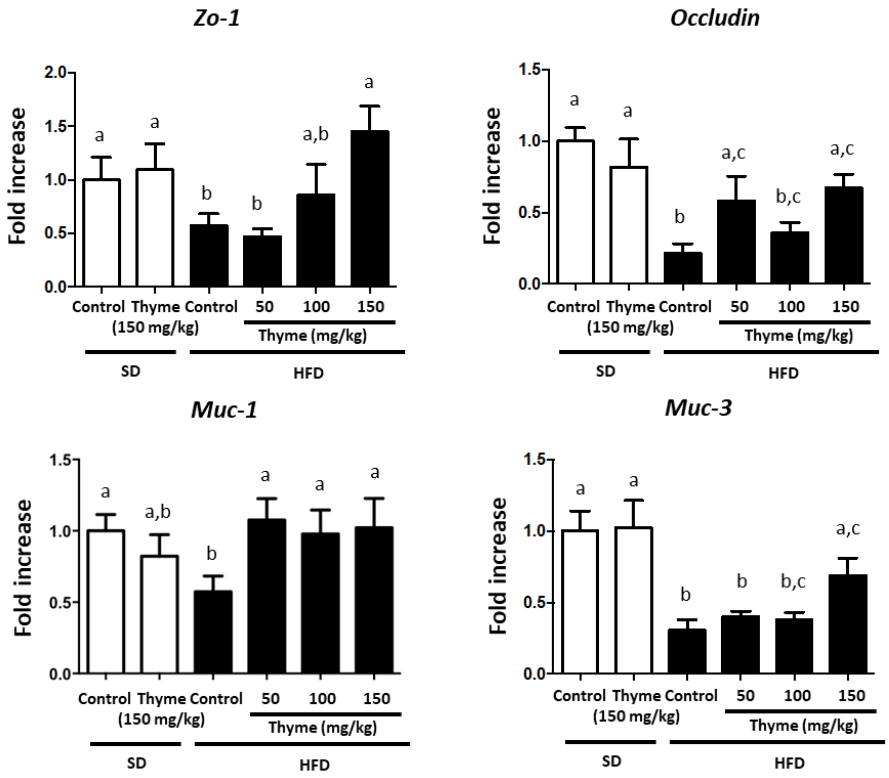

Figure 19. Effects of the treatment with the thyme extract on: *(A) plasma LPS levels and Tlr4 gene expression in liver. (B) mRNA levels of some markers of intestinal barrier integrity Zo-1, Occludin, Muc-1 and Muc-3. Data are expressed as means ± SEM (n = 10). Groups with different letters statistically differ (p < 0.05).*

1.3. Thyme extract administration prevents endothelial dysfunction and exerts an antioxidant response.

Aorta endothelium-dependent vasodilator responses to acetylcholine were evaluated in the different experimental groups. We found a significant relationship between obesity and endothelial dysfunction, since control obese mice showed a reduction in the maximal relaxant response to acetylcholine in comparison with SD mice (Emax values were 44.5 ± 3.9% and 79.4 ± 3.8% in the HFD and SD groups, respectively) (Figure 20A). Conversely, the administration of thyme extract to HFD mice ameliorated the relaxation response induced by acetylcholine without obtaining statistical differences in the Emax values compared to control SD mice (Figure 20A).

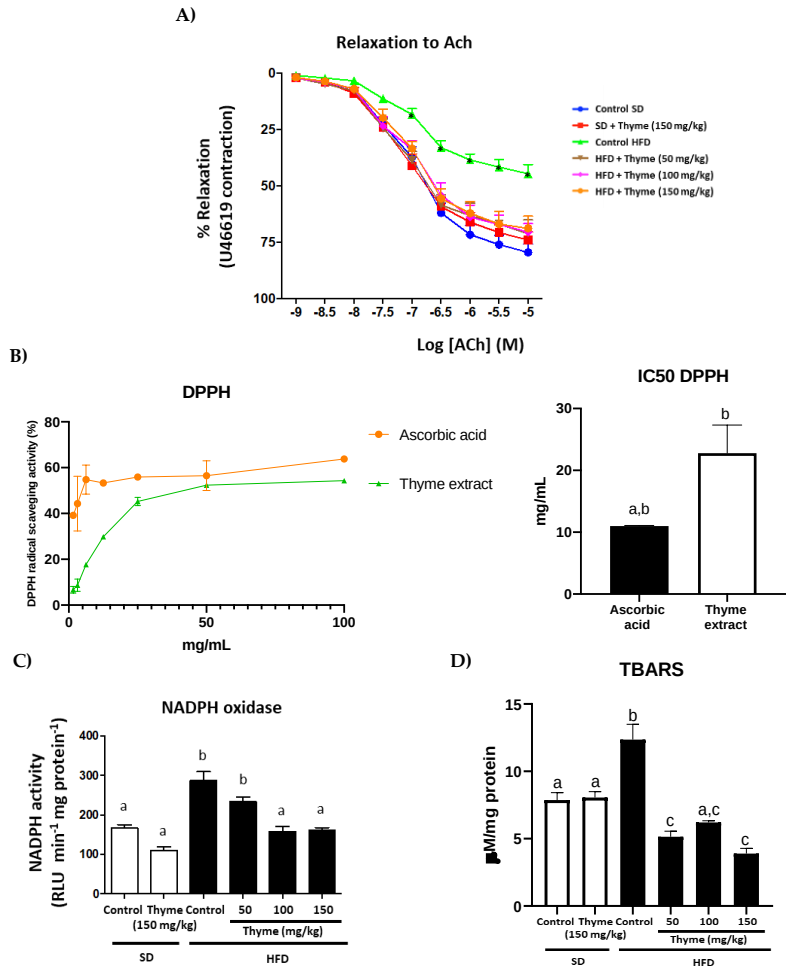

Figure 20. Impact of thyme extract on endothelial function and oxidative stress. *(A) Endothelium-dependent relaxation to acetylcholine after contraction with U46619. (B) DPPH activity scavenging of thyme extract and ascorbic acid and their IC_{50} values. (C) Aortic NADPH oxidase activity. (D) TBARS production in liver lysates. Data are*

expressed as means ± SEM (n = 10). Groups with different letters statistically differ (p < 0.05).

The antioxidant activity of the extract was also evaluated. Firstly, we aimed to determine the ability of the extract to neutralize the organic free radical DPPH, which is widely used in the evaluation of the antioxidant capacity of numerous compounds. We observed that thyme extract was able to neutralize the DPPH free radicals via hydrogen donating activity by 29.8%, 45.2%, 52.4% and 54.3%, at concentrations of 12.5, 25, 50 and 100 mg/mL, respectively (Figure 20B). Moreover, the IC_{50} value for thyme extract was 22.8 ± 4.5 mg/mL whereas the IC_{50} determined for ascorbic acids was 11 ± 0.1 mg/mL (Figure 20B).

Similarly, when NADPH oxidase activity was evaluated in aortic rings, this was significantly higher in HFD mice than in non-obese mice (Figure 20C); however, thyme extract significantly decreased it (Figure 20C). The antioxidant capacity of thyme extract was also evaluated by the TBARS assay in liver samples. According to reported studies, our analysis indicated that the mice that consumed the HFD exhibited TBARS values significantly higher than both SD groups (Figure 20D). Conversely, the administration of thyme extract in HFD-fed mice was able to significantly reduce the TBARS values (Figure 20D).

1.4. Thyme extract treatment restores gut dysbiosis in HFD fed mice.

Obesity-associated dysbiosis was observed when a microbiome analysis of the intestinal contents was performed in the different experimental groups (Figure 21). In fact, beta diversity determination through the principal coordinate analysis (PCoA) revealed clear differences in the microbial communities of control SD and untreated HFD mice (Figure 21A). Additionally, PCoA analysis showed a higher similarity between the microbial communities present in thyme-treated mice (100 and 150 mg/kg/day) and control lean mice than those present in the control HFD group (Figure 21A). Additionally, it was found that the most representative phyla in the gut microbiota of the different experimental groups were *Bacillota* (previously named *Firmicutes*) and *Bacteroidota* (previously named *Bacteroidetes*) (Figure 21A). Moreover, we evaluated the impact of the treatment on the F/B ratio, which is widely used as a marker of gut dysbiosis. This ratio was found significantly increased in control HFD mice compared to SD mice and the treatment with thyme extract at 150 mg/kg/day substantially restored the values of this ratio (Figure 21A).

Moreover, a significant decrease in the alpha diversity indexes (Chao1, phylogenetic diversity whole tree and Shannon) was observed in untreated obese mice in comparison with control SD-fed mice (Figure 21B). However, the highest dose of the thyme extract was able to significantly increase the Chao1 richness, obtaining similar values to those in non-obese mice (Figure 21B).

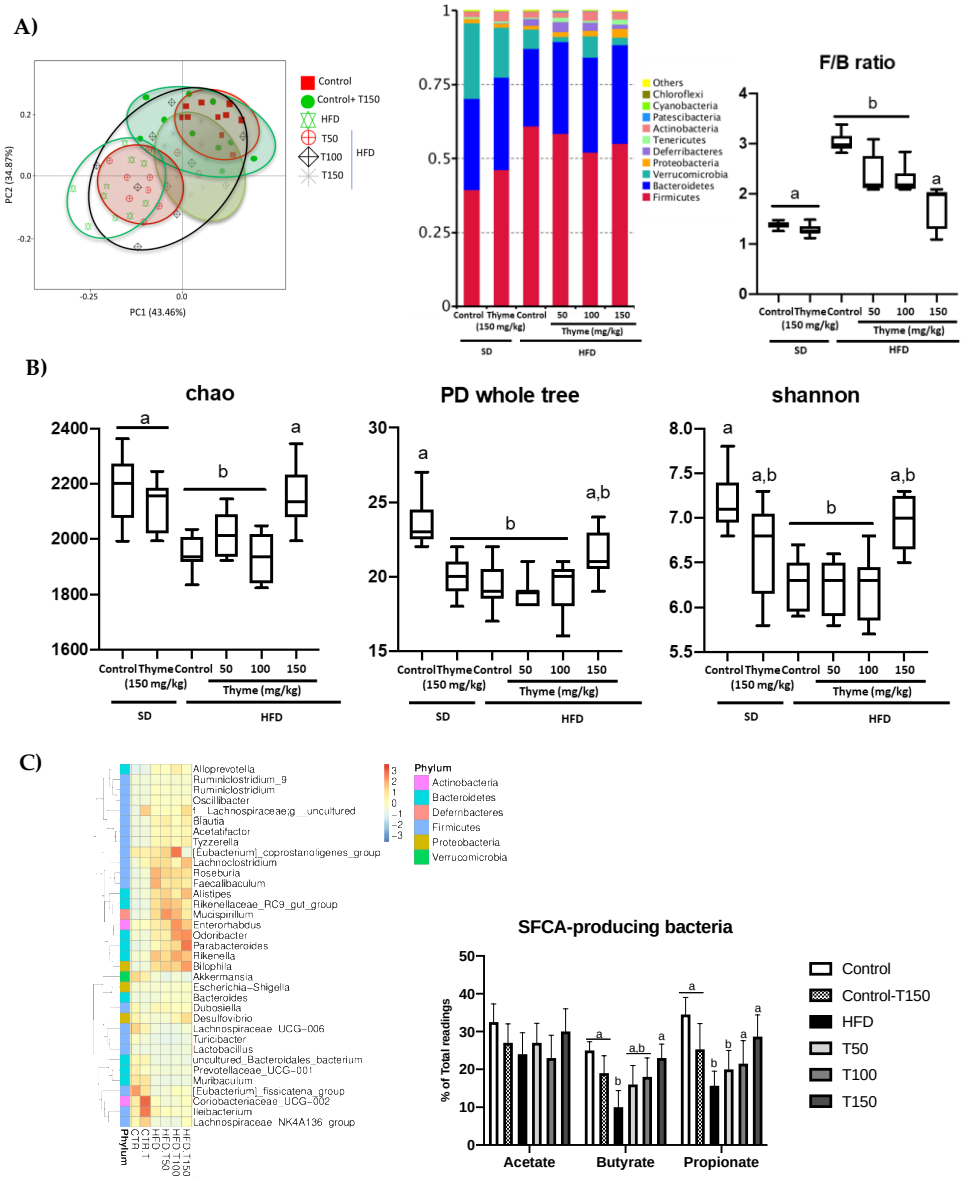

Figure 21. Effects of Thyme extract administration on: *(A) Beta-diversity by principal coordinate analysis score plot, bacterial community (phyla) and the F/B ratio; (B) microbiome alpha diversity (Chao1, PD whole tree and Shannon index) and (C) SCFAs-producing bacteria levels in each group of mice. Data are expressed as means ± SEM (n = 10). Groups with different letters statistically differ ($p < 0.05$).*

Then, the relative abundance of the different microbial genera present in the intestinal microbiota was studied and control HFD mice exhibited an increased proportion of *Faecalibaculum* and *Roseburia* (phylum Bacillota), *Mucispirillum* (phylum Deferribacteres) and *Rikenella* (phylum *Bacteroidota*), in comparison with non-obese mice (Figure 21C). Importantly, the proportion in the sequences of these bacterial genera was normalized with thyme treatment in obese mice (Figure 21C).

Lastly, SCFA-producing bacteria levels were analyzed in the faecal contents of each experimental group (Figure 21D). Levels of butyrate- and propionate-producing bacteria were found significantly downregulated in control HFD mice compared to untreated SD mice (Figure 21D). However, the treatment with the highest dose of thyme resulted in a significant increase in the counts of these bacteria (Figure 21D).

2. EFFECTS OF THE MULBERRY LEAF EXTRACT ADMINISTRATION IN HIGH FAT DIET-INDUCED OBESITY.

Different studies have previously reported the pharmacological properties exerted by extracts obtained from the leaves of *Morus alba*, including antioxidant, anti-inflammatory and anti-obesogenic activities (455, 529, 530). In order to know if the prebiotic properties of this extract could be involved in these actions, it was assayed in the experimental model of obesity induced by HFD in mice, with special attention to its impact on gut microbiota modulation. All these effects were compared with those obtained with metformin, a drug currently used in the treatment of type 2 diabetes.

2.1. *Morus alba* extract prevents body weight gain, reduces fat deposits and improves glucose tolerance.

As previously shown, the HFD consumption resulted in an increase in body weight gain in comparison with those mice fed with a SD from the first week (Figure 22A), which was significantly reduced by the treatment with metformin (Figure 22A). Similarly, the administration of the extract (10 mg/kg/day) significantly reduced the increase in body weight from day 10 onwards (Figure 22A). Interestingly, the inhibition in body weight gain shown by both treatments was not associated with a satiating effect; in fact, no significant differences were observed when energy intake was evaluated in the different HFD-fed groups of mice (Figure 22B). Then, both treatments induced a lower feed efficiency when compared to the control HFD fed group (Figure 22B).

Consistent with the body weight gain data, the deposits of epididymal, abdominal and brown fat were significantly higher in untreated HFD mice when compared to the SD group (Figure 23). Conversely, the treatment with the *Morus alba* extract resulted in a significant reduction of epididymal fat deposits. Similarly, mice treated with metformin exhibited a lower accumulation of epididymal and abdominal fat (Figure 23A). The expansion of fat depots is linked to a hypertrophy of the adipocytes, which was evidenced by a significant increase of the epididymal adipocyte area in untreated HFD-fed mice in comparison to SD-fed mice (Figure 23B). This adipocyte hypertrophy was significantly reduced in those mice treated with metformin or the plant extract (Figure 24B and C). In addition, mice treated with either *Morus alba* extract or metformin exhibited a lower infiltration of immune cells in epididymal adipose tissue sections when compared to untreated HFD-fed mice (Figure 23C)

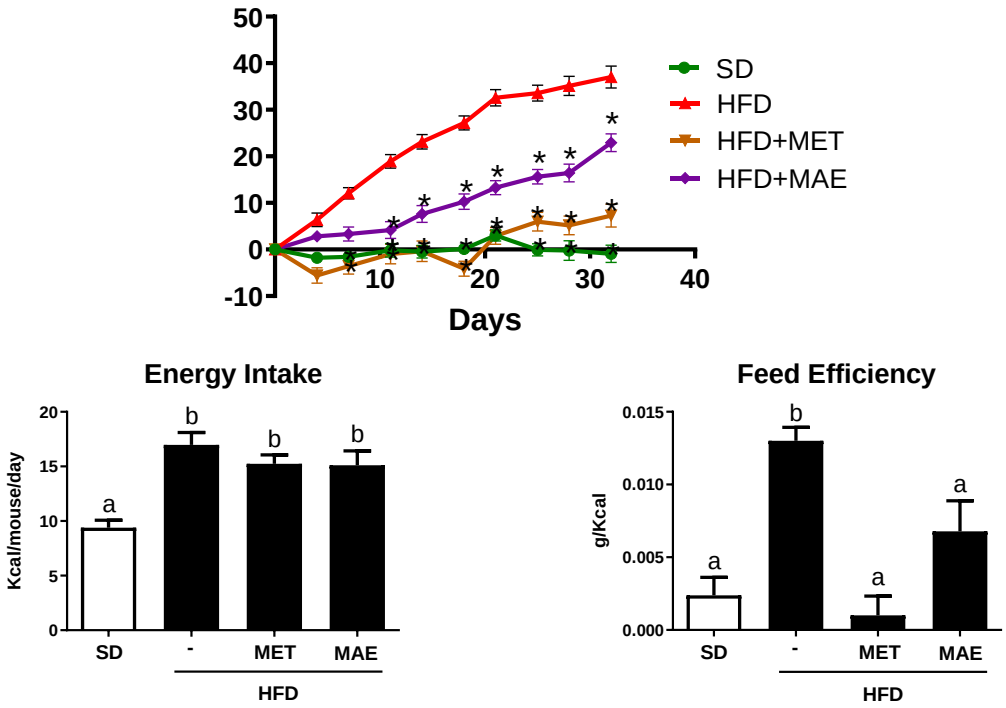

Figure 22. Effects of mulberry extract administration on body weight evolution, energy intake and feed efficiency. *Data are graphed as means ± SEM (n = 10). * = p < 0.05 vs. HFD control group. Groups with different letters statistically differ (p < 0.05).*

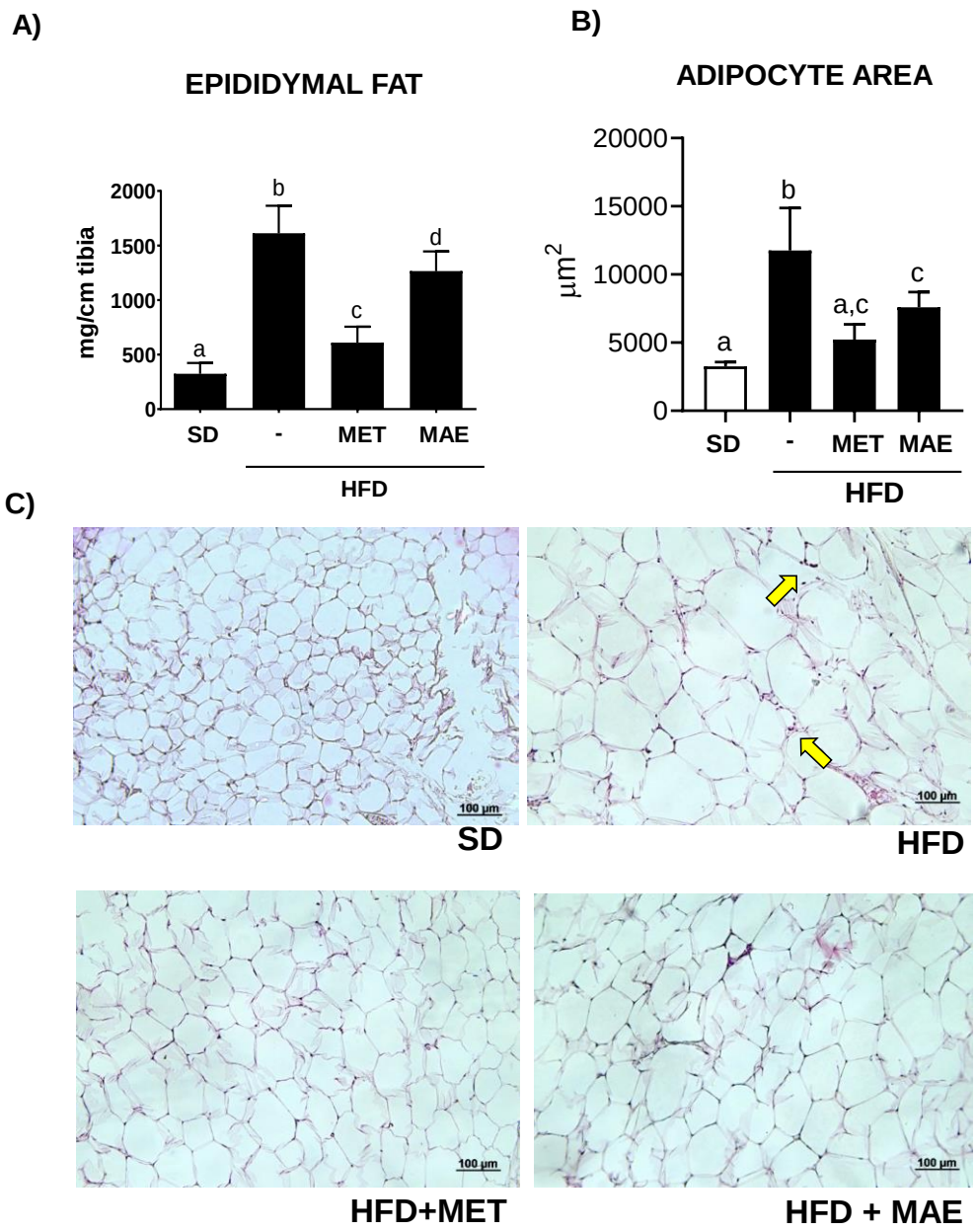

Figure 23. Impact of Morus alba extract supplementation on *(A) epididymal fat deposits weight and (B) on adipocyte area from (C) epididymal fat stained with haematoxilin and eosin. Groups with different letters statistically differ ($p < 0.05$). Yellow arrows show cell immune infiltrations.*

Considering the impact of the extract against the HFD diet induced adiposity, the hepatic steatosis process was also studied. As compared to SD control mice, exposure to HFD induced a significant accumulation of fat in the liver (macrovesicular steatosis) (Figure

24), which was characterized by the presence of lipid droplets (yellow arrows) within hepatocytes cytoplasm (Figure 24). The administration of the extract or metformin resulted in a significant reduction in hepatic steatosis, since hepatocytes displayed mainly a single small-sized lipid droplet or multiple lipid vesicles of very small size in their cytoplasm (Figure 24).

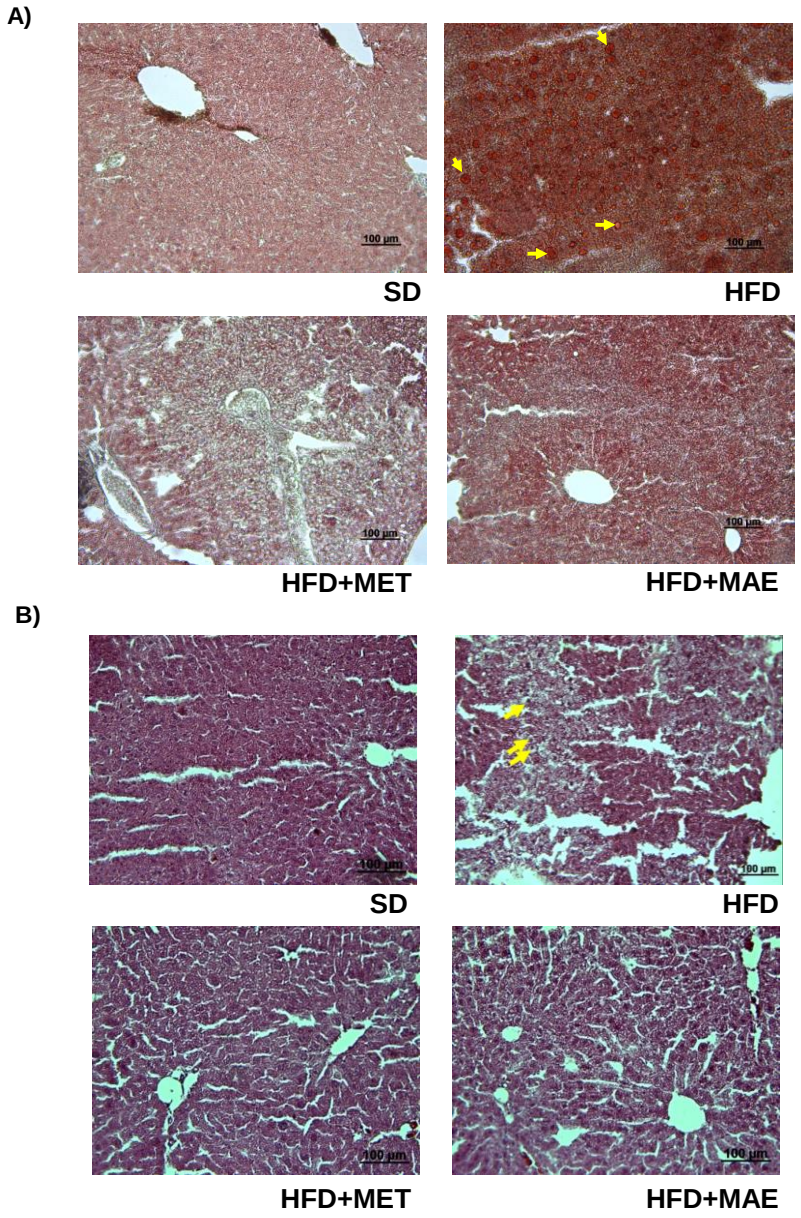

Figure 24. Impact of the Morus alba extract supplementation in hepatic steatosis induced by HFD-fed mice *evaluated by (A) oil-red staining and (B) haematoxilin and*

eosin staining. Yellow arrows indicate the presence of lipid vacuoles in the hepatocyte cytoplasm.

The effect of the *Morus alba* extract in the glucose homeostasis was also assayed through the glucose tolerance test in which glucose was intraperitoneally administered and glycemic levels were determined at different times. As it is shown in the glycemic curves represented in Figure 25A, control HFD-fed mice showed a higher peak of the glycemic values 15 min after glucose injection in comparison with control SD mice (Figure 25A).

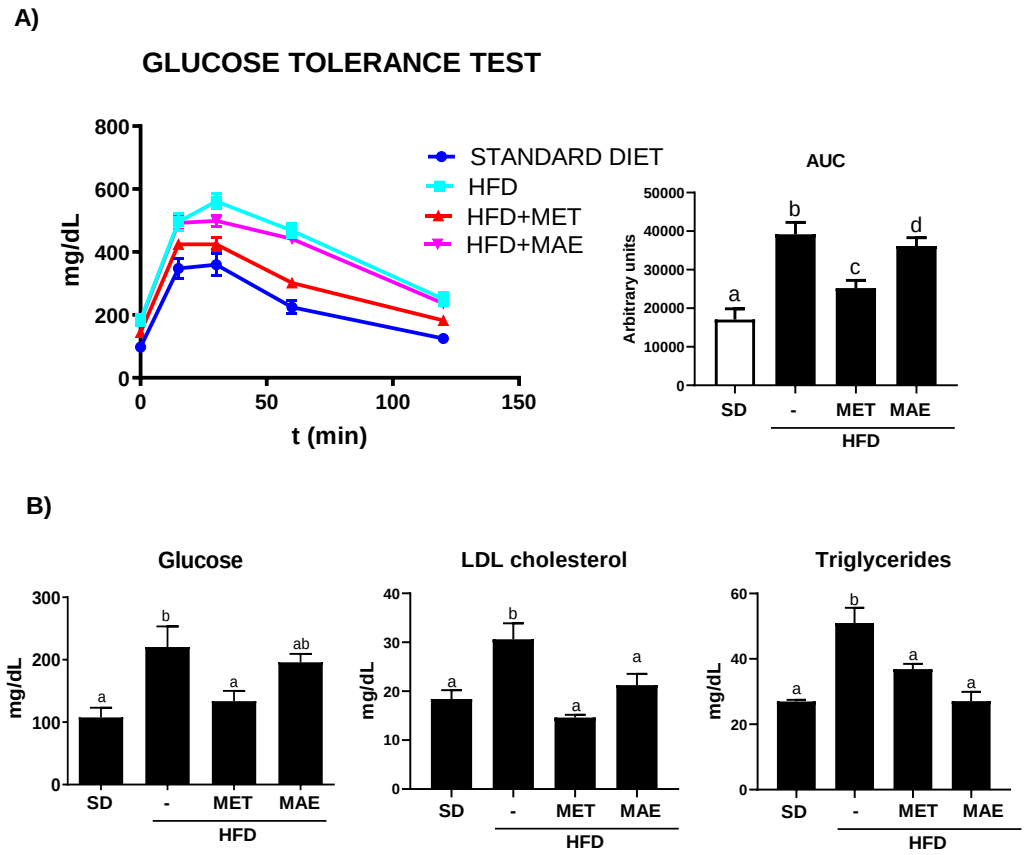

Figure 25. Impact of Morus alba extract (MAE) in (A) glucose tolerance test and area under glycemic curve (AUC). *(B) Plasmatic levels of glucose, LDL-cholesterol and triglycerides. Data are presented as means ± SEM (n = 10). Groups with different letters statistically differ (p < 0.05).*

Additionally, blood glucose remained elevated in control obese mice at all determined times when compared to the normal glycemic curve obtained in the group of SD-fed mice (Figure 25A). As a result, a significant increase of the glycemic AUC in control obese

mice was observed (Figure 25A). Of note, the antidiabetic drug metformin was able to significantly reduce the peak of glycemia and maintain glucose levels below those obtained in control HFD-fed mice (Figure 25A), thus leading to a significant reduction of glycemic AUC (Figure 25A). Remarkably, mice receiving the extract also showed lower plasma glucose concentrations at all time points compared to untreated HFD-fed control mice (Figure 25A), also resulting in a significant reduction in the AUC (Figure 25A). Similarly, levels of blood glucose were determined at the end of the assay, and they were lower in both groups of treated mice than in the obese control group, although the significant differences were only achieved in those mice treated with metformin (Figure 25B).

The biochemical results also evidenced the obesity-induced alterations in lipid profile. Consequently, HFD supplementation to mice resulted in hypercholesterolemia and hypertriglyceridemia in comparison with control diet-fed mice, with higher levels of both LDL-cholesterol and triglycerides (Figure 25B). The impaired lipid homeostasis was significantly restored by the administration of *Morus alba* extract to obese mice, reducing LDL and triglycerides (Figure 25B).

2.2. *Morus alba* extract administration improved the inflammatory status and redox homeostasis.

It is well known that HFD-induced obesity is associated with a systemic inflammatory status and leads to a metabolically activation of different tissues such as adipose tissue and the liver. Therefore, the effect of the extract on the inflammatory status in liver and fat tissue was evaluated. Thus, the results revealed an increase of the different proinflammatory mediators in both tissues, including IL-6, MAPK, AKT, UCP1 and COX-2. In epididymal fat tissue, HFD-fed mice showed a higher expression of phosphorylated p38 MAPK and AKT in comparison with lean mice, which is associated with the glucose and lipidic alterations described above (Figure 26). Surprisingly, only the extract treatment was able to significantly counteract this effect (Figure 26). Additionally, the protein expression of COX-2 was also determined. It has been reported that HFD increases COX-2 levels produced by metabolically activated fat tissue macrophages (531). Correspondingly, the HFD-fed mice showed a significant increase of COX-2 expression on fat tissue compared to lean control mice (Figure 26), which was reduced in those treated obese mice; however, although no statistical differences were obtained in comparison with the obese control group, no differences were observed either when compared with control lean mice (Figure 26). Mitochondrial uncoupling protein-1 (UCP1) is the hallmark of brown adipocytes responsible for cold- and diet-induced

thermogenesis. Although UCP1 is not properly an inflammatory marker, many reports have indicated that UCP1 deficiency exacerbates the systemic and vascular inflammatory process. Accordingly, the protein quantification performed in fat tissue showed that HFD supplementation significantly reduced the UCP1 expression compared to the control lean group (Figure 26). Interestingly, both treatments, *Morus alba* extract and metformin, significantly restored the UCP1 protein expression levels (Figure 26).

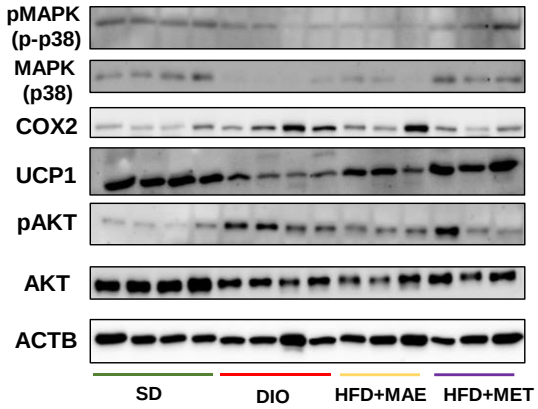

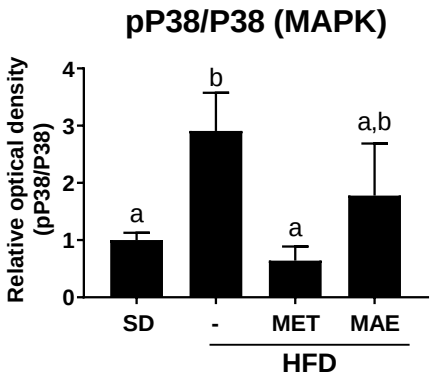

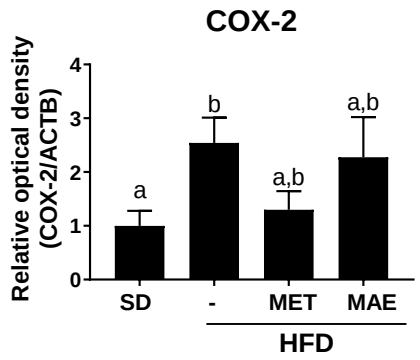

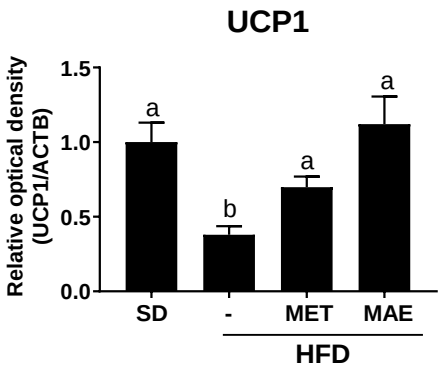

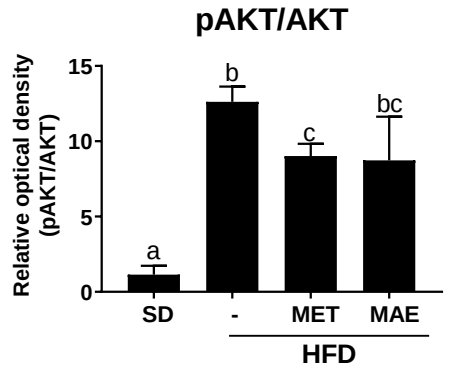

Figure 26. Impact of the Morus alba extract on inflammatory and metabolic-related markers analyzed in epididymal adipose tissue. *Data are presented as means ± SEM (n = 10). Groups with different letters statistically differ (p < 0.05).*

In the liver, HFD-fed mice showed a higher expression of phosphorylated p38 MAPK and IL-6, in comparison with the SD control group, being closely related with the hepatic steatosis and the inflammatory cell infiltration that occurred in the liver (Figure 27A). Of note, both the extract and metformin showed a significant reduction of the protein expression from these mediators (Figure 27A).

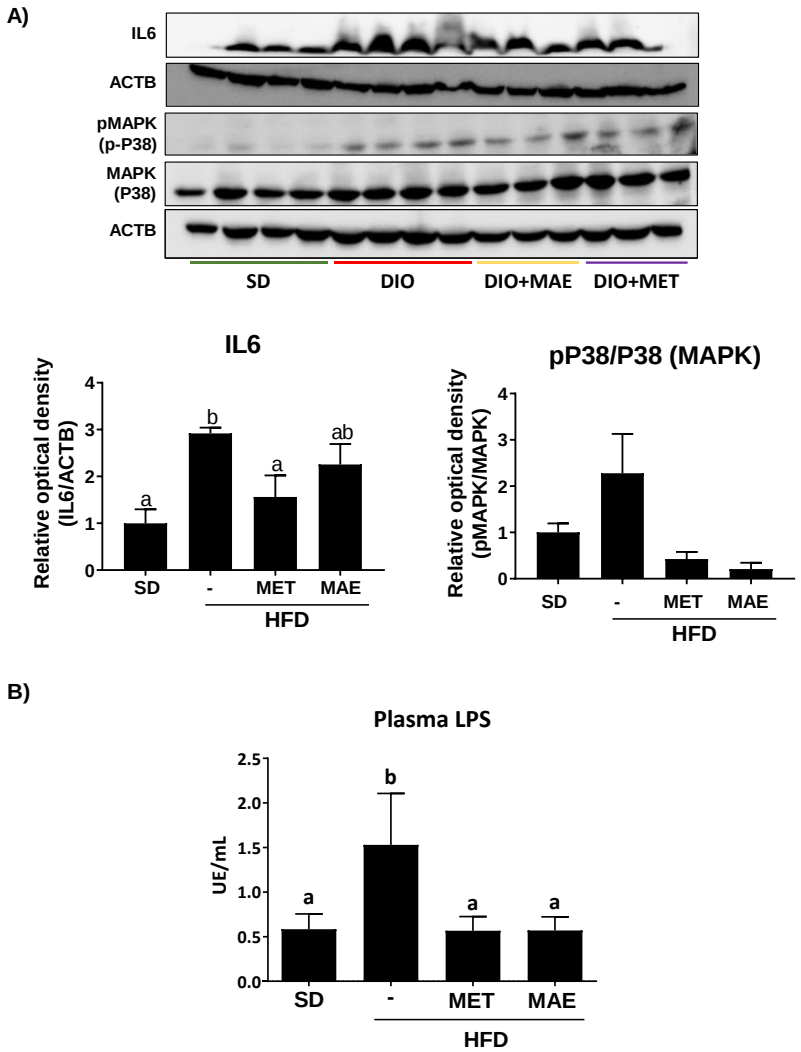

Figure 27. Effect of Morus alba extract on *(A) inflammatory markers studies in liver samples and (B) LPS plasmatic levels. Data are presented as means ± SEM (n = 10). Groups with different letters statistically differ (p < 0.05).*

In addition, the impairment in glucose and lipid metabolism evidenced in HFD-fed mice was related to a notable increase of the plasma levels of LPS (Figure 27B). As commented before, HFDs increase the intestinal permeability and the systemic exposure to bacterial LPS and, subsequently, the metabolic endotoxemia is established. In this sense, the *Morus alba* extract supplementation and metformin administration significantly reduced the metabolic endotoxemia through decreasing plasma LPS (Figure 27B).

Cardiovascular problems are one of the main comorbidities associated with obesity. Since obesity-associated oxidative stress can have an important role in the development of the cardiovascular complications, through the excessive generation of ROS, the activity of the enzyme NADPH oxidase, the main source of ROS in aortic rings, was measured. The results showed that there was a significant increase of NADPH oxidase activity in HFD-fed mice, whereas the treatments with *Morus alba* or metformin were able to significantly reduce it (Figure 28A). Additionally, and in order to confirm the antioxidant effects of this plant extract (455, 532), the TBARS quantification was determined. In line with previous reports, HFD consumption significantly increased TBARS values compared to SD group (Figure 28B), and the administration of the extract or metformin to HFD-fed mice reduced these TBARS values (Figure 28B).

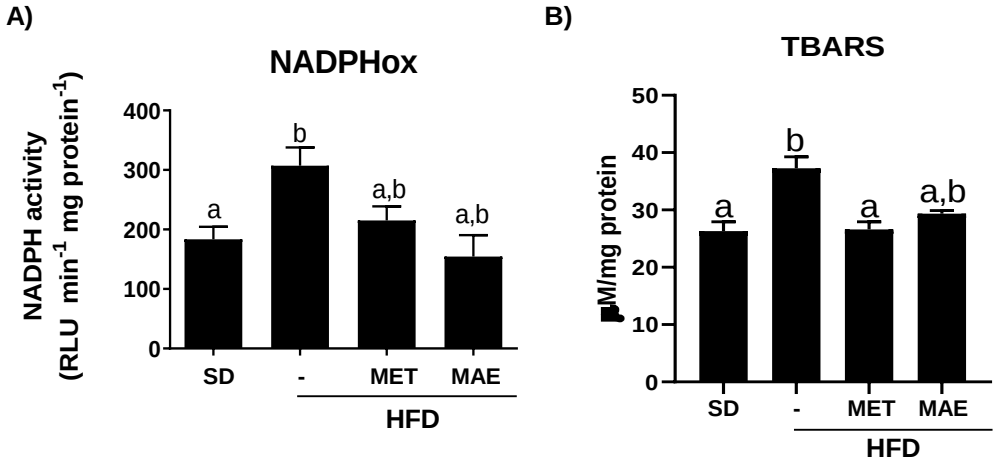

Figure 28. Effect of Morus alba extract on (A) NADPH oxidase activity and (B) TBARS levels*. Data are presented as means ± SEM (n = 10). Groups with different letters statistically differ (p < 0.05).*

2.3. *Morus alba* extract treatment ameliorates gut dysbiosis in obese mice.

As previously commented, it has been widely reported that obesity is associated with changes in gut microbiome composition, thus leading to a situation of dysbiosis. Therefore, to investigate the effects of the *Morus alba* leaf extract on gut microbiota in HFD-induced obese mice, the 16S rDNA sequencing was evaluated in the intestinal contents. Firstly, the alpha diversity, characterized by Shannon diversity, Observed ASVs and Simpson index, was determined. The results revealed that HFD intervention did not have a significant impact on these ecological features evaluated (Figure 29A). Secondly, the PCoA plot visualizing the beta diversity with Bray–Curtis distance showed a clear separation between HFD group and SD-fed mice (p-value = 0.006) (Figure 29B). Conversely, dissimilarity-based PCoA indicated no significant clustering of the gut microbiota between the treatments and HFD-fed mice (Figure 29B). Moreover, the effects of the *Morus alba* leaf extract on the abundance of gut microbiota at the phylum level was measured. The results indicated that the phyla taxonomic profiling was mainly composed of *Actinomycetota, Bacteroidota, Bacillota, Desulfobacterota, Pseudomonadota* and *Verrucomicrobiota* (Figure 29C). When HFD group was compared to SD control, the obese mice exhibited a notable increase in the *Bacteroidota, Pseudomonadota* and *Verrucomicrobia* abundance and a significant decrease in the *Actinomycetota, Bacillota, Desulfobacterota* abundances, thus resulting in a reduction of F/B ratio (FigureVIIID). *Morus alba* leaf extract supplementation significantly modulated the phyla abundance, thus showing a profile more similar to SD group (Figure 29C). Correspondingly, the F/B ratio was significantly reestablished by the treatment (Figure 29D).

At the genus level, significant differences in the relative abundances of *Akkermansia*, *Alistipes*, *Alloprevotella*, *Parabacteroides*, *Desulfovibrio*, *Enterorhabdus*, *Lactobacillus*, *Turibacter were obtained* (Figure 29E). Specifically, in the control HFD-fed group, *Akkermansia*, *Alistipes* and *Parabacteroides* abundances were boosted whereas *Desulfovibrio*, *Enterorhabdus*, *Lactobacillus* and *Turicibacter* abundances were diminished compared to the SD control group (Figure 29E). *Morus alba* leaf extract administration was able to significantly reduce *Alistipes* compared to the HFD group (Figure 29E). Remarkably, the plant extract treatment provoked an increase of two exclusively genus, *Faecalibaculum* and *Pseudomonas* (Figure 29E). Correspondingly, the determination of the histogram of linear discriminant analysis (LDA) and volcano plot indicated that obese mice group was characterized by a significantly higher proportion of

Alistipes, while in the group treated with the extract, *Pseudomonas* abundance increased significantly (Figure 30A and B).

Lastly, the Venn diagram showed that the SD, HFD, *Morus alba* extract and metformin contained 22, 7, 8 and 14 ASVs, respectively (Figure 30C). Additionally, there was 1 common ASV between the SD and HFD groups. Only 1 common ASV was obtained between the plant extract group and HFD-fed mice (Figure 30C).

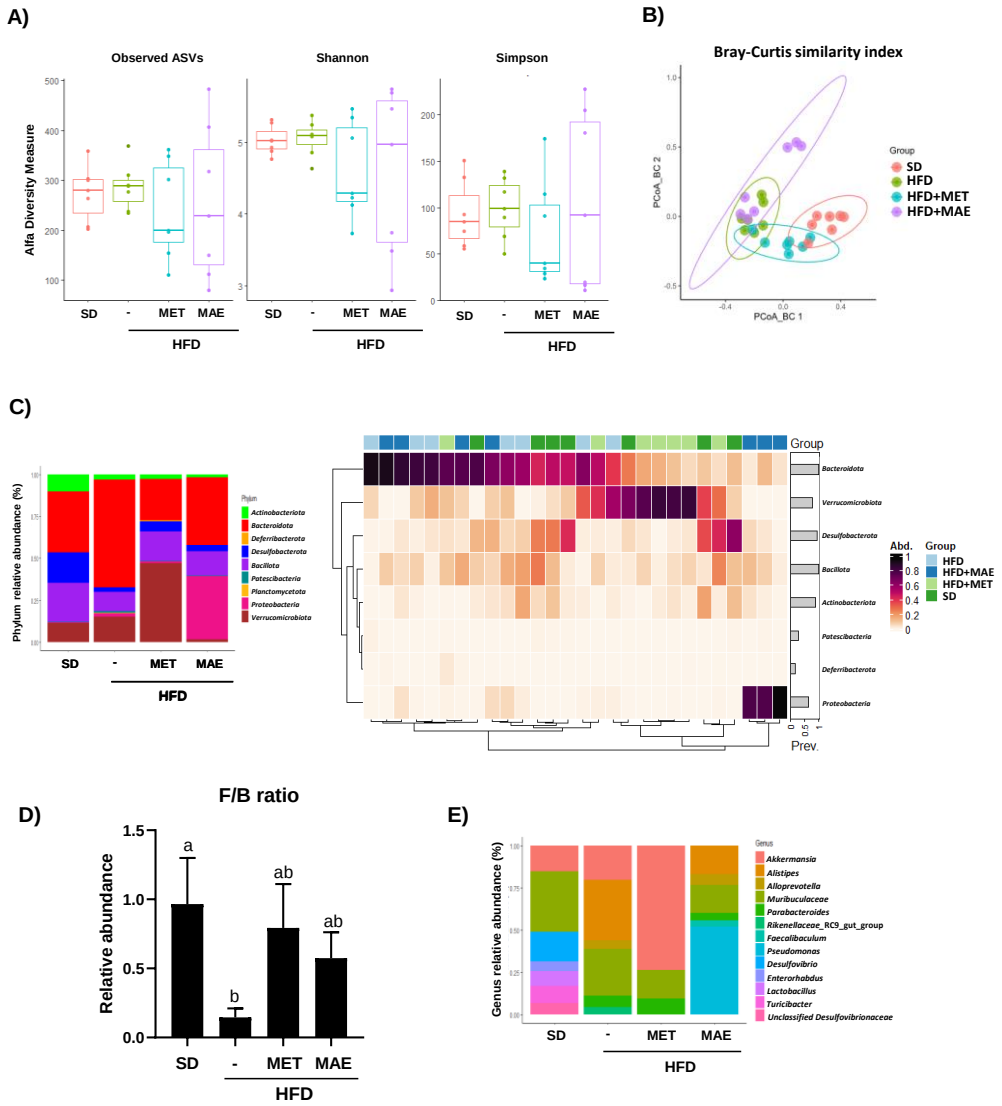

Figure 29. Effects of Morus alba extract supplementation on: *(A) alpha diversity indexes (Observed ASVs, Shannon and Simpson); (B) beta diversity analyzed by Bray-Curtis similarity index; (C) bacterial phyla composition; (D) F/B ratio and (E) bacterial genera relative abundance in each group of mice. Data are expressed as means ± SEM. Groups with different letters statistically differ ($p < 0.05$).*

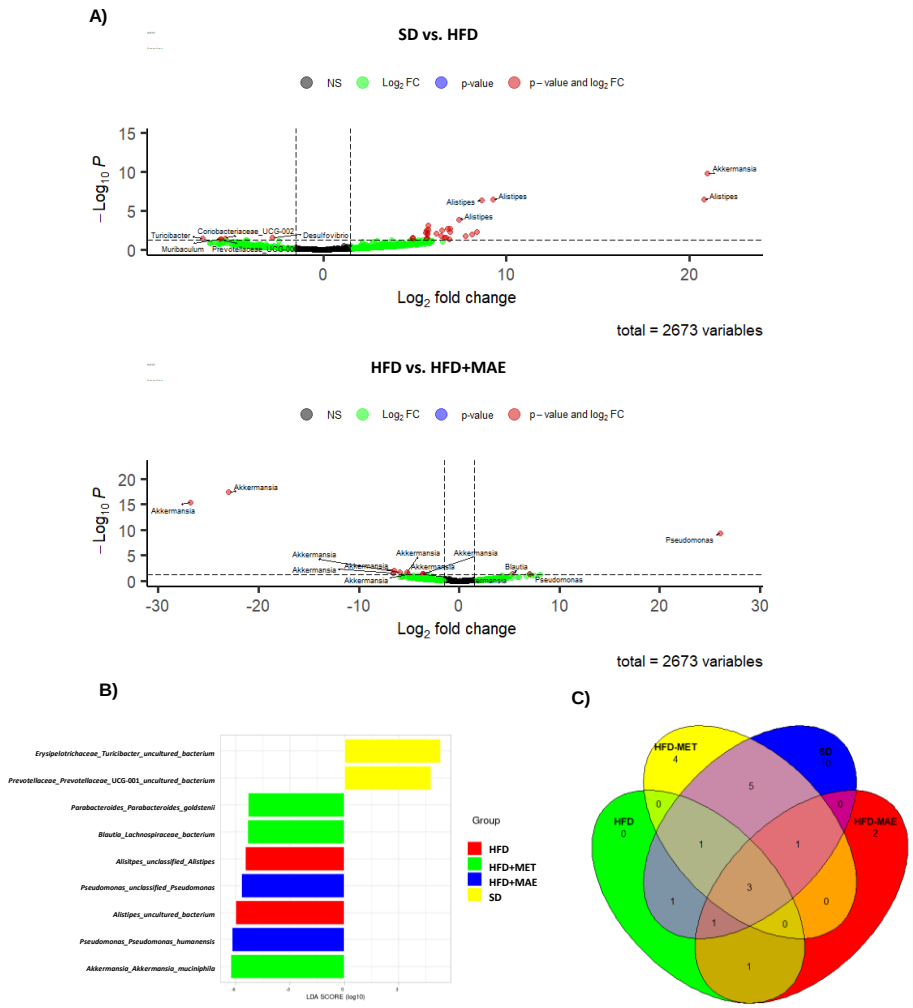

Figure 30. Effect of Morus alba extract on gut microbiota profile. *(A) Volcano plot indicating the upregulated and downregulated ASVs in HFD-fed mice when compared to SD mice (up) and those upregulated and downregulated in Morus alba-treated mice in comparison with untreated HFD mice (down). (B) Histogram of the LDA scores for differentially abundant bacterial genera in each experimental group. Negative LDA scores represent bacterial genera over-abundant in HFD-fed groups of mice while positive represent bacterial groups overrepresented in SD-fed mice. (C) A Venn diagram showing the number of ASVs which are unique and common to each experimental group.*

II. EVALUATION OF THE EFFECT OF TIGECYCLINE ON COLORECTAL CANCER.

1. TIGECYCLINE EXERTS AN ANTIPROLIFERATIVE EFFECT *IN VITRO*

The antiproliferative effect of tigecycline was evaluated using clonogenic and MTS assays in the colon cancer cell lines HCT116 and Caco-2, as well as in the epithelial cell line derived from the normal colon mucosa NCM356. Treatment with tigecycline reduced proliferation (Figure 31A) and clonogenic capacity (Figure 31B) of all the cell lines tested in a dose-dependent manner. Similar results were obtained when these cells were treated with 5-FU, although a more pronounced cytotoxic effect was observed in the MTS assay (Figure 31A).

The antiproliferative effect exerted by tigecycline was confirmed by immunofluorescence assay using the antibody anti-Ki67 (Figure 31C). Ki67 is a protein used as a proliferation marker that is highly expressed in the nucleus of cycling cells but strongly down-regulated in resting cells that are in phase G0 (533). Tigecycline and 5-FU caused a significant reduction of the percentage of cells in proliferation, based on the ratio between the $Ki67^+$ cells and the total number of cells (Figure 31C). As expected, this result was accompanied by a significant reduction in the Mean Fluorescence Intensity (MFI) of the anti-Ki67 antibody (Figure 31C), indicating reduced levels of this marker in the nucleus of treated cells.

Then, we studied the molecular mechanisms involved in the anti-proliferative effects of tigecycline, focusing on the role of β-catenin (CTNNB1), which is a component of the Wnt signaling pathway that plays an important role in the development of several types of cancer, including CRC (534-536). In normal conditions, β-catenin is located in the cell cytoplasm and it is phosphorylated to subsequently undergo proteasome degradation. The presence of a stimulus, such as Wnt, or a pathological situation like cancer, promotes the aberrant accumulation of β-catenin, and its translocation to the nucleus. Then, nuclear β-catenin is involved in the overexpression of proliferation and survival genes such as *MYC* and *AXIN2*. Western blot analysis performed in nuclear lysates revealed that levels of nuclear CTNNB1 were reduced in those cells treated with tigecycline or 5-

FU in comparison with untreated cells (Figure 32A). This effect was associated with an increase in CTNNB1 cytoplasmic levels thus lowering nuclear/cytoplasmic ratio in comparison with non-treated cells (Figure 32A).

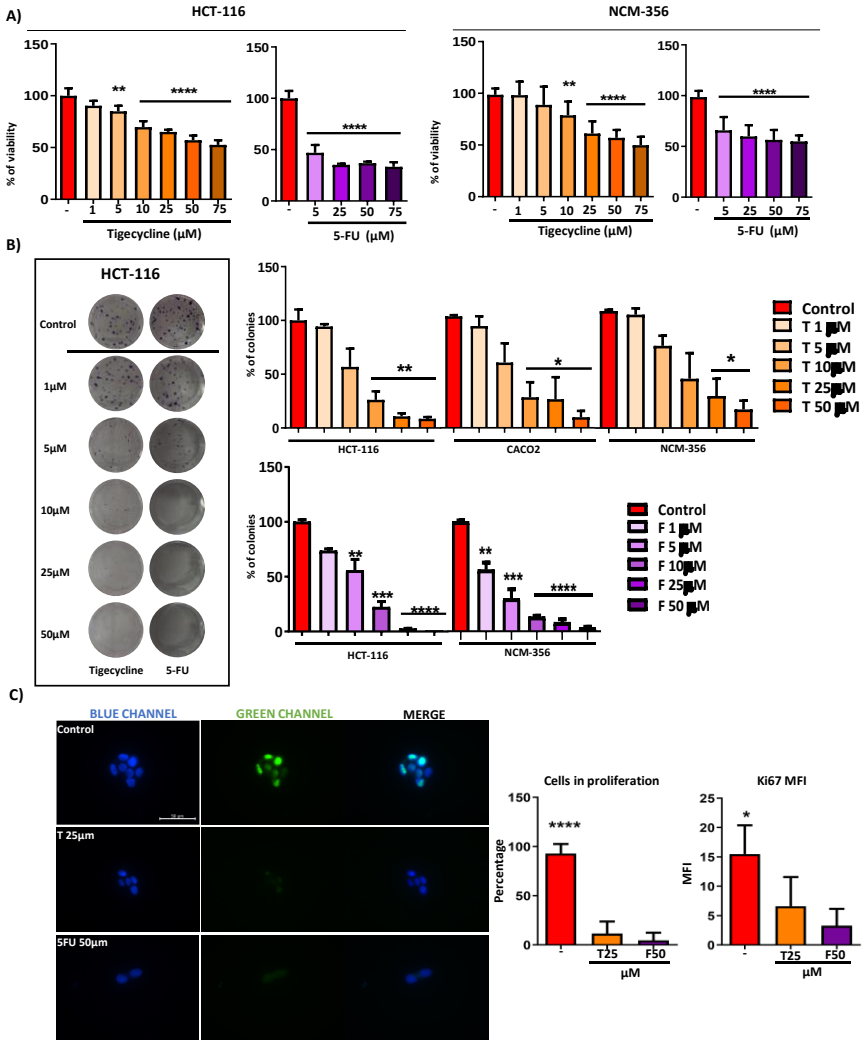

Figure 31. In vitro anti-proliferative effect of tigecycline and 5-FU. (*A) Cell proliferation evaluated by MTT assay (B) Clonogenic assay in HCT116, Caco-2 and NCM356 cell lines treated with different doses of tigecycline or 5-FU. (C) Immunofluorescence representative images of Ki67 (green) staining in HCT116 cells non-treated or treated with tigecycline or 5-FU, cells in proliferation based on ki-67 positive cells and total cells (right and up) and ki-67 mean fluorescence intensity (MFI) (right and down). Scale bar: 50 µm. Data are presented as mean ± SEM. *P < 0.05, **P < .01, ***P < .001 vs. control.*

This result indicates that the antibiotic hinders the translocation of this CTNNB1 to the nucleus and it could be explained considering the ability of tigecycline to increase the phosphorylation of cytoplasmic CTNNB1, a step that is required for its degradation (Figure 32A). Consequently, tigecycline and 5-FU reduced MYC levels (Figure 32A), a downstream component of Wnt/β-catenin pathway. In addition, tigecycline also inhibited STAT3 activation (Figure 32A), which promotes nuclear accumulation of CTNNB1 (145).

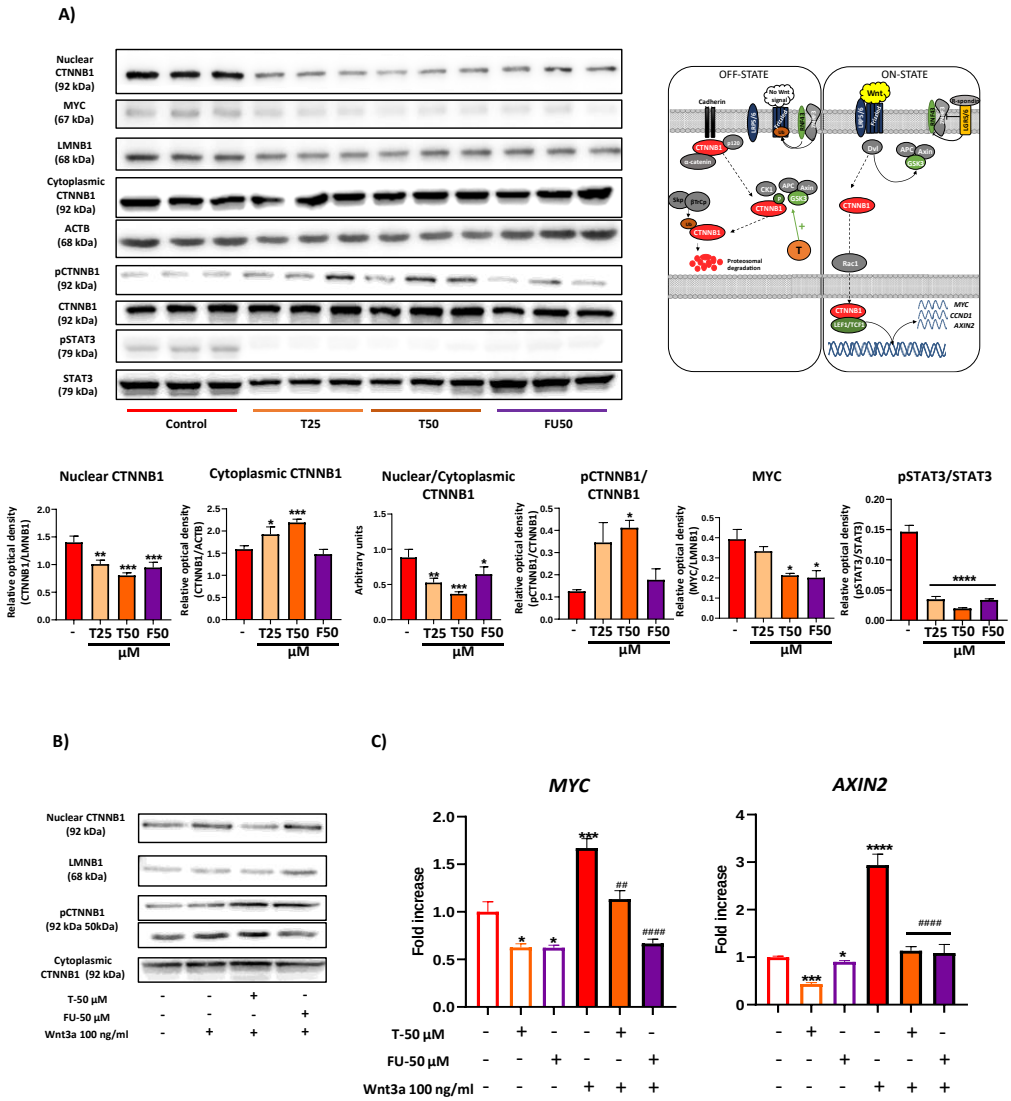

Figure 32. Molecular mechanisms involved in the anti-proliferative effect of tigecycline and 5-FU: *effect on Wnt/β-catenin pathway. (A) Impact on β-catenin nuclear and cytoplasmic levels analyzed by Western blot in basal conditions or (B) stimulated with Wnt3a (C) Effect on the expression of Wnt/β-catenin target genes in the presence*

*or absence of Wnt. Data are presented as mean ± SEM. *P < 0.05, **P < .01, ***P < .001, ****P<.0001 vs. control. #P < 0.05, ##P < .01, ###P < .001, ####P<.0001 vs. control + Wnt.*

To confirm these results, additional experiments were performed in which the Wnt/β-catenin pathway was stimulated with Wnt3a in HCT116 cells. As expected, the stimulation caused a reduction of the CTNNB1 phosphorylation, together with an increment of nuclear CTNNB1 (Figure 32B), thus resulting in the upregulation of *AXIN2* and *MYC.* Importantly, tigecycline and 5-FU enhanced CTNNB1 phosphorylation and reduced its nuclear translocation, evidenced by lower nuclear CTNNB1 levels in treated cells (Figure 32B). Downregulated expression of CTNNB1 target genes, *MYC* and *AXIN2*, was also observed with tigecycline and 5-FU (Figure 32C). Therefore, we confirmed that tigecycline and 5-FU act as inhibitors of the Wnt/β-catenin pathway in colon tumor cells, both in basal and Wnt3a-stimulated proliferation.

3. TIGECYCLINE SHOWS PRO-APOPTOTIC EFFECTS IN COLON CANCER CELL LINES.

The pro-apoptotic capacity of tigecycline was evaluated using the ANXV / PI assay in HCT116 cells. We observed a dose-response effect in the percentage of $ANXV^+PI^-$ cells (Figure 33A), thus revealing its ability to promote early apoptosis after 48 h of treatment. No significant differences in the number of late apoptotic or necrotic cells ($ANXV^+PI^+$) were found. These results were confirmed by performing a TUNEL assay. As expected, tigecycline significantly increased the staining of brown (apoptotic) nuclei (Figure 33B). Similarly, the control drug 5-FU achieved a significant increase in the percentage of apoptotic cells (Figure 33B).

Next, we aimed to characterize the molecular mechanisms by which tigecycline drove its apoptotic effect by investigating the impact of the drug on the three molecular pathways involved in the programmed death process: extrinsic, intrinsic and ER-mediated apoptosis. We observed that the cellular pathways involved in 5-FU-mediated apoptosis were slightly different from those engaged by tigecycline (Figures 34, 35 and 36).

When considering the extrinsic pathway, tigecycline (25 μM) increased the levels of cleaved CASP8, as well as the ratio between the cleaved and the full-length form (Figure 34) with a trend to reduce full-length CASP8, without statistical significance (Figure 34). Caspase 8 is considered to be a caspase initiator, which requires its proteolytic cleavage for activation. Moreover, it has been reported that the cleavage of CASP8 is necessary for the recognition of other substrates, such as executioner caspases and the pro-

apoptotic BCL2 family member BID. Subsequently, the impact of the treatments in the last steps of the extrinsic apoptosis pathway was also evaluated. Tigecycline increased significantly CASP9 and the cleaved form of the executioner CASP7 (Figure 34). Levels of CASP9 and cleaved CASP7 were also increased by 5-FU, which also upregulated CASP3 and their active forms (Figure 34). CASP3 and CASP7 activation lead to the cleavage of PARP, which is responsible for creating breaks in the DNA to cause cell death (163). We found that tigecycline promoted the cleavage of PARP and reduced the levels of full length PARP leading to a significant increment of the ratio (Figure 34). This action was even more intense with the 5FU treatment (Figure 34). These results support that treatment with tigecycline exerts a pro-apoptotic effect, as shown by 5-FU.

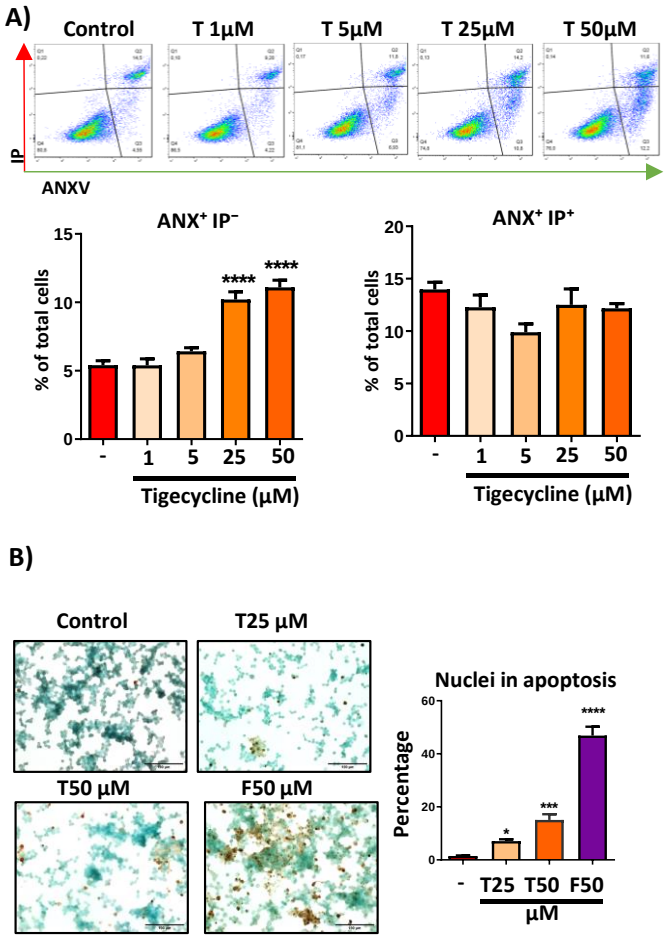

Figure 33. Pro-apoptotic effect of tigecycline and 5-FU in vitro. *(A) Apoptosis study by ANXV-PI assay in HCT-116 cell line (B) Tunel assay in HCT-116 cell. Data are presented as mean ± SEM. *P < 0.05, **P < .01, ***P < .001, ****P<.0001 vs. control.*

Besides, tigecycline increased the levels of both BID and tBID, even though this increase was not statistically significant (Figure 34). Truncation of BID (tBID) by cleaved CASP8 on the mitochondrial membrane is required for the formation of pores and the release of cytochrome C oxidase to the cytosol, and it has been reported that BID acts as a link between the extrinsic pathway and the intrinsic pathway of apoptosis (537). Interestingly, the incubation of tumor cells with either tigecycline or 5-FU significantly upregulates the levels of BAX and its oligomer (Figure 35). BAX is a member of the BCL2 family proteins that oligomerizes and promotes a mitochondrial outer membrane permeabilization (538). BCL2 binds BAX and inactivates it and its pore-forming function. Therefore, BCL2 favors cell survival, being the ratio BAX/BCL2 an indicator of the cell apoptosis state. Although the levels of BCL2 protein were not significantly modified by tigecycline or 5-FU, both compounds increased the BAX/BCL2 ratio (Figure 35). Consequently, cytochrome C oxidase was upregulated in those cells incubated with tigecycline (Figure 35). Additionally, TP53 protein also plays an important role in the intrinsic apoptotic pathway and we found that it was upregulated by 5-FU, but not by tigecycline (Figure 35) that acts downstream increasing BCL2L11 (BIM) levels (Figure 35).

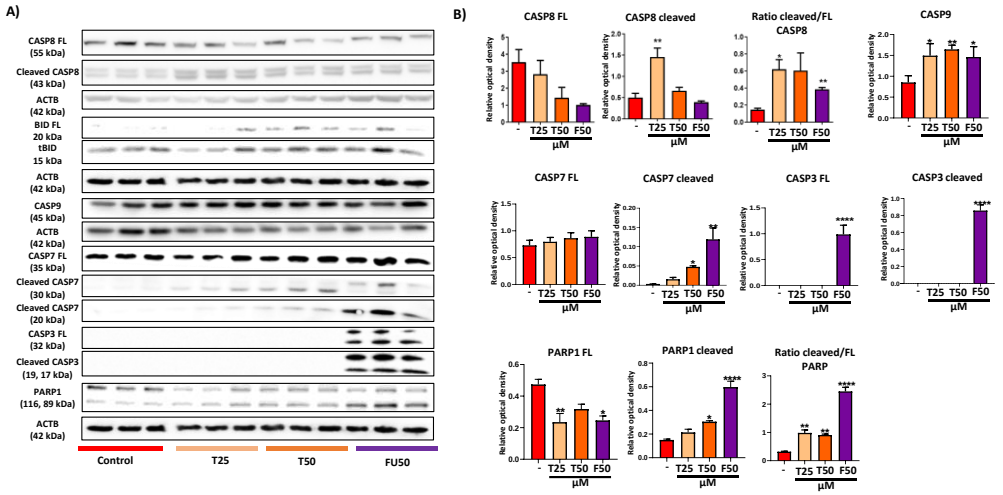

Figure 34. Pro-apoptotic effect of tigecycline and 5-FU in vitro. Impact on extrinsic apoptotic pathway. *(A) Western blot bands of several markers involved in extrinsic-mediated apoptosis and (B) their quantification. Data are presented as mean ± SEM. *P < 0.05, **P < .01, ***P < .001, ****P<.0001 vs. control.*

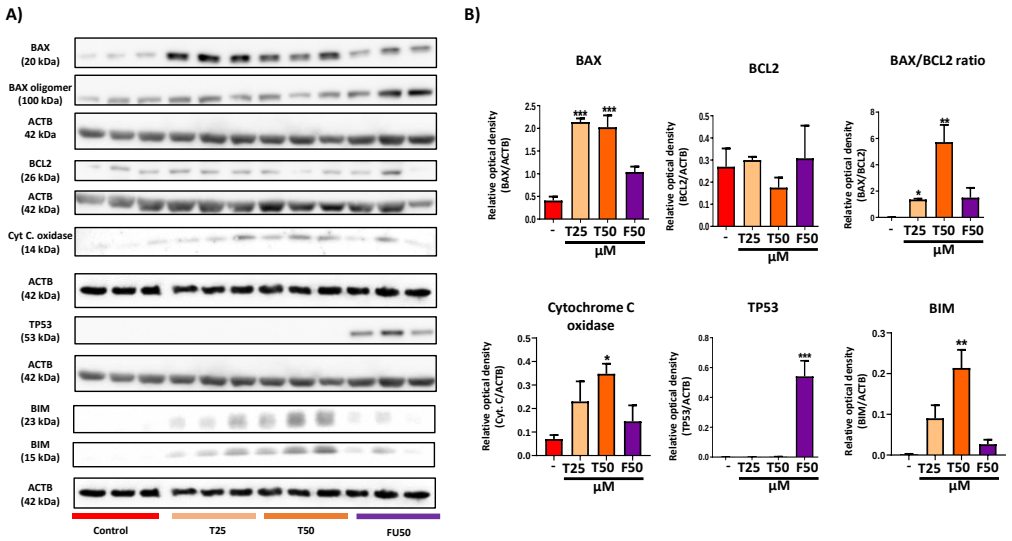

Figure 35. Pro-apoptotic effect of tigecycline and 5-FU in vitro. Impact on mitochondrial apoptotic pathway. *(A) Western blot bands of several markers involved in intrinsic-mediated apoptosis and (B) their quantification. Data are presented as mean ± SEM. *P < 0.05, **P < .01, ***P < .001, ****P<.0001 vs. control.*

The pro-apoptotic effects of both tigecycline and 5-FU also involve the ER pathway, although in different ways (Figure 36).

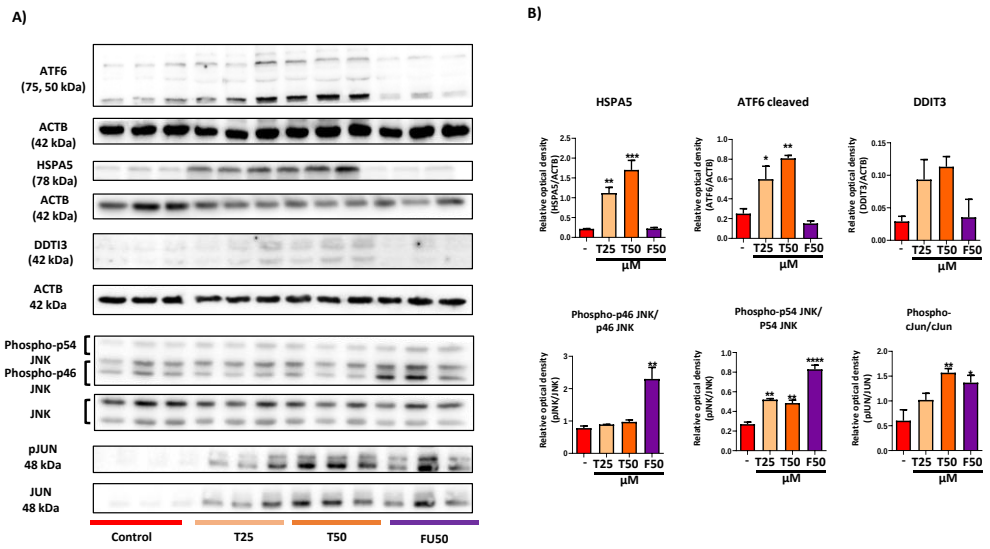

Figure 36. Pro-apoptotic effect of tigecycline and 5-FU in vitro. *Impact on ER-mediated apoptosis. (A) Western blot bands of several markers involved in ER-mediated apoptosis and (B) their quantification. Data are presented as mean ± SEM. *P < 0.05, **P < .01, ***P < .001, ****P<.0001 vs. control.*

Tigecycline increased the levels of the ER-stress marker immunoglobulin heavy chain-binding protein (HSPA5, also called BIP or GRP78) (Figure 36). Similarly, tigecycline induced the cleavage and activation of ATF6, which resulted in an upregulation of CHOP (DDIT3) (Figure 36), a protein that links the ER and mitochondrial pathways. Conversely, 5-FU did not significantly modify the levels of ATF6 or DDIT3 (Figure 36) but increased the levels of the phosphorylated active form of JNK (Figure 36), which justifies its ability to promote apoptosis through ER pathway. Although tigecycline also increased the levels of phospho-JNK, this was only observed when the p54 isoform was considered, and with a lower efficacy in comparison with 5-FU (Figure 36). Furthermore, both, tigecycline and 5-FU, significantly increased the ratio between phospho-JUN and JUN (Figure 36), thus favoring the activation of this proapoptotic ligand.

4. EFFECT OF TIGECYCLINE ON STEMNESS PROPERTIES *IN VITRO.*

CSCs are considered to be responsible for the initiation of the cancer process, as well as other cancer-associated malignancies such as metastasis, multidrug resistance and tumor recurrence. Therefore, CSCs could be considered one of the most promising targets for cancer treatment. In fact, much of current research focuses on the characterization of these CSCs, and the search for new effective therapies against them. Tetracyclines have proven to be effective against metastasis, one of the main complications in cancer. This beneficial effect is mainly due to their capacity to interfere with the activity of MMPs and angiogenesis. Considering all the above, tigecycline could have a beneficial impact against the initiation of tumor process by acting on CSCs. To confirm this, we first obtained colonospheres from colon cancer lines and characterized the effects of tigecycline against the malignancy properties of CSCs.

4.1. TIGECYCLINE REDUCED VIABILITY AND CLONOGENICITY OF COLONOSPHERES.

To evaluate the effects of tigecycline on colon CSCs, colonospheres were obtained from HCT116 and CMT93 cancer cell lines (Figure 37A). Then, the impact of tigecycline on the functional characteristics of CSCs was assayed through the analysis of SFE, cell viability and their clonogenicity capacity.

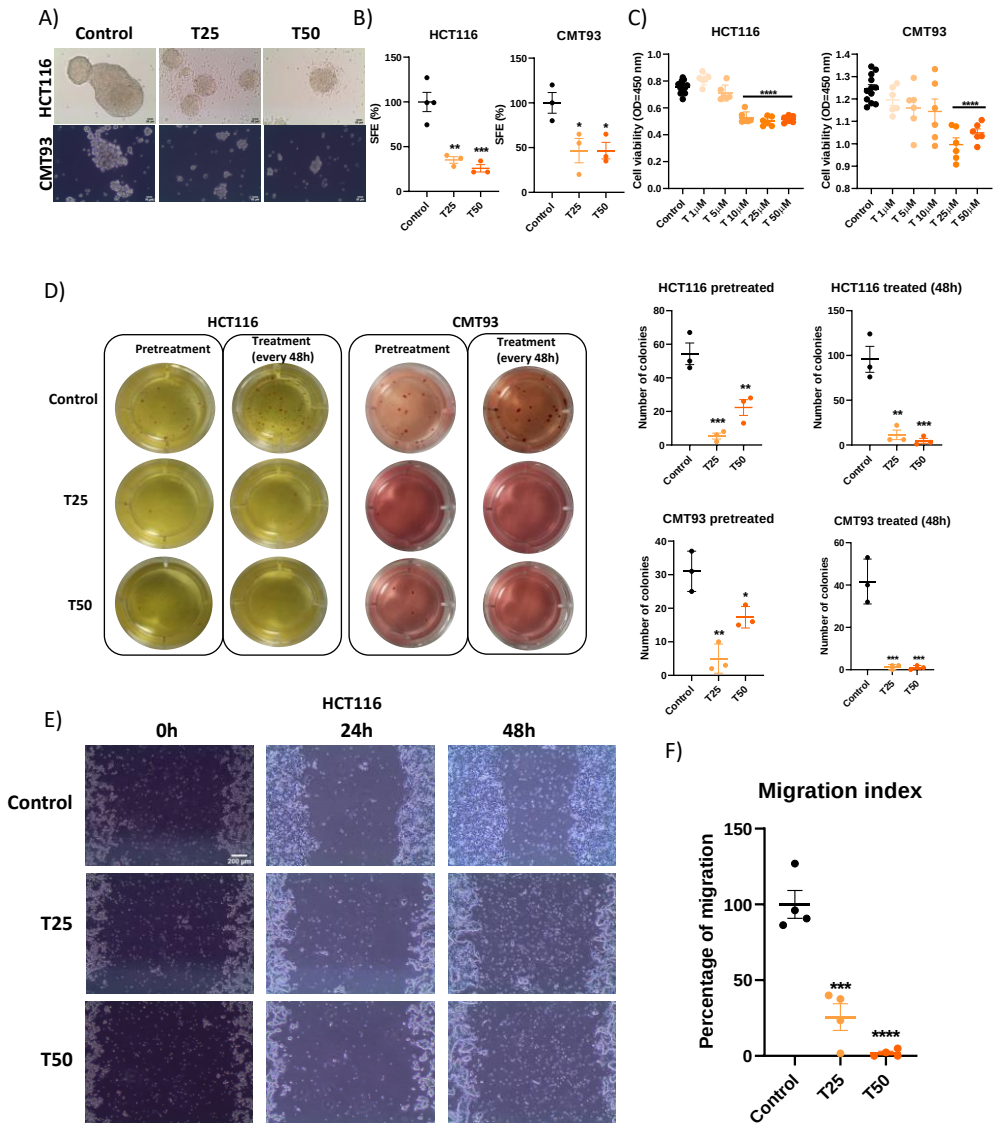

Figure 37. Impact of tigecycline on colon spheroids. *(A) Representative images of HCT116 (up) and CMT93 (down) colonospheres formed from different tigecycline doses (0, 25 and 50 µM). Scale bar = 50µM. (B) Sphere-forming efficiency (SFE) percentage after the treatment of HCT116 (left) and CMT93 (right) colonospheres with tigecycline (0, 25 and 50 µM) (n=3-4) (C) Cell viability evaluated by CCK8 assay after treatment with tigecycline (0, 1, 5, 10, 25 and 50 µM) for 48 h in HCT116 (left) and CMT93 (right) derived colonospheres (n=6). (D) Representative images of HCT-116 (left) and CMT-93 (middle) colonies after being pretreated with tigecycline for 48 h or treated every 48h for 21 days once seeded with different doses (0, 25 and 50 µM) and quantification of the number of colonies in each cell line and condition (right). (D) Wound healing assay performed on*

*HCT116 cells treated with tigecycline at 0, 25 and 50 µM. Images were taken at 0, 24 and 48 h after wounding. Scale bar: 200 µm (E) Migration index based on the results of wound healing assay. Data are graphed as mean ± SEM (*P < 0.05, **P < 0.01, ***P < 0.001, ****P < 0.0001 vs. Control).*

The incubation of HCT116 and CMT93-derived colonospheres with tigecycline resulted in morphological and size changes (Figure 37A). Indeed, tigecycline markedly reduced their size and induced a disruption of their integrity as it is shown in Figure 37A. The reduction in spheroids volume and number resulted in significantly lower levels of the SFE parameter in those colonospheres treated with tigecycline (Figure 37B), thus interfering in the self-renewal capacity of CSCs. In concordance with these results, HCT116 and CMT93-derived CSCs showed a significant reduction in their viability after being incubated with tigecycline 25 µM, 50 µM and, even 10 µM in HCT116 CSCs (Figure 37C). Regardless of murine or human origin of these cells, the clonogenicity of CSCs was reduced when they were pre-treated or treated every 48h with tigecycline (Figure 37D). These data suggest that tigecycline was able to diminish the viability, clonogenicity and self-renewal capacities of CSCs derived from HCT116 and CMT93 cell lines.

Cell migration is a key process that occurs throughout the entire development of the tumor and it is of special relevance in the invasion of adjacent tissues, as well as in cancer metastasis (539). The migratory capacity of HCT116 cells was evaluated in presence of tigecycline by the wound healing assay. We observed that tigecycline reduced the migration of HCT116 (Figure 37E) resulting in a significant reduction of the migration index (Figure 37F), which was calculated as the percentage of wound regeneration considering 100% regeneration in control cells. These results demonstrate that tigecycline is able to reduce the number of invading cells, which can prevent the metastasis process.

CSCs are further characterized by presenting enhanced resistance to apoptosis. Therefore, targeting the apoptotic pathway to induce cell death has been long considered a promising therapeutic strategy for cancer. Based on the pro-apoptotic effect of tigecycline described in the first objective, we aimed to investigate if this drug was also able to induce apoptosis in CSCs derived from HCT116 and CMT93 cell lines. Using ANXV/PI flow cytometry we observed that tigecycline at 25µM and 50µM was able to induce apoptosis in HCT116 cell line, thus significantly increasing the levels of $ANXV^+PI^+$ cell population (Figure 38A and B). On the other hand no significant differences in the number of late apoptotic or necrotic cells ($ANXV^+PI^+$) were found (Figure 38B). Moreover,

the treatment did not cause any impact on apoptosis ($ANXV^+PI^-$ population) or necrosis ($ANXV^+PI^+$) of CMT93 cells (Figure 38A and C). These results suggest that HCT116 cells are more sensitive to tigecycline-induced apoptosis than CMT93 cells, thus contributing this action to the reduction of CSCs viability observed.

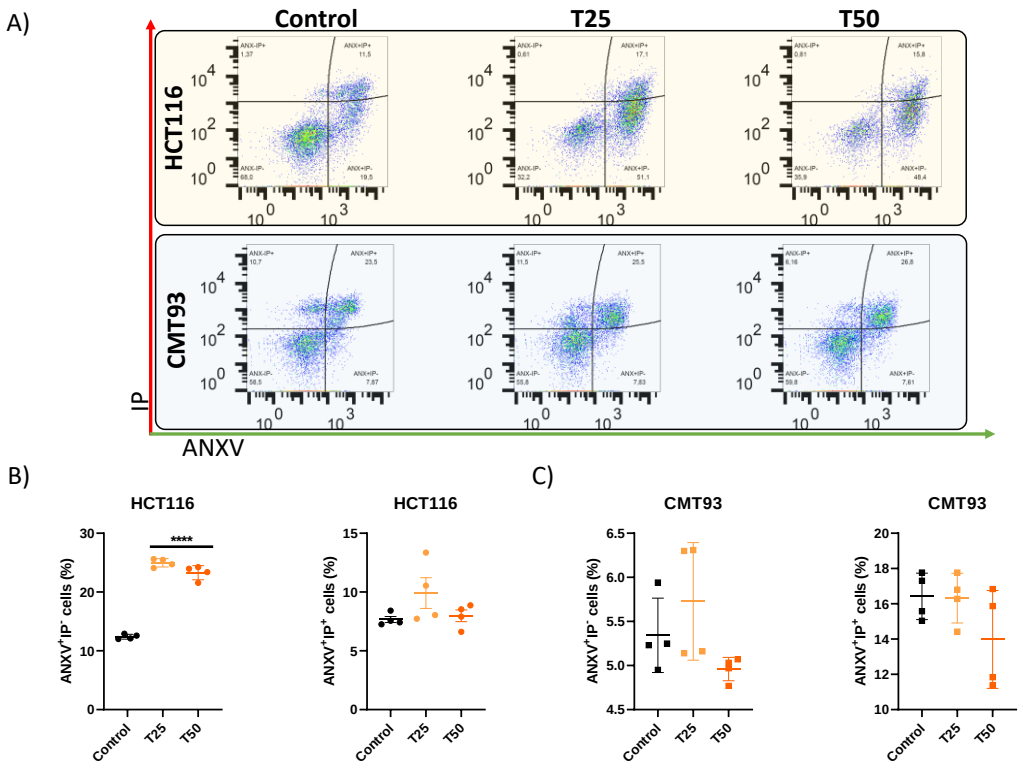

Figure 38. Tigecycline induces apoptosis in colon CSCs. *(A) ANXV PI flow cytometry analysis carried out in HCT116 (up) and CMT93 cells derived from secondary spheroids and treated with tigecycline at 0, 25 and 50 μM for 72h. Percentage of (B) HCT116 and (C) CMT93 cells in apoptosis (left) and late apoptosis or necrosis (right) after tigecycline treatment. Data are graphed as mean ± SEM (*P < 0.05, **P < 0.01, ***P < 0.001, ****P < 0.0001 vs. Control).*

4.2. COLON CSCs POPULATIONS WERE REDUCED BY TIGECYCLINE TREATMENT

Molecularly, colorectal CSCs are identified via a group of surface markers among which CD133, CD44, LGR5, and increased ALDH1 activity stand out (540, 541). Thus, these markers were evaluated in these cells in order to confirm if the effects observed after

their incubation with tigecycline on colonospheres viability, clonogenicity and apoptosis were linked to a reduction of CSC population (Figure 39).

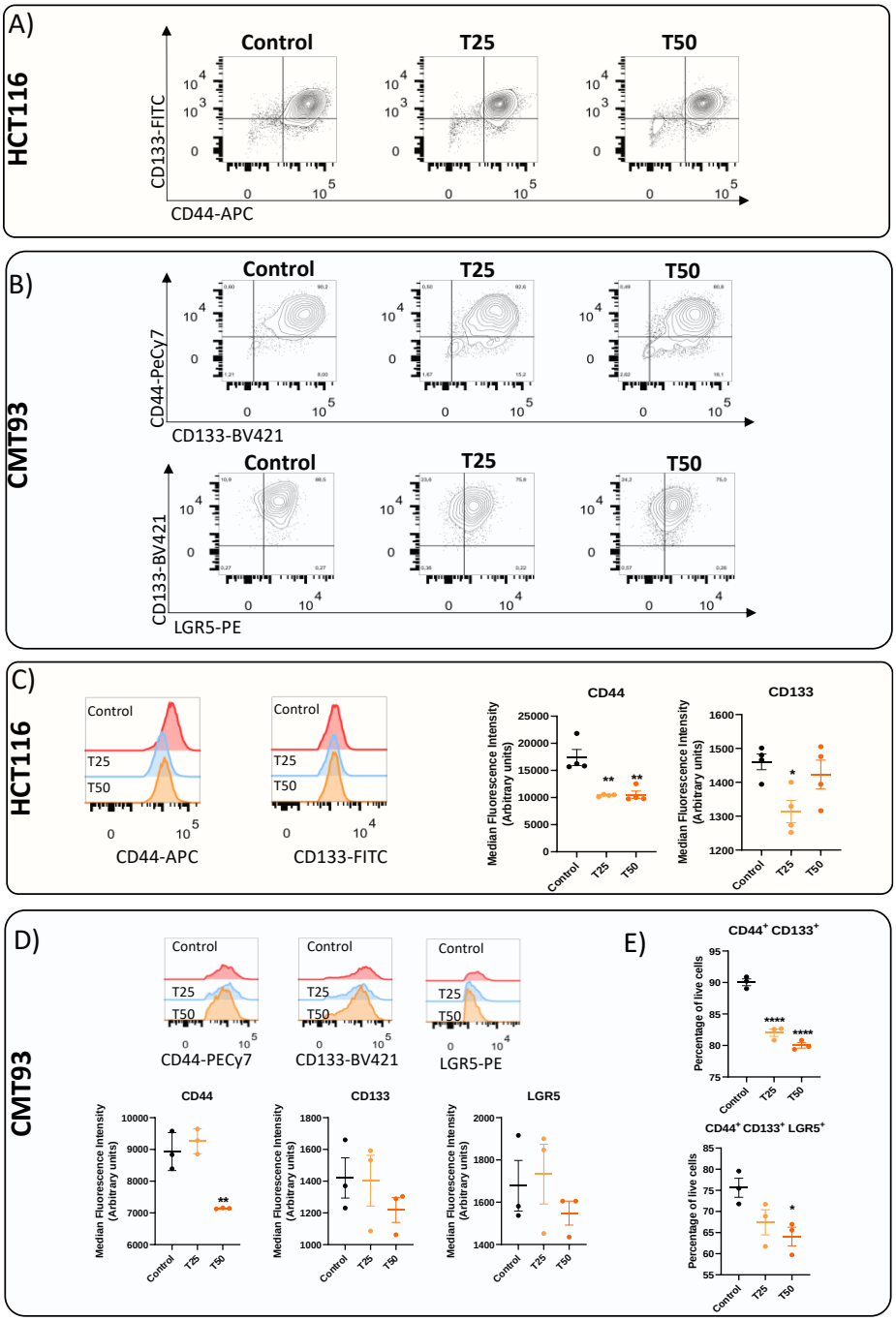

Figure 39. Colon CSCs population is reduced by tigecycline in secondary colonospheres derived from HCT116 and CMT93 cell lines. *(A) Flow cytometry analysis of CD133⁺/CD44⁺ cell populations in HCT116 cells derived from secondary*

*colonospheres and treated with tigecycline for 72 h. (B) Flow cytometry analysis of CD133⁺/CD44⁺/LGR5⁺ cell populations in CMT93 cells derived from secondary colonospheres and treated with tigecycline for 72 h. (C) Representative histograms showing CD44 and CD133 staining and quantification of the median fluorescence intensity for each marker in HCT116 cells after being treated with tigecycline. (D) Representative histograms showing CD44, CD133 and LGR5 staining and quantification of the median fluorescence intensity for each marker in CMT93 cells after being treated with tigecycline. (E) Percentage of CD44⁺CD133⁺ and CD44⁺CD133⁺LGR5⁺ cell populations in CMT93 derived from secondary colonospheres. Data are graphed as mean ± SEM (*P < 0.05, **P < 0.01, ***P < 0.001, ****P < 0.0001 vs. Control).*

First, the cells that integrated the colonospheres obtained from HCT116 and CMT93 cell lines were positive for CD133, CD44 (Figure 39A and B) and LGR5 (Figure 39B), thus supporting the fact that these colonospheres were mainly integrated by CSCs. Then, when the impact of tigecycline on colon CSC populations was evaluated, the results revealed that the compound was able to significantly reduce the expression levels of the different markers expressed by CSCs in both HCT116 and CMT93 cells (Figure 39C and D). Indeed, tigecycline reduced the expression of CD133 and CD44 in HCT116, as evidenced by a reduction of the median fluorescence intensity of these markers (Figure 39C). This effect was also observed in CMT93 cells, although it showed statistical significance only for the CD44 marker and when cells were treated with the highest concentration (50 µM) (Figure 39D). However, when double ($CD44^+CD133^+$) triple positive ($CD44^+CD133^+LGR5^+$) populations were considered, a significant decrease of their expression levels was observed when cells were treated with tigecycline (Figure 39E).

The impact of tigecycline on the CSC population was confirmed when ALDH activity was analyzed. The enzyme ALDH has been reported to play a key role in the development of cancer drug resistance (542). As it is shown in Figure 40A and B, both HCT116 and CMT93 cells expressed ALDH and the activity of this enzyme were significantly inhibited in presence of tigecycline (Figure 40A and B), and neutralized when cells were treated with the ALDH inhibitor DEAB (not shown).

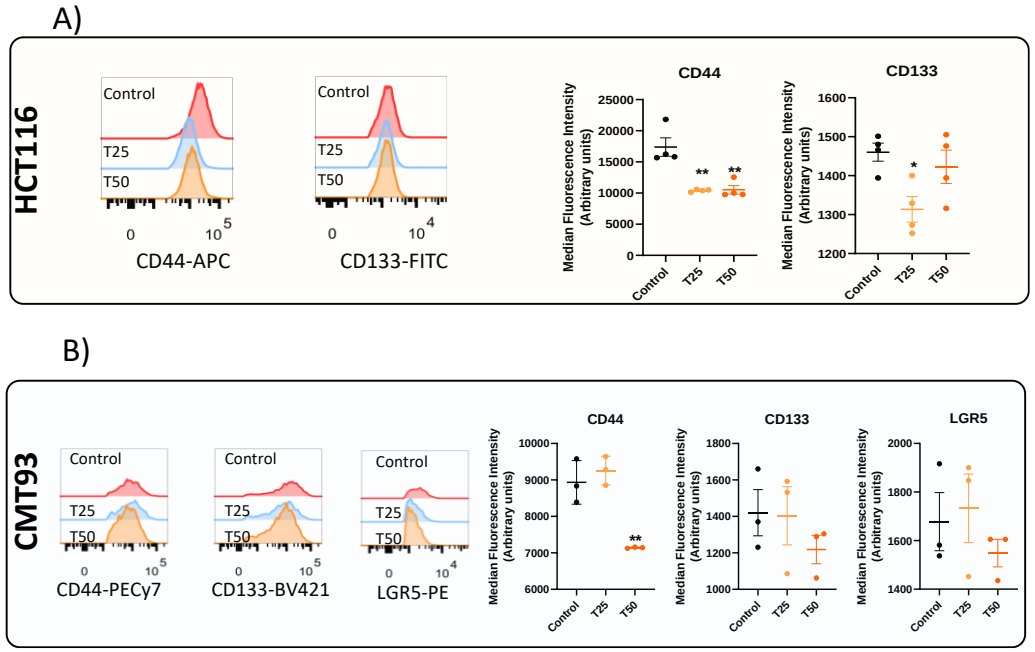

Figure 40. Colon CSC ALDH activity is reduced by tigecycline in secondary colonospheres *derived from (A) HCT116 and (B) CMT93 cell lines. The treatment with tigecycline lasted for 72 h and the ALDH inhibitor N,N-diethylaminobenzaldehyde (DEAB) was used as positive control. Data are graphed as mean ± SEM (*P < 0.05, **P < 0.01, ***P < 0.001, ****P < 0.0001 vs. Control).*

4.3. IMPACT OF TIGECYCLINE ON PLURIPOTENCY AND EMT-RELATED GENES IN COLON CSCs

It is widely accepted the importance of the EMT process in the generation of CSCs; for this reason, the ability of tigecycline to impair this process was evaluated as a mechanism to decrease the levels of colon CSCs.

Preliminary results carried out in HCT116 cell monolayer revealed that levels of e-cadherin (CDH1), an epithelial cell marker, was significantly lower in untreated cells than in those treated with tigecycline (Figure 41A), thus indicating that tigecycline is able to hinder the EMT process and favors the epithelial phenotype over the mesenchymal one. The increased levels of CDH1 observed after tigecycline incubation could be associated with a significant reduction of the transcription factor SNAI1 (Figure 41A), which is considered a repressor of CDH1 that favors the EMT. Surprisingly, this action was observed with tigecycline, but not with the control drug 5-FU (Figure 41A). In

concordance with these results, the expression of *CDH2*, the n-cadherin gene, was significantly decreased in those cells treated with tigecycline (Figure 41B). Unlike e-cadherin, n-cadherin promotes the EMT process, thus favoring the formation of CSCs (543).

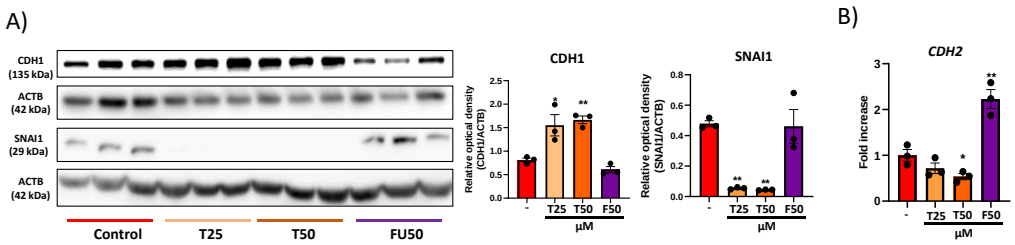

Figure 41. Tigecycline reduces the EMT process in HCT116 cell monolayer. *(A) Representative western blot bands and quantification of EMT-related markers expressed in HCT116 cell monolayer after being treated with tigecycline or 5-FU. (B) Expression levels of CDH2 gene in HCT116 cell monolayer treated with tigecycline or 5-FU for 24h. Data are graphed as mean ± SEM (*P < 0.05, **P < 0.01, ***P < 0.001, ****P < 0.0001 vs. Control).*

Then, the effects of tigecycline on the EMT process was also evaluated in secondary colonospheres obtained from HCT116 and CMT93 cancer cell lines. In line with the results obtained for HCT116 cell monolayer, tigecycline was also able to reduce SNAI1 levels in both HCT116 (Figure 42A) and CMT93 cells (Figure 42B).

Moreover, RT-qPCR analysis supported the results obtained by Western blot analysis revealing that HCT116 colonospheres treated with tigecycline showed an upregulation of *CDH1* accompanied by an downregulation of *SNAI1* gene expression (Figure 32C). Moreover, tigecycline also reduced the expression of *OCT4B,* a short isoform of OCT4 that induces EMT and cancer dissemination (544). Stemmer et al., (2018) reported that SNAI1 can interact with CTNNB1 and stimulate the Wnt/β-catenin pathway, which also promotes the EMT (234). As it was reported in the first objective of the present Thesis, tigecycline was able to reduce CTNNB1 levels. This effect was also carried out in HCT116 cells derived from secondary colonospheres where tigecycline achieved a reduction of *CTNNB1* expression (Figure 32C) and protein levels (Figure 32D).

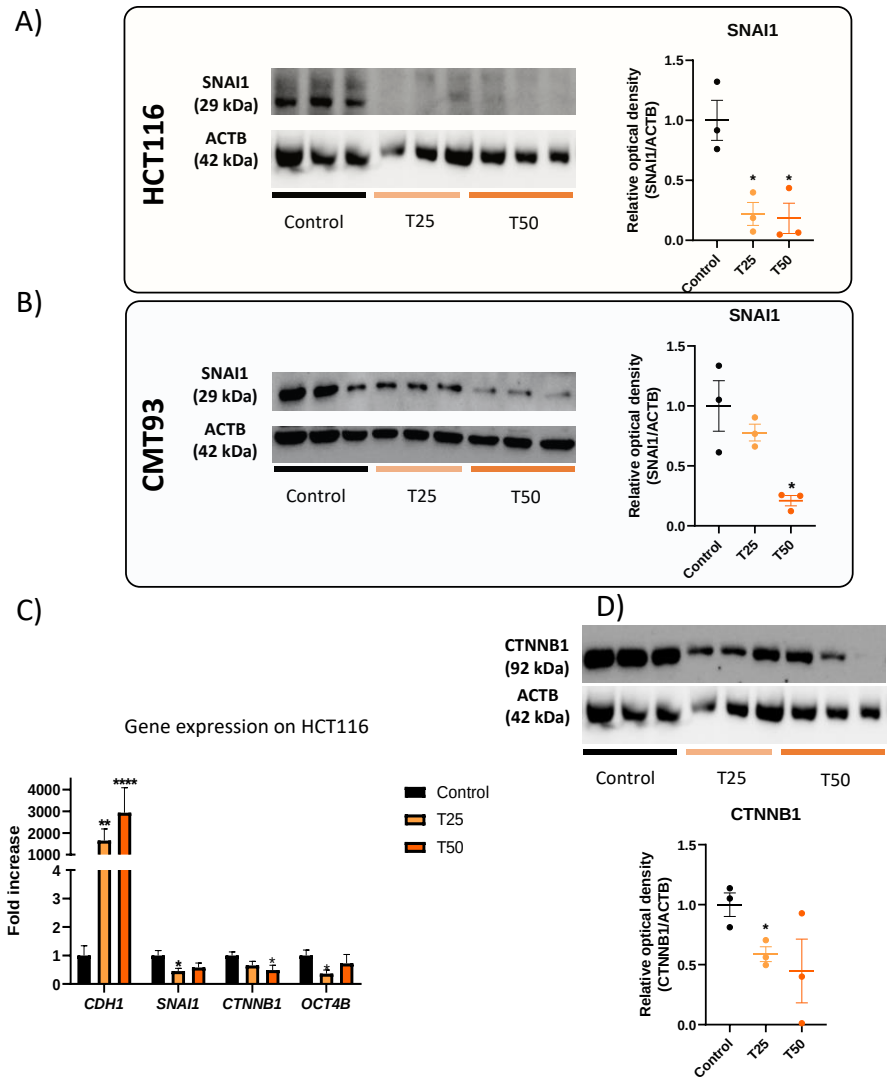

Figure 42. Tigecycline reduces the levels of pluripotency and EMT-related genes in secondary colonospheres. *Impact of tigecycline in SNAI1 levels evaluated by Western blot on (A) HCT116 and (B) CMT93 cancer cell lines. (C) Expression levels of EMT-related genes in HCT116 colonospheres treated with tigecycline at 0, 25 or 50 µM for 6h. (D) Impact of tigecycline treatment on CTNNB1 protein levels on HCT116 colonospheres. Data are graphed as mean ± SEM (*P < 0.05, **P < 0.01, ***P < 0.001, ****P < 0.0001 vs. Control).*

4.4. IMPACT OF TIGECYCLINE ON TUMORIGENESIS IN A HCT116 XENOGRAFT MURINE MODEL

In order to know if the beneficial effects achieved by tigecycline could be extrapolated *in vivo,* two different experiments were designed. In the first experiment, secondary colonospheres were incubated for 48h with tigecycline (50 µM), and then, they were subcutaneously injected in the right flank of NSG mice, whereas untreated cells were injected in the left flank as control. As it is shown in Figure 43A and B, tumors generated by non-treated cells displayed higher volume than those generated by treated cells.

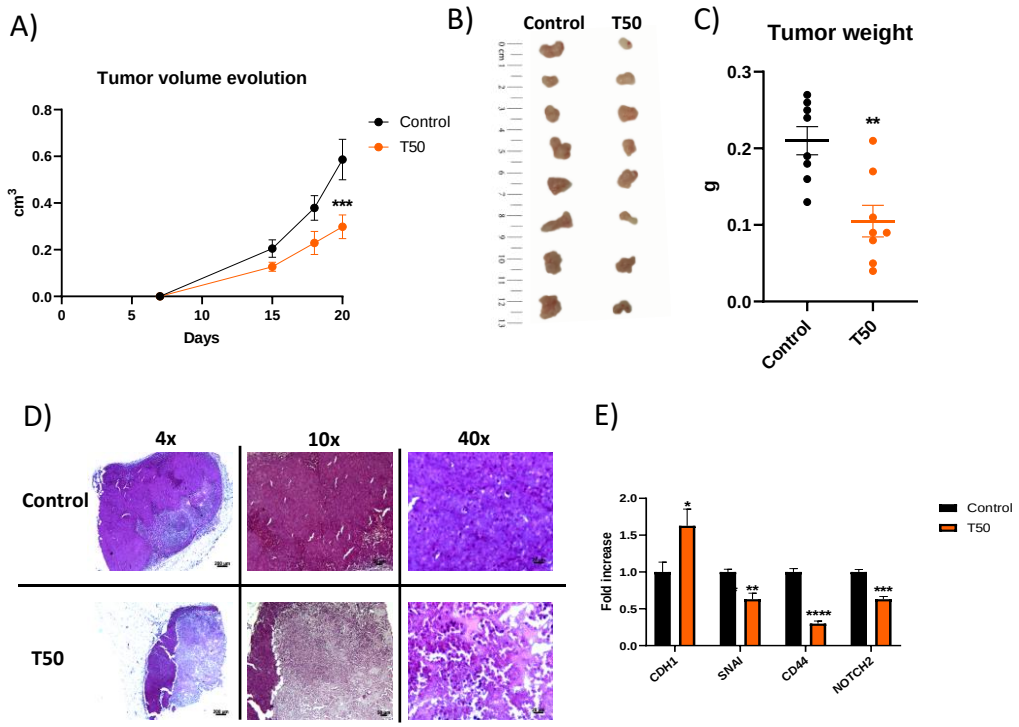

Figure 43. Tumorigenic capacity of HCT116 xenograft after being treated with tigecycline 50 µM ex vivo. *(A) Tumor volume evolution. (B) Representative image of the tumor size of both groups of mice. (C) Tumor weight. (D) Representative images of H&E staining of tumor sections from mice receiving tigecycline-treated or untreated cells. Scale bar: 200 µm for 4x images; 50 µm for 10x images; and 20 µm for 40x images. (E) Gene expression analysis of CSC and EMT-related genes in untreated and tigecycline-treated HCT116 cells. Data are graphed as mean ± SEM (*P < 0.05, **P < 0.01, ***P < 0.001, ****P < 0.0001 vs. Control).*

Moreover, 28 days after cell inoculation, mice were sacrificed and tumors were removed and weighed, obtaining a significantly lower weight in those tumors generated from treated cells than in those generated by untreated cells (Figure 43C). Histologically, typical tumor cell morphology was observed in control xenograft characterized by high nucleus/cytoplasm ratio, cytoplasmic basophilia and active mitosis (Figure 43D). Conversely, the structural integrity of the tumor was altered when cells were previously treated with tigecycline, which induced apoptotic features such as loss of intercellular contact, presence of a high amount of connective tissue in intercellular spaces, as well as an increase in cells in an apoptotic state (cytoplasm and chromatin condensation) (545, 546) (Figure 43D). Moreover, gene expression analysis carried out in these cells showed significant differences in CSC-related genes (*CDH1, SNAI1, CD44* and *NOTCH2*) between untreated and treated cells (Figure 43E).

In the second experiment, the effects of orally administered tigecycline (25 and 50 mg/kg/day) were evaluated in a HCT116 xenograft model in mice. With this aim, secondary spheres were injected in the right flank of NSG mice, starting the tigecycline treatment two weeks later. Interestingly, a significant reduction in tumor volume evolution was observed in those mice treated with the highest dose of tigecycline (Figure 44A and B), accompanied by a marked decrease in tumor weight at the end of the assay (Figure 44C).

The antitumor effect of tigecycline was also evidenced by a reduction in tumor metabolism in those treated mice (Figure 44D). Moreover, tumors from mice treated with tigecycline showed a higher expression of *CDH1* when compared with control mice. In addition, expression levels of EMT-related genes such as *SNAI1*, *SOX2* and *NANOG* were significantly higher in control mice than in those treated with tigecycline (Figure 44E). In accordance with the effects obtained *in vitro,* the treatment with tigecycline resulted in a significant reduction of CTNNB1 levels (Figure 44F and G)

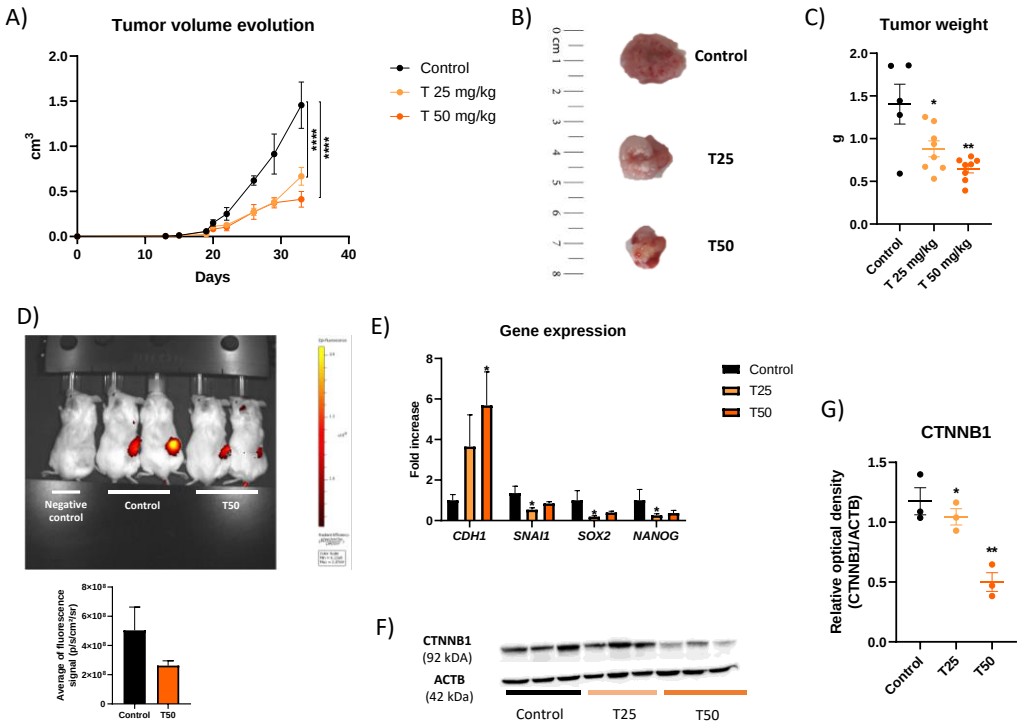

Figure 44. Effect of oral administration of tigecycline on HCT116 xenograft mice. *(A) Tumor volume evolution. (B) Representative image of the tumor size of each group of mice. (C) Tumor weight. (D) Representative IVIS imaging obtained at the end of the assay (up) of a negative control mouse (up and left), two control-untreated mice (up and middle) and two mice treated with tigecycline 50 mg/kg (up and right). Average of fluorescence in the tumor region (down). (E) Gene expression analysis of CSC and EMT-related genes. (F) Western blot bands and (G) their quantification of CTNNB1 levels in control mice and in those treated with tigecycline 25 or 50 mg/kg/day. Data are graphed as mean ± SEM (*P < 0.05, **P < 0.01, ***P < 0.001, ****P < 0.0001 vs. Control).*

5. TIGECYCLINE ATTENUATES TUMORIGENESIS IN AOM/DSS TREATED MICE.

In order to confirm the anti-tumoral effects of tigecycline evidenced in vitro, the antibiotic was assayed in an experimental model of CAC in mice, the AOM/DSS model. The results revealed that no mortality was observed in those mice treated with the highest dose of tigecycline or with 5-FU, whereas it occurred in the control CAC group (90% survival) and in that treated with the lower dose of tigecycline (80% survival); however, no statistical

differences in survival rates were observed among groups (Figure 45A). As evidenced by colonoscopy images and score (calculated as previously described by Becker C. et al., (518), the administration of either tigecycline or 5-FU exerted beneficial effects ameliorating tumoral progression (Figure 45B). This amelioration of the disease was confirmed the day of the end of the experiment when colons were obtained, rinsed and longitudinally opened in order to count the number of tumors. Importantly, tigecycline and 5-FU were able to significantly reduce the number and size of tumors (Figure 45C-F). Additionally, histological analysis confirmed these observations and showed a higher number of adenocarcinomas in non-treated CAC mice than in treated mice (Figure 46A).

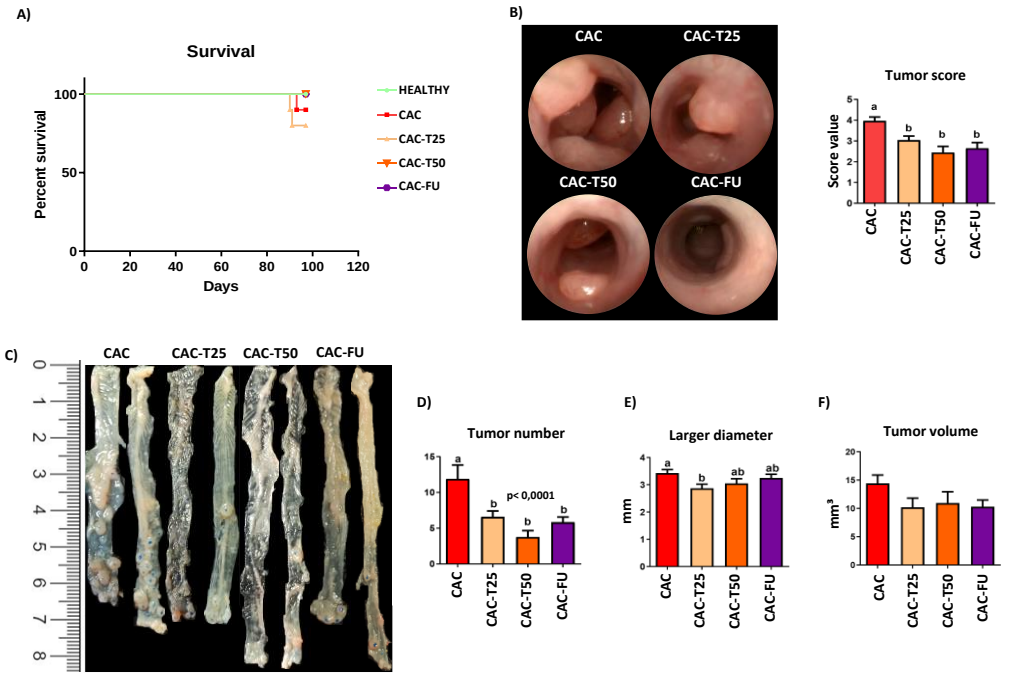

Figure 45. Effect of tigecycline and 5-FU on murine CAC model and impact on tumorigenesis. *(A) Survival rates. (B) Representative colonoscopy images and tumor score based on the size of the tumor evaluated by colonoscopy (B). (C) Representative colon images of CAC, CAC-T25, CAC-T50 and CAC-FU mice, (D) tumor number, (E) tumor size and (F) tumor volume. Data are presented as mean ± SEM. Bars with different letters differ statistically (P<0.05).*

Furthermore, the immunofluorescence analysis carried out with anti-Ki67 supports the antiproliferative effect of tigecycline and 5-FU, which results in a reduction of the proliferation index (Figure 46B).

Additional determinations were performed to characterize the molecular mechanisms underlying these antiproliferative effects. Thus, the inhibitory effects exerted by

tigecycline on CAC progression seemed to be mediated by modulation of the Wnt/β-catenin signaling pathway, thus confirming the in vitro results commented above. In fact, and similarly to that observed *in vitro*, tigecycline inhibited STAT3 activation in CAC mice, resulting in a reduction of the ratio phospho-STAT3/STAT3 (Figure 47A and B). Subsequently, the treatment ameliorated the expression of the downstream genes *Ccnd1* and *Mmp9,* which were upregulated in control CAC mice (Figure 47B). Furthermore, a trend to reduce the colonic levels of CTNNB1 was observed with both tigecycline and 5-FU (Figure 47A and B). The antiproliferative effect observed may be also due to the inhibitory effects of tigecycline on AKT activation, thus resulting in a reduction of the phospho-AKT/AKT ratio, which was increased in control CAC mice (Figure 47A and B). This effect was also observed with 5-FU treatment and it could be associated with a significant downregulation of *Angpt2,* an important mediator in the angiogenesis process. The effects of tigecycline on CSCs populations were also evaluated by flow cytometry analysis. An increase in $LGR5^+$ and $LGR5^+CD44^+$ CSCs populations was found in control CAC mice, whereas the treatment with tigecycline significantly reduced the levels of both populations (Figure 47C). When the impact of tigecycline on CSCs formation was evaluated, a significant reduction in SNAI1 levels was observed in those mice treated with tigecycline in comparison with the CAC group (Figure 47D).

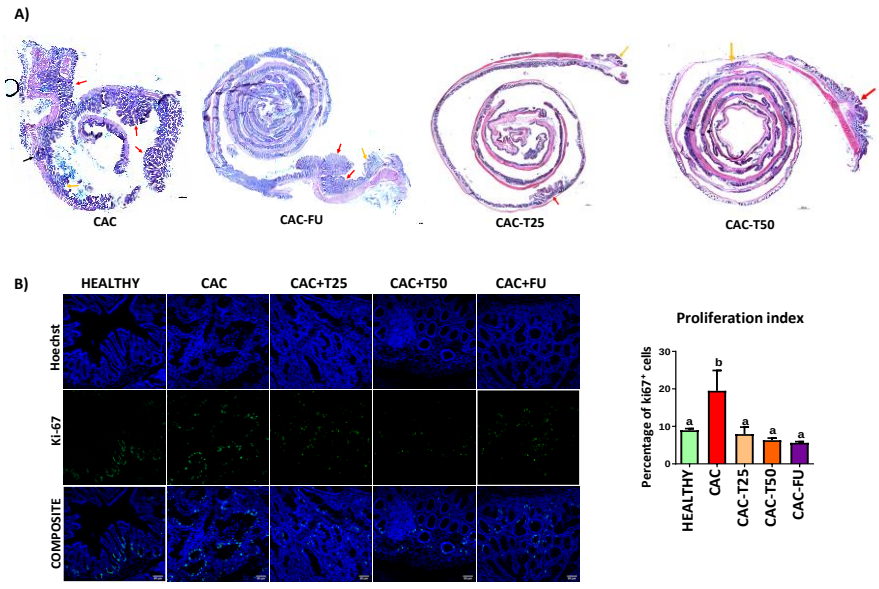

Figure 46. Histological study of colon from CAC mice treated with tigecycline and 5-FU. *(A) Representative colon sections stained with haematoxylin, eosin and alcian*

blue. Adenocarcinomas are indicated with red arrows, adenomas with blue arrows and a lymph node with black arrow. (B) Ki67 immunofluorescence staining (green) was conducted to identify actively proliferating cells and proliferation index was calculated from the percentage of ki67-positive cells in ratio to total cells per field. Data are presented as mean ± SEM. Bars with different letters differ statistically (P<0.05).

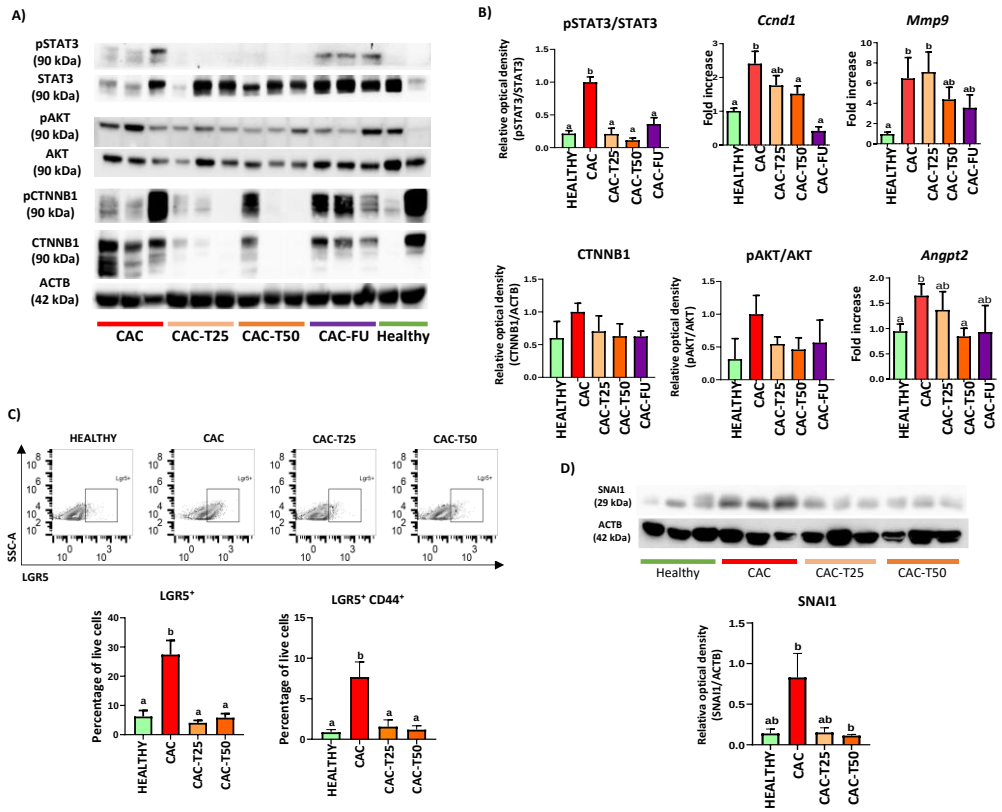

Figure 47. Impact of tigecycline and 5-FU on cell proliferation and stemness in CAC mice. *(A) Western blot bands, (B) protein quantification and gene expression of several markers involved in cell proliferation evaluated and detected in colon.(C) Representative flow cytometry analysis of LGR5⁺ population and quantification of LGR5⁺ and LGR5⁺CD44⁺ cell populations in each experimental group. (D) Changes in SNAI1 levels induced by the CAC process and tigecycline treatment analyzed by western blot in colon. Data are presented as mean ± SEM. Bars with different letters differ statistically (P<0.05).*

Moreover, the anti-tumor effect of tigecycline was also related to a pro-apoptotic impact. The TUNEL assay showed an increase in the number of apoptotic cells in mice treated with either tigecycline or 5-FU (Figure 48A). In accordance with the *in vitro* results

described above, the apoptosis induction exerted by tigecycline in CAC mice involved the increase the levels of CASP7, both full length and cleaved (Figure 48B and C). Moreover, tigecycline and 5-FU treated mice also normalized the levels of BCL2 compared to CAC-mice (Figure 48B and C), which can also contribute to the pro-apoptotic effect.

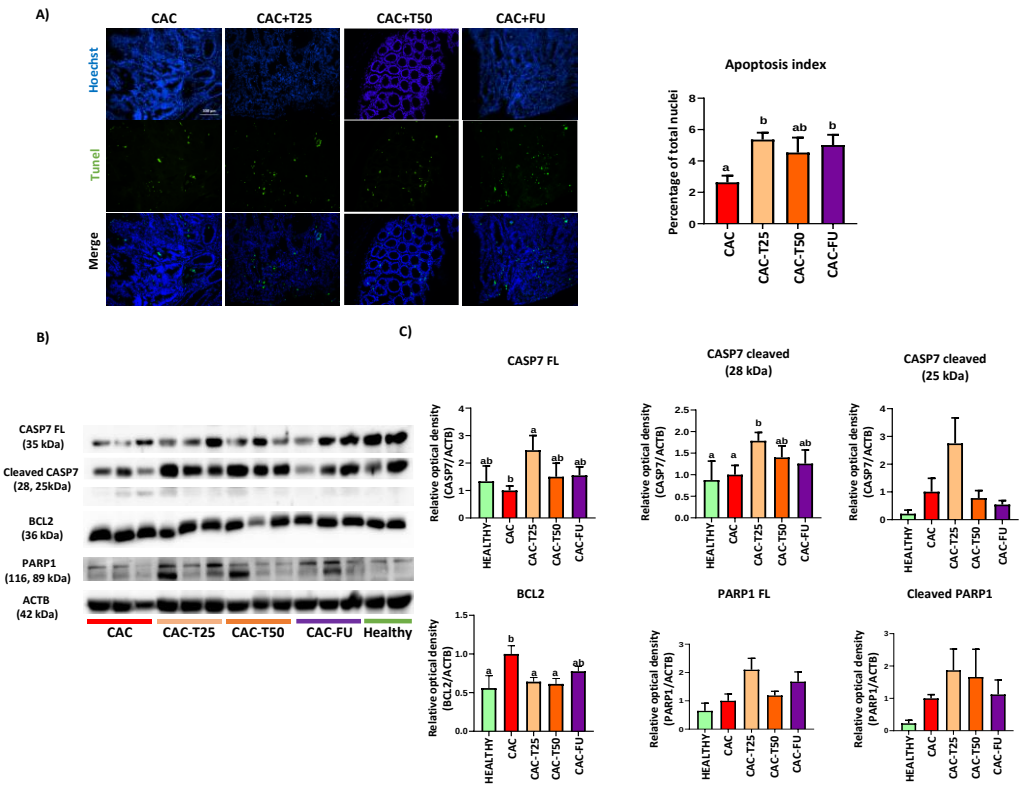

Figure 48. Apoptotic effect of tigecycline and 5-FU on CAC mice. *(A) Representative fluorescence images of Tunel assay-stained (apoptosis) colonic tissue sections from CAC, CAC-T25, CAC-T50 and CAC-FU mice. Apoptotic cells are stained in green and nuclei in blue (Hoechst). The apoptosis index was calculated as Tunel⁺ cells/total cells per field. (B) Western blot bands and (C) quantification of several markers Data are presented as mean ± SEM. Bars with different letters differ statistically (P<0.05).involved in apoptosis and cell survival analyzed in colon tissue.*

The inflammatory status of the disease was assessed throughout the induction process by monitoring the DAI (Figure 49A). 5-FU treatment did not show any statistical

differences in comparison with the CAC control group at the end of the assay, but tigecycline significantly reduced DAI values (Figure 49A). Accordingly, tigecycline inhibited the expression of some cytokines involved in the tumor-associated inflammatory response in the colon, like *Tnfa*, *Il6*, *Il17a* and *Il23a* (Figure 49B).

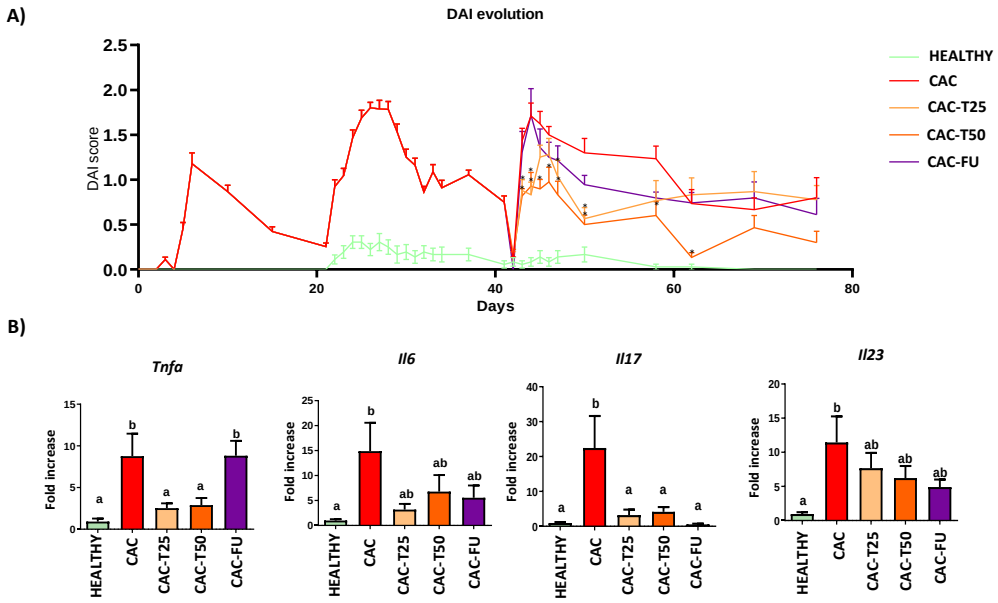

Figure 49. Effect of tigecycline and 5-FU on CRC-associated inflammation. *(A) DAI score. (B) Impact on the cytokines gene expression quantified by real-time qPCR. Fold increase was calculated vs. control group. Data are presented as mean ± SEM. Bars with different letters differ statistically (P<0.05).*

When the impact of the tigecycline on the myeloid populations from colon ($CD45^+CD11b^+$) and lymphoid cells in MLNs ($CD3^+CD4^+$/$CD3^+CD8^+$) was analyzed, a reduced infiltration of myeloid cells ($CD45^+CD11b^+$) into the colon was observed (Figure 49A). Also, similar numbers of $CD3^+CD4^+$ cells among the T cells from MLNs were observed in the different groups, together with a significant reduction of $CD8^+$ CTLs in CAC group (Figure 49B and C). When the $CD3^+CD4^+IFN\gamma^+$ (Th1 phenotype) population was considered, the highest dose of tigecycline produced a significant increase (Figure 49C). Interestingly, this increment has been associated with a protective response against CAC through favoring the recruitment of CTLs (547). In fact, when CTL population was analyzed, tigecycline and 5-FU increased its level in comparison with

non-treated CAC-mice (Figure 49C), particularly those CTLs with interferon-γ (IFNγ) production (Tc1) (Figure 49C).

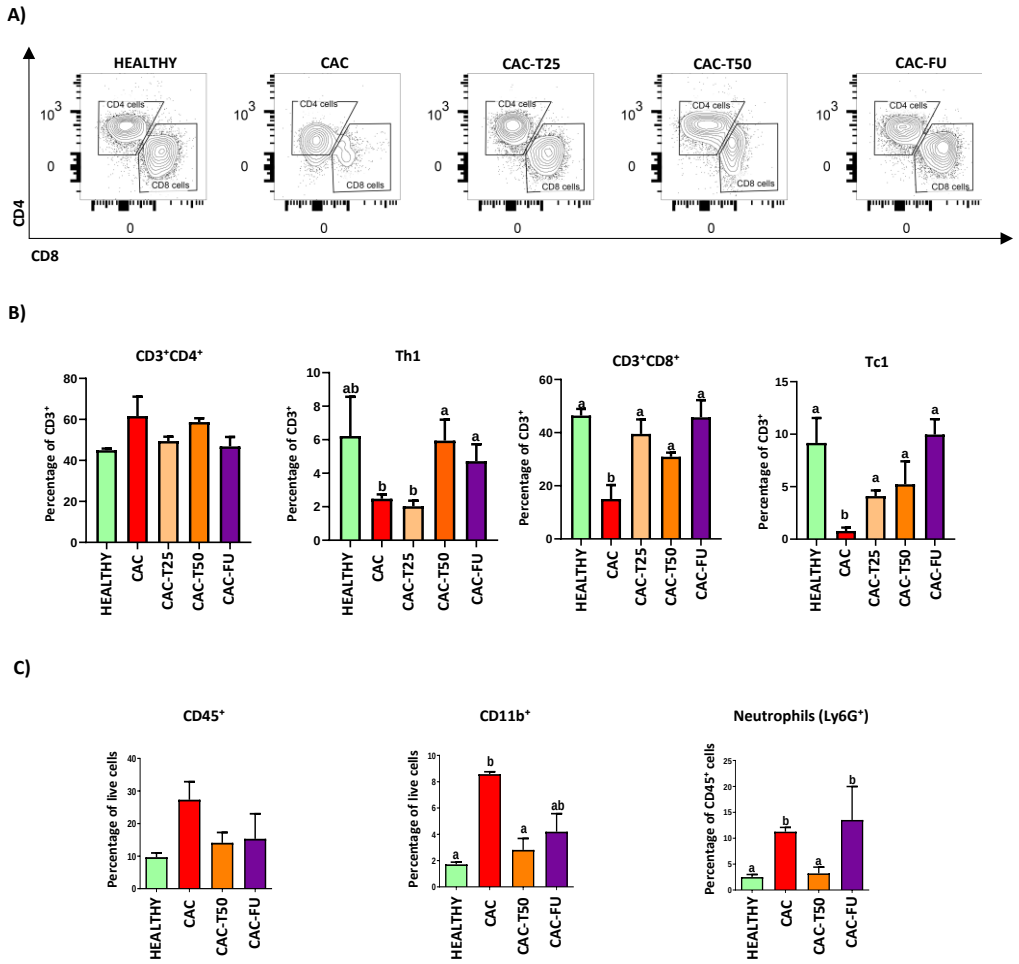

Figure 49. Effect of tigecycline and 5-FU on cell immune populations in CAC mice. *(A) Representative dot plots from HEALTHY, CAC, CAC-T25, CAC-T50 and CAC-FU mice showing the CD4 vs. CD8 T lymphocyte distribution. (B) $CD3^+CD4^+$, Th1, $CD3^+CD8^+$, Tc1 and (C) $CD45^+$, $CD11b^+$ and Neutrophils populations levels in HEALTHY, CAC, CAC-T25, CAC-T50 and CAC-FU mice groups. Data are presented as mean ± SEM. Bars with different letters differ statistically (P<0.05).*

The effect of tigecycline treatment on gut dysbiosis was also explored since this microbiota alteration plays a pivotal role in CRC development, as evidenced both in human and in experimental models. The analysis of 16S rRNA sequencing results confirmed that microbiota composition was clearly modified in control CAC mice

compared to healthy mice. However, the administration of tigecycline (25 mg/kg) or 5-FU treatment showed a clear impact on gut microbiota composition, since the treatments significantly increased alpha diversity, calculated by different indexes (observed species, Shannon, ACE, and Simpson), in comparison with untreated CAC group (Figure 50A). Conversely, diversity indexes were lower in those mice treated with the highest dose of tigecycline (50 mg/kg) (Figure 50A), most probably due to the antibiotic effect exerted at this dose. Besides, the beta diversity determined by weighted unifrac analysis revealed a clear separation in the PCoA between healthy and control CAC group, indicating that the homeostasis of gut microbiota was dramatically disrupted by the AOM/DSS administration to mice (Figure 50B). Remarkably, the 5-FU mice and the lowest dose of tigecycline showed more resemblance to the healthy group (Figure 50B). Consistently, the Venn diagram (prevalence 75%) showed that there were only 4 common OTUs among healthy and CAC groups, and that the highest number of shared OTUs was presented among healthy group and tigecycline group (25 mg/kg, 48 shared OTUs) (Figure 50C).

The gut microbiota composition and their abundance were also determined in more detail. As shown in Figure 50D, the relative taxonomic composition at the phylum level mainly contained *Bacillota*, *Bacteroidota*, *Pseudomonadota* and *Verrucomicrobiota.* Additionally, the relative abundance of *Bacillota* and *Actinomycetota* was diminished in the control CAC group in comparison with the healthy group, whereas *Bacteroidota*, *Pseudomonadota*, and *Verrucomicrobiota* levels were increased (Figure 50D). Notably, the administration of tigecycline attenuated the modification in the gut microbiota composition caused by AOM/DSS administration (Figure 50D). Furthermore, the control CAC group showed a significant reduction of the F/B ratio when compared to healthy control mice. Importantly, the treatment with the lowest dose of tigecycline significantly increased this ratio (Figure 50E). At genus level, the heatmap showed that the abundance of some of the bacteria was increased in the CAC group when compared to healthy mice (*Akkermansia*, *Turicibacter*, *Lachnospiraceae*, *Desulfovibrio* and *Enterorhabdus*) (Figure 50F), whereas other genera were reduced (*Coriobacteriaceae*, *Lactobacillus*, and *Dubosiella*) (Figure 50F).

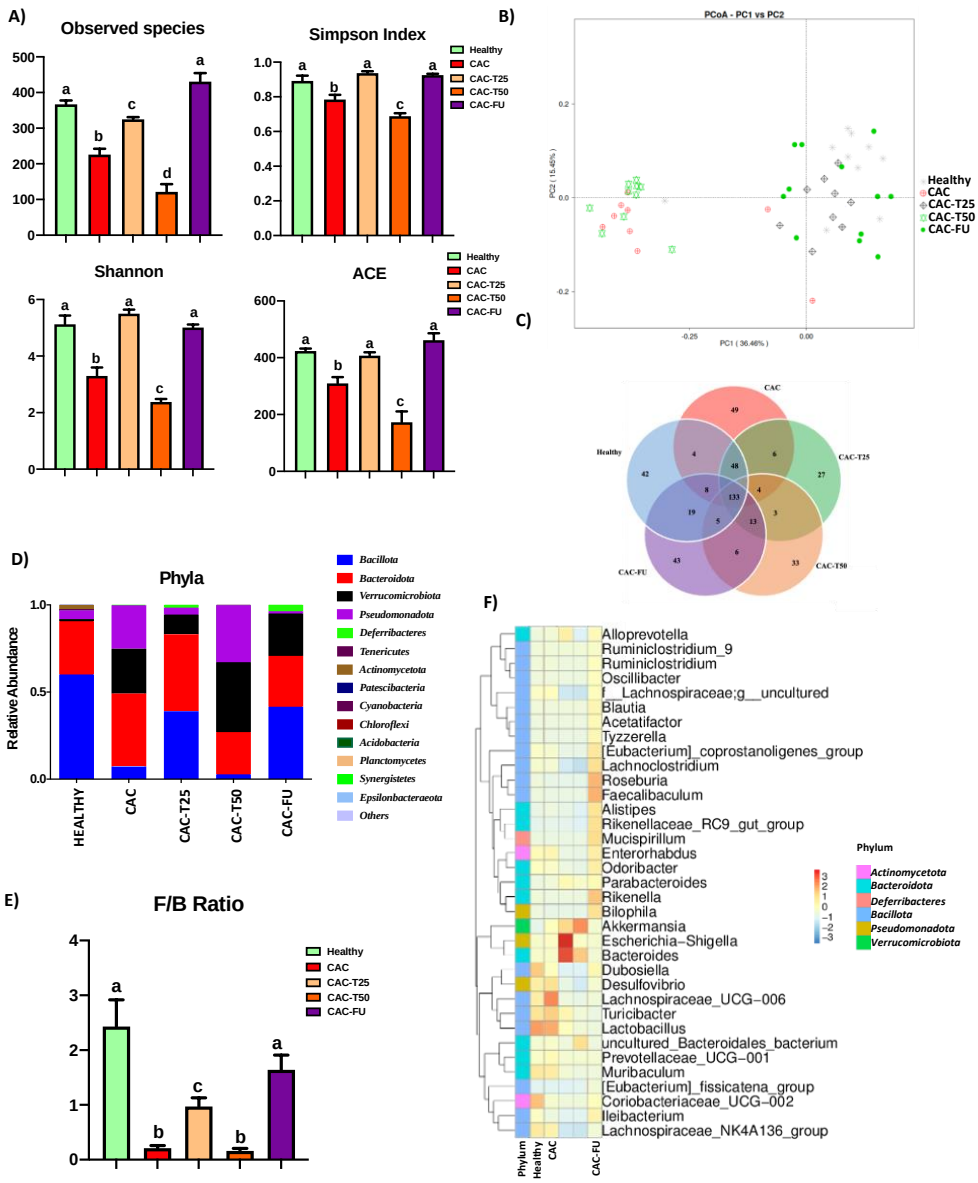

Figure 50. Effect of tigecycline and 5-FU on gut microbiota composition. *(A) Microbiome diversity indexes calculated after fecal microbiota Illumina sequencing: observed species, Simpson index, Shannon index and ACE index. (B) β-diversity by principal coordinate analysis score plot. (C) A Venn diagram showing the number of OTUs which are unique and common to each experimental group. (D) Distribution histogram of relative abundance of taxa. (E) Bacillota/Bateroidota (named F/B) ratio in each experimental group (F) A heatmap showing the taxonomic signatures at the genus*

level. Data are presented as mean ± SEM. Bars with different letters differ statistically (P<0.05).

The Volcano plots provide information about the amount of OTUs that are downregulated and upregulated with respect to the control CAC group. Specifically, in healthy and CAC-FU the higher number of OTUs were upregulated, 93 and 130 OTUs, respectively (Figure 51A). When the Venn diagram was determined with the upregulated OTUs the results showed that none of them were shared among the four groups. Conversely, one of them, corresponding to *Parabacteroides* genus, was observed among the three treated groups (Figure 51B). Moreover, 6 OTUs were up-regulated and shared among mice treated with the two doses of tigecycline (Figure 51B): *Enterobacteriaceae* family, *Akkermansia* and *Bacteroides* genera, as well as, *Parabacteroides distasonis* and *uncultured Bacteroidales bacterium* bacterial species (Figure 51B). Additionally, in tigecycline-treated mice, the higher number of OTUs were found downregulated when compared to the control CAC group: 87 and 130 OTUs, respectively (Figure 51B). Three of them were significantly downregulated, and shared in the three groups of treated mice: *Dubosiella* genus and *Dubosiella newyorkinensis* and *Clostridium sp. ASF502* bacterial species (Figure 51B). When tigecycline treated groups were compared only two bacterial genera (*Faecalibaculum* and *A2* from *Lachnospiraceae)* were decreased and shared (Figure 51B).

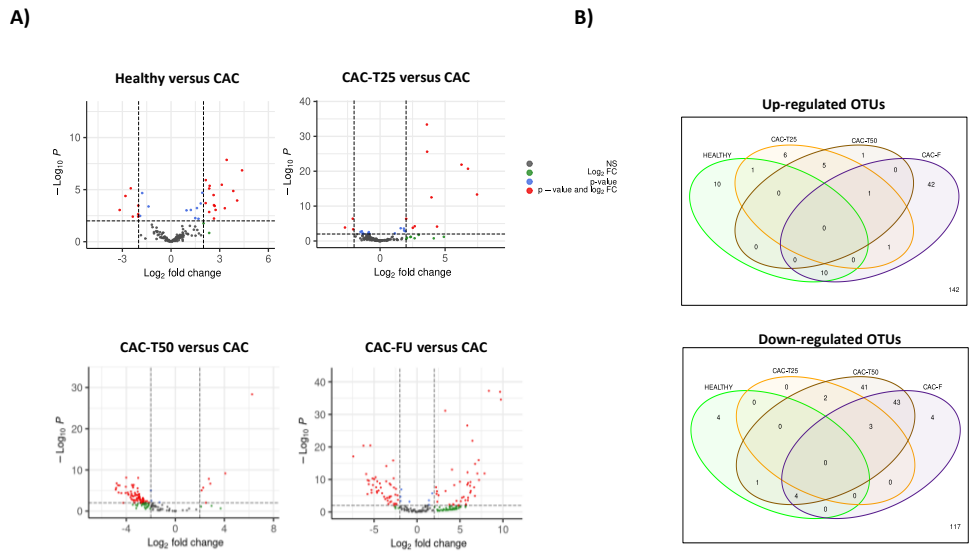

Figure 51. Effect of tigecycline and 5-FU on gut microbiota composition. *(A) Volcano plot indicating the upregulated and downregulated OTUs in Healthy, CAC-T25, CAC-T50 and CAC-FU in comparison with those OTUs determined on CAC group. (B)*

Venn-diagrams that show the down-regulated shared OTUs and the up-regulated shared OTUs between Healthy, CAC-T25, CAC-T50 and CAC-FU when compared with the CAC group.

When focused on OTUs shared in both treated and healthy mice, *Ruminococcus 1* and *Erysipelatoclostridium* genera, *Lachnospiraceae bacterium* COE1 and *Clostridium* sp. Clone-47 species were found down-regulated in healthy, CAC-T50 and CAC-FU groups (Figure 51B). Additionally, the genus *Ruminococcaceae* UCG-013 was decreased in healthy and tigecycline 50 mg/kg treated mice (Figure 51B).

III. CHARACTERIZATION OF THE IMPACT OF OBESITY IN CRC DEVELOPMENT: IMPACT OF TIGECYCLINE IN A OBESITY-ASSOCIATED CAC MODEL.

1. ADIPOSE CELL-DERIVED METABOLITES CONTRIBUTE TO THE PROLIFERATION AND CLONOGENICITY OF TUMOR CELLS.

As it is widely known, overweight and obese patients suffer from hypertrophy and hyperplasia in adipose tissue that lead to fat accumulation. It has been reported that adipocytes are a source of metabolites that can be involved in the pathogenesis of cancer (548), thus justifying that obesity has been considered as a risk factor for the development of CRC. Therefore, and in order to study the association between obesity and cancer, the impact of the conditioned medium of ADSCs and differentiated adipocytes on the clonogenicity of HCT116 colon cancer cells was evaluated. A significant increase in the number of colonies and size of HCT116 cells was observed when they were incubated with the conditioned medium of both ADSCs and differentiated adipocytes (Figure 52A).

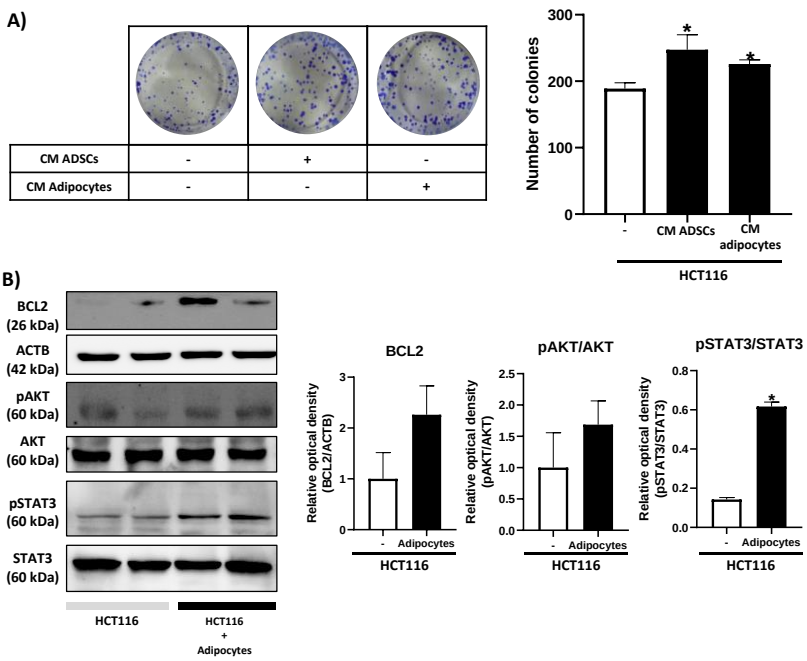

Figure 52. Adipose cells increase the tumorigenicity of colon cancer cells. *(A) Clonogenicity capacity of HCT116 cells is increased after being incubated with 10%*

*conditioned medium (CM) of ADSCs or adipocytes. (B) Western blot analysis of survival and proliferation markers carried out in HCT116 cells co-cultured with adipocytes. Data are graphed as mean ± SEM (*P < 0.05, **P < 0.01, ***P < 0.001, ****P < 0.0001 vs. Control).*

These results suggested that adipose cells secrete metabolites that contribute to the clonogenicity of tumor cells. Then, additional experiments were performed to characterize the molecular mechanisms involved in this effect, i.e., in the growth of tumor cells induced by adipose cells. The results revealed that the coculture of HCT116 with adipocytes expressed higher levels of the survival marker BCL2, as well as further activation of AKT and STAT3, although only the latter showed statistical differences (Figure 52B). Therefore, these results may provide a mechanistic explanation by which adipose cells could increase the tumorigenesis of colon cancer cells.

2. TIGECYCLINE MITIGATES THE DISEASE SEVERITY IN A MODEL OF OBESITY-ASSOCIATED CAC.

In order to further study the complex relationships between obesity and CRC, a murine model that combined both pathologies was designed. As shown in Figure 53A, C57Bl/6 mice were fed SD or HFD for 10 weeks and then, AOM was intraperitoneally administered to these mice. Subsequently, mice were subjected to three cycles of DSS at 2% in drinking water to promote CAC. At the beginning of the third cycle, a group of HFD mice was treated with tigecycline at 25 mg/kg/day in order to evaluate the impact of this drug in obesity-associated CAC.

As expected, mice fed HFD resulted in a significant increase in body weight when compared to those mice fed SD (Figure 53B). Obesity is characterized by impairment of the glucose metabolism due to the development of insulin resistance, with high levels of insulin and glucose in plasma, and this metabolism alteration has been associated with a higher risk of colon cancer development development (549). Thus, the GTT was performed one week before the end of the experiment, and the results revealed that control obese CAC mice showed significantly higher blood glucose levels than the SD-fed group (Figure 53C). Conversely, tigecycline treatment resulted in a faster recovery of blood glucose levels, although there were no significant differences in the AUC of glycemia when compared to untreated obese mice (Figure 53C and D).

The presence of both comorbidities, CRC and obesity resulted in higher mortality, although no significant differences were found with respect to that obtained in lean mice

with CAC (Figure 53E). The treatment with tigecycline was not able to reverse the mortality percentage suffered by obese mice submitted to CAC (Figure 53E).

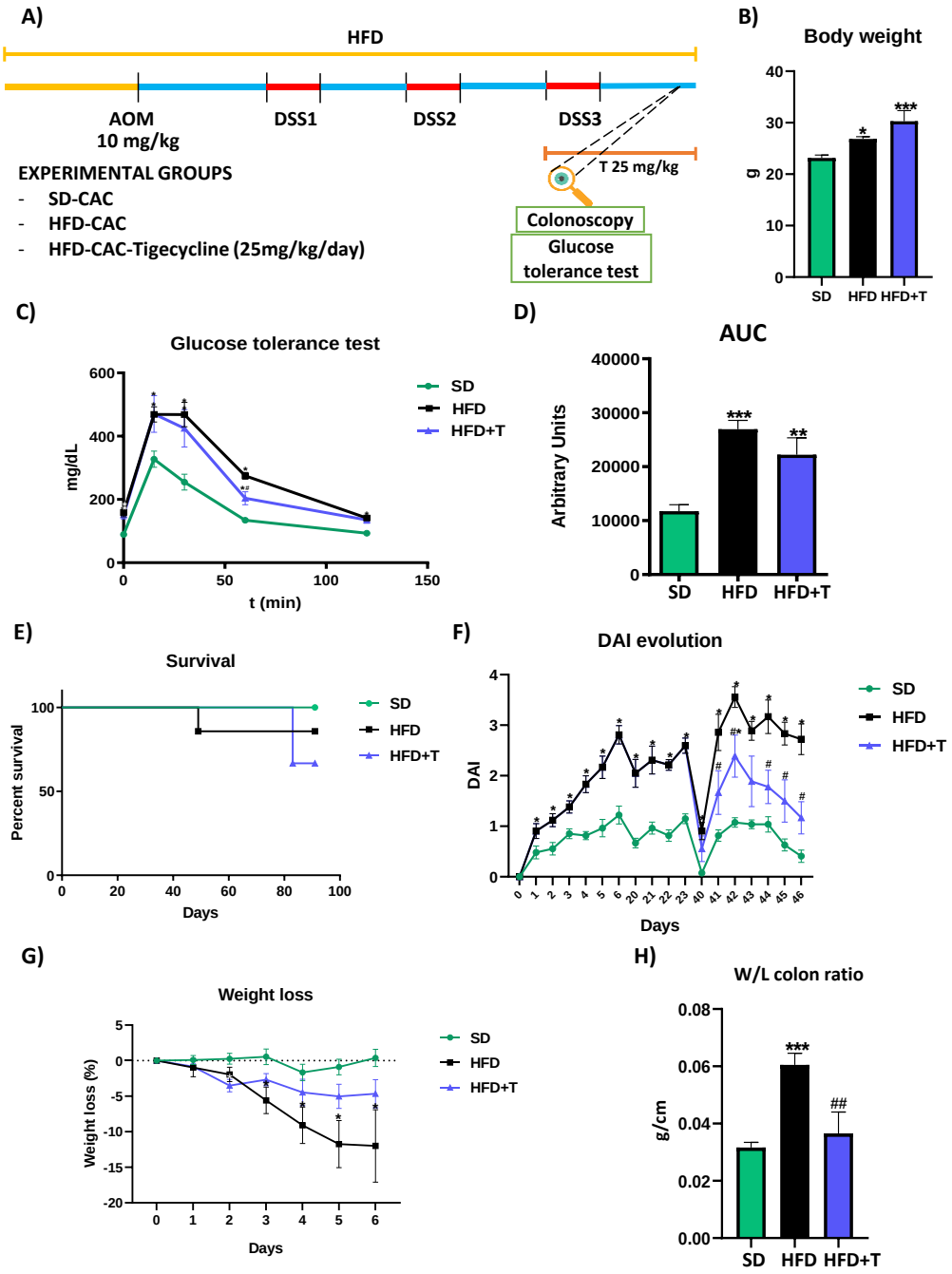

Figure 53. Tigecycline attenuates the disease severity in a model of obesity-associated CAC. *(A) C57Bl/6 mice were fed with a SD or HFD before being subjected to CAC induction through the intraperitoneally injection of 10 mg/kg of AOM followed by*

*three cycles of DSS interspersed with weeks of rest. A group of obese mice with cancer was treated with tigecycline during the last 7 weeks of the assay. Moreover, a week before the endpoint a glucose tolerance test and a colonoscopy were carried out. (B) Body weight of mice at the end of the experiment. (C) Glucose tolerance test. (D) Area under the curve (AUC) of glycemia of each group of mice. (E) Percentage survival. (F) Disease Activity Index (DAI) and (G) weight loss index were determined daily during the three DSS cycles. (H) Colon weight/length (W/L) ratio. Data are graphed as mean ± SEM (*P < 0.05, **P < 0.01, ***P < 0.001, ****P < 0.0001 vs. CAC control SD mice and $^{\#}$P < 0.05, $^{\#\#}$P < 0.01, $^{\#\#\#}$P < 0.001, $^{\#\#\#\#}$P < 0.0001 vs. CAC control HFD mice).*

Moreover, it has been reported that obesity negatively influences the inflammatory status in IBD patients, thus accelerating the development of the CAC process (382, 550). In accordance with previous studies, obese mice with CAC presented more severe inflammatory features than SD mice, as evidenced by the DAI score measured in each cycle of DSS incorporation to drinking water (Figure 53F). Conversely, the antiinflammatory properties associated to tigecycline resulted in an amelioration of the cancer-associated inflammation, since a significant reduction in DAI score values in these animals were observed when compared to untreated obese mice (Figure 53F). In addition, the severity of the disease was associated with a higher percentage of weight loss in obese mice with cancer that was attenuated by the tigecycline treatment (Figure 53G). During colitis development there is a shortening and thickening of the colon, thus resulting in an increase in the colon weight/length (W/L) ratio, being this a marker commonly used to evaluate colitis severity (551). In correlation with DAI score values, control obese mice showed a significant increase in the W/L ratio when compared to SD fed mice and those obese mice treated with tigecycline (Figure 53H).

3. TIGECYCLINE ADMINISTRATION REDUCED THE TUMORIGENESIS IN OBESITY-ASSOCIATED CAC MICE.

The evaluation of the tumorigenesis process in the different experimental groups by colonoscopy revealed an increase in tumor number and size grade in untreated HFD-mice when compared to those fed with SD (Figure 54A), thus resulting in an increase of endoscopic index of tumor severity (Figure 54B). Conversely, obese mice treated with

tigecycline exhibited a significant reduction in tumor number and size, which resulted in a significant reduction in the endoscopic index of tumor severity when compared to untreated obese mice (Figure 54B).

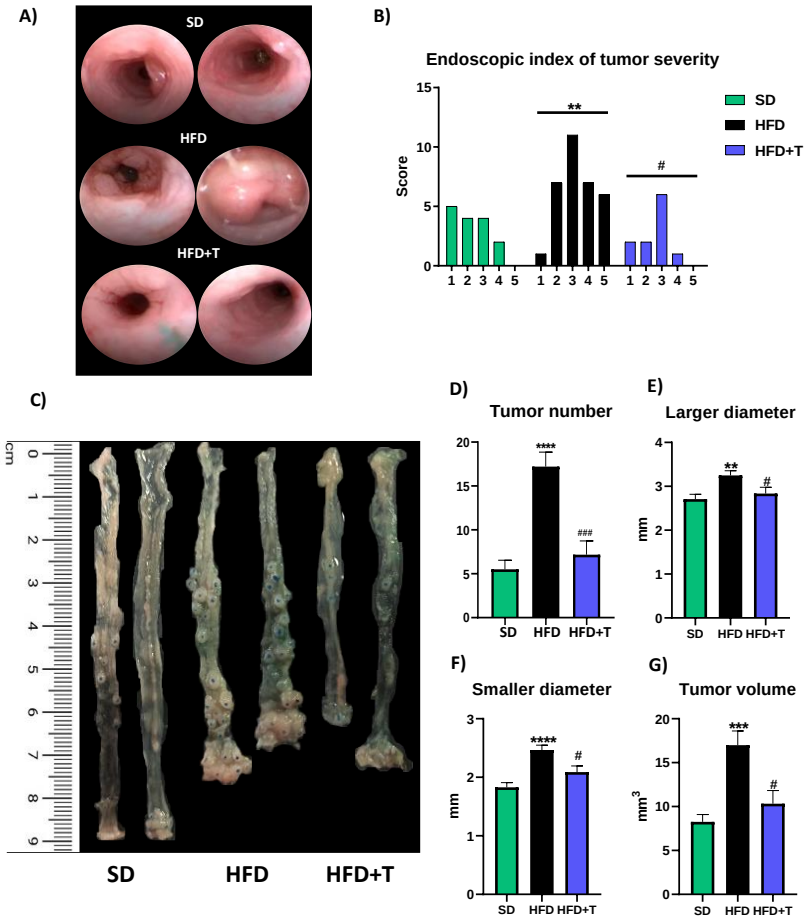

Figure 54. Tigecycline administration to obese mice with CAC reduces tumor burden and size. *(A) Representative images taken from a colonoscopy carried out one week before mice were sacrificed. (B) Endoscopic index of tumor severity based on the size of the tumors observed during the colonoscopy and calculated as previously described by Becker and colleagues (2006) (518). (C) Representative images of colons removed from SD, HFD and HFD+Tigecycline after their sacrifice. (D) Tumor number, (E) larger diameter, (F) smaller diameter and (G) tumor volume. Values are graphed as mean ± SEM (*P < 0.05, **P < 0.01, ***P < 0.001, ****P < 0.0001 vs. CAC control SD mice and #P < 0.05, ##P < 0.01, ###P < 0.001, ####P < 0.0001 vs. CAC control HFD mice).*

Once mice were sacrificed, tumor load and size were analyzed in the colonic segments. Supporting the colonoscopy observations, untreated HFD-fed mice showed a significant

increase of tumor burden compared to SD mice, while tigecycline treatment mitigated the tumorigenesis and resulted in a significant reduction in the number of tumors (Figure 54C and D). Additionally, obesity promoted the generation of larger tumors, resulting in a significant increase in both the larger (Figure 54E) and smaller (Figure 54F) diameter of tumors and, therefore, in the tumor volume (Figure 54G). The treatment with tigecycline not only mitigated the negative impact of obesity on tumor burden, but also managed to significantly reduce the size grade of the tumors (Figure 54E-G).

The histological analysis of the representative colonic sections revealed that, in the case of HFD untreated-mice, all specimens analyzed showed adenocarcinoma-type lesions with signs of submucosal invasiveness in some cases (Figure 55A and B). Conversely, the lesions observed in both SD and HFD tigecycline-treated mice were adenomes, without signs of submucosal invasion (Figure 55A and B). Moreover, in neoplastic areas, higher immune cell infiltration, together with lower number of goblet cells with an altered pattern of mucin secretion was observed in obese untreated-mice submitted to CAC in comparison with both SD and HFD tigecycline-treated mice (Figure 55A). These data suggest that obesity accelerates the malignancy of tumors, thus turning cancer to further advanced stages with tissue invasive capacity, while the treatment with tigecycline hinders this advance.

In order to better characterize the underlying mechanisms by which obesity aggravates tumorigenesis in CAC mice, cell proliferation was evaluated by the Ki67 staining in the colonic sections (Figure 55C). The results showed a significantly increased number of $Ki67^+$ cells in untreated HFD-fed CAC mice when compared to SD-fed CAC mice, thus revealing a significant increase of the proliferation index (Figure 55D), calculated through the percentage of the ratio between $Ki67^+$ cells and total number of cells per field. In turn, the treatment with tigecycline achieved a significant reduction in the number of $Ki67^+$ cells leading to a reduction of the proliferation index (Figure 55D).

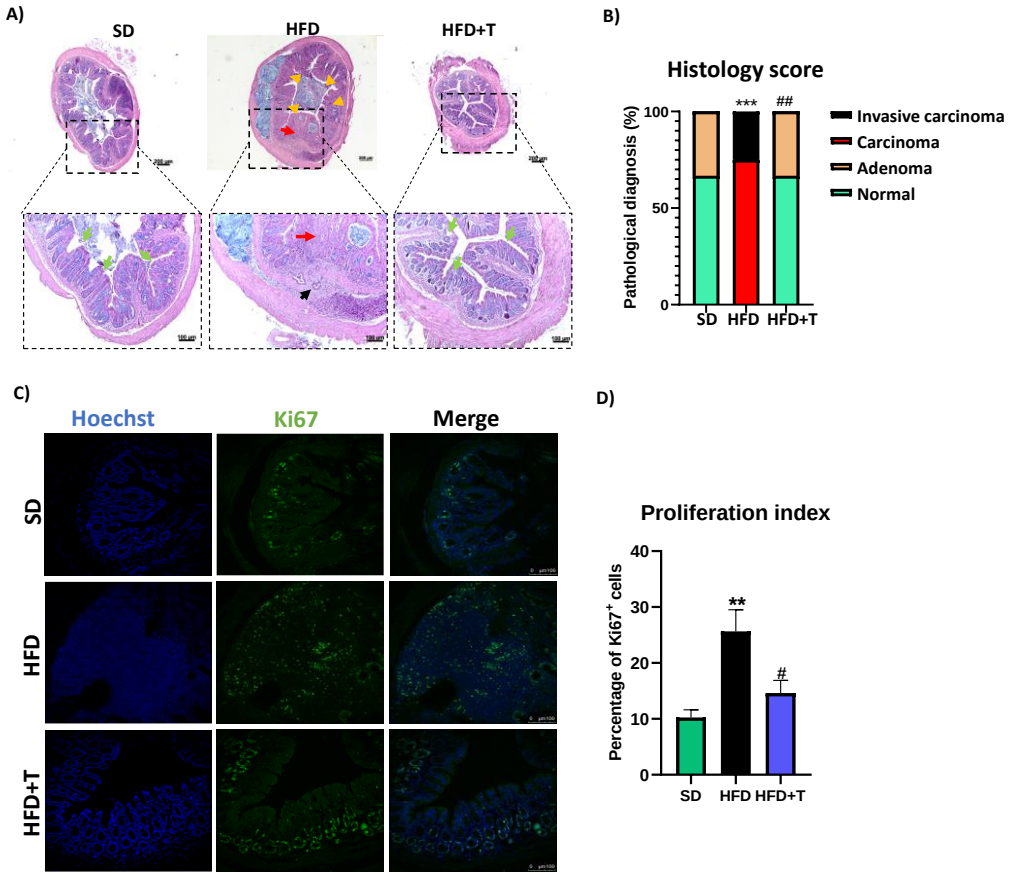

Figure 55. Tigecycline ameliorated the adenocarcinoma-like lesions with invasive capacity, which was associated with a reduction in the proliferation index in obese mice with CAC. *(A) Representative colonic sections of SD, HFD and HFD+T mice stained with haematoxylin, eosin and alcian blue. Scale bar: 200 µm (up) and 100 µm (low). Green arrow: healthy tissue; Yellow arrowhead: adenome; red arrow: adenocarcinoma; black arrow: invasive tumor. (B) Histology score based on the lesions observed in each group of mice. (C) Ki67 immunofluorescence staining (green) in colonic sections of SD, HFD and HFD+T mice. Scale bar: 100 µm. (D) Proliferation index calculated from the percentage of ki67-positive cells in ratio to total cells per field. Data are graphed as mean ± SEM (*P < 0.05, **P < 0.01, ***P < 0.001, ****P < 0.0001 vs. CAC control SD mice and $^{\#}$P < 0.05, $^{\#\#}$P < 0.01, $^{\#\#\#}$P < 0.001, $^{\#\#\#\#}$P < 0.0001 vs. CAC control HFD mice).*

4. IMPACT OF TIGECYCLINE ON ADIPOSE-DERIVED METABOLITES AND THEIR INVOLVEMENT IN CAC DEVELOPMENT.

As commented above, several factors, which are altered in obesity, have an important impact in cancer development and contribute to the activation of molecular pathways involved in tumor growth. In fact, it has been demonstrated that adipose-derived adipokines, like leptin, and cytokines, like IL-6, are involved in the overstimulation of proliferative molecular pathways, such as JAK/STAT3, PI3K/AKT and the widely known Wnt/β-catenin route (552, 553). IL-6 has been found to be increased in both obese and CRC patients (554, 555). In the present study, the levels of IL-6 were significantly upregulated in the inguinal fat deposits, as evidenced when both gene expression (Figure 56A) and protein levels were determined (Figure 56B). In turn, mice treated with tigecycline exhibited a downregulation of *Il6* gene expression (Figure 56A) and protein levels (Figure 56B). In concordance with these results, a significant increase in the activation of STAT3, evidenced by an increase in the pSTAT3/STAT3 ratio, was observed in untreated obese mice when compared to SD mice (Figure 56C). Tigecycline administration significantly inhibited colonic STAT3 activation in HFD-fed CAC, which was associated with a significant reduction in the active form of STAT3 in these mice (Figure 56C).

PPARγ is a transcription factor found in adipose tissue that plays a crucial role in adipocyte differentiation and function (556). Moreover, it has been linked to antiinflammatory and antineoplastic effects through the induction of apoptosis, as well as the inhibition of proliferation and angiogenesis (557-559). One of the main mechanisms involved in the antitumor effects of PPARγ is due to its ability to upregulate *PTEN* expression, which is a tumor suppressor gene that reduces cell migration and proliferation through halting PI3K/AKT signaling pathway (557, 560). Thus, when levels of PPARγ in inguinal fat samples were analyzed, a significant decrease was observed in HFD mice with CAC, regardless of the treatment (Figure 56D). Then, the state of the PI3K/AKT pathway was evaluated in colonic samples.

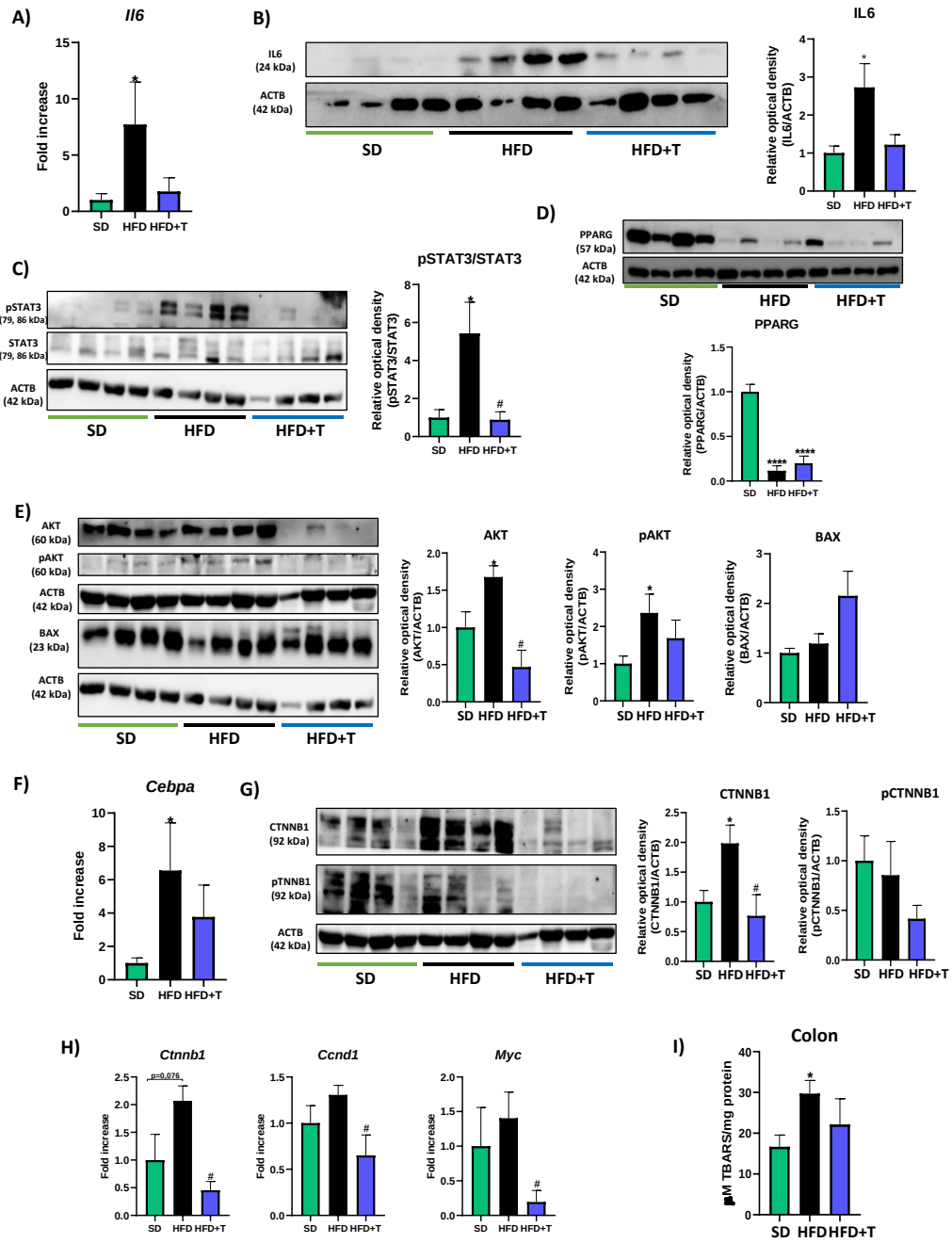

Figure 56. Impact of adipose-derived metabolites in tumorigenesis and its modulation by tigecycline. *(A) Il6 gene expression and (B) IL-6 protein levels in inguinal fat samples. (C) Colonic western blot analysis of phospho STAT3 and STAT3 and ratio of their values. (D) PPARγ Western blot bands analyzed in inguinal fat samples and their quantification by densitometry. (E) Western blot of AKT, phospho-AKT and BAX proteins in colon samples and densitometric analysis. (F) Cebpa gene expression in inguinal fat*

*samples obtained from SD, HFD and HFD+tigecycline mice. (G) Quantification of CTNNB1 and phospho-CTNNB1 levels in colon samples by Western blot and quantification by densitometry. (H) Gene expression analysis of Ctnnb1, Ccnd1 and Myc in colon specimens. (I) TBARS production in colon. Data are graphed as mean ± SEM (*P < 0.05, **P < 0.01, ***P < 0.001, ****P < 0.0001 vs. CAC control SD mice and $^{\#}$P < 0.05, $^{\#\#}$P < 0.01, $^{\#\#\#}$P < 0.001, $^{\#\#\#\#}$P < 0.0001 vs. CAC control HFD mice).*

As expected, there was an increase of the activation of AKT in untreated obese mice submitted to CAC, which resulted in a significant increase of the phosphoAKT/AKT ratio compared to the corresponding control SD mice (Figure 56E). This effect may be associated with the increased cell proliferation index observed in colon sections from obese control mice. Despite tigecycline was not able to restore PPARγ levels in the adipose tissue of CAC-obese mice, the compound interfered with the crosstalk PPARγ/AKT, being able to significantly reduce the activation of AKT, thus reducing the ratio phospho-AKT/AKT (Figure 56E). Moreover, the activation of the PI3K/AKT pathway is associated with the suppression of BAX activity, inducing an antiapoptotic effect in tumor cells (561). BAX levels were also analyzed in the colonic tissue, and no significant differences were observed among groups, although a trend was noted in tigecycline treated mice (Figure 56E).

C/EBPα is another important mediator in the regulation of adipogenesis, whose levels have been found to be increased in obesity (562, 563). Moreover, this transcription factor is involved in the pathogenesis of cancer, being recently reported that its upregulation contributes to CRC growth, metastasis and poor survival outcome (564). Furthermore, it has been reported that C/EBPα exerts its oncogenic role by targeting the Wnt/β-catenin pathway, thus upregulating *Myc* and *Ccnd1* gene expression (564). A significant increase in *Cebpa* expression was observed in the inguinal fat of untreated obese mice with CAC compared to SD-fed mice (Figure 56F). This action may be associated with the impact of obesity in total CTNNB1 levels in colonic tissue, where a significant increase of this marker was found in HFD-untreated mice in comparison to SD mice (Figure 56G). Although tigecycline did not have significant effect on *Cebpa* expression (Figure 56F), it significantly reduced total CTNNB1 protein levels (Figure 56G), although no significant differences were obtained with the phosphorylated form of CTNNB1 among groups (Figure 56G). In concordance to these results, tigecycline was able to significantly downregulate the expression of CTNNB1 target genes: *Ccnd1* and *Myc*, as well as, the *Ctnnb1* gene itself (Figure 56H).

Finally, lipid peroxidation has been reported to be increased in obesity, which is associated with increased production of MDA. As previously stated, MDA may act as a mutagen and induce alterations in the colonocytes that contribute to the initiation and progression of CRC (358, 362). A significant increase in the production of MDA was observed in the colonic specimens from untreated obese mice when compared to those fed with a SD, which was significantly reduced in those CAC-obese mice treated with tigecycline (Figure 56I).

5. TIGECYCLINE ADMINISTRATION MODULATES THE IMMUNE RESPONSE INVOLVED IN CAC DEVELOPMENT.

As commented above, the inflammatory process plays an important role in the initiation and progression of CRC. Moreover, the infiltration of immune cells, such as macrophages, in the tumor microenvironment may promote tumorigenesis in CRC due to the release of several cytokines and other mediators that can suppress the tumoricidal activity of lymphocytes and stimulate tumor growth (565, 566). Therefore, we aimed to further characterize the immune response involved in the pathogenesis of obesity-associated CAC. In accordance with the macroscopic observations described above, the gene expression analysis showed an upregulation of the proinflammatory cytokines *Il17a* and *Il23p19* in colonic tissue from HFD untreated mice compared to those mice fed a SD (Figure 57A). Both cytokines have a pivotal role in the stimulation of the Th17 response, which has been reported to negatively influence the prognosis of CRC (339, 567). The administration of tigecycline resulted in a significant downregulation of both proinflammatory cytokines (Figure 57A).

The inflammatory status in HFD-untreated mice was associated with a significant increase in the colonic infiltration of $CD45^+$ cells and a trend to increase $CD11b^+$ cell levels in comparison to those fed SD (Figure 57B). Mice treated with tigecycline exhibited a slight decrease in the colonic infiltration of these immune cells (Figure 57B), although additional experiments to increase the number of samples analyzed is necessary to confirm these observations.

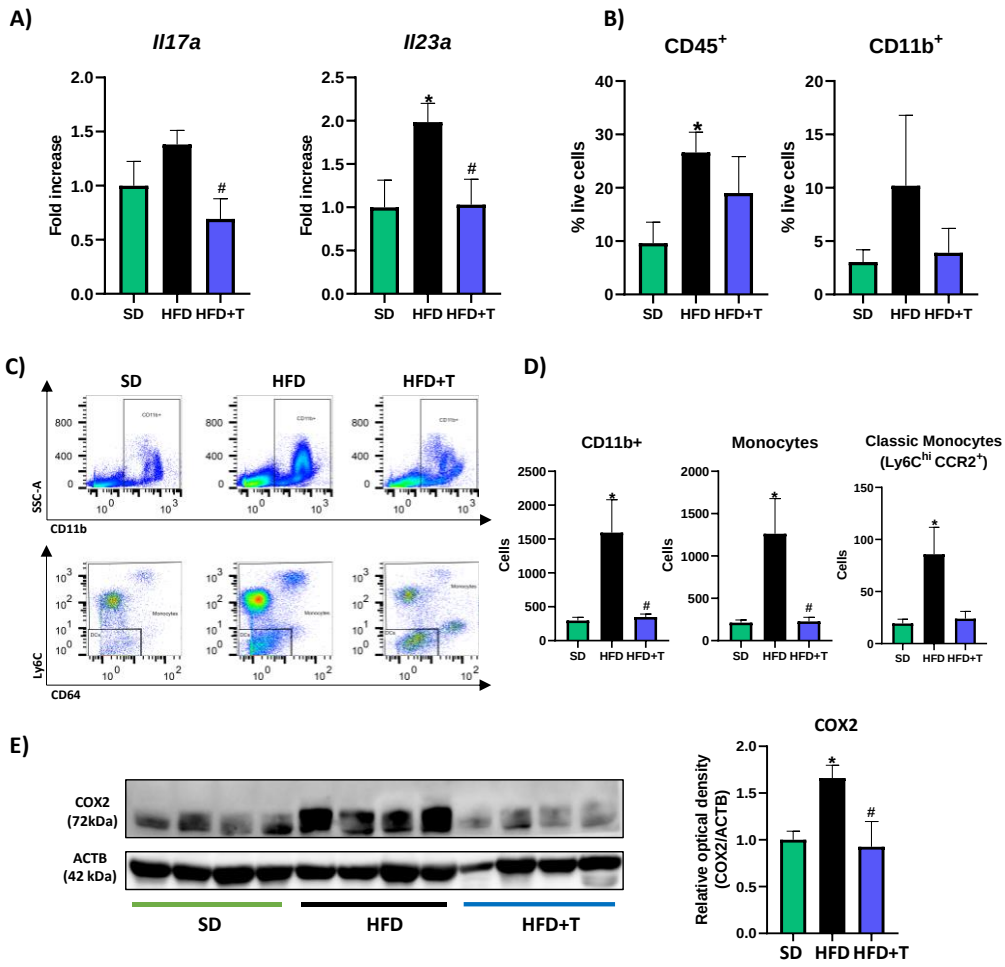

Figure 57. Tigecycline attenuates the inflammatory status altered in the colon of obese-CAC mice through a modulation of the myeloid compartment in blood. *(A) Cytokine gene expression in colon tissue. (B) Percentage of CD45$^+$ and CD11b$^+$ with respect to the total number of cells analyzed by flow cytometry in colon samples. (C) Representative gates from SD, HFD, and HFD+T mice showing the abundance of CD11b$^+$ cells (up) and monocytic cells (down) in blood. (D) Total number of CD11b$^+$ cells, monocytes and classic monocytes (Ly6C^{hi}CCR2$^+$) in blood. (E) Representative Western-blot bands of COX2 levels in colon tissue in the three experimental groups and their densitometric quantification. Data are graphed as mean ± SEM (*P < 0.05, **P < 0.01, ***P < 0.001, ****P < 0.0001 vs. CAC control SD mice and $^{\#}$P < 0.05, $^{\#\#}$P < 0.01, $^{\#\#\#}$P < 0.001, $^{\#\#\#\#}$P < 0.0001 vs. CAC control HFD mice).*

The results were more evident when monocyte populations were evaluated in blood samples by using flow cytometry. Regarding the number of circulating CD11b$^+$ myeloid

cells, the analysis showed a clear difference between SD- and HFD-CAC control mice, being this population significantly higher in the latter (Figure 57C and D). Surprisingly, mice treated with tigecycline showed a significant reduction in $CD11b^+$ circulating cells (Figure 57D), in concordance with previous studies performed with tetracyclines in the DSS model of experimental colitis (477). When the largest population of myeloid cells was considered, the monocytic-macrophagic population, differences among groups were also observed (Figure 57C and D). Indeed, levels of monocytic cells were significantly higher in HFD-fed CAC mice when compared to either SD or HFD-fed mice treated with tigecycline (Figure 57D). It has been reported that circulating $CCR2^+$ monocytes are recruited to the tumor microenvironment by tumor cells and, once there, they become immunosuppressive TAMs that promote cancer malignancy (568). Then, the levels of the $Ly6C^{hi}CCR2^+$ subpopulation of monocytes were determined in blood samples, which are considered as classical activated monocytes. The results revealed that this classic monocytic population was significantly increased in HFD-fed CAC mice in comparison with lean CAC mice (Figure 57D). Additionally, the treatment with tigecycline reduced $Ly6C^{hi}CCR2^+$ monocyte levels, although no significant differences were observed (Figure 57D).

Previous studies have reported the presence of upregulated levels of COX-2 enzyme in peripheral blood monocytes and local macrophages in CRC patients (569). As previously stated, COX-2 activity linked to PGE_2 overproduction has a crucial role in the pathogenesis and malignancy of CAC and obesity-associated CRC (328). In view of the described results for myeloid populations,the COX-2 levels in the colonic tissue from the different experimental groups of mice were evaluated. Obesity was associated with a significant increase in COX-2 levels in untreated HFD-fed CAC mice in comparison with mice fed a SD (Figure 57E). Conversely, tigecycline was able to significantly prevent this increase in COX-2 levels (Figure 57E). COX-2 downregulation may be associated with the reduction of STAT3 and AKT activation, as previously described in the present study (315).

Finally, the adaptive immune response also plays an important role in the progression of CRC. Therefore, the immune cell population at MLNs was evaluated by flow cytometry. Interestingly, the samples from HFD-fed CAC mice treated with tigecycline exhibited more than three times the number of $CD45^+$ cells compared to the other experimental groups (Figure 58A). About 15% of total $CD45^+$ cells turned out to be $CD3^+$ lymphocytes in tigecycline-treated mice, whereas this percentage was below 5% in control SD-fed or HFD-fed CAC mice (Figure 58A). A more detailed analysis of T cell subpopulations revealed that levels of $CD4^+$ and $CD8^+$ T cells were slightly downregulated in HFD-fed

CAC mice in comparison with lean mice, but this effect was masked by the marked increase in both cell populations in mice treated with tigecycline (Figure 58A and B). As it previously discussed, an increase in $CD8^+$ T cells is associated with a better CRC prognosis (191). Moreover, the administration of tigecycline resulted in a marked increase in B cells levels in MLNs in comparison with both control groups of mice (Figure 58A). The role of B lymphocytes in CRC development is controversial, but it has been reported that an increase of B cells in CRC is associated with a better prognosis due to their ability to cooperate with $CD8^+$ T lymphocytes in the immune response against cancer (570, 571).

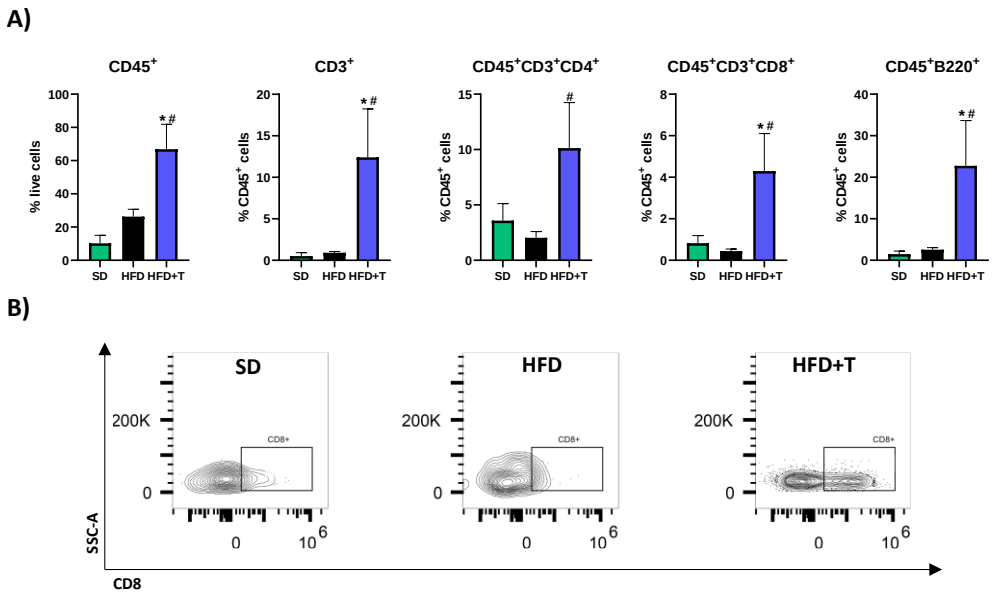

Figure 58. Impact of tigecycline in lymphocyte populations in MLNs analyzed by flow cytometry. *(A) Percentage of $CD45^+$ cells, $CD3^+$ cells, $CD45^+CD3^+CD4^+$ T lymphocytes, $CD45^+CD8^+$ T cells and $CD45^+B220^+$ B lymphocytes. (B) Representative gates from SD, HFD, and HFD+T mice showing the abundance of $CD8^+$ T cells in MLNs. Data are graphed as mean ± SEM (*P < 0.05, **P < 0.01, ***P < 0.001, ****P < 0.0001 vs. CAC control SD mice and $^{\#}P < 0.05$, $^{\#\#}P < 0.01$, $^{\#\#\#}P < 0.001$, $^{\#\#\#\#}P < 0.0001$ vs. CAC control HFD mice).*

6. TIGECYCLINE MODULATES THE GUT MICROBIOTA IN HFD-CAC MICE

The impact of tigecycline on gut microbiota composition was also explored since dysbiosis is a common feature in both diseases, obesity and CRC. Firstly, the alpha diversity was analyzed by determining different biodiversity indexes (Shannon, Simpson and Observed ASVs). Although no significant differences were obtained among control groups when these indexes were analyzed (Figure 59A), their values were reduced in the gut microbiota from HFD-fed CAC mice treated with tigecycline (Figure 59A). Next, the beta diversity was determined by Bray-Curtis dissimilarity index analysis. The metric multidimensional scaling, called PCoA plot, showed a clear separation among the three experimental groups (Figure 59B), thus indicating high differences in the composition of the bacterial communities from each group.

Next, we determined the composition of the bacterial phyla in each experimental group of mice. The two main bacterial phyla in the gut microbiota, *Bacteroidota* and *Bacillota,* were found downregulated in obese mice in comparison with lean mice (Figure 59C). On the other hand, an increase in *Verrucomicrobiota* phylum levels was observed in obese mice. In fact, this phylum became the most predominant in those mice treated with tigecycline (Figure 59C). Interestingly, *Desulfobacterota* phylum was increased in untreated obese mice but not in those treated with tigecycline. In the latter, an increase in *Proteobacteria* in comparison with the other two groups was reported (Figure 59C). Regarding the abundance of bacterial genus, it was noteworthy that obese mice exhibited an increase in *Akkermansia* genus levels, making this rise more marked in treated mice (Figure 59D). Moreover, the relative abundance of *Alistipes* was especially increased in untreated obese mice (Figure 59D). It is also necessary to mention that *Parabacteroides* relative abundance was higher in those mice treated with tigecycline when compared to control groups (Figure 59D). Lastly, when the abundance of bacterial species was studied, we found that *Akkermansia muciniphila* was the most abundant bacterial species in both, untreated and treated obese mice. In the latter, it is also noteworthy the increase in *Parabacteroides goldsteinii* abundance, which is the second bacterial species more abundant in this group (Figure 59E). On the other hand, SD fed mice showed increased levels of *Unclassified Lachnospiraceae_NK4A136_group, Akkermansia muciniphila* and *Uncultured_Bacteroidales* (Figure 59E).

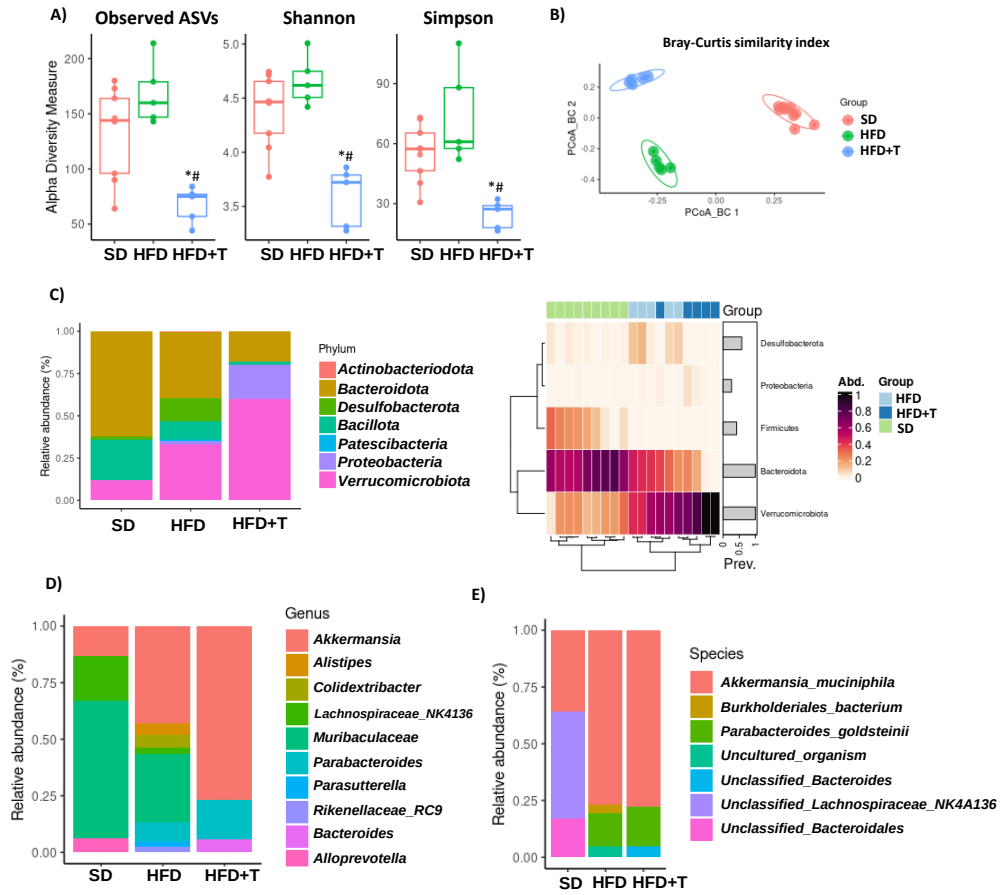

Figure 59. Tigecycline modulates microbiota composition in HFD-fed mice with CAC. *(A) Alpha-diversity indexes of stool microbiota (observed ASVs, Shannon index and Simpson index) (B) Beta-diversity index by Bray-Curtis analysis. (C) Distribution histogram of relative abundance of bacterial phyla; (D) genera and (E) species. Data are graphed as mean ± SEM (*P < 0.05 vs. CAC control SD mice and #P < 0.05 vs. CAC control HFD mice).*

Correspondingly, the volcano plot analysis showed that HFD-fed mice treated with tigecycline presented significantly lower levels of *Muribaculaceae* than control SD and HFD groups (Figure 60A). Moreover, tigecycline significantly increased *Akkermansia, Parabacteroides* and *Enterobacter* genera in comparison with SD-fed mice, being the latter genus also significantly increased when compared to control HFD mice (Figure 60A). Similarly, LDA histogram indicated that the control HFD group was characterized by a significantly higher proportion of *Alistipes*, *Odoribacter* and *Burkholderiales* while in the HFD-fed group treated with tigecycline, levels of *Parabacteroides goldsteinii,*

Akkermansia muciniphila and *Citrobacter europaeus* were increased in comparison with the SD and HFD control groups (Figure 60B).

Finally, the Venn diagram showed that SD, HFD and HFD-T groups only shared 2 ASVs being the number of shared ASVs higher between the SD and HFD-T (9) groups than HFD and HFD-T (4) mice groups (Figure 60C). Additionally, there was no common ASV between the SD and HFD groups (Figure 60C).

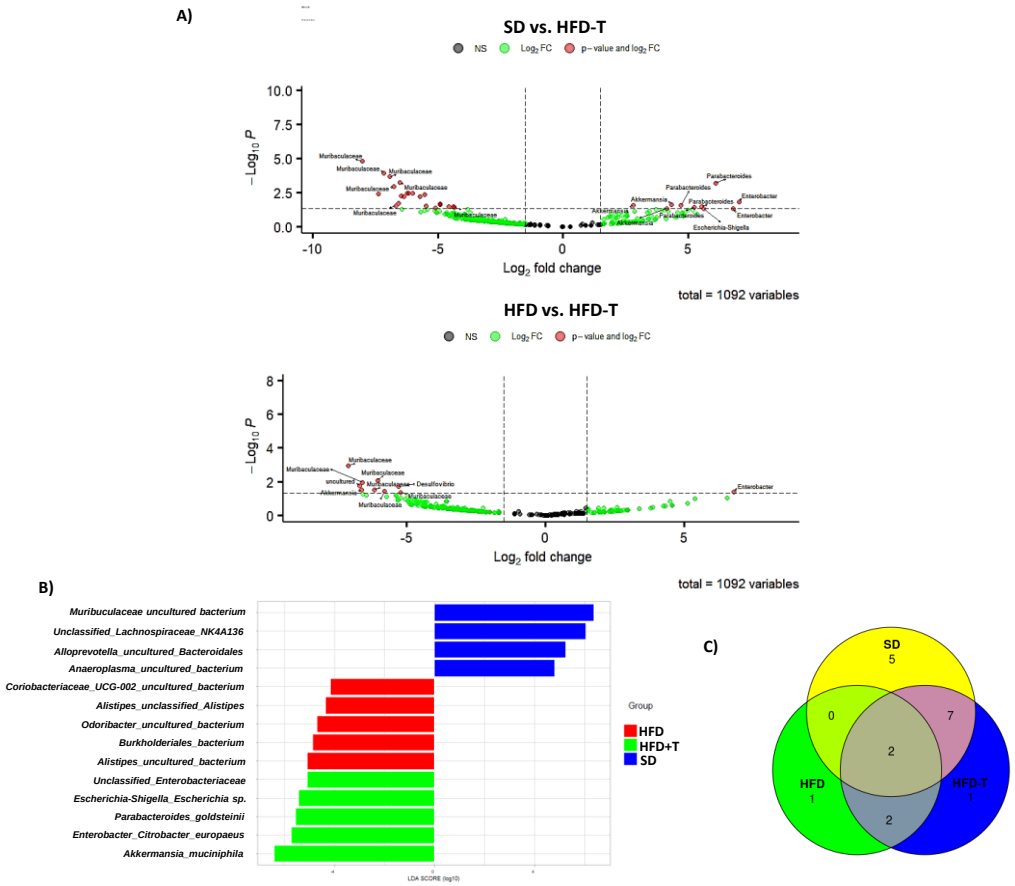

Figure 60. Impact of tigecycline on microbiota profile in HFD mice. *(A) Volcano plot indicating the upregulated and downregulated ASVs in HFD-T mice when compared to SD mice (up) and those upregulated and downregulated in HFD-T mice in comparison with untreated HFD mice (down). (B) LDA scores for differentially abundant bacterial taxa in each experimental group. Negative LDA scores represent bacterial genera over-abundant in HFD-fed groups of mice while positive represent bacterial groups overrepresented in SD-fed mice. (C) A Venn diagram showing the number of ASVs which are unique and common to each experimental group.*

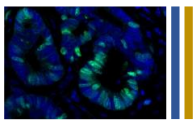

DISCUSSION

DISCUSSION

Actually, obesity is considered to be one of the most relevant public health issues, with increasing prevalence in the last decades probably due to urbanization, sedentary lifestyle, and increased consumption of high-calorie processed food. In fact, WHO estimates that by 2025, approximately 167 million people will be overweight or obese (572). Of note, obesity constitutes a crucial risk factor for non-communicable conditions, including metabolic diseases (diabetes), cardiovascular diseases (stroke, hypertension or atherosclerosis), psychological problems and cancer, including colorectal cancer. Regarding the latter, it has been reported that obese people have a nearly doubled risk of suffering early-onset CRC (573). Additionally, epidemiological data suggests that around 11% of CRC cancer cases have been attributed to overweight and obesity in Europe in the last decade (345).

Therefore, the association between obesity and CRC is well documented, although the link between both diseases is not fully characterized. Different hypothesis have suggested that alterations in insulin signaling and the development of a systemic and chronic low-grade inflammatory state could be involved in the convergence of obesity and CRC (382, 574, 575). Moreover, it has been widely demonstrated that obesity can induce gut dysbiosis. In fact, it has been reported that experimental obesity induced by HFD in mice can induce a shift in the microbial populations associated with an impairment of the gut barrier function and the onset of an inflammatory state that increases the risk of CRC through diverse mechanisms (576). The complexity of both diseases together, obesity and CRC, with the lack of efficacy and safety of existing drugs in certain population groups encourages the search for new strategies against these conditions. In this scenario, the main objective of the present study was to establish the role of the altered microbiota in the development of obesity and CRC, as well as the search for new therapies and targets based on the modulation of this microbiota to simultaneously act against both diseases. With this aim, firstly, the management of both diseases was addressed separately, in a murine model of diet-induced obesity and in CAC model; and, secondly, as a whole entity in a murine model of obesity-associated CRC.

The present study was divided into three parts. In the first, two different experiments showed that plant extracts obtained from leaves of *Thymus serpyllum* and *Morus alba* exerted prebiotic effects that resulted in an amelioration of obesity. In the second, and based on the fact that the pharmacological profile of tigecycline combines antibiotic

activity and many other non-antibiotic properties, this tetracycline resulted an appropriate drug in the management of CRC, as evidenced in the *in vitro* assays and in a murine model of CAC. Finally, in the third part of this study, the impact of obesity in the malignancy of CRC was reported in a murine model of obesity-associated CRC, in which tigecycline achieved a substantial effectiveness.

1. THE GUT MICROBIOME MODULATION BY PREBIOTIC TREATMENT AS POTENTIAL TREAMENT IN THE OBESITY

Lifestyle modification is the first line of action for the management of obesity. However, many obese individuals do not achieve long-lasting benefits since it is difficult for them to adhere to the lifestyle changes due to their physical and psychological condition (577). Another way to address the problem of obesity is through drug therapy. The most commonly used drugs approved by the Food and Drug Administration (FDA) for the long-term treatment of obesity include orlistat, phentermine/topiramate, naltrexone/bupropion, and liraglutide (578). Unfortunately, the lack of efficacy of some of these drugs, which has been questioned in recent meta-analysis, or their high cost and high incidence of adverse effects make their use difficult (578). Additionally, bariatric surgery yields substantial weight loss but its high cost and the risk of serious complications make it only suitable for cases of severe obesity (577). These findings have prompted the use of alternative therapies against obesity, highlighting the use of plant extracts with proven and safe anti-obesogenic properties (579, 580). In this scenario, *Thymus serpyllum* and *Morus alba* are two plant species containing different bioactive compounds, such as flavonoids and phenolic acids, that have previously demonstrated therapeutic potential against many diseases, including those metabolic disorders associated with obesity such as diabetes and dyslipidemia (461, 581-583) Based on these findings, in the current Thesis, two well chemically-characterized extracts from *Thymus serpyllum* and *Morus alba* were assayed in a murine model of diet-induced obesity, paying special attention to their capacity to modulate gut microbiota profile.

The administration of both extracts to obese mice resulted in a significant reduction in body weight gain, which was associated with a reduction in the accumulation of fat deposits. These actions were exerted without affecting satiety of mice, as evidenced by a similar energy intake among the different groups fed with HFD, thus discarding an

anorexigenic action for these plant extracts. In consequence, other underlying mechanisms should be involved in the feed efficiency reduction observed.

Rosmarinic acid, one of the major bioactive compounds presents in both extracts, has reported to exert anti-adipogenic activity through the downregulation of transcription factors involved in the maturation of human adipocytes, especially targeting C/EBPα, FABP4 and SREBP1 (584). Additionally, it has already been reported the ability of a *Morus alba* leaf extract to interfere with the expression of these transcription factors (585). Similarly, thyme treatment demonstrated a reduction in the expression of these makers in HFD-fed mice leading to a reduction in adiposity. It has been reported that the excess of fat in obese individuals facilitates accumulation and the impairment in the function of different organs such as the liver. In fact, one of the main disorders associated with obesity is the non-alcoholic fatty liver disease (NAFLD), which is characterized by hepatic steatosis (586). For this reason, the impact of the treatments in the development of fatty liver was studied, and the results obtained with the histological studies revealed the improvement of liver steatosis exerted by the extracts. It is well known that this situation of hepatic steatosis is usually linked to altered glucose and lipid metabolism, as well as to the development of systemic inflammation (586). This was confirmed in the present study, since HFD-induced obesity was associated with an alteration of the glucidic and lipidic metabolism, which was ameliorated in those obese mice treated with the thyme and mulberry extracts. Supporting this, both treatments were able to improve the systemic glucose intolerance associated with the obese phenotype when the glucose tolerance test was performed one week before sacrificing the mice.

In a postprandial physiological situation, the increase in blood glucose stimulates the release of insulin from the pancreas and, once in blood, it reaches different target tissues and binds to its receptor. This action triggers the activation of the PI3K/AKT cascade, in which phospho-AKT promotes the translocation of the glucose transporter (GLUT) to the plasma membrane, thus inducing the entry of glucose into the cell (587). However, obesity is associated with an increased risk of insulin resistance development (588-590). This phenomenon is mainly associated with the chronic inflammatory state observed in obese patients and it leads to hyperinsulinemia and hyperglycemia (591). In the present study, although there were no differences in the insulin levels among the different groups of mice, it was shown a reduction in the insulin resistance in those mice treated with thyme, evidenced by a significant decrease of HOMA-IR, which is an index developed by Matthews et al. (1985) that is widely used for the estimation of insulin resistance (592). This amelioration of the insulin signaling induced by thyme promoted the upregulation of

Glut2 expression in the liver, which resulted in the improvement of glucose uptake by this organ and the subsequent glycemic reduction described in obese mice.

As it was commented above, PI3K/AKT pathway has an important role in insulin-mediated glucose homeostasis (593). In adipose tissue, the activation of this signaling cascade results in the promotion of lipid biosynthesis and the suppression of lipolysis. Therefore, activated AKT contributes to increased fat deposits (594). Additionally, it has been reported that insulin resistance may result in an overactivation of PI3K/AKT pathway (593). This would justify that, in obese mice, the high and sustained levels of blood glucose would result in the activation of AKT, in comparison with lean mice. Moreover, this action may be involved in the increased fat accumulation observed in untreated obese mice. Interestingly, a reduction in the activation of AKT was observed in those obese mice treated with metformin or mulberry leaf extract, which could be related to the amelioration of the glucidic metabolism profile and the substantial reduction of fat deposits observed in these mice.

AMPK has also a pivotal role in metabolism, being considered as an energy sensor. When this enzyme is phosphorylated (active form), catabolic pathways such as lipid oxidation and glycolysis are triggered, thus increasing the energy expenditure (595). Thyme extract was able to increase the phosphorylation of AMPK, thus leading to its activation. This action may contribute to the reduction of energy efficiency observed in mice treated with this extract, as well as to the amelioration of the glycemic profile. In this scenario, it is necessary to highlight UCP1 protein, which is a major regulator of adipose energy expenditure and metabolic homeostasis (596). UCP1 uncouples the proton motive force generated in the mitochondria from ATP production to produce heat, thus increasing the energy expenditure. A deficiency of this protein in mice is associated with increased weight gain and development of obesity. Conversely, an overexpression of *Ucp1* is associated with an anti-obesity effect (597). In fact, UCP1 is considered a promising molecular target to thermogenesis enhancement and obesity treatment (598). Of note, *Morus alba* extract was able to significantly increase the UCP1 levels downregulated in obese mice, and this may be considered one of the main mechanisms involved in the anti-obesity effects for this plant extract.

Moreover, AMPK activation is also associated with the blockade of ATP-consuming anabolic pathways including fatty acid synthesis and cholesterol and triacylglycerol synthesis (599). Both plant extracts, thyme and mulberry, achieved a significant amelioration of lipid profile evidenced by a reduction in triglycerides and LDL/HDL ratio.

AMPK not only exerts an essential role in regulating metabolism pathways, but also acts by controlling the inflammatory response through the the inhibition of NF-κB activation

pathway and reducing the expression of pro-inflammatory cytokines, such as IL-1β, TNFα and IL-6 (600). Moreover, it has been described that AMPKα1$^{-/-}$ mice exhibit an overactivation of JNK and STAT3 pathways, which are also involved in the inflammatory state characteristic of obesity (601). *Thymus serpyllum* and *Morus alba* leaf extracts showed beneficial effects against the increased inflammation present in HFD-mice. On one hand, thyme extract was able to reduce the expression of the pro-inflammatory cytokines TNFα and IL-6 in both epididymal fat and the liver, as well as MCP1 chemokine expression in the liver. The ability of *Thymus serpyllum* extract to induce the activation of AMPK in obese mice could explain the impact of this extract in the reduction of the expression of these pro-inflammatory mediators, as well as of *Jnk1* and *Jnk2*. On the other hand, *Morus alba* extract also exerted a beneficial impact on the inflammatory status evidenced in obesity by reducing the protein levels of COX-2 in epididymal fat and IL-6 levels in the liver. The activation of COX-2 in epididymal adipose tissue has been correlated with inflammation, insulin resistance and fatty liver in HFD obese rats (602). Moreover, HFD feeding is associated with an overexpression of *Il6* in the liver that contributes to the low grade inflammation process observed in obesity (603). The ability of *Morus alba* extract to reduce the levels of these inflammatory mediators suggests an amelioration of the inflammation in obese mice.

One of the most accepted hypotheses to explain the systemic inflammatory state linked to fat diet lies in the absorption of bacterial components such as LPS that causes a metabolic endotoxemia (604). LPS penetration is associated with gut dysbiosis and an impairment of the gut barrier integrity after high-fat exposure (604, 605). It has been reported that HFD consumption inhibits the secretion of mucin 2 through the induction of ER stress (605). Moreover, gut dysbiosis associated with obesity results in the release of LPS by Gram-negative bacteria that diffuses through the altered tight junctions or is incorporated into chylomicrons (394). Once in the systemic circulation, LPS binds to the LPS-binding protein and this complex activates the CD14 receptor, which in turn stimulates TLR4 activation on resident macrophages of different organs such as liver and adipose tissue (604). The activation of TLR4 leads to a pro-inflammatory response characterized by an increase of pro-inflammatory cytokine production (604). These findings were confirmed in the present study, in which an increased level of plasmatic LPS was found in control mice fed a HFD compared to those fed a normal diet. Interestingly, this metabolic endotoxemia was reduced in those groups of mice treated with the two leaf extracts evaluated, thyme or mulberry, as well as in those mice treated with metformin. Moreover, an amelioration of the gut barrier integrity functions was

observed in mice administered with thyme extract, an action that contributes to the reduction of LPS absorption in these mice.

The existence of obesity-associated gut dysbiosis was also confirmed in the present study. Conversely to the data presented in the first study when the thyme extract was evaluated the alpha diversity was not significantly modified in the mulberry evaluation assay. This could be explained because different methods of microbiome analysis were performed in both studies. In the second one, the gut microbiome was analyzed using ASVs. In this sense, it has been recently reported that microbial diversity results can be markedly affected by both the filtering strategy and ASVs- or OTUs- based analysis (606). Despite this, the gut dysbiosis produced by the HFD intake was confirmed in both studies when the beta diversity was determined. These results suggest that HFD impacts on the bacterial microorganisms involved on the efficacy for energy harvesting (387-389). Interestingly, the treatments with both plant extract assayed were associated with a modulation of gut dysbiosis. Thus, when obese mice were treated with thyme extract, a restoration in all these dysbiosis-related indexes was observed, resulting in the increase of the biodiversity and richness of microbial communities in the gut of HFD mice. Moreover, both extract treatments normalized the levels of *Bacteroidota* and *Bacillota* phyla. Changes in bacteria genera were also found in obese mice compared to lean mice. In the evaluation of the thyme extract study, untreated HFD mice exhibited a higher relative abundance of *Faecalibaculum* and *Roseburia* than in SD-fed mice. It has been shown that these both bacteria genera are increased in experimental obesity and can participate in the generation of the inflammatory status, lipid disorders and gut epithelial barrier impairment (607-609). Consequently, the restoration of these bacteria levels observed in those mice treated with thyme extract could be associated with its beneficial effects in HFD-mice, including restoration of gut barrier integrity, amelioration of the systemic inflammatory response and improvement of the lipid and glucose metabolic function. Furthermore, SCFAs are important bacterial metabolites with well described anti-inflammatory properties (610), and able to enhance the intestinal barrier integrity (611) and regulate the body weight by controlling food intake (612). For this reason, the beneficial effects exerted by thyme extract could be also related with an increase in the SCFA-producing bacteria, especially with an increase in butyrate- and propionate-producing bacteria. Elevated gut microbiota-derived butyrate and propionate levels are associated with several beneficial effects, including antiinflammatory activity (613, 614), improved insulin sensitivity and energy expenditure (615). When the *Morus alba* extract was evaluated, the HFD administration modified many different bacterial genus. The treatment significantly modulated many of them. Remarkably, a reduction of *Alistipes*

genus abundance was obtained by the extract plant treatment. Of note, there is no consensus about the role attribute dto these bacteria. Thus, *Alistipes* may have protective effects against some diseases, including liver fibrosis, colitis, cancer immunotherapy, and cardiovascular disease. However, several reports have indicated that *Alistipes* is pathogenic in CRC and is associated with gut inflammation (616). Additionally, the extract treatment increased *Faecalibaculum* content, which was reduced in the untreated HFD-fed mice. These are gram-positive obligate anaerobes with high fermentation ability, especially butyrate production, and then, they have been associated with the SCFAs production and carbohydrate metabolism (617). Consequently, the amelioration of the obesity-associated dysbiosis in thyme- and *Morus alba*-treated obese mice may contribute to the beneficial effects observed in this experimental model of diet-induced obesity.

Lastly, the administration of *Thymus serpyllum* and *Morus alba* leaf extracts to HFD-fed mice resulted in an antioxidant effect evidenced by a reduction of lipid peroxidation byproducts, as well as a downregulation of endothelial NADPH oxidase activity, which is involved in the pathophysiology of vascular diseases such as hypertension and stroke through the production of ROS (superoxide and hydrogen peroxide) (618, 619). In fact, the effect of the thyme extract on the enzymatic activity of NADPH oxidase could explain the enhancement of endothelial function described. This antioxidant activity together with the antiinflammatory and hypocholesterolemic actions may converge in a lower risk of atherosclerosis development and subsequent cardiovascular diseases, beneficial effect in which the rosmarinic acid may be involved (620).

The effects summarized above provide convincing evidence about the ability of *Thymus serpyllum* and *Morus alba* leaf extracts to exhibit anti-obesity activity and ameliorate the associated disorders with this condition. Therefore, these extracts can be considered as promising candidates in the treatment of obesity, as well as in the prevention of other associated diseases, among them cardiovascular diseases, type II diabetes and even cancer.

2. ANTITUMORAL EFFECT OF TIGECYCLINE.

CRC incidence and mortality rates are still high at present, being the third most common cancer worldwide. Moreover, CRC is considered a morbidity associated with different diseases, among which IBD and obesity stand out. Although it is true that relevant advances have been made in both the diagnosis and the treatment of this cancer, the high side effects associated with the chemotherapy, together with the lack of an optimal

efficacy in some population groups, make necessary continuous research in this field to find new therapies that complement the existing ones. It is widely known that one of the main problems associated with cancer is metastasis, since, once is presented, there is a drastic increase in the mortality of patients, being the survival rates among people diagnosed with metastatic CRC approximately 70% to 75% for patients diagnosed beyond 1 year, 30% to 35% beyond 3 years and fewer than 20% beyond 5 years from diagnosis (621).

It is well recognized for the great heterogeneity in the cells that form the tumor, which can also challenge current therapies. Of note, the presence of cells with stem properties has been associated with a higher tumor malignancy since they are responsible for recurrences and metastasis (622). Moreover, most current theories that attempt to explain cancer origin point to CSCs as key cells in this process (623). However, as it has been already mentioned, cancer is one of the most complex diseases in which different cell types are involved in addition to the tumor cells themselves. In fact, accumulating evidence suggests a dynamic interaction between tumor cells and their microenvironment, which contributes to cancer development (624). Thus, understanding the molecular mechanisms that govern the crosstalk between the tumor and its environment can be used as a novel strategy to hinder tumor progression (624). Additionally, gut microbiota has also an important role in the pathogenesis of CRC to the point that Tjalsma and colleges (2012) proposed a model in which different bacterial species were classified as “drivers” or “passengers”, based on their ability to initiate or promote the tumor process in CRC, respectively (408). Nowadays, these findings are being studied in depth in order to find out which microorganisms can be really involved in this process and even which metabolites derived from this bacteria can cause tumorigenesis. Recent studies have identified a family of DNA damage-inducing microbial metabolites called indolimines, which are produced by Gram-negative bacteria such as *Morganella morganii*. Strains of this bacteria species are enriched in the gut microbiota of both IBD and CRC patients, and are characterized by containing an enzyme, aspartate aminotransferase, which has an essential role in indolimine production, a metabolite that causes the exacerbation of tumor burden in a preclinical model of CRC (625). Also, it has been proposed that *Fusobacterium nucleatum* is a CRC “driver bacteria” that may be involved in the initiation and progression of the disease due to the presence of virulence factors, such as the adhesion molecule FadA, able to trigger the activation of Wnt/β-catenin signaling pathway, thus inducing the proliferation of colon epithelial cells (412, 413). These findings suggest that the altered microbiota composition can be considered as a target for novel therapies against CRC (626, 627). In addition,

some studies support the efficacy of therapies based on the modulation of gut microbiota, such as probiotics, prebiotics, FMT and antibiotics in the treatment of CRC (414, 437, 628, 629).

Tetracyclines are a family of valuable drugs that were initially discovered to deal with large antibiotic resistance problems in the last century. However, the chemical modifications introduced in these compounds not only increased their effectiveness as antibiotics, but also improved their pharmacological profile, endowing them with interesting pharmacodynamic properties that make them very attractive for the treatment of several diseases. In fact, numerous clinical trials are currently in progress evaluating the effects of different against various pathologies, including inflammatory acne (630), periodontitis (631), refractory high grade gliomas (632), among others. Furthermore, some of these pharmacological properties have made these drugs to be considered as promising agents in the management of cancer (489, 490).

In the current study the effectiveness of tigecycline, a third generation tetracycline, has been demonstrated in the treatment of CRC both *in vitro* and *in vivo* in two murine models of CRC: a HCT116 xenograft model and in a CAC model. Moreover, the complexity of CRC has been studied in the current Thesis, addressing the impact of the treatment on each of the hallmarks of this disease: uncontrolled proliferation, apoptosis and immune evasion, as well as in the properties of CSCs, which are responsible for the origin, invasion and metastasis. Moreover, our findings provide the first evidence that tigecycline exerts an anti-proliferative and pro-apoptotic effect, as well as immunomodulatory properties and the ability to modulate gut dysbiosis in CRC.

Supporting this, different antibiotic drugs, including tigecycline, have been recently reported to inhibit the growth of various types of tumor cells and show positive therapeutic effects in cancer patients (633, 634) . The antitumor mechanisms of tigecycline remain unidentified, but one of them could be the capacity of tigecycline to regulate cell proliferation rate. In this regard, almost 80% of CRC patients (110) show mutations in APC gene which lead to alterations on Wnt/β-catenin signaling pathway. In fact, CTNNB1 aberrant activation and nuclear translocation boost the expression of oncogenes involved in cell cycle and proliferation such as *AXIN2, MYC* and *CCND1* (108), thus increasing cell proliferation and promoting the tumorigenesis process, including migration, invasion, apoptosis evasion and chemoresistance (635). The current study demonstrates that tigecycline suppressed tumorigenesis by downregulating the Wnt/β-catenin signaling pathway, confirming previous studies in cervical squamous cell carcinoma (634). It has been shown that tigecycline was able to increase the phosphorylation of CTNNB1 in colon tumor cells, even when this signaling pathway was overactivated in presence of

Wnt3a ligand. This action resulted in an increased degradation of CTNNB1 and subsequent reduction of the translocation of this protein to the cell nucleus, hindering the expression of genes involved in cell proliferation such as *MYC* and *AXIN2.* In addition, tigecycline interfered with other molecular pathways involved in cell proliferation, and downregulated them. Importantly, tigecycline treatment resulted in a reduction of the STAT3 activation both *in vitro* and *in vivo.* In this regard, there is evidence that STAT3 signaling contributes to the stimulation of *CCND1* and *MYC* expression and promotes cell-cycle progression and proliferation (146). Moreover, STAT3 contributes to tumor malignancy through the up-regulation of *BCL2* and MMPs such as *MMP9* (636, 637). Accordingly, we found that tigecycline treatment decreased the expression of these markers, which could explain its capacity to inhibit STAT3 activation. These molecular mechanisms underlying the antiproliferative effect exerted by tigecycline support previous findings related to other tetracyclines and antibiotics (637, 638). In fact, tetracyclines have been shown to exert an antiproliferative effect in various cancers including liver cancer, cervical carcinoma and colorectal adenocarcinoma (497, 498, 639). In addition to interfere with the molecular pathways involved in the cell proliferation, tigecycline has been shown to inhibit mitochondrial translation by reducing the levels of cytochrome c oxidase-1 and 2 and glucose-regulated protein 78 (GRP78), leading to a decrease in the mitochondrial membrane potential, respiration and ATP levels (640). Therefore, the impact of tigecycline on the mitochondrial function can contribute to the antiproliferative effect described in this study.

As it is widely known, evasion of cell death is one of the hallmarks of cancer. Previous studies have evidenced that tetracyclines can induce apoptosis in different cell lines, including tumor cells (499, 500, 641). Besides, it has been previously reported that tigecycline is able to induce apoptosis by activating cytochrome C and caspase 3 cleavage in different type of tumor cells (633, 642), which was corroborated by our findings. Interestingly, when the apoptotic activity of tigecycline was compared to that observed with 5-FU, both *in vitro* and *in vivo*, the molecular mechanisms involved in tigecycline-mediated apoptosis seemed to be different from those displayed by 5-FU. The latter activated intrinsic apoptosis through TP53 upregulation, whereas tigecycline exerted its action downstream, at BAX level. Moreover, our findings revealed that CASP3 and CASP7 were the main apoptosis executioners in 5-FU treatment, whereas CASP7 was involved in the tigecycline-mediated apoptosis. Importantly, both treatments led to PARP1 cleavage and cell death. Of note, this action has been algo previously reported for different anticancer drugs, such as etoposide, being considered as an early marker of chemotherapy-induced apoptosis (643). Furthermore, it has been demonstrated that both

treatments, 5-FU and tigecycline, targeted ER-mediated apoptosis markers, favoring the induction of cell death through this pathway. 5-FU increased the ER-mediated apoptosis through the activation of the two isoforms of JNK. Tigecycline also acted at this level, however, it only facilitated the activation of the p54 isoform, which, according to Waetzig V et al., 2003, was enough for taxol-mediated apoptosis (644). Unlike what occurs with 5-FU, tigecycline also activated this pathway through its action on ATF6. These findings were in concordance with previous studies carried out with different tetracyclines, which reported the ability of minocycline to induce apoptosis through the ER pathway, both *in vitro* and in xenograft models (641).

As it has been commented above, the idea that cancers are driven by CSCs is widely accepted. These CSCs are able to differentiate into the different tumor cell types promoting the origin of the cancer and maintaining the ability to self-renew (645). Besides, CSCs contribute to therapy resistance and metastasis development, thus making them attractive potential targets for the treatment of CRC. Previously studies have shown the efficacy of tetracyclines in CSCs populations, as well as in the EMT process, which is a key mechanism in the origin of these CSCs (646, 647). These actions, together with the ability of tetracyclines to inhibit MMPs, make this family of drugs potential candidates in the treatment of cancer metastasis (479). In the present study, tigecycline was able to exert beneficial effects against colon CSC populations, EMT and metastatic properties of colon CSCs.

Self-renewal capacity is essential for maintenance of CSCs, conferring them an enhanced longevity (648). Our findings have revealed for the first time that tigecycline was able to inhibit colon CSCs clonogenicity and self-renewal due to its ability to alter the integrity and reduce the size of secondary colonospheres. This action was evidenced by a reduction of the sphere-forming efficiency in HCT116 and CMT93 colonospheres treated with tigecycline, and it resulted in a reduction of those $CD44^+CD133^+LGR5^+ALDH^+$ cells, which are identified as colon CSCs (541). Furthermore, apoptosis evasion is one of the main mechanisms by which CSCs remain latents in the stem cell niche, thus resulting in chemoresistance. In addition to the pro-apoptotic effect previously described *in vitro* and *in vivo*, tigecycline was able to induce apoptosis in HCT116-derived CSCs. Therefore, these accumulating findings suggest that tigecycline ameliorated CRC by reducing the levels of CSCs.

These results are in the line of those obtained by doxycycline, another member of tetracyclines family, which has been shown to reduce CD44 and ALDH1 expression in CSCs from patients with early breast cancer (649). Moreover, doxycycline was able to inhibit the EMT process in breast cancer cell lines. In particular, doxycycline has reduced

the proliferation of CSCs, its self-renewal ability as well as the expression of EMT-related genes such as *OCT4, SOX2, NANOG, MYC* and *CD44* (646). Additionally, the effects of doxycycline on EMT process has been also evidenced in the lung cancer cells NCI-H446 and A549, thus resulting in a suppression of the activity of EMT-related transcription factors such as Twist1/2, SNAI1/2, AP1 and STAT3 (650). In these studies, doxycycline also reduced the migration capacity of tumor cells, a key step in the tumor invasion and metastasis (646, 650). Supporting these results, tigecycline was able to reduce the migration ability of HCT116 cells and to hinder the EMT process in both HCT116 and CMT93 cell lines, a key event in the generation of CSCs. The underlying mechanism mainly involved in this activity seemed to be related with the downregulation of SNAI1, a transcription factor that promotes the mesenchymal phenotype through the inhibition of E-cadherin (651). The SNAI1 repression observed after tigecycline treatment resulted in an increase of E-cadherin levels and a reduction of N-cadherin (*CDH2*) gene expression, both actions associated with an epithelial phenotype rather than the mesenchymal one (543).

Additionally, it has been reported that the Wnt/β-catenin pathway is also involved in CSCs generation (652). Indeed, increased Wnt activity has been found in CSCs from multiple human tumor types, including digestive tumors and breast cancer (653). Furthermore, LGR5 is a receptor for R-spondins that exerts an important role in the regulation of the Wnt/β-catenin pathway, stimulating it. In fact, LGR5 is considered a surface marker of CSCs both in humans and mice (654, 655). Moreover, CD44, another marker of CSCs, is a target gene of the Wnt/β-catenin signaling pathway. Throughout this thesis, the role of tigecycline in the inhibition of beta catenin has been revealed. Additionally, levels of this key marker have been reduced in HCT116-derived colonospheres, indicating a downregulation of CTNNB1 in CSCs that are part of these biological structures. Moreover, β-catenin is also associated with an up-regulation of the pluripotency gene *NANOG* in an Oct-3/4-dependent manner. Additionally, OCT4 is an essential transcription factor for maintaining the self-renewal and the pluripotency of stem cells and it is associated with the degree of malignancy and the drug-resistance of cancer (656). Furthermore, SOX2 has been linked to EMT, chemoresistance, and stem properties (657). Interestingly, a downregulation in the expression of *NANOG, OCT4B* and *SOX2* genes have been observed in those HCT116 cells treated with tigecycline. These underlying mechanisms carried out by tigecycline on CSC populations are responsible for the tumor growth reduction reported in HCT116 xenograft mice, in both cases, when the treatment was carried out previously to the cell inoculation and after, once the tumor was already embedded and growing subcutaneously.

As previously stated, tumor microenvironment is also an important factor to understand the biology of cancer. Tumor microenvironment consists of tumor stromal cells including fibroblast, endothelial cells and immune cells, as well as the non-cellular components of extracellular matrix such as collagen, fibronectin, hyaluronan… (624). Tumor microenvironment has an essential role in the progression and prognosis of CRC, and the immune cells of this environment play a dual role in cancer development (658). On the one hand, chronic inflammatory stimuli triggers cancer initiation and progression, as occurs in this experimental CAC model, and in IBD patients, who have an increased risk of developing CRC (659). On the other hand, the immune system also plays an important role attacking the tumor cells. In CRC, altered Th1/Th2 response contributes to tumor progression, while enhanced Th1 population is associated with a better prognosis (660). Furthermore, cytotoxic $CD8^+$ T cells are the preferred immune cells for tumor surveillance, being the most powerful effectors in immune cancer targeting (661). Accordingly, the present study showed that the development of CAC was associated with a depletion of T cells, specifically CTLs in the colon of non-treated CAC mice; however, the treatment with tigecycline and 5-FU restored cytotoxic T cells levels. In fact, 5-FU and the lowest dose of tigecycline significantly increased Tc1 cells, which are characterized by their antitumor effect, being IFNγ producers and considered an indicator of $CD8^+$ T cells activation (547) . Based on these findings, tigecycline was able to modulate the immune response towards an antitumoral phenotype through the mitigation of the inflammatory response that drives CRC development, and the restoration of the adaptive response involved in a tumoricidal effect. Finally, it is well accepted that alterations in gut microbiota composition contribute to tumor development and are associated with CRC (662). Although it is not clear whether this dysbiosis has a causal role or its secondary to the environmental changes produced by tumor onset, there is enough evidence supporting the role of certain bacteria in cancer initiation and progression, as well as in cancer protection (408, 662). Therefore, modulation of this altered microbiota composition in CRC with drugs such as antibiotics, could be considered a complementary therapeutic approach (627). Correspondingly, our results in the CAC model confirm the existence of a dysbiotic status in the CAC control group, characterized by a reduced microbial diversity, as previously reported (663), being tigecycline able to restored this microbial diversity. Supporting the clinical importance of this activity, other antibiotics, including different tetracyclines, have shown the ability to modulate the dysbiosis in oncology patients (664). Over the last decade, several bacteria species have gained interest for their involvement in colorectal carcinogenesis (662). *Akkermansia muciniphila* stands out among these species for its anti-inflammatory and protective functions on gut barrier

(665). The relationship between *Akkermansia muciniphila* and CRC remains controversial. Different studies have shown an enrichment of *Akkermansia* in CRC patients (666), while others have reported that it can mitigate tumorigenesis in CRC with capacity to boost the effect of existing antitumor treatments (667). In this study we observed an increase in *Akkermansia* genus in CAC mice compared to healthy mice, as well as increased levels in mice treated with tigecycline, which may contribute to its beneficial effect. Additionally, *Parabacteroides distasonis* is a gram-negative anaerobic bacterium that has been associated with an attenuation of tumorigenesis and inflammation by interfering production of cytokines and proliferation mediators, such as AKT (668). Tigecycline treatment increased levels of *P. distasonis,* which can be related to the modulation of the inflammatory markers and the promotion of the intestinal barrier integrity, as reported previously in other studies (668). Indeed, the correlation analysis showed a negative association between *Akkermansia* genus or *P. distasonis* and some macroscopic parameters such as tumor number, size and DAI, as well as molecular markers of proliferation (STAT3, CTNNB1 and *Ccnd1* gene expression), survival (BCL2), stemness (SNAI1) or inflammation (*Il6, Il17a, Il23a, Tnfa* gene expression). Moreover, *Akkermansia* sp. or *P. distasonis* abundance is positively correlated with apoptosis (Tunel and CASP7) and cytotoxic activity ($CD8^+$ and Tc1 response) (Figure 61). Consequently, the connection between both bacteria species can contribute to tumorigenesis attenuation.

Human colonic microbiota can process a wide range of substrates that escape digestion by the host. Among *Bacillota*, the *Lachnospiraceae* and *Ruminococcaceae* species hydrolyze starch and other sugars to produce butyrate and other SCFAs. Initially, these SCFA-producing species have been associated with an improvement of the outcomes in different clinical settings, including CRC and IBD (669). Despite this, other studies have reported an increase in *Lachnospiraceae* and *Ruminococcus* genera in CRC patients (670). Here, a down-regulation of *Ruminococcus* and *Lachnospiraceae* species have been found in healthy and treated groups when compared with control CAC.

On the other hand, bacterial species from the *Erysipelatoclostridium* genus, such as *E. ruminantium* and *E. ramosum,* have been reported to be increased in adenoma (671). In this regard, we found a lower abundance of *Erysipelatoclostridium* in both healthy and tigecycline treated groups, in comparison with untreated group. Indeed, in this study, it has been also shown a positive correlation between tumor size and markers associated with tumor progression and the abundance of *Ruminococcaceae* UCG-013*, Ruminococcus 1, Lachnospiraceae A2, Lachnospiraceae bacterium* COE1 and *Erysipelatoclostridium* (Figure 61)

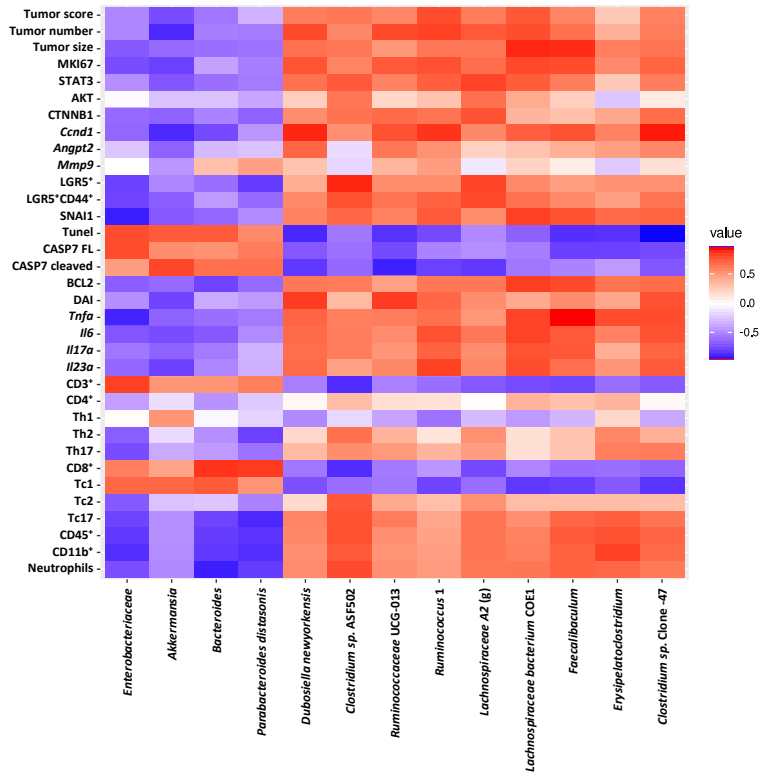

Figure 61. Heat-map of correlations between gut microbiota changes and different features analyzed in vivo between tigecycline-treated mice and untreated-CAC mice.

In conclusion, this study demonstrated the capacity of tigecycline to induce a sustained attenuation of tumorigenesis in CRC, evidenced by a reduced tumor number and characterized by reduction of tumor cells proliferation, induction of apoptosis, as well as amelioration of inflammation and modulation of gut dysbiosis. Therefore, our data support the treatment with tigecycline as a novel therapeutic strategy against CRC.

3. CHARACTERIZATION OF THE IMPACT OF OBESITY IN CRC DEVELOPMENT: IMPACT OF TIGECYCLINE IN A OBESITY-ASSOCIATED CAC MODEL.

It is widely accepted that obesity is considered a risk factor for CRC development. Different epidemiological studies have identified several dietary and lifestyle factors that either promote or protect against CRC. Among the risk factors, a key role has been ascribed to high body fat accumulation in overweight and obese people (672), and

abdominal adiposity has been positively associated with CRC for both men and women (673). Different factors contribute to the crosstalk between obesity and CRC, and different hypotheses have been formulated to explain this association. Firstly, metabolic changes occurring in obese patients lead to a dysregulation in the levels of some metabolites that may participate in tumorigenesis, such as insulin (673). Moreover, the chronic inflammatory state displayed in obesity may contribute to colon cancer development through the release of cytokines, such as IL-6, that activates several proliferation molecular pathways (382). Additionally, lipid peroxidation is a key process in the relationship between these two comorbidities, since different byproducts (4-HNE and MDA) possess a toxic profile and mutagenic properties (674). Finally, obesity and CRC share a status of gut dysbiosis, which has been evidenced to contribute to cancer development. In fact, metabolites derived from this altered microbiota composition have been found to contribute to the tumor process (421). In this scenario, the use of therapies that modulate this microbiota composition may interfere in the severity of CRC induced by the obese phenotype. Thus, beneficial effects against CRC development have been proven by modulating the microbiota profile in preclinical models of obesity-associated CRC (423, 427). Based on these findings, and taking into account the beneficial impact of the tigecycline described before, the characterization of the impact of this antibiotic in a murine model of obesity-associated CRC was another of the objectives proposed of this Thesis. Interestingly, these results can be considered as the first evidence of the effect of tigecycline on the treatment of obesity-associated CRC.

High blood glucose levels and hyperinsulinemia have been associated with a higher risk of CRC (549). Moreover, hyperglycemia is linked to an increase in cancer malignancy phenotype, which may be related to high levels of the enzyme glutamine-fructose-6-phosphate amidotransferase in colon carcinoma biopsies (675). Also, this hyperglycemia in obese subjects is a manifestation of insulin resistance and hyperinsulinemia. It is well known that the binding of insulin to its receptor activates the PI3K/AKT/mTOR and MAPK pathways, which subsequently exert downstream metabolic and cellular proliferation effects (374). Additionally, some experimental studies have evidenced that insulin can display antiapoptotic actions that together with its mitogenic capacity result in an induction of colonic tumors (676, 677). Accordingly, the HFD administration to mice resulted in a significant increase in body weight and higher levels of blood glucose in comparison with SD-fed mice. Conversely, although tigecycline treatment did not cause any significant differences in body weight, the drug reduced the glycemic levels and it may be associated with a high insulin sensitivity in these mice, probably because of the antiinflammatory effect exerted by this tetracycline. As previously stated,

hyperinsulinemia induces the activation of mitogenic pathways and this action is mainly carried out by an upregulation of the insulin growth factor 1 (374, 678). Furthermore, PI3K/AKT/mTOR molecular signaling pathway is involved in the tumor growth induced by insulin. Accordingly, untreated HFD-fed mice showed an increase in AKT activation in colonic tissue compared to SD-fed mice, thus indicating that the PI3K/AKT/mTOR signaling pathway is overactivated in control obese mice, and the treatment with tigecycline reduced it. This pathway seems to be involved in the increased cell proliferation rates and tumor growth observed in untreated HFD-fed mice, which showed a higher tumor number and size than those SD-fed mice or tigecycline-treated obese mice. Supporting this, it has been demonstrated that both rapamycin (as mTORC1 inhibitor) and metformin (AMPK-activator, able to inhibit AKT/mTOR activation) have been shown to block tumor formation in experimentally-induced cancer models (679-681).

The systemic and chronic low-grade inflammatory state displayed in obese individuals contributes to several disorders linked to this disease, like insulin resistance, and it is also considered a key player in the crosstalk between obesity and CRC (574). In concordance with these findings, higher signs of inflammation have been seen in untreated obese mice when compared with control SD and HFD-treated mice. In fact, control HFD group exhibited higher macroscopic features of inflammation (DAI score and colon W/L ratio), as well as increased levels of cell immune populations in blood and colon, and upregulated expression of pro-inflammatory cytokines in both colon and fat tissue. Regarding immune cells populations, it has been reported that obese patients have a high number of classical monocytes in peripheral blood, which is correlated with BMI and body fat accumulation (682). Moreover, classical monocytes levels are increased in peripheral blood of IBD patients (683). Moreover, some mediators are released from the tumor microenvironment, such as VEGF and chemokines, that contribute to the recruitment of monocytes into the primary tumor (684). Classical activated monocytes transmigrate to colon where are differentiated into resident macrophages and dendritic cells depending on the cytokines and microbial products environment (685). In IBD-associated cancer has been found that part of these monocytes are differentiated into tumor-associated macrophages that contribute to the tumor progression (686). Similarly, a significant increase in classic monocytes $Ly6C^{hi}CCR2^{+}$ was found in peripheral blood of untreated obese mice when compared to SD-fed and tigecycline-treated groups of mice. This increment in peripheral blood mononuclear cells was correlated with a significant increase of $CD45^{+}$ cells levels in the colon of control HFD mice in comparison with SD-fed mice. Subsequently, high levels of

the proinflammatory cytokines *Il17a* and *Il23a,* which have been described to contribute to tumorigenesis (687), were found in untreated obese mice in comparison with both, SD and HFD-tigecycline groups. Furthermore, mice treated with tigecycline exhibited a significant increase in $CD4^+$ and $CD8^+$ T lymphocytes, as well as in B lymphocytes ($B220^+$) in MLN in comparison with the other two experimental groups, similarly to those results previously described in the present Thesis, which may contribute to anti-tumor effect of tigecycline.

As commented above, inflammation can contribute to cancer development through different mechanisms including induction of oxidative stress, impairment of the immune response, aberrant cell signaling, upregulation of proliferative and anti-apoptotic pathways, as well as angiogenesis and cell migration, in which the overexpression of different transcription factors within tumor cells, like NF-κB, STATs or HIF1α, seems to play a key role (688). Confirming this, in the present study, IL6 levels were found to be upregulated in colon and fat deposits in untreated HFD-fed mice when compared to the other two experimental groups. Wunderlich CM and colleagues (2018) have reported that this cytokine exacerbates tumorigenesis in obesity-associated CRC through a shift in macrophage polarization towards CC-chemokine-ligand-20 (CCL-20)-producing macrophages that promote tumor development (382). Moreover, IL-6/JAK/STAT3 signaling axis is aberrantly hyperactivated in many types of cancer, including CRC, and it is associated with poor clinical prognosis, since it increases the tumor malignancy through the promotion of cell proliferation, survival, invasiveness and metastasis (689). This signaling cascade has been analyzed in the obesity-associated CRC model used in this study and, according to these findings, an overactivation of STAT3 has been found in control HFD mice when compared to SD-fed mice. In concordance with previous results described throughout this Thesis, tigecycline was able to hinder the activation of STAT3, and this effect resulted in the amelioration of the disease. As commented above, STAT3 is involved in cell proliferation and invasiveness, which were observed in the histological analysis carried out in colonic samples of untreated HFD-fed mice, where severe neoplastic lesions with invasive and hyperproliferation features were found in comparison with the other two groups of mice. Moreover, it is known that STAT3 is involved in the activation of the Wnt/β-catenin signaling pathway, which also contributes to cell proliferation and tumor growth (143). As previously reported, Wnt/β-catenin axis was also overactivated in untreated obese mice when compared to SD-fed mice, driving an upregulation of β-catenin target genes such as *Ccnd1* and *Myc*, which are involved in cell proliferation (421, 427). Moreover, it has been described that some metabolites that

are involved in adipogenesis, such as CEBP/α, can increase the activity of β-catenin, thus linking obesity and cancer (564). Indeed, a significant upregulation of the expression of this marker was found in the inguinal fat of HFD-mice. In concordance with the results related to body weight and adiposity, tigecycline treatment did not cause any significant impact on *Cebpa* gene expression, however a significant reduction in β-catenin levels and β-catenin target genes was observed in colonic specimens from HFD-mice treated with this drug due to its inherent capacity to inhibit this proliferation marker. Similarly, PPARγ is another transcription factor that plays a key role in the regulation of adipogenesis and obesity-associated inflammation. Moreover, PPARγ is also considered as a tumor suppressor in CRC due to its action on different targets including a downregulation of β-catenin (690, 691) and an induction of apoptosis through the upregulation of the tumor suppressor gene *TP53* (692) and the activation of the JNK pathway (693). In fact, some clinical trials were initiated at the beginning or this century to evaluate the effect of thiazolidinediones on CRC (694, 695), PPARγ ligands that have been used clinically to treat type 2 diabetes (696). In concordance with these findings, a significant reduction of PPARγ levels were found in inguinal fat samples from both obese mice groups when compared to lean mice. Tigecycline treatment did not cause any significant differences in PPARγ levels compared to control HFD mice, however the treatment achieved a downregulation of the activity of signaling pathways targeted by this transcription factor, specifically those in which AKT and the β-catenin are involved.

Oxidative stress and lipid dysregulation in obese individuals is linked to elevated levels of ROS, which may cause DNA mutations directly or through the formation of reactive lipid peroxidation byproducts such as MDA and 4-HNE (697, 698). Therefore, these compounds may be considered as genotoxic agents or tumor promoters (698). Accordingly, lipid peroxidation was indirectly measured in colon specimens from each group of mice and a significant increase in the byproducts of this reaction were found in untreated HFD mice when compared to SD-fed mice. The treatment with tigecycline reduced the levels of these compounds although no significant differences were found.

Finally, it is widely accepted that the gut microbiota plays an important role in the pathogenesis of obesity and CRC. Therefore, it could also act as a link between both pathologies worsening their prognosis and evolution. Consequently, the use of therapies that modulate the microbiota may constitute an optimal approach for the management of obesity and CRC separately as well as in patients with concomitant diseases (699, 700). The administration of a antibiotic cocktail (0.2 g/L ampicillin, neomycin, and metronidazole, and 0.1 g/L vancomycin) in drinking water to HFD mice with CRC induced by AOM/DSS resulted in an inhibition of tumor development (421). This beneficial impact

of antibiotics administration on obesity-associated CRC has also been proven by Liu et al., (2020)(701). They showed an acceleration of the adenoma-adenocarcinoma sequence in HFD mice due to the dysbiosis that takes place in mice with both co-morbidities. Although it has been reported that HFD promotes intestinal dysbiosis, the impact on microbial diversity and richness is controversial. In fact, some authors have shown a reduction in alpha-diversity indexes in obesity-associated CRC preclinical models (421, 426) whereas others have reported no significant differences in microbial diversity and richness between HFD-fed mice and SD-fed mice with CRC (422, 423, 428). In this study no significant differences were observed in alpha-diversity indexes when comparing SD-fed mice and those fed with a HFD. This finding could be explained considering that both groups of mice have been submitted to a CAC induction process that may impair the gut microbiota composition. Moreover, these results are in the line of those obtained in the second assay of HFD induced obesity in which the *Morus alba* extract was assayed. However, the antibiotic effect of tigecycline resulted in a reduction of alpha-diversity indexes in comparison with the other two groups of mice. According to previous studies, the dysbiosis induced by HFD was mainly evidenced when beta-diversity was analyzed (423). In this study, different groups of mice exhibited a significant dissimilarity between their microbial communities when the Bray-Curtis analysis was performed. Thus, the results indicated that the microbiota profile in each group of mice was different. Interestingly, tigecycline treatment in HFD mice modulated the gut microbiome composition showing a microbiota profile similar to the CAC group treated with tigecycline in normal weight mice. Hence, these findings suggest that regardless of obesity, tigecycline modulated the gut microbiota similarly. In this sense, HFD mice treated with tigecycline contained a higher relative abundance of *Akkermansia* and *Parabacteroides* bacterial genera than those mice fed a SD or a HFD. As previously commented, some beneficial effects have been attributed to these two bacterial genera when they are present in the microbiota of CRC subjects (667, 702, 703). Among the bacterial species of these genera, the treatment with tigecycline to HFD-fed mice achieved a significant increase of *Parabacteroides goldsteinii,* which has been positively correlated with an anti-tumor activity and the production of SCFAs (703).

Moreover, it has been reported that changes in *Muribaculaceae* (also named family S24-7) relative abundance occurred during tumorigenesis in AOM/DSS mice (704). Additionally, previous studies have identified *Muribuculaceae* as capable of degrading carbohydrates and its levels have been found downregulated with high-fat diet intake (705, 706). In line with these findings, *Muribaculaceae* family relative abundance was found decreased in HFD mice treated with AOM/DSS in comparison with those fed a SD

(422). Accordingly, LDA score carried out in this study showed that SD-fed mice contained higher levels of *Muribaculaceae_uncultred_bacterium* than those fed a HFD or treated with tigecycline. However, it is noteworthy that a reduction of this bacterial family induced by antibiotics or probiotics supplementation is associated with a better prognosis of the disease (707, 708). Consequently, these findings could explain the correlation between the reduction of *Muribaculaceae* induced by tigecycline and the beneficial effects exerted by this drug in obesity-associated CRC.

Additionally, the shared ASVs between the different groups were mapped in the Venn diagram. Curiously, *Desufovibrio* sp. was only found in the tigecycline treated group. Moreover, the results showed that this bacterial species was upregulated in tigecycline treated mice compared with HFD control mice. The increase of this bacterial genus has been associated with the inflammatory process and cell proliferation through SH_2 production (709). However, some authors have also described beneficial effects attributed to *Desulfovibrio* enrichment in AOM/DSS treated mice (710, 711).

Finally, *Alistipes* is a bacterial genus whose increased levels have been also associated with the intake of HFD and obesity (712, 713). In line with these findings, a substantial gain in the relative abundance of *Alistipes* was found in control HFD-fed mice from the different studies carried out in the present Thesis. Additionally, enrichment of *Alistipes* sp. has been linked to an increase of pro-tumoral metabolites such as lysophosphatidic acid and lysophosphatidylcholine that result in a higher tumorigenesis in HFD-fed mice with CRC (421). Accordingly, a significant increase in *Alistipes* abundance was observed in untreated HFD-fed mice in comparison with SD-fed mice and HFD-fed mice treated with tigecycline. Consequently, these changes in *Alistipes* sp. richness could explain the significant increase of the tumorigenesis process observed in the untreated HFD group.

Therefore, different studies performed in the current Thesis have shown that the gut dysbiosis situation described in the obesity induced model was similar to that observed in the obesity-associated cancer model. Of note, *Alistipes* abundance was increased in both untreated HFD and HFD-CAC mice. Therefore, the results obtained in this study would support that in both diseases, cancer and obesity, similar changes on the gut microbiota composition were promoted. Moreover, it has been demonstrated that tigecycline was able to modulate the intestinal microbiota towards similar profiles regardless of obesity status. In this sense, this modulation was associated with the increased bacterial taxa associated with beneficial effects against CRC, such as *Parabacteroides goldsteinii, Parabacteroides distasonis* and *Akkermansia muciniphila.*

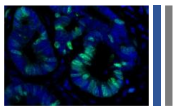

CONCLUSIONS

CONCLUSIONS

1. The extracts obtained from aerial parts of *Thymus serpyllum* and leaves of *Morus alba* showed beneficial effects in a murine model of high fat diet-induced obesity. The extracts ameliorated the inflammatory state, which was associated to the antioxidant activity of their phenolic compounds, and improved the obesity-associated gut dysbiosis, due to their prebiotic properties.
2. Tigecycline, a tetracycline with antibiotic and immunomodulatory properties, exerted an antitumor effect against several colon cancer cell lines. This effect was linked to an antiproliferative and proapoptotic activity, most probably mediated by the inhibition of the molecular pathways involved in cell proliferation, such as Wnt/β-catenin and JAK/STAT3, and the activation of the extrinsic, intrinsic and endoplasmic reticulum apoptosis pathways. Besides, tigecycline interfered with the epithelial mesenchymal transition process leading to a reduction in colon CSC populations, mainly attributed to its capacity to reduce SNAI1 levels.
3. In the murine model of AOM/DSS induced colitis-associated colorectal cancer, tigecycline administration reduced tumorigenesis via modulation of the immune system towards an anti-inflammatory status and enhancement of the T cytotoxic response. Moreover, tigecycline treatment reduced tumor cell proliferation and increased the proapoptotic effect, mainly through enhancing CASP7 levels. Additionally, tigecycline modulated gut microbiota by increasing specified bacterial taxa, such as *Parabacteroides distasonis* and *Akkermansia sp*., which have been associated with antitumor and anti-inflammatory profiles, and decreasing potential pathobionts like *Dubosiella sp*.
4. Obesity promoted the aggravation of the tumorigenesis process in a murine model of obesity-associated CAC, which was associated with an increase of chronic low-grade inflammation and the increased oxidative stress. Additionally, the high-fat diet intake induced an intestinal dysbiosis that resulted in an increase in some bacteria taxa involved in the crosstalk between obesity and CRC such as *Alistipes* sp.
5. In the murine model of obesity-associated CAC, tigecycline treatment lessened tumor worsening induced by high-fat diet. This effect could be derived from the antiproliferative and immunomodulatory properties showed by tigecycline, together with its capacity to modulate the gut dysbiosis increasing beneficial bacterial species such as *Parabacteroides goldsteinii* and *Akkermansia muciniphila*.

6. Gut microbiota modulation by prebiotics or antibiotics as well as their combination could be considered as potential novel therapeutic strategies in the management of obesity and/or colorectal cancer. Additionally, this therapeutic target could be considered for the prevention of colorectal cancer in high-risk patients.

CONCLUSIONES

1. Los extractos obtenidos de partes aéreas de *Thymus serpyllum* y hojas de *Morus alba* mostraron efectos beneficiosos en un modelo murino de obesidad inducida por dieta rica en grasa. En este sentido, los extractos mejoraron el estado inflamatorio, asociado a la actividad antioxidante de sus compuestos fenólicos, y mejoraron la disbiosis intestinal asociada a la obesidad, debido a sus propiedades prebióticas.
2. La tigeciclina, una tetraciclina con propiedades antibióticas e inmunomoduladoras, ejerció un efecto antitumoral en diferentes líneas celulares de cáncer de colon. Este efecto se relacionó con una actividad antiproliferativa y proapoptótica, íntimamente asociada con la inhibición de las vías moleculares implicadas en la proliferación celular, como Wnt/β-catenina y JAK/STAT3, y la activación de la apoptosis extrínseca, intrínseca y del retículo endoplásmico. Además, la tigeciclina impactó en el proceso de transición epitelio-mesénquima, que condujo a una reducción de las poblaciones de células madre del cáncer de colon, atribuida principalmente a su capacidad para reducir los niveles de SNAI1.
3. En el modelo murino de cáncer colorrectal asociado a colitis inducido por AOM/DSS, la administración de tigeciclina redujo la tumorigénesis a través de la modulación del sistema inmunitario hacia un estado antiinflamatorio y la mejora de la respuesta T citotóxica. Además, el tratamiento con tigeciclina redujo la proliferación de células tumorales y aumentó el efecto proapoptótico, principalmente mediante la mejora de los niveles de CASP7. Además, la tigeciclina moduló la microbiota intestinal aumentando taxones bacterianos específicos, como *Parabacteroides distasonis* y *Akkermansia sp.,* asociados a perfiles antitumorales y antiinflamatorios, y disminuyendo las poblaciones de patógenos potenciales como *Dubosiella sp*.
4. La obesidad agravó la tumorigénesis en un modelo murino de obesidad asociada a cáncer colorrectal, efecto asociado con un incremento de la inflamación crónica subclínica y del estrés oxidativo. Además, la ingesta de una dieta rica en grasa indujo una disbiosis intestinal que resultó en un incremento de ciertos taxones bacterianos involucrados en la comunicación entre la obesidad y el cáncer colorrectal como *Alistipes* sp.
5. En el modelo murino de CAC asociado a obesidad, el tratamiento con tigeciclina redujo el agravamiento del proceso tumoral inducido por una dieta rica en grasa.

Este efecto podría derivarse de las propiedades antiproliferativas e inmunomoduladoras que presenta la tigeciclina, junto con su capacidad para modular la disbiosis intestinal aumentando especies bacterianas beneficiosas como *Parabacteroides goldsteinii* y *Akkermansia muciniphila*.

6. La modulación de la microbiota intestinal por prebióticos o antibióticos, así como por su combinación, podrían considerarse una posible estrategia terapéutica novedosa en el manejo de la obesidad y/o el cáncer colorrectal. Además, esta diana terapéutica podría llegar a convertirse en una aproximación óptima para la prevención del cáncer colorrectal en pacientes de alto riesgo.

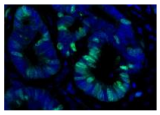

REFERENCES

REFERENCES

1. American Cancer Society. The History of Cancer [Internet] 2023 [Accesed on 10.01.22] Available from: https://www.cancer.org/treatment/understanding-your-diagnosis/history-of-cancer.html.
2. Sirica AE. Classification of Neoplasms. In: Sirica AE, editor. The Pathobiology of Neoplasia. Boston, MA: Springer US; 1989. p. 25-38.
3. World Health Organization. Cancer [Internet] 2023 [Accesed on 15.01.22] Available from: https://www.who.int/health-topics/cancer#tab=tab_1.
4. Hajdu SI. A note from history: the first printed case reports of cancer. Cancer. 2010;116(10):2493-8.
5. Hajdu SI. Thoughts about the cause of cancer. Cancer. 2006;106(8):1643-9.
6. Mitrus I, Bryndza E, Sochanik A, Szala S. Evolving models of tumor origin and progression. Tumour Biol. 2012;33(4):911-7.
7. Garrison FH. The history of cancer. Bull N Y Acad Med. 1926;2(4):179-85.
8. Talmadge JE, Fidler IJ. AACR centennial series: the biology of cancer metastasis: historical perspective. Cancer research. 2010;70(14):5649-69.
9. Neoplastic Diseases: A Treatise on Tumours. By James Ewing, A.M., M.D., Sc.D., Professor of Pathology at Cornell University Medical College, N.Y.; Pathologist to the Memorial Hospital. Third edition. Royal 8vo. Pp. 1127, with 546 illustrations. 1928. Philadelphia and London: W. B. Saunders Co. Ltd. 63s. net. 1928;16(61):174-5.
10. Cooper M. Regenerative Pathologies: Stem Cells, Teratomas and Theories of Cancer. 2009;1(1 %J Medicine Studies):55-66.
11. Capp JP. Cancer Stem Cells: From Historical Roots to a New Perspective. J Oncol. 2019;2019:5189232.
12. Whitman RC. Somatic Mutations as a Factor in the Production of Cancer: A Critical Review of v. Hansemann's Theory of Anaplasia in the Light of Modern Knowledge of Genetics. The Journal of Cancer Research. 1919;4(2):181-202.
13. Leon P. Bignold BLDC, Hubertus P. A. Jersmann. David Paul von Hansemann: Contributions to Oncology2007.
14. Hansford S, Huntsman DG. Boveri at 100: Theodor Boveri and genetic predisposition to cancer. J Pathol. 2014;234(2):142-5.
15. Muller HJ. The Production of Mutations by X-Rays. Proc Natl Acad Sci U S A. 1928;14(9):714-26.
16. Watson JD, Crick FH. Molecular structure of nucleic acids: a structure for deoxyribose nucleic acid. J.D. Watson and F.H.C. Crick. Published in Nature, number 4356 April 25, 1953. Nature. 1974;248(5451):765.
17. Potter VR. Initiation and promotion in cancer formation: the importance of studies on intercellular communication. Yale J Biol Med. 1980;53(5):367-84.

18. Pitot HC. The molecular biology of carcinogenesis. Cancer. 1993;72(3 Suppl):962-70.
19. Luch A. Nature and nurture - lessons from chemical carcinogenesis. Nat Rev Cancer. 2005;5(2):113-25.
20. Bishop JM. The molecular genetics of cancer. Science. 1987;235(4786):305-11.
21. Nowell PC. The clonal evolution of tumor cell populations. Science. 1976;194(4260):23-8.
22. Foo J, Leder K, Michor F. Stochastic dynamics of cancer initiation. Phys Biol. 2011;8(1):015002.
23. Tomasetti C, Vogelstein B, Parmigiani G. Half or more of the somatic mutations in cancers of self-renewing tissues originate prior to tumor initiation. Proc Natl Acad Sci U S A. 2013;110(6):1999-2004.
24. Melzer C, von der Ohe J, Lehnert H, Ungefroren H, Hass R. Cancer stem cell niche models and contribution by mesenchymal stroma/stem cells. Mol Cancer. 2017;16(1):28.
25. Lobo NA, Shimono Y, Qian D, Clarke MF. The biology of cancer stem cells. Annu Rev Cell Dev Biol. 2007;23:675-99.
26. Lapidot T, Sirard C, Vormoor J, Murdoch B, Hoang T, Caceres-Cortes J, et al. A cell initiating human acute myeloid leukaemia after transplantation into SCID mice. Nature. 1994;367(6464):645-8.
27. Massard C, Deutsch E, Soria JC. Tumour stem cell-targeted treatment: elimination or differentiation. Ann Oncol. 2006;17(11):1620-4.
28. Plaks V, Kong N, Werb Z. The cancer stem cell niche: how essential is the niche in regulating stemness of tumor cells? Cell Stem Cell. 2015;16(3):225-38.
29. Borovski T, De Sousa EMF, Vermeulen L, Medema JP. Cancer stem cell niche: the place to be. Cancer research. 2011;71(3):634-9.
30. Rich JN. Cancer stem cells: understanding tumor hierarchy and heterogeneity. Medicine (Baltimore). 2016;95(1 Suppl 1):S2-S7.
31. Hass R, Gunji H, Datta R, Kharbanda S, Hartmann A, Weichselbaum R, et al. Differentiation and retrodifferentiation of human myeloid leukemia cells is associated with reversible induction of cell cycle-regulatory genes. Cancer Res. 1992;52(6):1445-50.
32. Cabillic F, Corlu A. Regulation of Transdifferentiation and Retrodifferentiation by Inflammatory Cytokines in Hepatocellular Carcinoma. Gastroenterology. 2016;151(4):607-15.
33. Hass R. Rejuvenation in distinct cell populations - What does it mean? Exp Gerontol. 2009;44(10):634-8.
34. Cancer National Institute. What Is Cancer? [Internet] 2021 [Accesed on 12.01.22] Available from: https://www.cancer.gov/about-cancer/understanding/what-is-cancer.
35. Greaves M, Maley CC. Clonal evolution in cancer. Nature. 2012;481(7381):306-13.
36. Ripple MJ, Parker Struckhoff A, Trillo-Tinoco J, Li L, Margolin DA, McGoey R, et al. Activation of c-Myc and Cyclin D1 by JCV T-Antigen and beta-catenin in colon cancer. PLoS One. 2014;9(9):e106257.

37. Iacopetta B. TP53 mutation in colorectal cancer. Hum Mutat. 2003;21(3):271-6.
38. Yoshida K, Miki Y. Role of BRCA1 and BRCA2 as regulators of DNA repair, transcription, and cell cycle in response to DNA damage. Cancer Sci. 2004;95(11):866-71.
39. Kontomanolis EN, Koutras A, Syllaios A, Schizas D, Mastoraki A, Garmpis N, et al. Role of Oncogenes and Tumor-suppressor Genes in Carcinogenesis: A Review. Anticancer research. 2020;40(11):6009-15.
40. Li GM. Mechanisms and functions of DNA mismatch repair. Cell Res. 2008;18(1):85-98.
41. Cooper GM. The cell : a molecular approach / Geoffrey M. Cooper: Washington, D.C. : Sunderland, Mass. : ASM Press ; Sinauer Associates, c2000.; 2000 [2nd ed.:[xxiv, 689 p. : ill. (some col.) ; 29 cm].
42. Hanahan D, Weinberg RA. Hallmarks of cancer: the next generation. Cell. 2011;144(5):646-74.
43. Dagogo-Jack I, Shaw AT. Tumour heterogeneity and resistance to cancer therapies. Nat Rev Clin Oncol. 2018;15(2):81-94.
44. Anderson NM, Simon MC. The tumor microenvironment. Curr Biol. 2020;30(16):R921-R5.
45. Truffi M, Sorrentino L, Corsi F. Fibroblasts in the Tumor Microenvironment. Adv Exp Med Biol. 2020;1234:15-29.
46. International Agency for Research on Cancer. About CANCER TODAY IARC, [Internet] 2020 [Accesed on 20.01.22] Available from: https://gco.iarc.fr/today/about#about-cancer-today.
47. World Cancer Research Fund International. Colorectal cancer statistics [Internet] 2023 [Accesed on 20.01.22] Available from: https://www.wcrf.org/cancer-trends/colorectal-cancer-statistics/.
48. American Cancer Society. About Colorectal Cancer [Internet] 2023 [Accesed on 20.01.22] Available from: https://www.cancer.org/content/dam/CRC/PDF/Public/8604.00.pdf.
49. Arnold M, Sierra MS, Laversanne M, Soerjomataram I, Jemal A, Bray F. Global patterns and trends in colorectal cancer incidence and mortality. Gut. 2017;66(4):683-91.
50. Henrikson NB, Webber EM, Goddard KA, Scrol A, Piper M, Williams MS, et al. Family history and the natural history of colorectal cancer: systematic review. Genet Med. 2015;17(9):702-12.
51. Bakhoum SF, Cantley LC. The Multifaceted Role of Chromosomal Instability in Cancer and Its Microenvironment. Cell. 2018;174(6):1347-60.
52. Munteanu I, Mastalier B. Genetics of colorectal cancer. Journal of medicine and life. 2014;7(4):507-11.
53. Yan H, Yuan W, Velculescu VE, Vogelstein B, Kinzler KW. Allelic variation in human gene expression. Science. 2002;297(5584):1143.
54. Aaltonen LA, Salovaara R, Kristo P, Canzian F, Hemminki A, Peltomaki P, et al. Incidence of hereditary nonpolyposis colorectal cancer and the feasibility of molecular screening for the disease. N Engl J Med. 1998;338(21):1481-7.
55. Hampel H, Frankel WL, Martin E, Arnold M, Khanduja K, Kuebler P, et al. Screening for the Lynch syndrome (hereditary nonpolyposis colorectal cancer). N Engl J Med. 2005;352(18):1851-60.

56. Roudko V, Cimen Bozkus C, Greenbaum B, Lucas A, Samstein R, Bhardwaj N. Lynch Syndrome and MSI-H Cancers: From Mechanisms to "Off-The-Shelf" Cancer Vaccines. Front Immunol. 2021;12:757804.
57. Win AK, Jenkins MA, Dowty JG, Antoniou AC, Lee A, Giles GG, et al. Prevalence and Penetrance of Major Genes and Polygenes for Colorectal Cancer. Cancer Epidemiol Biomarkers Prev. 2017;26(3):404-12.
58. Vasen HF, Tomlinson I, Castells A. Clinical management of hereditary colorectal cancer syndromes. Nat Rev Gastroenterol Hepatol. 2015;12(2):88-97.
59. Esteller M. Aberrant DNA methylation as a cancer-inducing mechanism. Annu Rev Pharmacol Toxicol. 2005;45:629-56.
60. Strathdee G, Brown R. Aberrant DNA methylation in cancer: potential clinical interventions. Expert Rev Mol Med. 2002;4(4):1-17.
61. Tse JWT, Jenkins LJ, Chionh F, Mariadason JM. Aberrant DNA Methylation in Colorectal Cancer: What Should We Target? Trends Cancer. 2017;3(10):698-712.
62. Weisenberger DJ, Siegmund KD, Campan M, Young J, Long TI, Faasse MA, et al. CpG island methylator phenotype underlies sporadic microsatellite instability and is tightly associated with BRAF mutation in colorectal cancer. Nat Genet. 2006;38(7):787-93.
63. White A, Ironmonger L, Steele RJC, Ormiston-Smith N, Crawford C, Seims A. A review of sex-related differences in colorectal cancer incidence, screening uptake, routes to diagnosis, cancer stage and survival in the UK. BMC Cancer. 2018;18(1):906.
64. Vuik FE, Nieuwenburg SA, Bardou M, Lansdorp-Vogelaar I, Dinis-Ribeiro M, Bento MJ, et al. Increasing incidence of colorectal cancer in young adults in Europe over the last 25 years. Gut. 2019;68(10):1820-6.
65. Botteri E, Iodice S, Bagnardi V, Raimondi S, Lowenfels AB, Maisonneuve P. Smoking and colorectal cancer: a meta-analysis. JAMA. 2008;300(23):2765-78.
66. Morris JS, Bradbury KE, Cross AJ, Gunter MJ, Murphy N. Physical activity, sedentary behaviour and colorectal cancer risk in the UK Biobank. Br J Cancer. 2018;118(6):920-9.
67. Cai S, Li Y, Ding Y, Chen K, Jin M. Alcohol drinking and the risk of colorectal cancer death: a meta-analysis. Eur J Cancer Prev. 2014;23(6):532-9.
68. Chan DS, Lau R, Aune D, Vieira R, Greenwood DC, Kampman E, et al. Red and processed meat and colorectal cancer incidence: meta-analysis of prospective studies. PLoS One. 2011;6(6):e20456.
69. Abrahami D, McDonald EG, Schnitzer ME, Barkun AN, Suissa S, Azoulay L. Proton pump inhibitors and risk of colorectal cancer. Gut. 2022;71(1):111-8.
70. Shin CM, Kim N, Han K, Kim B, Jung JH, Oh TJ, et al. Anti-diabetic medications and the risk for colorectal cancer: A population-based nested case-control study. Cancer Epidemiol. 2020;64:101658.
71. Eaden JA, Abrams KR, Mayberry JF. The risk of colorectal cancer in ulcerative colitis: a meta-analysis. Gut. 2001;48(4):526-35.
72. Bajpai M, Seril DN, Van Gurp J, Geng X, Alvarez J, Minacapelli CD, et al. Effect of Long-Term Mesalamine Therapy on Cancer-Associated Gene Expression in Colonic Mucosa of Patients with Ulcerative Colitis. Dig Dis Sci. 2019;64(3):740-50.

73. Ma Y, Yang Y, Wang F, Zhang P, Shi C, Zou Y, et al. Obesity and risk of colorectal cancer: a systematic review of prospective studies. PLoS One. 2013;8(1):e53916.
74. Moghaddam AA, Woodward M, Huxley R. Obesity and risk of colorectal cancer: a meta-analysis of 31 studies with 70,000 events. Cancer Epidemiol Biomarkers Prev. 2007;16(12):2533-47.
75. Kostic AD, Chun E, Robertson L, Glickman JN, Gallini CA, Michaud M, et al. Fusobacterium nucleatum potentiates intestinal tumorigenesis and modulates the tumor-immune microenvironment. Cell Host Microbe. 2013;14(2):207-15.
76. Nakatsu G, Li X, Zhou H, Sheng J, Wong SH, Wu WK, et al. Gut mucosal microbiome across stages of colorectal carcinogenesis. Nat Commun. 2015;6:8727.
77. Ogino S, Goel A. Molecular classification and correlates in colorectal cancer. J Mol Diagn. 2008;10(1):13-27.
78. Grady WM, Carethers JM. Genomic and epigenetic instability in colorectal cancer pathogenesis. Gastroenterology. 2008;135(4):1079-99.
79. Dekker E, Tanis PJ, Vleugels JLA, Kasi PM, Wallace MB. Colorectal cancer. Lancet (London, England). 2019;394(10207):1467-80.
80. Lengauer C, Kinzler KW, Vogelstein B. Genetic instabilities in human cancers. Nature. 1998;396(6712):643-9.
81. Pino MS, Chung DC. The chromosomal instability pathway in colon cancer. Gastroenterology. 2010;138(6):2059-72.
82. Fearon ER, Vogelstein B. A genetic model for colorectal tumorigenesis. Cell. 1990;61(5):759-67.
83. Kinzler KW, Vogelstein B. Lessons from hereditary colorectal cancer. Cell. 1996;87(2):159-70.
84. Jen J, Powell SM, Papadopoulos N, Smith KJ, Hamilton SR, Vogelstein B, et al. Molecular determinants of dysplasia in colorectal lesions. Cancer research. 1994;54(21):5523-6.
85. Smith AJ, Stern HS, Penner M, Hay K, Mitri A, Bapat BV, et al. Somatic APC and K-ras codon 12 mutations in aberrant crypt foci from human colons. Cancer research. 1994;54(21):5527-30.
86. Fearon ER. Molecular genetics of colorectal cancer. Annu Rev Pathol. 2011;6:479-507.
87. Shpitz B, Hay K, Medline A, Bruce WR, Bull SB, Gallinger S, et al. Natural history of aberrant crypt foci. A surgical approach. Dis Colon Rectum. 1996;39(7):763-7.
88. Hawkins NJ, Bariol C, Ward RL. The serrated neoplasia pathway. Pathology. 2002;34(6):548-55.
89. Rashtak S, Rego R, Sweetser SR, Sinicrope FA. Sessile Serrated Polyps and Colon Cancer Prevention. Cancer Prev Res (Phila). 2017;10(5):270-8.
90. Snover DC. Update on the serrated pathway to colorectal carcinoma. Hum Pathol. 2011;42(1):1-10.
91. Toyota M, Ahuja N, Ohe-Toyota M, Herman JG, Baylin SB, Issa JP. CpG island methylator phenotype in colorectal cancer. Proc Natl Acad Sci U S A. 1999;96(15):8681-6.

92. Ogino S, Kawasaki T, Kirkner GJ, Loda M, Fuchs CS. CpG island methylator phenotype-low (CIMP-low) in colorectal cancer: possible associations with male sex and KRAS mutations. J Mol Diagn. 2006;8(5):582-8.
93. Lao VV, Grady WM. Epigenetics and colorectal cancer. Nat Rev Gastroenterol Hepatol. 2011;8(12):686-700.
94. Bettington M, Walker N, Clouston A, Brown I, Leggett B, Whitehall V. The serrated pathway to colorectal carcinoma: current concepts and challenges. Histopathology. 2013;62(3):367-86.
95. Hewish M, Lord CJ, Martin SA, Cunningham D, Ashworth A. Mismatch repair deficient colorectal cancer in the era of personalized treatment. Nat Rev Clin Oncol. 2010;7(4):197-208.
96. Guinney J, Dienstmann R, Wang X, de Reynies A, Schlicker A, Soneson C, et al. The consensus molecular subtypes of colorectal cancer. Nat Med. 2015;21(11):1350-6.
97. Fessler E, Medema JP. Colorectal Cancer Subtypes: Developmental Origin and Microenvironmental Regulation. Trends Cancer. 2016;2(9):505-18.
98. Zeki SS, Graham TA, Wright NA. Stem cells and their implications for colorectal cancer. Nat Rev Gastroenterol Hepatol. 2011;8(2):90-100.
99. Hanahan D, Weinberg RA. The hallmarks of cancer. Cell. 2000;100(1):57-70.
100. Hanahan D. Hallmarks of Cancer: New Dimensions. Cancer Discov. 2022;12(1):31-46.
101. Smit WL, Spaan CN, Johannes de Boer R, Ramesh P, Martins Garcia T, Meijer BJ, et al. Driver mutations of the adenoma-carcinoma sequence govern the intestinal epithelial global translational capacity. Proc Natl Acad Sci U S A. 2020;117(41):25560-70.
102. Pai SG, Carneiro BA, Mota JM, Costa R, Leite CA, Barroso-Sousa R, et al. Wnt/beta-catenin pathway: modulating anticancer immune response. J Hematol Oncol. 2017;10(1):101.
103. Fearnhead NS, Britton MP, Bodmer WF. The ABC of APC. Hum Mol Genet. 2001;10(7):721-33.
104. Qian J, Steigerwald K, Combs KA, Barton MC, Groden J. Caspase cleavage of the APC tumor suppressor and release of an amino-terminal domain is required for the transcription-independent function of APC in apoptosis. Oncogene. 2007;26(33):4872-6.
105. Gumbiner BM. Signal transduction of beta-catenin. Curr Opin Cell Biol. 1995;7(5):634-40.
106. Rubinfeld B, Albert I, Porfiri E, Fiol C, Munemitsu S, Polakis P. Binding of GSK3beta to the APC-beta-catenin complex and regulation of complex assembly. Science. 1996;272(5264):1023-6.
107. Su Y, Fu C, Ishikawa S, Stella A, Kojima M, Shitoh K, et al. APC is essential for targeting phosphorylated beta-catenin to the SCFbeta-TrCP ubiquitin ligase. Mol Cell. 2008;32(5):652-61.
108. Shang S, Hua F, Hu ZW. The regulation of beta-catenin activity and function in cancer: therapeutic opportunities. Oncotarget. 2017;8(20):33972-89.
109. Bienz M, Clevers H. Linking colorectal cancer to Wnt signaling. Cell. 2000;103(2):311-20.

110. Korinek V, Barker N, Morin PJ, van Wichen D, de Weger R, Kinzler KW, et al. Constitutive transcriptional activation by a beta-catenin-Tcf complex in APC-/- colon carcinoma. Science. 1997;275(5307):1784-7.
111. Pines G, Kostler WJ, Yarden Y. Oncogenic mutant forms of EGFR: lessons in signal transduction and targets for cancer therapy. FEBS Lett. 2010;584(12):2699-706.
112. Krasinskas AM. EGFR Signaling in Colorectal Carcinoma. Patholog Res Int. 2011;2011:932932.
113. Chia CM, Winston RM, Handyside AH. EGF, TGF-alpha and EGFR expression in human preimplantation embryos. Development. 1995;121(2):299-307.
114. Citri A, Yarden Y. EGF-ERBB signalling: towards the systems level. Nat Rev Mol Cell Biol. 2006;7(7):505-16.
115. Goldstein NS, Armin M. Epidermal growth factor receptor immunohistochemical reactivity in patients with American Joint Committee on Cancer Stage IV colon adenocarcinoma. Cancer. 2001;92(5):1331-46.
116. Jonker DJ, O'Callaghan CJ, Karapetis CS, Zalcberg JR, Tu D, Au HJ, et al. Cetuximab for the treatment of colorectal cancer. N Engl J Med. 2007;357(20):2040-8.
117. Fang JY, Richardson BC. The MAPK signalling pathways and colorectal cancer. Lancet Oncol. 2005;6(5):322-7.
118. Sasaoka T, Langlois WJ, Leitner JW, Draznin B, Olefsky JM. The signaling pathway coupling epidermal growth factor receptors to activation of p21ras. Journal of Biological Chemistry. 1994;269(51):32621-5.
119. Keshamouni VG, Mattingly RR, Reddy KB. Mechanism of 17-beta-estradiol-induced Erk1/2 activation in breast cancer cells. A role for HER2 AND PKC-delta. J Biol Chem. 2002;277(25):22558-65.
120. Qiu ZH, Leslie CC. Protein kinase C-dependent and -independent pathways of mitogen-activated protein kinase activation in macrophages by stimuli that activate phospholipase A2. Journal of Biological Chemistry. 1994;269(30):19480-7.
121. Dong C, Davis RJ, Flavell RA. MAP kinases in the immune response. Annu Rev Immunol. 2002;20:55-72.
122. Boulton TG, Nye SH, Robbins DJ, Ip NY, Radziejewska E, Morgenbesser SD, et al. ERKs: a family of protein-serine/threonine kinases that are activated and tyrosine phosphorylated in response to insulin and NGF. Cell. 1991;65(4):663-75.
123. Chen DB, Davis JS. Epidermal growth factor induces c-fos and c-jun mRNA via Raf-1/MEK1/ERK-dependent and -independent pathways in bovine luteal cells. Mol Cell Endocrinol. 2003;200(1-2):141-54.
124. Lewis TS, Shapiro PS, Ahn NG. Signal transduction through MAP kinase cascades. Adv Cancer Res. 1998;74:49-139.
125. Koveitypour Z, Panahi F, Vakilian M, Peymani M, Seyed Forootan F, Nasr Esfahani MH, et al. Signaling pathways involved in colorectal cancer progression. Cell Biosci. 2019;9:97.
126. Cox AD, Fesik SW, Kimmelman AC, Luo J, Der CJ. Drugging the undruggable RAS: Mission possible? Nat Rev Drug Discov. 2014;13(11):828-51.

127. Tejpar S, Bertagnolli M, Bosman F, Lenz HJ, Garraway L, Waldman F, et al. Prognostic and predictive biomarkers in resected colon cancer: current status and future perspectives for integrating genomics into biomarker discovery. The oncologist. 2010;15(4):390-404.
128. Johnston SR. Farnesyl transferase inhibitors: a novel targeted tnerapy for cancer. Lancet Oncol. 2001;2(1):18-26.
129. Frattini M, Saletti P, Molinari F, De Dosso S. EGFR signaling in colorectal cancer: a clinical perspective. Gastrointestinal Cancer: Targets and Therapy. 2015.
130. Malinowsky K, Nitsche U, Janssen KP, Bader FG, Spath C, Drecoll E, et al. Activation of the PI3K/AKT pathway correlates with prognosis in stage II colon cancer. Br J Cancer. 2014;110(8):2081-9.
131. Sarbassov DD, Guertin DA, Ali SM, Sabatini DM. Phosphorylation and regulation of Akt/PKB by the rictor-mTOR complex. Science. 2005;307(5712):1098-101.
132. Yu JS, Cui W. Proliferation, survival and metabolism: the role of PI3K/AKT/mTOR signalling in pluripotency and cell fate determination. Development. 2016;143(17):3050-60.
133. Maehama T, Dixon JE. The tumor suppressor, PTEN/MMAC1, dephosphorylates the lipid second messenger, phosphatidylinositol 3,4,5-trisphosphate. J Biol Chem. 1998;273(22):13375-8.
134. Gao T, Furnari F, Newton AC. PHLPP: a phosphatase that directly dephosphorylates Akt, promotes apoptosis, and suppresses tumor growth. Mol Cell. 2005;18(1):13-24.
135. Danielsen SA, Eide PW, Nesbakken A, Guren T, Leithe E, Lothe RA. Portrait of the PI3K/AKT pathway in colorectal cancer. Biochim Biophys Acta. 2015;1855(1):104-21.
136. Sato S, Fujita N, Tsuruo T. Involvement of 3-phosphoinositide-dependent protein kinase-1 in the MEK/MAPK signal transduction pathway. J Biol Chem. 2004;279(32):33759-67.
137. Tang S, Yuan X, Song J, Chen Y, Tan X, Li Q. Association analyses of the JAK/STAT signaling pathway with the progression and prognosis of colon cancer. Oncol Lett. 2019;17(1):159-64.
138. Gargalionis AN, Papavassiliou KA, Papavassiliou AG. Targeting STAT3 Signaling Pathway in Colorectal Cancer. Biomedicines. 2021;9(8).
139. Kamran MZ, Patil P, Gude RP. Role of STAT3 in cancer metastasis and translational advances. Biomed Res Int. 2013;2013:421821.
140. Babon JJ, Varghese LN, Nicola NA. Inhibition of IL-6 family cytokines by SOCS3. Semin Immunol. 2014;26(1):13-9.
141. Hu X, Li J, Fu M, Zhao X, Wang W. The JAK/STAT signaling pathway: from bench to clinic. Signal Transduct Target Ther. 2021;6(1):402.
142. Corvinus FM, Orth C, Moriggl R, Tsareva SA, Wagner S, Pfitzner EB, et al. Persistent STAT3 activation in colon cancer is associated with enhanced cell proliferation and tumor growth. Neoplasia. 2005;7(6):545-55.
143. Bromberg JF, Wrzeszczynska MH, Devgan G, Zhao Y, Pestell RG, Albanese C, et al. Stat3 as an oncogene. Cell. 1999;98(3):295-303.

144. Grivennikov S, Karin E, Terzic J, Mucida D, Yu GY, Vallabhapurapu S, et al. IL-6 and Stat3 are required for survival of intestinal epithelial cells and development of colitis-associated cancer. Cancer Cell. 2009;15(2):103-13.
145. Kawada M, Seno H, Uenoyama Y, Sawabu T, Kanda N, Fukui H, et al. Signal transducers and activators of transcription 3 activation is involved in nuclear accumulation of beta-catenin in colorectal cancer. Cancer research. 2006;66(6):2913-7.
146. Luo J, Yan R, He X, He J. Constitutive activation of STAT3 and cyclin D1 overexpression contribute to proliferation, migration and invasion in gastric cancer cells. American journal of translational research. 2017;9(12):5671-7.
147. Bhattacharya S, Ray RM, Johnson LR. STAT3-mediated transcription of Bcl-2, Mcl-1 and c-IAP2 prevents apoptosis in polyamine-depleted cells. Biochem J. 2005;392(Pt 2):335-44.
148. Xie TX, Wei D, Liu M, Gao AC, Ali-Osman F, Sawaya R, et al. Stat3 activation regulates the expression of matrix metalloproteinase-2 and tumor invasion and metastasis. Oncogene. 2004;23(20):3550-60.
149. Dechow TN, Pedranzini L, Leitch A, Leslie K, Gerald WL, Linkov I, et al. Requirement of matrix metalloproteinase-9 for the transformation of human mammary epithelial cells by Stat3-C. Proc Natl Acad Sci U S A. 2004;101(29):10602-7.
150. Itoh M, Murata T, Suzuki T, Shindoh M, Nakajima K, Imai K, et al. Requirement of STAT3 activation for maximal collagenase-1 (MMP-1) induction by epidermal growth factor and malignant characteristics in T24 bladder cancer cells. Oncogene. 2006;25(8):1195-204.
151. Wei D, Le X, Zheng L, Wang L, Frey JA, Gao AC, et al. Stat3 activation regulates the expression of vascular endothelial growth factor and human pancreatic cancer angiogenesis and metastasis. Oncogene. 2003;22(3):319-29.
152. Semenza GL. Targeting HIF-1 for cancer therapy. Nat Rev Cancer. 2003;3(10):721-32.
153. Norbury CJ, Hickson ID. Cellular responses to DNA damage. Annu Rev Pharmacol Toxicol. 2001;41:367-401.
154. Elmore S. Apoptosis: a review of programmed cell death. Toxicol Pathol. 2007;35(4):495-516.
155. Locksley RM, Killeen N, Lenardo MJ. The TNF and TNF receptor superfamilies: integrating mammalian biology. Cell. 2001;104(4):487-501.
156. Ashkenazi A, Dixit VM. Death receptors: signaling and modulation. Science. 1998;281(5381):1305-8.
157. Kischkel FC, Hellbardt S, Behrmann I, Germer M, Pawlita M, Krammer PH, et al. Cytotoxicity-dependent APO-1 (Fas/CD95)-associated proteins form a death-inducing signaling complex (DISC) with the receptor. EMBO J. 1995;14(22):5579-88.
158. Saelens X, Festjens N, Vande Walle L, van Gurp M, van Loo G, Vandenabeele P. Toxic proteins released from mitochondria in cell death. Oncogene. 2004;23(16):2861-74.
159. Shamas-Din A, Brahmbhatt H, Leber B, Andrews DW. BH3-only proteins: Orchestrators of apoptosis. Biochim Biophys Acta. 2011;1813(4):508-20.
160. Chinnaiyan AM. The apoptosome: heart and soul of the cell death machine. Neoplasia. 1999;1(1):5-15.

161. Wong RS. Apoptosis in cancer: from pathogenesis to treatment. J Exp Clin Cancer Res. 2011;30(1):87.
162. van Loo G, van Gurp M, Depuydt B, Srinivasula SM, Rodriguez I, Alnemri ES, et al. The serine protease Omi/HtrA2 is released from mitochondria during apoptosis. Omi interacts with caspase-inhibitor XIAP and induces enhanced caspase activity. Cell Death Differ. 2002;9(1):20-6.
163. Gobeil S, Boucher CC, Nadeau D, Poirier GG. Characterization of the necrotic cleavage of poly(ADP-ribose) polymerase (PARP-1): implication of lysosomal proteases. Cell Death Differ. 2001;8(6):588-94.
164. Chaitanya GV, Steven AJ, Babu PP. PARP-1 cleavage fragments: signatures of cell-death proteases in neurodegeneration. Cell Commun Signal. 2010;8:31.
165. Marchi S, Patergnani S, Missiroli S, Morciano G, Rimessi A, Wieckowski MR, et al. Mitochondrial and endoplasmic reticulum calcium homeostasis and cell death. Cell Calcium. 2018;69:62-72.
166. Breckenridge DG, Germain M, Mathai JP, Nguyen M, Shore GC. Regulation of apoptosis by endoplasmic reticulum pathways. Oncogene. 2003;22(53):8608-18.
167. Chang TK, Lawrence DA, Lu M, Tan J, Harnoss JM, Marsters SA, et al. Coordination between Two Branches of the Unfolded Protein Response Determines Apoptotic Cell Fate. Mol Cell. 2018;71(4):629-36 e5.
168. Haze K, Yoshida H, Yanagi H, Yura T, Mori K. Mammalian transcription factor ATF6 is synthesized as a transmembrane protein and activated by proteolysis in response to endoplasmic reticulum stress. Mol Biol Cell. 1999;10(11):3787-99.
169. Sano R, Reed JC. ER stress-induced cell death mechanisms. Biochim Biophys Acta. 2013;1833(12):3460-70.
170. Hu H, Tian M, Ding C, Yu S. The C/EBP Homologous Protein (CHOP) Transcription Factor Functions in Endoplasmic Reticulum Stress-Induced Apoptosis and Microbial Infection. Front Immunol. 2018;9:3083.
171. Morishima N, Nakanishi K, Nakano A. Activating transcription factor-6 (ATF6) mediates apoptosis with reduction of myeloid cell leukemia sequence 1 (Mcl-1) protein via induction of WW domain binding protein 1. J Biol Chem. 2011;286(40):35227-35.
172. Nakagawa T, Zhu H, Morishima N, Li E, Xu J, Yankner BA, et al. Caspase-12 mediates endoplasmic-reticulum-specific apoptosis and cytotoxicity by amyloid-beta. Nature. 2000;403(6765):98-103.
173. Hitomi J, Katayama T, Taniguchi M, Honda A, Imaizumi K, Tohyama M. Apoptosis induced by endoplasmic reticulum stress depends on activation of caspase-3 via caspase-12. Neurosci Lett. 2004;357(2):127-30.
174. Fernald K, Kurokawa M. Evading apoptosis in cancer. Trends Cell Biol. 2013;23(12):620-33.
175. Korsmeyer SJ. Chromosomal translocations in lymphoid malignancies reveal novel proto-oncogenes. Annu Rev Immunol. 1992;10:785-807.
176. Vaux DL, Cory S, Adams JM. Bcl-2 gene promotes haemopoietic cell survival and cooperates with c-myc to immortalize pre-B cells. Nature. 1988;335(6189):440-2.

177. Strasser A, Harris AW, Bath ML, Cory S. Novel primitive lymphoid tumours induced in transgenic mice by cooperation between myc and bcl-2. Nature. 1990;348(6299):331-3.
178. Baugh EH, Ke H, Levine AJ, Bonneau RA, Chan CS. Why are there hotspot mutations in the TP53 gene in human cancers? Cell Death Differ. 2018;25(1):154-60.
179. Harris CC. p53 tumor suppressor gene: from the basic research laboratory to the clinic--an abridged historical perspective. Carcinogenesis. 1996;17(6):1187-98.
180. Oda E, Ohki R, Murasawa H, Nemoto J, Shibue T, Yamashita T, et al. Noxa, a BH3-only member of the Bcl-2 family and candidate mediator of p53-induced apoptosis. Science. 2000;288(5468):1053-8.
181. Nakano K, Vousden KH. PUMA, a novel proapoptotic gene, is induced by p53. Mol Cell. 2001;7(3):683-94.
182. Mills JR, Hippo Y, Robert F, Chen SM, Malina A, Lin CJ, et al. mTORC1 promotes survival through translational control of Mcl-1. Proc Natl Acad Sci U S A. 2008;105(31):10853-8.
183. Waldner M, Schimanski CC, Neurath MF. Colon cancer and the immune system: the role of tumor invading T cells. World J Gastroenterol. 2006;12(45):7233-8.
184. Pancione M, Giordano G, Remo A, Febbraro A, Sabatino L, Manfrin E, et al. Immune escape mechanisms in colorectal cancer pathogenesis and liver metastasis. J Immunol Res. 2014;2014:686879.
185. Sun W, Wei FQ, Li WJ, Wei JW, Zhong H, Wen YH, et al. A positive-feedback loop between tumour infiltrating activated Treg cells and type 2-skewed macrophages is essential for progression of laryngeal squamous cell carcinoma. Br J Cancer. 2017;117(11):1631-43.
186. Grizzi F, Bianchi P, Malesci A, Laghi L. Prognostic value of innate and adaptive immunity in colorectal cancer. World J Gastroenterol. 2013;19(2):174-84.
187. Jayasingam SD, Citartan M, Thang TH, Mat Zin AA, Ang KC, Ch'ng ES. Evaluating the Polarization of Tumor-Associated Macrophages Into M1 and M2 Phenotypes in Human Cancer Tissue: Technicalities and Challenges in Routine Clinical Practice. Front Oncol. 2019;9:1512.
188. Lan J, Sun L, Xu F, Liu L, Hu F, Song D, et al. M2 Macrophage-Derived Exosomes Promote Cell Migration and Invasion in Colon Cancer. Cancer research. 2019;79(1):146-58.
189. Oshi M, Tokumaru Y, Asaoka M, Yan L, Satyananda V, Matsuyama R, et al. M1 Macrophage and M1/M2 ratio defined by transcriptomic signatures resemble only part of their conventional clinical characteristics in breast cancer. Sci Rep. 2020;10(1):16554.
190. Diederichsen AC, Hjelmborg J, Christensen PB, Zeuthen J, Fenger C. Prognostic value of the CD4+/CD8+ ratio of tumour infiltrating lymphocytes in colorectal cancer and HLA-DR expression on tumour cells. Cancer Immunol Immunother. 2003;52(7):423-8.
191. Lalos A, Tulek A, Tosti N, Mechera R, Wilhelm A, Soysal S, et al. Prognostic significance of CD8+ T-cells density in stage III colorectal cancer depends on SDF-1 expression. Sci Rep. 2021;11(1):775.

192. Olguin JE, Medina-Andrade I, Rodriguez T, Rodriguez-Sosa M, Terrazas LI. Relevance of Regulatory T Cells during Colorectal Cancer Development. Cancers (Basel). 2020;12(7).
193. Aristin Revilla S, Kranenburg O, Coffer PJ. Colorectal Cancer-Infiltrating Regulatory T Cells: Functional Heterogeneity, Metabolic Adaptation, and Therapeutic Targeting. Front Immunol. 2022;13:903564.
194. Chen DS, Mellman I. Elements of cancer immunity and the cancer-immune set point. Nature. 2017;541(7637):321-30.
195. Goping IS, Barry M, Liston P, Sawchuk T, Constantinescu G, Michalak KM, et al. Granzyme B-induced apoptosis requires both direct caspase activation and relief of caspase inhibition. Immunity. 2003;18(3):355-65.
196. Brunner T, Wasem C, Torgler R, Cima I, Jakob S, Corazza N. Fas (CD95/Apo-1) ligand regulation in T cell homeostasis, cell-mediated cytotoxicity and immune pathology. Semin Immunol. 2003;15(3):167-76.
197. Folkman J. Tumor angiogenesis: therapeutic implications. N Engl J Med. 1971;285(21):1182-6.
198. Holmgren L, O'Reilly MS, Folkman J. Dormancy of micrometastases: balanced proliferation and apoptosis in the presence of angiogenesis suppression. Nat Med. 1995;1(2):149-53.
199. Parangi S, O'Reilly M, Christofori G, Holmgren L, Grosfeld J, Folkman J, et al. Antiangiogenic therapy of transgenic mice impairs de novo tumor growth. Proc Natl Acad Sci U S A. 1996;93(5):2002-7.
200. Baeriswyl V, Christofori G. The angiogenic switch in carcinogenesis. Semin Cancer Biol. 2009;19(5):329-37.
201. George ML, Tutton MG, Janssen F, Arnaout A, Abulafi AM, Eccles SA, et al. VEGF-A, VEGF-C, and VEGF-D in colorectal cancer progression. Neoplasia. 2001;3(5):420-7.
202. Liu Y, Tamimi RM, Collins LC, Schnitt SJ, Gilmore HL, Connolly JL, et al. The association between vascular endothelial growth factor expression in invasive breast cancer and survival varies with intrinsic subtypes and use of adjuvant systemic therapy: results from the Nurses' Health Study. Breast Cancer Res Treat. 2011;129(1):175-84.
203. Mezquita P, Parghi SS, Brandvold KA, Ruddell A. Myc regulates VEGF production in B cells by stimulating initiation of VEGF mRNA translation. Oncogene. 2005;24(5):889-901.
204. Zuazo-Gaztelu I, Casanovas O. Unraveling the Role of Angiogenesis in Cancer Ecosystems. Front Oncol. 2018;8:248.
205. Fagiani E, Christofori G. Angiopoietins in angiogenesis. Cancer letters. 2013;328(1):18-26.
206. Compagni A, Wilgenbus P, Impagnatiello MA, Cotten M, Christofori G. Fibroblast growth factors are required for efficient tumor angiogenesis. Cancer research. 2000;60(24):7163-9.
207. Ferrari G, Cook BD, Terushkin V, Pintucci G, Mignatti P. Transforming growth factor-beta 1 (TGF-beta1) induces angiogenesis through vascular endothelial growth factor (VEGF)-mediated apoptosis. J Cell Physiol. 2009;219(2):449-58.
208. Carmeliet P, Jain RK. Angiogenesis in cancer and other diseases. Nature. 2000;407(6801):249-57.

209. Carmeliet P. VEGF as a key mediator of angiogenesis in cancer. Oncology. 2005;69 Suppl 3:4-10.
210. Kim M, Jang K, Miller P, Picon-Ruiz M, Yeasky TM, El-Ashry D, et al. VEGFA links self-renewal and metastasis by inducing Sox2 to repress miR-452, driving Slug. Oncogene. 2017;36(36):5199-211.
211. Ferrara N, Hillan KJ, Novotny W. Bevacizumab (Avastin), a humanized anti-VEGF monoclonal antibody for cancer therapy. Biochem Biophys Res Commun. 2005;333(2):328-35.
212. Fares J, Fares MY, Khachfe HH, Salhab HA, Fares Y. Molecular principles of metastasis: a hallmark of cancer revisited. Signal Transduct Target Ther. 2020;5(1):28.
213. Steeg PS. Tumor metastasis: mechanistic insights and clinical challenges. Nat Med. 2006;12(8):895-904.
214. Pretzsch E, Bosch F, Neumann J, Ganschow P, Bazhin A, Guba M, et al. Mechanisms of Metastasis in Colorectal Cancer and Metastatic Organotropism: Hematogenous versus Peritoneal Spread. J Oncol. 2019;2019:7407190.
215. Pan Z, Peng J, Lin J, Chen G, Wu X, Lu Z, et al. Is there a survival benefit from adjuvant chemotherapy for patients with liver oligometastases from colorectal cancer after curative resection? Cancer Commun (Lond). 2018;38(1):29.
216. Franko J, Shi Q, Meyers JP, Maughan TS, Adams RA, Seymour MT, et al. Prognosis of patients with peritoneal metastatic colorectal cancer given systemic therapy: an analysis of individual patient data from prospective randomised trials from the Analysis and Research in Cancers of the Digestive System (ARCAD) database. Lancet Oncol. 2016;17(12):1709-19.
217. Paschos KA, Majeed AW, Bird NC. Natural history of hepatic metastases from colorectal cancer--pathobiological pathways with clinical significance. World J Gastroenterol. 2014;20(14):3719-37.
218. Valastyan S, Weinberg RA. Tumor metastasis: molecular insights and evolving paradigms. Cell. 2011;147(2):275-92.
219. Zwager LW, Bastiaansen BAJ, Montazeri NSM, Hompes R, Barresi V, Ichimasa K, et al. Deep Submucosal Invasion Is Not an Independent Risk Factor for Lymph Node Metastasis in T1 Colorectal Cancer: A Meta-Analysis. Gastroenterology. 2022;163(1):174-89.
220. Tateishi Y, Nakanishi Y, Taniguchi H, Shimoda T, Umemura S. Pathological prognostic factors predicting lymph node metastasis in submucosal invasive (T1) colorectal carcinoma. Mod Pathol. 2010;23(8):1068-72.
221. Cao H, Xu E, Liu H, Wan L, Lai M. Epithelial-mesenchymal transition in colorectal cancer metastasis: A system review. Pathol Res Pract. 2015;211(8):557-69.
222. Pena C, Garcia JM, Silva J, Garcia V, Rodriguez R, Alonso I, et al. E-cadherin and vitamin D receptor regulation by SNAIL and ZEB1 in colon cancer: clinicopathological correlations. Hum Mol Genet. 2005;14(22):3361-70.
223. He X, Chen Z, Jia M, Zhao X. Downregulated E-cadherin expression indicates worse prognosis in Asian patients with colorectal cancer: evidence from meta-analysis. PLoS One. 2013;8(7):e70858.

224. Dorudi S, Sheffield JP, Poulsom R, Northover JM, Hart IR. E-cadherin expression in colorectal cancer. An immunocytochemical and in situ hybridization study. The American journal of pathology. 1993;142(4):981-6.
225. Berx G, Strumane K, Comijn J, Van Roy F. E-cadherin controlling epithelial differentiation in human carcinomas. Nature Genetics. 2001;27(4):43-.
226. Liu CY, Lin HH, Tang MJ, Wang YK. Vimentin contributes to epithelial-mesenchymal transition cancer cell mechanics by mediating cytoskeletal organization and focal adhesion maturation. Oncotarget. 2015;6(18):15966-83.
227. Toiyama Y, Yasuda H, Saigusa S, Tanaka K, Inoue Y, Goel A, et al. Increased expression of Slug and Vimentin as novel predictive biomarkers for lymph node metastasis and poor prognosis in colorectal cancer. Carcinogenesis. 2013;34(11):2548-57.
228. Batlle E, Sancho E, Franci C, Dominguez D, Monfar M, Baulida J, et al. The transcription factor snail is a repressor of E-cadherin gene expression in epithelial tumour cells. Nat Cell Biol. 2000;2(2):84-9.
229. Comijn J, Berx G, Vermassen P, Verschueren K, van Grunsven L, Bruyneel E, et al. The two-handed E box binding zinc finger protein SIP1 downregulates E-cadherin and induces invasion. Mol Cell. 2001;7(6):1267-78.
230. Yang J, Mani SA, Donaher JL, Ramaswamy S, Itzykson RA, Come C, et al. Twist, a master regulator of morphogenesis, plays an essential role in tumor metastasis. Cell. 2004;117(7):927-39.
231. Amack JD. Cellular dynamics of EMT: lessons from live in vivo imaging of embryonic development. Cell Communication and Signaling. 2021;19(1):79.
232. Han X, Fang X, Lou X, Hua D, Ding W, Foltz G, et al. Silencing SOX2 induced mesenchymal-epithelial transition and its expression predicts liver and lymph node metastasis of CRC patients. PLoS One. 2012;7(8):e41335.
233. Dai X, Ge J, Wang X, Qian X, Zhang C, Li X. OCT4 regulates epithelial-mesenchymal transition and its knockdown inhibits colorectal cancer cell migration and invasion. Oncol Rep. 2013;29(1):155-60.
234. Stemmer V, de Craene B, Berx G, Behrens J. Snail promotes Wnt target gene expression and interacts with beta-catenin. Oncogene. 2008;27(37):5075-80.
235. Suman S, Kurisetty V, Das TP, Vadodkar A, Ramos G, Lakshmanaswamy R, et al. Activation of AKT signaling promotes epithelial-mesenchymal transition and tumor growth in colorectal cancer cells. Mol Carcinog. 2014;53 Suppl 1:E151-60.
236. Xiong H, Hong J, Du W, Lin YW, Ren LL, Wang YC, et al. Roles of STAT3 and ZEB1 proteins in E-cadherin down-regulation and human colorectal cancer epithelial-mesenchymal transition. J Biol Chem. 2012;287(8):5819-32.
237. Cottonham CL, Kaneko S, Xu L. miR-21 and miR-31 converge on TIAM1 to regulate migration and invasion of colon carcinoma cells. J Biol Chem. 2010;285(46):35293-302.
238. Gregory PA, Bert AG, Paterson EL, Barry SC, Tsykin A, Farshid G, et al. The miR-200 family and miR-205 regulate epithelial to mesenchymal transition by targeting ZEB1 and SIP1. Nat Cell Biol. 2008;10(5):593-601.
239. Wu J, Wu G, Lv L, Ren YF, Zhang XJ, Xue YF, et al. MicroRNA-34a inhibits migration and invasion of colon cancer cells via targeting to Fra-1. Carcinogenesis. 2012;33(3):519-28.

240. Karagiannis GS, Poutahidis T, Erdman SE, Kirsch R, Riddell RH, Diamandis EP. Cancer-associated fibroblasts drive the progression of metastasis through both paracrine and mechanical pressure on cancer tissue. Mol Cancer Res. 2012;10(11):1403-18.
241. Li Y, Wang L, Pappan L, Galliher-Beckley A, Shi J. IL-1beta promotes stemness and invasiveness of colon cancer cells through Zeb1 activation. Mol Cancer. 2012;11:87.
242. Cheng XS, Li YF, Tan J, Sun B, Xiao YC, Fang XB, et al. CCL20 and CXCL8 synergize to promote progression and poor survival outcome in patients with colorectal cancer by collaborative induction of the epithelial-mesenchymal transition. Cancer letters. 2014;348(1-2):77-87.
243. Rokavec M, Oner MG, Li H, Jackstadt R, Jiang L, Lodygin D, et al. IL-6R/STAT3/miR-34a feedback loop promotes EMT-mediated colorectal cancer invasion and metastasis. J Clin Invest. 2014;124(4):1853-67.
244. Prall F. Tumour budding in colorectal carcinoma. Histopathology. 2007;50(1):151-62.
245. Zlobec I, Lugli A. Epithelial mesenchymal transition and tumor budding in aggressive colorectal cancer: tumor budding as oncotarget. Oncotarget. 2010;1(7):651-61.
246. Guzińska-Ustymowicz K. MMP-9 and cathepsin B expression in tumor budding as an indicator of a more aggressive phenotype of colorectal cancer (CRC). Anticancer research. 2006;26(2b):1589-94.
247. Masaki T, Sugiyama M, Matsuoka H, Abe N, Izumisato Y, Sakamoto A, et al. Coexpression of matrilysin and laminin-5 gamma2 chain may contribute to tumor cell migration in colorectal carcinomas. Dig Dis Sci. 2003;48(7):1262-7.
248. Joyce JA, Pollard JW. Microenvironmental regulation of metastasis. Nat Rev Cancer. 2009;9(4):239-52.
249. Kim SH, Choi SJ, Park JS, Lee J, Cho YB, Kang MW, et al. Tropism between hepatic and pulmonary metastases in colorectal cancers. Oncol Rep. 2012;28(2):459-64.
250. Psaila B, Lyden D. The metastatic niche: adapting the foreign soil. Nat Rev Cancer. 2009;9(4):285-93.
251. van der Wath RC, Gardiner BS, Burgess AW, Smith DW. Cell organisation in the colonic crypt: a theoretical comparison of the pedigree and niche concepts. PLoS One. 2013;8(9):e73204.
252. Fanali C, Lucchetti D, Farina M, Corbi M, Cufino V, Cittadini A, et al. Cancer stem cells in colorectal cancer from pathogenesis to therapy: controversies and perspectives. World J Gastroenterol. 2014;20(4):923-42.
253. Barker N, Ridgway RA, van Es JH, van de Wetering M, Begthel H, van den Born M, et al. Crypt stem cells as the cells-of-origin of intestinal cancer. Nature. 2009;457(7229):608-11.
254. Merlos-Suarez A, Barriga FM, Jung P, Iglesias M, Cespedes MV, Rossell D, et al. The intestinal stem cell signature identifies colorectal cancer stem cells and predicts disease relapse. Cell Stem Cell. 2011;8(5):511-24.
255. Carmon KS, Gong X, Lin Q, Thomas A, Liu Q. R-spondins function as ligands of the orphan receptors LGR4 and LGR5 to regulate Wnt/beta-catenin signaling. Proc Natl Acad Sci U S A. 2011;108(28):11452-7.

256. Fan XS, Wu HY, Yu HP, Zhou Q, Zhang YF, Huang Q. Expression of Lgr5 in human colorectal carcinogenesis and its potential correlation with beta-catenin. Int J Colorectal Dis. 2010;25(5):583-90.
257. Wu XS, Xi HQ, Chen L. Lgr5 is a potential marker of colorectal carcinoma stem cells that correlates with patient survival. World J Surg Oncol. 2012;10:244.
258. de Sousa e Melo F, Kurtova AV, Harnoss JM, Kljavin N, Hoeck JD, Hung J, et al. A distinct role for Lgr5(+) stem cells in primary and metastatic colon cancer. Nature. 2017;543(7647):676-80.
259. Kobayashi S, Yamada-Okabe H, Suzuki M, Natori O, Kato A, Matsubara K, et al. LGR5-positive colon cancer stem cells interconvert with drug-resistant LGR5-negative cells and are capable of tumor reconstitution. Stem Cells. 2012;30(12):2631-44.
260. Barker N, van Es JH, Kuipers J, Kujala P, van den Born M, Cozijnsen M, et al. Identification of stem cells in small intestine and colon by marker gene Lgr5. Nature. 2007;449(7165):1003-7.
261. Shimokawa M, Ohta Y, Nishikori S, Matano M, Takano A, Fujii M, et al. Visualization and targeting of LGR5(+) human colon cancer stem cells. Nature. 2017;545(7653):187-92.
262. Hirsch D, Barker N, McNeil N, Hu Y, Camps J, McKinnon K, et al. LGR5 positivity defines stem-like cells in colorectal cancer. Carcinogenesis. 2014;35(4):849-58.
263. Barzegar Behrooz A, Syahir A, Ahmad S. CD133: beyond a cancer stem cell biomarker. J Drug Target. 2019;27(3):257-69.
264. O'Brien CA, Pollett A, Gallinger S, Dick JE. A human colon cancer cell capable of initiating tumour growth in immunodeficient mice. Nature. 2007;445(7123):106-10.
265. Yin AH, Miraglia S, Zanjani ED, Almeida-Porada G, Ogawa M, Leary AG, et al. AC133, a novel marker for human hematopoietic stem and progenitor cells. Blood. 1997;90(12):5002-12.
266. Ricci-Vitiani L, Lombardi DG, Pilozzi E, Biffoni M, Todaro M, Peschle C, et al. Identification and expansion of human colon-cancer-initiating cells. Nature. 2007;445(7123):111-5.
267. Fang DD, Kim YJ, Lee CN, Aggarwal S, McKinnon K, Mesmer D, et al. Expansion of CD133(+) colon cancer cultures retaining stem cell properties to enable cancer stem cell target discovery. Br J Cancer. 2010;102(8):1265-75.
268. Mak AB, Nixon AM, Kittanakom S, Stewart JM, Chen GI, Curak J, et al. Regulation of CD133 by HDAC6 promotes beta-catenin signaling to suppress cancer cell differentiation. Cell Rep. 2012;2(4):951-63.
269. Wei Y, Jiang Y, Zou F, Liu Y, Wang S, Xu N, et al. Activation of PI3K/Akt pathway by CD133-p85 interaction promotes tumorigenic capacity of glioma stem cells. Proc Natl Acad Sci U S A. 2013;110(17):6829-34.
270. Adini A, Adini I, Ghosh K, Benny O, Pravda E, Hu R, et al. The stem cell marker prominin-1/CD133 interacts with vascular endothelial growth factor and potentiates its action. Angiogenesis. 2013;16(2):405-16.
271. Ding Q, Miyazaki Y, Tsukasa K, Matsubara S, Yoshimitsu M, Takao S. CD133 facilitates epithelial-mesenchymal transition through interaction with the ERK pathway in pancreatic cancer metastasis. Mol Cancer. 2014;13:15.

272. Chen KL, Pan F, Jiang H, Chen JF, Pei L, Xie FW, et al. Highly enriched CD133(+)CD44(+) stem-like cells with CD133(+)CD44(high) metastatic subset in HCT116 colon cancer cells. Clin Exp Metastasis. 2011;28(8):751-63.
273. Su YJ, Lai HM, Chang YW, Chen GY, Lee JL. Direct reprogramming of stem cell properties in colon cancer cells by CD44. EMBO J. 2011;30(15):3186-99.
274. Subramaniam V, Vincent IR, Gardner H, Chan E, Dhamko H, Jothy S. CD44 regulates cell migration in human colon cancer cells via Lyn kinase and AKT phosphorylation. Exp Mol Pathol. 2007;83(2):207-15.
275. Rezaee M, Gheytanchi E, Madjd Z, Mehrazma M. Clinicopathological Significance of Tumor Stem Cell Markers ALDH1 and CD133 in Colorectal Carcinoma. Iran J Pathol. 2021;16(1):40-50.
276. Yin H, Gao T, Xie J, Huang Z, Zhang X, Yang F, et al. FUBP1 promotes colorectal cancer stemness and metastasis via DVL1-mediated activation of Wnt/beta-catenin signaling. Molecular oncology. 2021;15(12):3490-512.
277. Tan X, Zhang Z, Yao H, Shen L. Tim-4 promotes the growth of colorectal cancer by activating angiogenesis and recruiting tumor-associated macrophages via the PI3K/AKT/mTOR signaling pathway. Cancer letters. 2018;436:119-28.
278. Duan JJ, Wang D, Cai J, Chen JJ, Zheng XX, Chen TQ, et al. An aldehyde dehydrogenase 1A3 inhibitor attenuates the metastasis of human colorectal cancer. Cancer letters. 2022;536:215662.
279. Phi LTH, Sari IN, Yang YG, Lee SH, Jun N, Kim KS, et al. Cancer Stem Cells (CSCs) in Drug Resistance and their Therapeutic Implications in Cancer Treatment. Stem Cells Int. 2018;2018:5416923.
280. Kreso A, O'Brien CA, van Galen P, Gan OI, Notta F, Brown AM, et al. Variable clonal repopulation dynamics influence chemotherapy response in colorectal cancer. Science. 2013;339(6119):543-8.
281. Hirschmann-Jax C, Foster AE, Wulf GG, Nuchtern JG, Jax TW, Gobel U, et al. A distinct "side population" of cells with high drug efflux capacity in human tumor cells. Proc Natl Acad Sci U S A. 2004;101(39):14228-33.
282. Ishimoto T, Nagano O, Yae T, Tamada M, Motohara T, Oshima H, et al. CD44 variant regulates redox status in cancer cells by stabilizing the xCT subunit of system xc(-) and thereby promotes tumor growth. Cancer Cell. 2011;19(3):387-400.
283. Rausch V, Liu L, Apel A, Rettig T, Gladkich J, Labsch S, et al. Autophagy mediates survival of pancreatic tumour-initiating cells in a hypoxic microenvironment. J Pathol. 2012;227(3):325-35.
284. Majumdar SR, Fletcher RH, Evans AT. How does colorectal cancer present? Symptoms, duration, and clues to location. Am J Gastroenterol. 1999;94(10):3039-45.
285. Baran B, Mert Ozupek N, Yerli Tetik N, Acar E, Bekcioglu O, Baskin Y. Difference Between Left-Sided and Right-Sided Colorectal Cancer: A Focused Review of Literature. Gastroenterology Res. 2018;11(4):264-73.
286. Valori R, Rey JF, Atkin WS, Bretthauer M, Senore C, Hoff G, et al. European guidelines for quality assurance in colorectal cancer screening and diagnosis. First Edition--Quality assurance in endoscopy in colorectal cancer screening and diagnosis. Endoscopy. 2012;44 Suppl 3:SE88-105.

287. Cunningham D, Atkin W, Lenz HJ, Lynch HT, Minsky B, Nordlinger B, et al. Colorectal cancer. Lancet (London, England). 2010;375(9719):1030-47.
288. Halloran SP, Launoy G, Zappa M, International Agency for Research on C. European guidelines for quality assurance in colorectal cancer screening and diagnosis. First Edition--Faecal occult blood testing. Endoscopy. 2012;44 Suppl 3:SE65-87.
289. Smith RA, Andrews KS, Brooks D, Fedewa SA, Manassaram-Baptiste D, Saslow D, et al. Cancer screening in the United States, 2019: A review of current American Cancer Society guidelines and current issues in cancer screening. CA Cancer J Clin. 2019;69(3):184-210.
290. Labianca R, Nordlinger B, Beretta GD, Mosconi S, Mandala M, Cervantes A, et al. Early colon cancer: ESMO Clinical Practice Guidelines for diagnosis, treatment and follow-up. Ann Oncol. 2013;24 Suppl 6:vi64-72.
291. Rosen RD SA. TNM Classification. StatPearls Publishing2022.
292. Hayashi N, Tanaka S, Hewett DG, Kaltenbach TR, Sano Y, Ponchon T, et al. Endoscopic prediction of deep submucosal invasive carcinoma: validation of the narrow-band imaging international colorectal endoscopic (NICE) classification. Gastrointest Endosc. 2013;78(4):625-32.
293. Sano Y, Tanaka S, Kudo SE, Saito S, Matsuda T, Wada Y, et al. Narrow-band imaging (NBI) magnifying endoscopic classification of colorectal tumors proposed by the Japan NBI Expert Team. Dig Endosc. 2016;28(5):526-33.
294. Backes Y, Schwartz MP, Ter Borg F, Wolfhagen FHJ, Groen JN, de Vos Tot Nederveen Cappel WH, et al. Multicentre prospective evaluation of real-time optical diagnosis of T1 colorectal cancer in large non-pedunculated colorectal polyps using narrow band imaging (the OPTICAL study). Gut. 2019;68(2):271-9.
295. Rodriguez-Bigas MA LE, Crane CH. Surgical Management of Colorectal Cancer. 6th ed2003.
296. American Cancer Society. Radiation Therapy for Colorectal Cancer [Internet] 2023 [Accesed on 30.01.22] Available from: https://www.cancer.org/cancer/colon-rectal-cancer/treating/radiation-therapy.htm.
297. Masui K, Gini B, Wykosky J, Zanca C, Mischel PS, Furnari FB, et al. A tale of two approaches: complementary mechanisms of cytotoxic and targeted therapy resistance may inform next-generation cancer treatments. Carcinogenesis. 2013;34(4):725-38.
298. Martino R, Gilard V, Desmoulin F, Malet-Martino M. Fluorine-19 or phosphorus-31 NMR spectroscopy: A suitable analytical technique for quantitative in vitro metabolic studies of fluorinated or phosphorylated drugs. Journal of Pharmaceutical and Biomedical Analysis. 2005;38(5):871-91.
299. Xie P, Mo JL, Liu JH, Li X, Tan LM, Zhang W, et al. Pharmacogenomics of 5-fluorouracil in colorectal cancer: review and update. Cell Oncol (Dordr). 2020;43(6):989-1001.
300. Twelves C, Wong A, Nowacki MP, Abt M, Burris H, 3rd, Carrato A, et al. Capecitabine as adjuvant treatment for stage III colon cancer. N Engl J Med. 2005;352(26):2696-704.
301. Andre T, Boni C, Mounedji-Boudiaf L, Navarro M, Tabernero J, Hickish T, et al. Oxaliplatin, fluorouracil, and leucovorin as adjuvant treatment for colon cancer. N Engl J Med. 2004;350(23):2343-51.

302. Andre T, Boni C, Navarro M, Tabernero J, Hickish T, Topham C, et al. Improved overall survival with oxaliplatin, fluorouracil, and leucovorin as adjuvant treatment in stage II or III colon cancer in the MOSAIC trial. J Clin Oncol. 2009;27(19):3109-16.
303. Pardini B, Kumar R, Naccarati A, Novotny J, Prasad RB, Forsti A, et al. 5-Fluorouracil-based chemotherapy for colorectal cancer and MTHFR/MTRR genotypes. Br J Clin Pharmacol. 2011;72(1):162-3.
304. Modulation of fluorouracil by leucovorin in patients with advanced colorectal cancer: evidence in terms of response rate. Advanced Colorectal Cancer Meta-Analysis Project. J Clin Oncol. 1992;10(6):896-903.
305. Comella P, Casaretti R, De Vita F, Avallone A, Orditura M, Petrillo A, et al. Concurrent irinotecan and 5-fluorouracil plus levo-folinic acid given every other week in the first-line management of advanced colorectal carcinoma: a phase I study of the Southern Italy Cooperative Oncology Group. Ann Oncol. 1999;10(8):915-21.
306. Goodman M. Managing the side effects of chemotherapy. Semin Oncol Nurs. 1989;5(2 Suppl 1):29-52.
307. Bohlius J, Bohlke K, Castelli R, Djulbegovic B, Lustberg MB, Martino M, et al. Management of Cancer-Associated Anemia With Erythropoiesis-Stimulating Agents: ASCO/ASH Clinical Practice Guideline Update. J Clin Oncol. 2019;37(15):1336-51.
308. Hurwitz H, Fehrenbacher L, Novotny W, Cartwright T, Hainsworth J, Heim W, et al. Bevacizumab plus irinotecan, fluorouracil, and leucovorin for metastatic colorectal cancer. N Engl J Med. 2004;350(23):2335-42.
309. Fantini MC, Guadagni I. From inflammation to colitis-associated colorectal cancer in inflammatory bowel disease: Pathogenesis and impact of current therapies. Dig Liver Dis. 2021;53(5):558-65.
310. Coussens LM, Werb Z. Inflammation and cancer. Nature. 2002;420(6917):860-7.
311. Terzic J, Grivennikov S, Karin E, Karin M. Inflammation and colon cancer. Gastroenterology. 2010;138(6):2101-14 e5.
312. Dobbins WO, 3rd. Dysplasia and malignancy in inflammatory bowel disease. Annu Rev Med. 1984;35:33-48.
313. Canavan C, Abrams KR, Mayberry J. Meta-analysis: colorectal and small bowel cancer risk in patients with Crohn's disease. Aliment Pharmacol Ther. 2006;23(8):1097-104.
314. Laukoetter MG, Mennigen R, Hannig CM, Osada N, Rijcken E, Vowinkel T, et al. Intestinal cancer risk in Crohn's disease: a meta-analysis. J Gastrointest Surg. 2011;15(4):576-83.
315. O'Connor PM, Lapointe TK, Beck PL, Buret AG. Mechanisms by which inflammation may increase intestinal cancer risk in inflammatory bowel disease. Inflamm Bowel Dis. 2010;16(8):1411-20.
316. Long AG, Lundsmith ET, Hamilton KE. Inflammation and Colorectal Cancer. Curr Colorectal Cancer Rep. 2017;13(4):341-51.
317. Rieder F, Fiocchi C. Mechanisms of tissue remodeling in inflammatory bowel disease. Dig Dis. 2013;31(2):186-93.
318. Vetrano S, Danese S. Colitis, microbiota, and colon cancer: an infernal triangle. Gastroenterology. 2013;144(2):461-3.

319. Souici AC, Mirkovitch J, Hausel P, Keefer LK, Felley-Bosco E. Transition mutation in codon 248 of the p53 tumor suppressor gene induced by reactive oxygen species and a nitric oxide-releasing compound. Carcinogenesis. 2000;21(2):281-7.
320. Brentnall TA, Crispin DA, Rabinovitch PS, Haggitt RC, Rubin CE, Stevens AC, et al. Mutations in the p53 gene: an early marker of neoplastic progression in ulcerative colitis. Gastroenterology. 1994;107(2):369-78.
321. Itzkowitz SH. Molecular biology of dysplasia and cancer in inflammatory bowel disease. Gastroenterol Clin North Am. 2006;35(3):553-71.
322. Matsumoto S, Hara T, Mitsuyama K, Yamamoto M, Tsuruta O, Sata M, et al. Essential roles of IL-6 trans-signaling in colonic epithelial cells, induced by the IL-6/soluble-IL-6 receptor derived from lamina propria macrophages, on the development of colitis-associated premalignant cancer in a murine model. J Immunol. 2010;184(3):1543-51.
323. Karin M, Lin A. NF-kappaB at the crossroads of life and death. Nat Immunol. 2002;3(3):221-7.
324. Karin M, Greten FR. NF-kappaB: linking inflammation and immunity to cancer development and progression. Nat Rev Immunol. 2005;5(10):749-59.
325. Singer, II, Kawka DW, Schloemann S, Tessner T, Riehl T, Stenson WF. Cyclooxygenase 2 is induced in colonic epithelial cells in inflammatory bowel disease. Gastroenterology. 1998;115(2):297-306.
326. Wang D, Dubois RN. The role of COX-2 in intestinal inflammation and colorectal cancer. Oncogene. 2010;29(6):781-8.
327. Jobin C, Morteau O, Han DS, Balfour Sartor R. Specific NF-kappaB blockade selectively inhibits tumour necrosis factor-alpha-induced COX-2 but not constitutive COX-1 gene expression in HT-29 cells. Immunology. 1998;95(4):537-43.
328. Hamoya T, Fujii G, Miyamoto S, Takahashi M, Totsuka Y, Wakabayashi K, et al. Effects of NSAIDs on the risk factors of colorectal cancer: a mini review. Genes Environ. 2016;38:6.
329. Kawamori T, Uchiya N, Sugimura T, Wakabayashi K. Enhancement of colon carcinogenesis by prostaglandin E2 administration. Carcinogenesis. 2003;24(5):985-90.
330. Wang D, Buchanan FG, Wang H, Dey SK, DuBois RN. Prostaglandin E2 enhances intestinal adenoma growth via activation of the Ras-mitogen-activated protein kinase cascade. Cancer research. 2005;65(5):1822-9.
331. Castellone MD, Teramoto H, Williams BO, Druey KM, Gutkind JS. Prostaglandin E2 promotes colon cancer cell growth through a Gs-axin-beta-catenin signaling axis. Science. 2005;310(5753):1504-10.
332. Sheng H, Shao J, Morrow JD, Beauchamp RD, DuBois RN. Modulation of apoptosis and Bcl-2 expression by prostaglandin E2 in human colon cancer cells. Cancer research. 1998;58(2):362-6.
333. Buchanan FG, Wang D, Bargiacchi F, DuBois RN. Prostaglandin E2 regulates cell migration via the intracellular activation of the epidermal growth factor receptor. J Biol Chem. 2003;278(37):35451-7.
334. Ito H, Duxbury M, Benoit E, Clancy TE, Zinner MJ, Ashley SW, et al. Prostaglandin E2 enhances pancreatic cancer invasiveness through an Ets-1-

dependent induction of matrix metalloproteinase-2. Cancer research. 2004;64(20):7439-46.
335. Wang D, DuBois RN. An inflammatory mediator, prostaglandin E2, in colorectal cancer. Cancer J. 2013;19(6):502-10.
336. Erreni M, Mantovani A, Allavena P. Tumor-associated Macrophages (TAM) and Inflammation in Colorectal Cancer. Cancer Microenviron. 2011;4(2):141-54.
337. Waldner MJ, Neurath MF. Colitis-associated cancer: the role of T cells in tumor development. Semin Immunopathol. 2009;31(2):249-56.
338. Nishimura T, Iwakabe K, Sekimoto M, Ohmi Y, Yahata T, Nakui M, et al. Distinct role of antigen-specific T helper type 1 (Th1) and Th2 cells in tumor eradication in vivo. J Exp Med. 1999;190(5):617-27.
339. De Simone V, Pallone F, Monteleone G, Stolfi C. Role of T(H)17 cytokines in the control of colorectal cancer. Oncoimmunology. 2013;2(12):e26617.
340. Ahern PP, Izcue A, Maloy KJ, Powrie F. The interleukin-23 axis in intestinal inflammation. Immunol Rev. 2008;226:147-59.
341. Maloy KJ, Kullberg MC. IL-23 and Th17 cytokines in intestinal homeostasis. Mucosal Immunol. 2008;1(5):339-49.
342. Langowski JL, Zhang X, Wu L, Mattson JD, Chen T, Smith K, et al. IL-23 promotes tumour incidence and growth. Nature. 2006;442(7101):461-5.
343. Grivennikov SI, Wang K, Mucida D, Stewart CA, Schnabl B, Jauch D, et al. Adenoma-linked barrier defects and microbial products drive IL-23/IL-17-mediated tumour growth. Nature. 2012;491(7423):254-8.
344. Nie W, Yu T, Sang Y, Gao X. Tumor-promoting effect of IL-23 in mammary cancer mediated by infiltration of M2 macrophages and neutrophils in tumor microenvironment. Biochem Biophys Res Commun. 2017;482(4):1400-6.
345. Bardou M, Barkun AN, Martel M. Obesity and colorectal cancer. Gut. 2013;62(6):933-47.
346. Larsson SC, Wolk A. Obesity and colon and rectal cancer risk: a meta-analysis of prospective studies. Am J Clin Nutr. 2007;86(3):556-65.
347. Cespedes Feliciano EM, Kroenke CH, Meyerhardt JA, Prado CM, Bradshaw PT, Dannenberg AJ, et al. Metabolic Dysfunction, Obesity, and Survival Among Patients With Early-Stage Colorectal Cancer. J Clin Oncol. 2016;34(30):3664-71.
348. Jensen BW, Bjerregaard LG, Angquist L, Gogenur I, Renehan AG, Osler M, et al. Change in weight status from childhood to early adulthood and late adulthood risk of colon cancer in men: a population-based cohort study. Int J Obes (Lond). 2018;42(10):1797-803.
349. Collaboration NCDRF. Worldwide trends in body-mass index, underweight, overweight, and obesity from 1975 to 2016: a pooled analysis of 2416 population-based measurement studies in 128.9 million children, adolescents, and adults. Lancet (London, England). 2017;390(10113):2627-42.
350. Ouchi N, Parker JL, Lugus JJ, Walsh K. Adipokines in inflammation and metabolic disease. Nat Rev Immunol. 2011;11(2):85-97.
351. Iyengar NM, Gucalp A, Dannenberg AJ, Hudis CA. Obesity and Cancer Mechanisms: Tumor Microenvironment and Inflammation. J Clin Oncol. 2016;34(35):4270-6.

352. Hursting SD, Digiovanni J, Dannenberg AJ, Azrad M, Leroith D, Demark-Wahnefried W, et al. Obesity, energy balance, and cancer: new opportunities for prevention. Cancer Prev Res (Phila). 2012;5(11):1260-72.
353. Bhat MI, Kapila R. Dietary metabolites derived from gut microbiota: critical modulators of epigenetic changes in mammals. Nutr Rev. 2017;75(5):374-89.
354. Rajagopalan H, Bardelli A, Lengauer C, Kinzler KW, Vogelstein B, Velculescu VE. Tumorigenesis: RAF/RAS oncogenes and mismatch-repair status. Nature. 2002;418(6901):934.
355. Park S, An J, Ha SY, Nam S, Kim JH. Immune signature as a potential marker for predicting response to immunotherapy in obesity-associated colorectal cancer. J Gastroenterol Hepatol. 2022;37(8):1579-87.
356. Furukawa S, Fujita T, Shimabukuro M, Iwaki M, Yamada Y, Nakajima Y, et al. Increased oxidative stress in obesity and its impact on metabolic syndrome. J Clin Invest. 2004;114(12):1752-61.
357. Skrzydlewska E, Sulkowski S, Koda M, Zalewski B, Kanczuga-Koda L, Sulkowska M. Lipid peroxidation and antioxidant status in colorectal cancer. World J Gastroenterol. 2005;11(3):403-6.
358. Mukai FH, Goldstein BD. Mutagenicity of malonaldehyde, a decomposition product of peroxidized polyunsaturated fatty acids. Science. 1976;191(4229):868-9.
359. Zhong H, Yin H. Role of lipid peroxidation derived 4-hydroxynonenal (4-HNE) in cancer: focusing on mitochondria. Redox Biol. 2015;4:193-9.
360. Ji Y, Dai Z, Wu G, Wu Z. 4-Hydroxy-2-nonenal induces apoptosis by activating ERK1/2 signaling and depleting intracellular glutathione in intestinal epithelial cells. Sci Rep. 2016;6:32929.
361. Uchida K, Kumagai T. 4-hydroxy-2-nonenal as a COX-2 inducer. Mol Aspects Med. 2003;24(4-5):213-8.
362. Sharma RA, Gescher A, Plastaras JP, Leuratti C, Singh R, Gallacher-Horley B, et al. Cyclooxygenase-2, malondialdehyde and pyrimidopurinone adducts of deoxyguanosine in human colon cells. Carcinogenesis. 2001;22(9):1557-60.
363. Wang D, Fu L, Sun H, Guo L, DuBois RN. Prostaglandin E2 Promotes Colorectal Cancer Stem Cell Expansion and Metastasis in Mice. Gastroenterology. 2015;149(7):1884-95 e4.
364. Zarrouki B, Soares AF, Guichardant M, Lagarde M, Geloen A. The lipid peroxidation end-product 4-HNE induces COX-2 expression through p38MAPK activation in 3T3-L1 adipose cell. FEBS Lett. 2007;581(13):2394-400.
365. Despres JP, Lemieux I. Abdominal obesity and metabolic syndrome. Nature. 2006;444(7121):881-7.
366. Esposito K, Chiodini P, Colao A, Lenzi A, Giugliano D. Metabolic syndrome and risk of cancer: a systematic review and meta-analysis. Diabetes Care. 2012;35(11):2402-11.
367. Brunner JE, Johnson CC, Zafar S, Peterson EL, Brunner JF, Mellinger RC. Colon cancer and polyps in acromegaly: increased risk associated with family history of colon cancer. Clin Endocrinol (Oxf). 1990;32(1):65-71.
368. Deng L, Gui Z, Zhao L, Wang J, Shen L. Diabetes mellitus and the incidence of colorectal cancer: an updated systematic review and meta-analysis. Dig Dis Sci. 2012;57(6):1576-85.

369. Zorena K, Jachimowicz-Duda O, Slezak D, Robakowska M, Mrugacz M. Adipokines and Obesity. Potential Link to Metabolic Disorders and Chronic Complications. Int J Mol Sci. 2020;21(10).
370. Divella R, De Luca R, Abbate I, Naglieri E, Daniele A. Obesity and cancer: the role of adipose tissue and adipo-cytokines-induced chronic inflammation. J Cancer. 2016;7(15):2346-59.
371. Yamaji T, Iwasaki M, Sasazuki S, Tsugane S. Interaction between adiponectin and leptin influences the risk of colorectal adenoma. Cancer research. 2010;70(13):5430-7.
372. Lu W, Huang Z, Li N, Liu H. Low circulating total adiponectin, especially its non-high-molecular weight fraction, represents a promising risk factor for colorectal cancer: a meta-analysis. Onco Targets Ther. 2018;11:2519-31.
373. Czech MP. Insulin action and resistance in obesity and type 2 diabetes. Nat Med. 2017;23(7):804-14.
374. Pollak MN, Schernhammer ES, Hankinson SE. Insulin-like growth factors and neoplasia. Nat Rev Cancer. 2004;4(7):505-18.
375. Miyamoto S, Yasui Y, Tanaka T, Ohigashi H, Murakami A. Suppressive effects of nobiletin on hyperleptinemia and colitis-related colon carcinogenesis in male ICR mice. Carcinogenesis. 2008;29(5):1057-63.
376. Wang D, Chen J, Chen H, Duan Z, Xu Q, Wei M, et al. Leptin regulates proliferation and apoptosis of colorectal carcinoma through PI3K/Akt/mTOR signalling pathway. J Biosci. 2012;37(1):91-101.
377. Jiang K, Chen B, Lou D, Zhang M, Shi Y, Dai W, et al. Systematic review and meta-analysis: association between obesity/overweight and surgical complications in IBD. Int J Colorectal Dis. 2022;37(7):1485-96.
378. Singh S, Dulai PS, Zarrinpar A, Ramamoorthy S, Sandborn WJ. Obesity in IBD: epidemiology, pathogenesis, disease course and treatment outcomes. Nat Rev Gastroenterol Hepatol. 2017;14(2):110-21.
379. Bilski J, Mazur-Bialy A, Wojcik D, Surmiak M, Magierowski M, Sliwowski Z, et al. Role of Obesity, Mesenteric Adipose Tissue, and Adipokines in Inflammatory Bowel Diseases. Biomolecules. 2019;9(12).
380. Shah SC, Itzkowitz SH. Colorectal Cancer in Inflammatory Bowel Disease: Mechanisms and Management. Gastroenterology. 2022;162(3):715-30 e3.
381. Coppack SW. Pro-inflammatory cytokines and adipose tissue. Proc Nutr Soc. 2001;60(3):349-56.
382. Wunderlich CM, Ackermann PJ, Ostermann AL, Adams-Quack P, Vogt MC, Tran ML, et al. Obesity exacerbates colitis-associated cancer via IL-6-regulated macrophage polarisation and CCL-20/CCR-6-mediated lymphocyte recruitment. Nat Commun. 2018;9(1):1646.
383. Rinninella E, Raoul P, Cintoni M, Franceschi F, Miggiano GAD, Gasbarrini A, et al. What is the Healthy Gut Microbiota Composition? A Changing Ecosystem across Age, Environment, Diet, and Diseases. Microorganisms. 2019;7(1).
384. Valdes AM, Walter J, Segal E, Spector TD. Role of the gut microbiota in nutrition and health. BMJ. 2018;361:k2179.

385. Castaner O, Goday A, Park YM, Lee SH, Magkos F, Shiow STE, et al. The Gut Microbiome Profile in Obesity: A Systematic Review. Int J Endocrinol. 2018;2018:4095789.
386. Turnbaugh PJ, Hamady M, Yatsunenko T, Cantarel BL, Duncan A, Ley RE, et al. A core gut microbiome in obese and lean twins. Nature. 2009;457(7228):480-4.
387. Turnbaugh PJ, Ley RE, Mahowald MA, Magrini V, Mardis ER, Gordon JI. An obesity-associated gut microbiome with increased capacity for energy harvest. Nature. 2006;444(7122):1027-31.
388. Ley RE, Turnbaugh PJ, Klein S, Gordon JI. Microbial ecology: human gut microbes associated with obesity. Nature. 2006;444(7122):1022-3.
389. Palmas V, Pisanu S, Madau V, Casula E, Deledda A, Cusano R, et al. Gut microbiota markers associated with obesity and overweight in Italian adults. Sci Rep. 2021;11(1):5532.
390. Gomes AC, Hoffmann C, Mota JF. The human gut microbiota: Metabolism and perspective in obesity. Gut Microbes. 2018;9(4):308-25.
391. Jin J, Cheng R, Ren Y, Shen X, Wang J, Xue Y, et al. Distinctive Gut Microbiota in Patients with Overweight and Obesity with Dyslipidemia and its Responses to Long-term Orlistat and Ezetimibe Intervention: A Randomized Controlled Open-label Trial. Front Pharmacol. 2021;12:732541.
392. Genser L, Aguanno D, Soula HA, Dong L, Trystram L, Assmann K, et al. Increased jejunal permeability in human obesity is revealed by a lipid challenge and is linked to inflammation and type 2 diabetes. J Pathol. 2018;246(2):217-30.
393. Radilla-Vazquez RB, Parra-Rojas I, Martinez-Hernandez NE, Marquez-Sandoval YF, Illades-Aguiar B, Castro-Alarcon N. Gut Microbiota and Metabolic Endotoxemia in Young Obese Mexican Subjects. Obes Facts. 2016;9(1):1-11.
394. Cani PD, Amar J, Iglesias MA, Poggi M, Knauf C, Bastelica D, et al. Metabolic endotoxemia initiates obesity and insulin resistance. Diabetes. 2007;56(7):1761-72.
395. Cani PD, Bibiloni R, Knauf C, Waget A, Neyrinck AM, Delzenne NM, et al. Changes in gut microbiota control metabolic endotoxemia-induced inflammation in high-fat diet-induced obesity and diabetes in mice. Diabetes. 2008;57(6):1470-81.
396. Guarner F, Malagelada JR. Gut flora in health and disease. Lancet (London, England). 2003;361(9356):512-9.
397. Coleman OI, Nunes T. Role of the Microbiota in Colorectal Cancer: Updates on Microbial Associations and Therapeutic Implications. Biores Open Access. 2016;5(1):279-88.
398. Song M, Chan AT, Sun J. Influence of the Gut Microbiome, Diet, and Environment on Risk of Colorectal Cancer. Gastroenterology. 2020;158(2):322-40.
399. Mori G, Rampelli S, Orena BS, Rengucci C, De Maio G, Barbieri G, et al. Shifts of Faecal Microbiota During Sporadic Colorectal Carcinogenesis. Sci Rep. 2018;8(1):10329.
400. Flemer B, Lynch DB, Brown JM, Jeffery IB, Ryan FJ, Claesson MJ, et al. Tumour-associated and non-tumour-associated microbiota in colorectal cancer. Gut. 2017;66(4):633-43.

401. Ahn J, Sinha R, Pei Z, Dominianni C, Wu J, Shi J, et al. Human gut microbiome and risk for colorectal cancer. J Natl Cancer Inst. 2013;105(24):1907-11.
402. Feng Q, Liang S, Jia H, Stadlmayr A, Tang L, Lan Z, et al. Gut microbiome development along the colorectal adenoma-carcinoma sequence. Nat Commun. 2015;6:6528.
403. Gao Z, Guo B, Gao R, Zhu Q, Qin H. Microbiota disbiosis is associated with colorectal cancer. Front Microbiol. 2015;6:20.
404. Kelly D, Yang L, Pei Z. Gut Microbiota, Fusobacteria, and Colorectal Cancer. Diseases. 2018;6(4).
405. Rebersek M. Gut microbiome and its role in colorectal cancer. BMC Cancer. 2021;21(1):1325.
406. Hou H, Chen D, Zhang K, Zhang W, Liu T, Wang S, et al. Gut microbiota-derived short-chain fatty acids and colorectal cancer: Ready for clinical translation? Cancer Lett. 2022;526:225-35.
407. Yachida S, Mizutani S, Shiroma H, Shiba S, Nakajima T, Sakamoto T, et al. Metagenomic and metabolomic analyses reveal distinct stage-specific phenotypes of the gut microbiota in colorectal cancer. Nat Med. 2019;25(6):968-76.
408. Tjalsma H, Boleij A, Marchesi JR, Dutilh BE. A bacterial driver-passenger model for colorectal cancer: beyond the usual suspects. Nat Rev Microbiol. 2012;10(8):575-82.
409. Tjalsma H, Boleij A. Subtyping of Streptococcus bovis group bacteria is needed to fully understand the clinical value of Streptococcus gallolyticus (S. bovis biotype I) infection as early sign of colonic malignancy. Int J Clin Pract. 2012;66(3):326.
410. Marchesi JR, Dutilh BE, Hall N, Peters WH, Roelofs R, Boleij A, et al. Towards the human colorectal cancer microbiome. PLoS One. 2011;6(5):e20447.
411. Abdulamir AS, Hafidh RR, Bakar FA. Molecular detection, quantification, and isolation of Streptococcus gallolyticus bacteria colonizing colorectal tumors: inflammation-driven potential of carcinogenesis via IL-1, COX-2, and IL-8. Mol Cancer. 2010;9:249.
412. Zhou Z, Chen J, Yao H, Hu H. Fusobacterium and Colorectal Cancer. Front Oncol. 2018;8:371.
413. Rubinstein MR, Wang X, Liu W, Hao Y, Cai G, Han YW. Fusobacterium nucleatum promotes colorectal carcinogenesis by modulating E-cadherin/beta-catenin signaling via its FadA adhesin. Cell Host Microbe. 2013;14(2):195-206.
414. Bullman S, Pedamallu CS, Sicinska E, Clancy TE, Zhang X, Cai D, et al. Analysis of Fusobacterium persistence and antibiotic response in colorectal cancer. Science. 2017;358(6369):1443-8.
415. Zamani S, Taslimi R, Sarabi A, Jasemi S, Sechi LA, Feizabadi MM. Enterotoxigenic Bacteroides fragilis: A Possible Etiological Candidate for Bacterially-Induced Colorectal Precancerous and Cancerous Lesions. Front Cell Infect Microbiol. 2019;9:449.
416. Ignacio A, Fernandes MR, Rodrigues VA, Groppo FC, Cardoso AL, Avila-Campos MJ, et al. Correlation between body mass index and faecal microbiota from children. Clin Microbiol Infect. 2016;22(3):258 e1-8.

417. Wu S, Rhee KJ, Albesiano E, Rabizadeh S, Wu X, Yen HR, et al. A human colonic commensal promotes colon tumorigenesis via activation of T helper type 17 T cell responses. Nat Med. 2009;15(9):1016-22.
418. Campisciano G, de Manzini N, Delbue S, Cason C, Cosola D, Basile G, et al. The Obesity-Related Gut Bacterial and Viral Dysbiosis Can Impact the Risk of Colon Cancer Development. Microorganisms. 2020;8(3).
419. Sanchez-Alcoholado L, Ordonez R, Otero A, Plaza-Andrade I, Laborda-Illanes A, Medina JA, et al. Gut Microbiota-Mediated Inflammation and Gut Permeability in Patients with Obesity and Colorectal Cancer. Int J Mol Sci. 2020;21(18).
420. He Q, Fu Y, Tian D, Yan W. The contrasting roles of inflammasomes in cancer. Am J Cancer Res. 2018;8(4):566-83.
421. Yang J, Wei H, Zhou Y, Szeto CH, Li C, Lin Y, et al. High-Fat Diet Promotes Colorectal Tumorigenesis Through Modulating Gut Microbiota and Metabolites. Gastroenterology. 2022;162(1):135-49 e2.
422. Bowers LW, Glenny EM, Punjala A, Lanman NA, Goldbaum A, Himbert C, et al. Weight Loss and/or Sulindac Mitigate Obesity-associated Transcriptome, Microbiome, and Protumor Effects in a Murine Model of Colon Cancer. Cancer Prev Res (Phila). 2022;15(8):481-95.
423. Broadfield LA, Saigal A, Szamosi JC, Hammill JA, Bezverbnaya K, Wang D, et al. Metformin-induced reductions in tumor growth involves modulation of the gut microbiome. Mol Metab. 2022;61:101498.
424. Song X, An Y, Chen D, Zhang W, Wu X, Li C, et al. Microbial metabolite deoxycholic acid promotes vasculogenic mimicry formation in intestinal carcinogenesis. Cancer Sci. 2022;113(2):459-77.
425. Lee PS, Nagabhushanam K, Ho CT, Pan MH. Inhibitory Effect of Garcinol on Obesity-Exacerbated, Colitis-Mediated Colon Carcinogenesis. Mol Nutr Food Res. 2021;65(17):e2100410.
426. Fei Y, Wang Y, Pang Y, Wang W, Zhu D, Xie M, et al. Xylooligosaccharide Modulates Gut Microbiota and Alleviates Colonic Inflammation Caused by High Fat Diet Induced Obesity. Front Physiol. 2019;10:1601.
427. Wang H, Guan L, Li J, Lai M, Wen X. The Effects of Berberine on the Gut Microbiota in Apc (min/+) Mice Fed with a High Fat Diet. Molecules. 2018;23(9).
428. Zeng H, Ishaq SL, Liu Z, Bukowski MR. Colonic aberrant crypt formation accompanies an increase of opportunistic pathogenic bacteria in C57BL/6 mice fed a high-fat diet. J Nutr Biochem. 2018;54:18-27.
429. Pfalzer AC, Kamanu FK, Parnell LD, Tai AK, Liu Z, Mason JB, et al. Interactions between the colonic transcriptome, metabolome, and microbiome in mouse models of obesity-induced intestinal cancer. Physiol Genomics. 2016;48(8):545-53.
430. Higashimura Y, Naito Y, Takagi T, Uchiyama K, Mizushima K, Ushiroda C, et al. Protective effect of agaro-oligosaccharides on gut dysbiosis and colon tumorigenesis in high-fat diet-fed mice. Am J Physiol Gastrointest Liver Physiol. 2016;310(6):G367-75.
431. Pfalzer AC, Nesbeth PD, Parnell LD, Iyer LK, Liu Z, Kane AV, et al. Diet- and Genetically-Induced Obesity Differentially Affect the Fecal Microbiome and Metabolome in Apc1638N Mice. PLoS One. 2015;10(8):e0135758.

432. Zhu G, Huang Q, Huang Y, Zheng W, Hua J, Yang S, et al. Lipopolysaccharide increases the release of VEGF-C that enhances cell motility and promotes lymphangiogenesis and lymphatic metastasis through the TLR4-NF-kappaB/JNK pathways in colorectal cancer. Oncotarget. 2016;7(45):73711-24.
433. Jia W, Xie G, Jia W. Bile acid-microbiota crosstalk in gastrointestinal inflammation and carcinogenesis. Nat Rev Gastroenterol Hepatol. 2018;15(2):111-28.
434. Gomes SD, Oliveira CS, Azevedo-Silva J, Casanova MR, Barreto J, Pereira H, et al. The Role of Diet Related Short-Chain Fatty Acids in Colorectal Cancer Metabolism and Survival: Prevention and Therapeutic Implications. Curr Med Chem. 2020;27(24):4087-108.
435. Alam Z, Shang X, Effat K, Kanwal F, He X, Li Y, et al. The potential role of prebiotics, probiotics, and synbiotics in adjuvant cancer therapy especially colorectal cancer. J Food Biochem. 2022;46(10):e14302.
436. Imai H, Saijo K, Komine K, Yoshida Y, Sasaki K, Suzuki A, et al. Antibiotics Improve the Treatment Efficacy of Oxaliplatin-Based but Not Irinotecan-Based Therapy in Advanced Colorectal Cancer Patients. J Oncol. 2020;2020:1701326.
437. Huang J, Zheng X, Kang W, Hao H, Mao Y, Zhang H, et al. Metagenomic and metabolomic analyses reveal synergistic effects of fecal microbiota transplantation and anti-PD-1 therapy on treating colorectal cancer. Front Immunol. 2022;13:874922.
438. Gibson GR, Scott KP, Rastall RA, Tuohy KM, Hotchkiss A, Dubert-Ferrandon A, et al. Dietary prebiotics: current status and new definition. Food Science & Technology Bulletin: Functional Foods. 2010;7(1):1-19.
439. Cerdo T, Garcia-Santos JA, M GB, Campoy C. The Role of Probiotics and Prebiotics in the Prevention and Treatment of Obesity. Nutrients. 2019;11(3).
440. Diez-Echave P, Vezza T, Rodriguez-Nogales A, Ruiz-Malagon AJ, Hidalgo-Garcia L, Garrido-Mesa J, et al. The prebiotic properties of Hibiscus sabdariffa extract contribute to the beneficial effects in diet-induced obesity in mice. Food Res Int. 2020;127:108722.
441. Vezza T, Garrido-Mesa J, Diez-Echave P, Hidalgo-Garcia L, Ruiz-Malagon AJ, Garcia F, et al. Allium-Derived Compound Propyl Propane Thiosulfonate (PTSO) Attenuates Metabolic Alterations in Mice Fed a High-Fat Diet through Its Anti-Inflammatory and Prebiotic Properties. Nutrients. 2021;13(8).
442. Zhou X, Liu X, He Q, Wang M, Lu H, You Y, et al. Ginger Extract Decreases Susceptibility to Dextran Sulfate Sodium-Induced Colitis in Mice Following Early Antibiotic Exposure. Front Med (Lausanne). 2021;8:755969.
443. Algieri F, Rodriguez-Nogales A, Garrido-Mesa N, Vezza T, Garrido-Mesa J, Utrilla MP, et al. Intestinal anti-inflammatory effects of oligosaccharides derived from lactulose in the trinitrobenzenesulfonic acid model of rat colitis. J Agric Food Chem. 2014;62(19):4285-97.
444. Rodriguez-Cabezas ME, Camuesco D, Arribas B, Garrido-Mesa N, Comalada M, Bailon E, et al. The combination of fructooligosaccharides and resistant starch shows prebiotic additive effects in rats. Clin Nutr. 2010;29(6):832-9.

445. Afshari K, Haddadi NS, Haj-Mirzaian A, Farzaei MH, Rohani MM, Akramian F, et al. Natural flavonoids for the prevention of colon cancer: A comprehensive review of preclinical and clinical studies. J Cell Physiol. 2019;234(12):21519-46.
446. Wu X, Xue L, Tata A, Song M, Neto CC, Xiao H. Bioactive Components of Polyphenol-Rich and Non-Polyphenol-Rich Cranberry Fruit Extracts and Their Chemopreventive Effects on Colitis-Associated Colon Cancer. J Agric Food Chem. 2020;68(25):6845-53.
447. Firrman J, Liu L, Mahalak K, Tanes C, Bittinger K, Tu V, et al. The impact of environmental pH on the gut microbiota community structure and short chain fatty acid production. FEMS Microbiol Ecol. 2022;98(5).
448. Walker AW, Duncan SH, McWilliam Leitch EC, Child MW, Flint HJ. pH and peptide supply can radically alter bacterial populations and short-chain fatty acid ratios within microbial communities from the human colon. Appl Environ Microbiol. 2005;71(7):3692-700.
449. Lu Y, Fan C, Li P, Lu Y, Chang X, Qi K. Short Chain Fatty Acids Prevent High-fat-diet-induced Obesity in Mice by Regulating G Protein-coupled Receptors and Gut Microbiota. Sci Rep. 2016;6:37589.
450. Chang PV, Hao L, Offermanns S, Medzhitov R. The microbial metabolite butyrate regulates intestinal macrophage function via histone deacetylase inhibition. Proc Natl Acad Sci U S A. 2014;111(6):2247-52.
451. Riggs MG, Whittaker RG, Neumann JR, Ingram VM. n-Butyrate causes histone modification in HeLa and Friend erythroleukaemia cells. Nature. 1977;268(5619):462-4.
452. Nieto G. A Review on Applications and Uses of Thymus in the Food Industry. Plants (Basel). 2020;9(8).
453. Lim SH, Choi CI. Pharmacological Properties of Morus nigra L. (Black Mulberry) as A Promising Nutraceutical Resource. Nutrients. 2019;11(2).
454. Chang BY, Koo BS, Kim SY. Pharmacological Activities for Morus alba L., Focusing on the Immunostimulatory Property from the Fruit Aqueous Extract. Foods. 2021;10(8).
455. Leyva-Jimenez FJ, Ruiz-Malagon AJ, Molina-Tijeras JA, Diez-Echave P, Vezza T, Hidalgo-Garcia L, et al. Comparative Study of the Antioxidant and Anti-Inflammatory Effects of Leaf Extracts from Four Different Morus alba Genotypes in High Fat Diet-Induced Obesity in Mice. Antioxidants (Basel). 2020;9(8).
456. de Oliveira AM, Mesquita Mda S, da Silva GC, de Oliveira Lima E, de Medeiros PL, Paiva PM, et al. Evaluation of Toxicity and Antimicrobial Activity of an Ethanolic Extract from Leaves of Morus alba L. (Moraceae). Evid Based Complement Alternat Med. 2015;2015:513978.
457. Dabili S, Fallah S, Aein M, Vatannejad A, Panahi G, Fadaei R, et al. Survey of the effect of doxorubicin and flavonoid extract of white Morus alba leaf on apoptosis induction in a-172 GBM cell line. Arch Physiol Biochem. 2019;125(2):136-41.
458. Ann JY, Eo H, Lim Y. Mulberry leaves (Morus alba L.) ameliorate obesity-induced hepatic lipogenesis, fibrosis, and oxidative stress in high-fat diet-fed mice. Genes Nutr. 2015;10(6):46.
459. Ruiz-Malagon AJ, Rodriguez-Sanchez MJ, Rodriguez-Sojo MJ, Vezza T, Pischel I, Algieri F, et al. Intestinal anti-inflammatory and visceral analgesic

effects of a Serpylli herba extract in an experimental model of irritable bowel syndrome in rats. Front Pharmacol. 2022;13:967644.
460. Bozkurt E, Atmaca H, Kisim A, Uzunoglu S, Uslu R, Karaca B. Effects of Thymus serpyllum extract on cell proliferation, apoptosis and epigenetic events in human breast cancer cells. Nutr Cancer. 2012;64(8):1245-50.
461. Azhar J, John P, Bhatti A. Thymus serpyllum Exhibits Anti-Diabetic Potential in Streptozotocin-Induced Diabetes Mellitus Type 2 Mice: A Combined Biochemical and In Vivo Study. Nutrients. 2022;14(17).
462. Feistel B, Suarez-Rizzo CG, Pischel I. Herba Thymi serpylli (Wild Thyme) – traditional herbal plant for digestive health. Zeitschrift für Phytotherapie. 2021;42(S 01):3.
463. Jarić S, Mitrović M, Karadžić B, Kostić O, Djurjević L, Pavlović M, et al. Plant resources used in Serbian medieval medicine. Ethnobotany and Ethnomedicine. Genetic Resources and Crop Evolution. 2014;61(7):1359-79.
464. Fachini-Queiroz FC, Kummer R, Estevao-Silva CF, Carvalho MD, Cunha JM, Grespan R, et al. Effects of Thymol and Carvacrol, Constituents of Thymus vulgaris L. Essential Oil, on the Inflammatory Response. Evid Based Complement Alternat Med. 2012;2012:657026.
465. Algieri F, Rodriguez-Nogales A, Garrido-Mesa N, Zorrilla P, Burkard N, Pischel I, et al. Intestinal anti-inflammatory activity of the Serpylli herba extract in experimental models of rodent colitis. J Crohns Colitis. 2014;8(8):775-88.
466. Hao JY, Wan Y, Yao XH, Zhao WG, Hu RZ, Chen C, et al. Effect of different planting areas on the chemical compositions and hypoglycemic and antioxidant activities of mulberry leaf extracts in Southern China. PLoS One. 2018;13(6):e0198072.
467. Harauma A, Murayama T, Ikeyama K, Sano H, Arai H, Takano R, et al. Mulberry leaf powder prevents atherosclerosis in apolipoprotein E-deficient mice. Biochem Biophys Res Commun. 2007;358(3):751-6.
468. Gryn A, Sperkowska B, Bazylak G. Determination of vitamin C and selected low molecular weight organic acids in aqueous extract of mulberry leaves used as dietary supplements. Current Issues of Pharmacy and Medical Sciences. 2013;26(2):221-4.
469. Zhang R, Zhang Q, Zhu S, Liu B, Liu F, Xu Y. Mulberry leaf (Morus alba L.): A review of its potential influences in mechanisms of action on metabolic diseases. Pharmacol Res. 2022;175:106029.
470. Chen C, Mohamad Razali UH, Saikim FH, Mahyudin A, Mohd Noor NQI. Morus alba L. Plant: Bioactive Compounds and Potential as a Functional Food Ingredient. Foods. 2021;10(3).
471. Eo HJ, Park JH, Park GH, Lee MH, Lee JR, Koo JS, et al. Anti-inflammatory and anti-cancer activity of mulberry (Morus alba L.) root bark. BMC Complement Altern Med. 2014;14:200.
472. Chan EWC, Wong SK, Tangah J, Inoue T, Chan HT. Phenolic constituents and anticancer properties of Morus alba (white mulberry) leaves. J Integr Med. 2020;18(3):189-95.
473. Deepa M, Sureshkumar T, Satheeshkumar PK, Priya S. Purified mulberry leaf lectin (MLL) induces apoptosis and cell cycle arrest in human breast cancer and colon cancer cells. Chem Biol Interact. 2012;200(1):38-44.

474. Chang CH, Chang YT, Tseng TH, Wang CJ. Mulberry leaf extract inhibit hepatocellular carcinoma cell proliferation via depressing IL-6 and TNF-alpha derived from adipocyte. J Food Drug Anal. 2018;26(3):1024-32.
475. Park HJ, Chi GY, Choi YH, Park SH. The root bark of Morus alba L. regulates tumor-associated macrophages by blocking recruitment and M2 polarization of macrophages. Phytother Res. 2020;34(12):3333-44.
476. Duggar BM. Aureomycin; a product of the continuing search for new antibiotics. Ann N Y Acad Sci. 1948;51(Art. 2):177-81.
477. Garrido-Mesa J, Rodriguez-Nogales A, Algieri F, Vezza T, Hidalgo-Garcia L, Garrido-Barros M, et al. Immunomodulatory tetracyclines shape the intestinal inflammatory response inducing mucosal healing and resolution. Br J Pharmacol. 2018;175(23):4353-70.
478. Rahmani M, Negro Alvarez SE, Hernandez EB. The potential use of tetracyclines in neurodegenerative diseases and the role of nano-based drug delivery systems. Eur J Pharm Sci. 2022;175:106237.
479. Saikali Z, Singh G. Doxycycline and other tetracyclines in the treatment of bone metastasis. Anticancer Drugs. 2003;14(10):773-8.
480. Grossman TH. Tetracycline Antibiotics and Resistance. Cold Spring Harb Perspect Med. 2016;6(4):a025387.
481. Smilack JD. The tetracyclines. Mayo Clin Proc. 1999;74(7):727-9.
482. Rusu A, Buta EL. The Development of Third-Generation Tetracycline Antibiotics and New Perspectives. Pharmaceutics. 2021;13(12).
483. Castro MM, Kandasamy AD, Youssef N, Schulz R. Matrix metalloproteinase inhibitor properties of tetracyclines: therapeutic potential in cardiovascular diseases. Pharmacol Res. 2011;64(6):551-60.
484. Bassett B, Subramaniyam S, Fan Y, Varney S, Pan H, Carneiro AMD, et al. Minocycline alleviates depression-like symptoms by rescuing decrease in neurogenesis in dorsal hippocampus via blocking microglia activation/phagocytosis. Brain Behav Immun. 2021;91:519-30.
485. Vezza T, Molina-Tijeras JA, Gonzalez-Cano R, Rodriguez-Nogales A, Garcia F, Galvez J, et al. Minocycline Prevents the Development of Key Features of Inflammation and Pain in DSS-induced Colitis in Mice. J Pain. 2023;24(2):304-19.
486. Protasoni M, Kroon AM, Taanman JW. Mitochondria as oncotarget: a comparison between the tetracycline analogs doxycycline and COL-3. Oncotarget. 2018;9(73):33818-31.
487. Wang Y, Xie F, Chen D, Wang L. Inhibition of mitochondrial respiration by tigecycline selectively targets thyroid carcinoma and increases chemosensitivity. Clin Exp Pharmacol Physiol. 2019;46(10):890-7.
488. Yang L, Yang J, Liu H, Lan J, Xu Y, Wu X, et al. Minocycline binds and inhibits LYN activity to prevent STAT3-meditated metastasis of colorectal cancer. Int J Biol Sci. 2022;18(6):2540-52.
489. Ali I, Alfarouk KO, Reshkin SJ, Ibrahim ME. Doxycycline as Potential Anti-cancer Agent. Anticancer Agents Med Chem. 2017;17(12):1617-23.
490. Antoszczak M, Markowska A, Markowska J, Huczynski A. Old wine in new bottles: Drug repurposing in oncology. Eur J Pharmacol. 2020;866:172784.

491. Yang J, Dong Z, Ren A, Fu G, Zhang K, Li C, et al. Antibiotic tigecycline inhibits cell proliferation, migration and invasion via down-regulating CCNE2 in pancreatic ductal adenocarcinoma. J Cell Mol Med. 2020;24(7):4245-60.
492. Sun J, Li G, Liu Y, Ma M, Song K, Li H, et al. Targeting histone deacetylase SIRT1 selectively eradicates EGFR TKI-resistant cancer stem cells via regulation of mitochondrial oxidative phosphorylation in lung adenocarcinoma. Neoplasia. 2020;22(1):33-46.
493. Ma R, Zhang Y, Wang W, Wu J, Yang Q, Xu W, et al. Inhibition of autophagy enhances the antitumour activity of tigecycline in multiple myeloma. J Cell Mol Med. 2018;22(12):5955-63.
494. Cheng J. Doxycycline sclerotherapy in children with head and neck lymphatic malformations. J Pediatr Surg. 2015;50(12):2143-6.
495. Zhu C, Yan X, Yu A, Wang Y. Doxycycline synergizes with doxorubicin to inhibit the proliferation of castration-resistant prostate cancer cells. Acta Biochim Biophys Sin (Shanghai). 2017;49(11):999-1007.
496. Fife RS, Sledge GW, Jr., Roth BJ, Proctor C. Effects of doxycycline on human prostate cancer cells in vitro. Cancer letters. 1998;127(1-2):37-41.
497. Sanchez-Burgos L, Navarro-Gonzalez B, Garcia-Martin S, Sirozh O, Mota-Pino J, Fueyo-Marcos E, et al. Activation of the integrated stress response is a vulnerability for multidrug-resistant FBXW7-deficient cells. EMBO Mol Med. 2022;14(9):e15855.
498. Zhou Y, Wang S, Wu W, Ling J, Li H, Jia Q, et al. Sustained activation of EGFR-ERK1/2 signaling limits the response to tigecycline-induced mitochondrial respiratory deficiency in liver cancer. EBioMedicine. 2023;87:104397.
499. Song H, Fares M, Maguire KR, Siden A, Potacova Z. Cytotoxic effects of tetracycline analogues (doxycycline, minocycline and COL-3) in acute myeloid leukemia HL-60 cells. PLoS One. 2014;9(12):e114457.
500. Pourgholami MH, Mekkawy AH, Badar S, Morris DL. Minocycline inhibits growth of epithelial ovarian cancer. Gynecol Oncol. 2012;125(2):433-40.
501. Griffin MO, Ceballos G, Villarreal FJ. Tetracycline compounds with non-antimicrobial organ protective properties: possible mechanisms of action. Pharmacol Res. 2011;63(2):102-7.
502. Smith Jr GN, Mickler EA, Hasty KA, Brandt KD. Specificity of inhibition of matrix metalloproteinase activity by doxycycline: Relationship to structure of the enzyme. Arthritis & Rheumatism. 1999;42(6):1140-6.
503. Guerin C, Laterra J, Masnyk T, Golub LM, Brem H. Selective endothelial growth inhibition by tetracyclines that inhibit collagenase. Biochem Biophys Res Commun. 1992;188(2):740-5.
504. Li CH, Liao PL, Yang YT, Huang SH, Lin CH, Cheng YW, et al. Minocycline accelerates hypoxia-inducible factor-1 alpha degradation and inhibits hypoxia-induced neovasculogenesis through prolyl hydroxylase, von Hippel-Lindau-dependent pathway. Arch Toxicol. 2014;88(3):659-71.
505. Krenn L. SERPYLLI HERBA Wild Thyme. SERIES O, editor. Notaries House, Chapel Street, Exeter EX1 1EZ, United Kingdom: EUROPEAN SCIENTIFIC COOPERATIVE ON PHYTOTHERAPY; 2014.
506. Cao Z, Zhang Z, Huang Z, Wang R, Yang A, Liao L, et al. Antitumor and immunomodulatory effects of low-dose 5-FU on hepatoma 22 tumor-bearing mice. Oncology letters. 2014;7(4):1260-4.

507. Ghosh S, Singh R, Vanwinkle ZM, Guo H, Vemula PK, Goel A, et al. Microbial metabolite restricts 5-fluorouracil-resistant colonic tumor progression by sensitizing drug transporters via regulation of FOXO3-FOXM1 axis. Theranostics. 2022;12(12):5574-95.
508. Malterud KE, Farbrot TL, Huse AE, Sund RB. Antioxidant and Radical Scavenging Effects of Anthraquinones and Anthrones. Pharmacology. 1993;47(suppl 1)(Suppl. 1):77-85.
509. Sekine S, Shibata T, Sakamoto M, Hirohashi S. Target disruption of the mutant β-catenin gene in colon cancer cell line HCT116: preservation of its malignant phenotype. Oncogene. 2002;21(38):5906-11.
510. Stauffer JS, Manzano LA, Balch GC, Merriman RL, Tanzer LR, Moyer MP. Development and characterization of normal colonic epithelial cell lines derived from normal mucosa of patients with colon cancer. The American Journal of Surgery. 1995;169(2):190-6.
511. Jiménez G, Hackenberg M, Catalina P, Boulaiz H, Griñán-Lisón C, García M, et al. Mesenchymal stem cell's secretome promotes selective enrichment of cancer stem-like cells with specific cytogenetic profile. Cancer letters. 2018;429:78-88.
512. Cruz-Lozano M, González-González A, Marchal JA, Muñoz-Muela E, Molina MP, Cara FE, et al. Hydroxytyrosol inhibits cancer stem cells and the metastatic capacity of triple-negative breast cancer cell lines by the simultaneous targeting of epithelial-to-mesenchymal transition, Wnt/β-catenin and TGFβ signaling pathways. European Journal of Nutrition. 2019;58(8):3207-19.
513. Griñán-Lisón C, Olivares-Urbano MA, Jiménez G, López-Ruiz E, Del Val C, Morata-Tarifa C, et al. miRNAs as radio-response biomarkers for breast cancer stem cells. Molecular oncology. 2020;14(3):556-70.
514. Smith PK, Krohn RI, Hermanson GT, Mallia AK, Gartner FH, Provenzano MD, et al. Measurement of protein using bicinchoninic acid. Analytical Biochemistry. 1985;150(1):76-85.
515. McGrath J, Drummond G, McLachlan E, Kilkenny C, Wainwright C. Guidelines for reporting experiments involving animals: the ARRIVE guidelines. 2010;160(7):1573-6.
516. Kilkenny C, Browne W, Cuthill IC, Emerson M, Altman DG. Animal research: reporting in vivo experiments: the ARRIVE guidelines. British journal of pharmacology. 2010;160(7):1577-9.
517. Diez-Echave P, Vezza T, Algieri F, Ruiz-Malagón AJ, Hidalgo-García L, García F, et al. The melatonergic agonist agomelatine ameliorates high fat diet-induced obesity in mice through the modulation of the gut microbiome. Biomedicine & pharmacotherapy = Biomedecine & pharmacotherapie. 2022;153:113445.
518. Becker C, Fantini MC, Neurath MF. High resolution colonoscopy in live mice. Nature Protocols. 2006;1(6):2900-4.
519. Ruiz-Malagón AJ, Rodríguez-Sojo MJ, Hidalgo-García L, Molina-Tijeras JA, García F, Pischel I, et al. The Antioxidant Activity of Thymus serpyllum Extract Protects against the Inflammatory State and Modulates Gut Dysbiosis in Diet-Induced Obesity in Mice. Antioxidants (Basel, Switzerland). 2022;11(6).
520. Toral M, Gómez-Guzmán M, Jiménez R, Romero M, Sánchez M, Utrilla MP, et al. The probiotic Lactobacillus coryniformis CECT5711 reduces the

vascular pro-oxidant and pro-inflammatory status in obese mice. Clinical science (London, England : 1979). 2014;127(1):33-45.
521. Zarzuelo MJ, Jiménez R, Galindo P, Sánchez M, Nieto A, Romero M, et al. Antihypertensive effects of peroxisome proliferator-activated receptor-β activation in spontaneously hypertensive rats. Hypertension (Dallas, Tex : 1979). 2011;58(4):733-43.
522. Bokulich NA, Subramanian S, Faith JJ, Gevers D, Gordon JI, Knight R, et al. Quality-filtering vastly improves diversity estimates from Illumina amplicon sequencing. Nature Methods. 2013;10(1):57-9.
523. Dhariwal A, Chong J, Habib S, King IL, Agellon LB, Xia J. MicrobiomeAnalyst: a web-based tool for comprehensive statistical, visual and meta-analysis of microbiome data. Nucleic Acids Res. 2017;45(W1):W180-W8.
524. Glöckner FO, Yilmaz P, Quast C, Gerken J, Beccati A, Ciuprina A, et al. 25 years of serving the community with ribosomal RNA gene reference databases and tools. Journal of Biotechnology. 2017;261:169-76.
525. Love MI, Huber W, Anders S. Moderated estimation of fold change and dispersion for RNA-seq data with DESeq2. Genome Biol. 2014;15(12):550.
526. Tilg H, Moschen AR. Inflammatory mechanisms in the regulation of insulin resistance. Molecular medicine (Cambridge, Mass). 2008;14(3-4):222-31.
527. Kola B, Grossman AB, Korbonits M. The role of AMP-activated protein kinase in obesity. Frontiers of hormone research. 2008;36:198-211.
528. Kalis C, Kanzler B, Lembo A, Poltorak A, Galanos C, Freudenberg MA. Toll-like receptor 4 expression levels determine the degree of LPS-susceptibility in mice. 2003;33(3):798-805.
529. Li R, Xue Z, Li S, Zhou J, Liu J, Zhang M, et al. Mulberry leaf polysaccharides ameliorate obesity through activation of brown adipose tissue and modulation of the gut microbiota in high-fat diet fed mice. Food & function. 2022;13(2):561-73.
530. Gunjal S, Ankola AV, Bhat K. In vitro antibacterial activity of ethanolic extract of Morus alba leaf against periodontal pathogens. Indian journal of dental research : official publication of Indian Society for Dental Research. 2015;26(5):533-6.
531. Viola A, Munari F, Sánchez-Rodríguez R, Scolaro T, Castegna A. The Metabolic Signature of Macrophage Responses. Front Immunol. 2019;10:1462.
532. Kim DS, Kang YM, Jin WY, Sung YY, Choi G, Kim HK. Antioxidant activities and polyphenol content of Morus alba leaf extracts collected from varying regions. Biomedical reports. 2014;2(5):675-80.
533. Gerdes J, Lemke H, Baisch H, Wacker HH, Schwab U, Stein H. Cell cycle analysis of a cell proliferation-associated human nuclear antigen defined by the monoclonal antibody Ki-67. J Immunol. 1984;133(4):1710-5.
534. Zhang M, Weng W, Zhang Q, Wu Y, Ni S, Tan C, et al. The lncRNA NEAT1 activates Wnt/β-catenin signaling and promotes colorectal cancer progression via interacting with DDX5. Journal of Hematology & Oncology. 2018;11(1):113.
535. Wei C-Y, Zhu M-X, Yang Y-W, Zhang P-F, Yang X, Peng R, et al. Downregulation of RNF128 activates Wnt/β-catenin signaling to induce cellular EMT and stemness via CD44 and CTTN ubiquitination in melanoma. Journal of Hematology & Oncology. 2019;12(1):21.

536. He S, Tang S. WNT/β-catenin signaling in the development of liver cancers. Biomed Pharmacother. 2020;132:110851.
537. Li H, Zhu H, Xu C-j, Yuan J. Cleavage of BID by Caspase 8 Mediates the Mitochondrial Damage in the Fas Pathway of Apoptosis. Cell. 1998;94(4):491-501.
538. Kalkavan H, Green DR. MOMP, cell suicide as a BCL-2 family business. Cell Death Differ. 2018;25(1):46-55.
539. Friedl P, Wolf K. Tumour-cell invasion and migration: diversity and escape mechanisms. Nat Rev Cancer. 2003;3(5):362-74.
540. Dalerba P, Dylla SJ, Park I-K, Liu R, Wang X, Cho RW, et al. Phenotypic characterization of human colorectal cancer stem cells. 2007;104(24):10158-63.
541. Zhou Y, Xia L, Wang H, Oyang L, Su M, Liu Q, et al. Cancer stem cells in progression of colorectal cancer. 2018;9(70).
542. Clark DW, Palle K. Aldehyde dehydrogenases in cancer stem cells: potential as therapeutic targets. Annals of translational medicine. 2016;4(24):518.
543. Loh C-Y, Chai J, Tang T, Wong W, Sethi G, Shanmugam M, et al. The E-Cadherin and N-Cadherin Switch in Epithelial-to-Mesenchymal Transition: Signaling, Therapeutic Implications, and Challenges. Cells. 2019;8(10).
544. Lin S-C, Chung C-H, Chung C-H, Kuo M-H, Hsieh C-H, Chiu Y-F, et al. OCT4B mediates hypoxia-induced cancer dissemination. Oncogene. 2019;38(7):1093-105.
545. Huang T-Y, Chang T-C, Chin Y-T, Pan Y-S, Chang W-J, Liu F-C, et al. NDAT Targets PI3K-Mediated PD-L1 Upregulation to Reduce Proliferation in Gefitinib-Resistant Colorectal Cancer. 2020;9(8):1830.
546. Gali-Muhtasib H, Ocker M, Kuester D, Krueger S, El-Hajj Z, Diestel A, et al. Thymoquinone reduces mouse colon tumor cell invasion and inhibits tumor growth in murine colon cancer models. Journal of Cellular and Molecular Medicine. 2007;12(1):330-42.
547. Bhat P, Leggatt G, Waterhouse N, Frazer IH. Interferon-γ derived from cytotoxic lymphocytes directly enhances their motility and cytotoxicity. Cell Death & Disease. 2017;8(6):e2836-e.
548. Tabuso M, Homer-Vanniasinkam S, Adya R, Arasaradnam RP. Role of tissue microenvironment resident adipocytes in colon cancer. World J Gastroenterol. 2017;23(32):5829-35.
549. Vulcan A, Manjer J, Ohlsson B. High blood glucose levels are associated with higher risk of colon cancer in men: a cohort study. BMC Cancer. 2017;17(1):842.
550. Pavelock N, Masood U, Minchenberg S, Heisig D. Effects of obesity on the course of inflammatory bowel disease. Baylor University Medical Center Proceedings. 2019;32(1):14-7.
551. Kim SH, Kwon D, Son SW, Jeong TB, Lee S, Kwak J-H, et al. Inflammatory responses of C57BL/6NKorl mice to dextran sulfate sodium-induced colitis: comparison between three C57BL/6 N sub-strains. Laboratory Animal Research. 2021;37(1).
552. Kern L, Mittenbühler M, Vesting A, Ostermann A, Wunderlich C, Wunderlich F. Obesity-Induced TNFα and IL-6 Signaling: The Missing Link

between Obesity and Inflammation—Driven Liver and Colorectal Cancers. Cancers. 2018;11(1).
553. Huang XF, Chen JZ. Obesity, the PI3K/Akt signal pathway and colon cancer. Obes Rev. 2009;10(6):610-6.
554. Knüpfer H, Preiss R. Serum interleukin-6 levels in colorectal cancer patients—a summary of published results. International Journal of Colorectal Disease. 2009;25(2):135-40.
555. El-Mikkawy DME, El-Sadek MA, El-Badawy MA, Samaha D. Circulating level of interleukin-6 in relation to body mass indices and lipid profile in Egyptian adults with overweight and obesity. Egyptian Rheumatology and Rehabilitation. 2020;47(1).
556. Rosen ED, Hsu C-H, Wang X, Sakai S, Freeman MW, Gonzalez FJ, et al. C/EBPα induces adipogenesis through PPARγ: a unified pathway. Genes & Development. 2002;16(1):22-6.
557. Motawi TK, Shaker OG, Ismail MF, Sayed NH. Peroxisome Proliferator-Activated Receptor Gamma in Obesity and Colorectal Cancer: the Role of Epigenetics. Scientific Reports. 2017;7(1).
558. Weng J-R, Chen C-Y, Pinzone JJ, Ringel MD, Chen C-S. Beyond peroxisome proliferator-activated receptor γ signaling: the multi-facets of the antitumor effect of thiazolidinediones %J Endocrine-Related Cancer Endocr Relat Cancer. 2006;13(2):401-13.
559. Panigrahy D, Singer S, Shen LQ, Butterfield CE, Freedman DA, Chen EJ, et al. PPARγ ligands inhibit primary tumor growth and metastasis by inhibiting angiogenesis. Journal of Clinical Investigation. 2002;110(7):923-32.
560. Tachibana K, Yamasaki D, Ishimoto K, Doi T. The Role of PPARs in Cancer. PPAR Research. 2008;2008:1-15.
561. Liu R, Chen Y, Liu G, Li C, Song Y, Cao Z, et al. PI3K/AKT pathway as a key link modulates the multidrug resistance of cancers. Cell Death & Disease. 2020;11(9).
562. Ren W, Guo J, Jiang F, Lu J, Ding Y, Li A, et al. CCAAT/Enhancer-Binding Protein α Is a Crucial Regulator of Human Fat Mass and Obesity Associated Gene Transcription and Expression. BioMed Research International. 2014;2014:406909.
563. Rolland V, Le Liepvre X, Houbiguian ML, Lavau M, Dugail I. C/EBP alpha expression in adipose tissue of genetically obese Zucker rats. Biochem Biophys Res Commun. 1995;207(2):761-7.
564. Mi L, Hu K, Wen X, Sun J, Wu A, Wang M, et al. Upregulation of C/EBPα contributes to colorectal cancer growth, metastasis and indicates poor survival outcome. American journal of cancer research. 2018;8(8):1449-65.
565. Porta C, Subhra Kumar B, Larghi P, Rubino L, Mancino A, Sica A. Tumor promotion by tumor-associated macrophages. Advances in experimental medicine and biology. 2007;604:67-86.
566. Wang H, Tian T, Zhang J. Tumor-Associated Macrophages (TAMs) in Colorectal Cancer (CRC): From Mechanism to Therapy and Prognosis. Int J Mol Sci. 2021;22(16).
567. Wang D, Yu W, Lian J, Wu Q, Liu S, Yang L, et al. Th17 cells inhibit CD8+ T cell migration by systematically downregulating CXCR3 expression via IL-

17A/STAT3 in advanced-stage colorectal cancer patients. Journal of Hematology & Oncology. 2020;13(1):68.
568. Grossman JG, Nywening TM, Belt BA, Panni RZ, Krasnick BA, DeNardo DG, et al. Recruitment of CCR2+ tumor associated macrophage to sites of liver metastasis confers a poor prognosis in human colorectal cancer. OncoImmunology. 2018;7(9):e1470729.
569. Inaba T, Sano H, Kawahito Y, Hla T, Akita K, Toda M, et al. Induction of cyclooxygenase-2 in monocyte/macrophage by mucins secreted from colon cancer cells. 2003;100(5):2736-41.
570. Edin S, Kaprio T, Hagström J, Larsson P, Mustonen H, Böckelman C, et al. The Prognostic Importance of CD20+ B lymphocytes in Colorectal Cancer and the Relation to Other Immune Cell subsets. Scientific Reports. 2019;9(1):19997.
571. Mullins CS, Gock M, Krohn M, Linnebacher M. Human Colorectal Carcinoma Infiltrating B Lymphocytes Are Active Secretors of the Immunoglobulin Isotypes A, G, and M. 2019;11(6):776.
572. World Health Organization. World Obesity Day 2022 – Accelerating action to stop obesity [Internet] 2022 [Accesed on 10.01.22] Available from: https://www.who.int/news/item/04-03-2022-world-obesity-day-2022-accelerating-action-to-stop-obesity.
573. Liu PH, Wu K, Ng K, Zauber AG, Nguyen LH, Song M, et al. Association of Obesity With Risk of Early-Onset Colorectal Cancer Among Women. JAMA Oncol. 2019;5(1):37-44.
574. Bou Malhab LJ, Abdel-Rahman WM. Obesity and Inflammation: Colorectal Cancer Engines. Curr Mol Pharmacol. 2022;15(4):620-46.
575. Cirillo F, Catellani C, Sartori C, Lazzeroni P, Amarri S, Street ME. Obesity, Insulin Resistance, and Colorectal Cancer: Could miRNA Dysregulation Play A Role? Int J Mol Sci. 2019;20(12).
576. Cox AJ, West NP, Cripps AW. Obesity, inflammation, and the gut microbiota. Lancet Diabetes Endocrinol. 2015;3(3):207-15.
577. Gadde KM, Martin CK, Berthoud HR, Heymsfield SB. Obesity: Pathophysiology and Management. J Am Coll Cardiol. 2018;71(1):69-84.
578. Tak YJ, Lee SY. Long-Term Efficacy and Safety of Anti-Obesity Treatment: Where Do We Stand? Curr Obes Rep. 2021;10(1):14-30.
579. Paul AK, Jahan R, Paul A, Mahboob T, Bondhon TA, Jannat K, et al. The Role of Medicinal and Aromatic Plants against Obesity and Arthritis: A Review. Nutrients. 2022;14(5).
580. Mopuri R, Islam MS. Medicinal plants and phytochemicals with anti-obesogenic potentials: A review. Biomed Pharmacother. 2017;89:1442-52.
581. Liu LK, Chou FP, Chen YC, Chyau CC, Ho HH, Wang CJ. Effects of mulberry (Morus alba L.) extracts on lipid homeostasis in vitro and in vivo. J Agric Food Chem. 2009;57(16):7605-11.
582. Ahn E, Lee J, Jeon YH, Choi SW, Kim E. Anti-diabetic effects of mulberry (Morus alba L.) branches and oxyresveratrol in streptozotocin-induced diabetic mice. Food Sci Biotechnol. 2017;26(6):1693-702.
583. Khani M, Motamedi P, Dehkhoda MR, Dabagh Nikukheslat S, Karimi P. Effect of thyme extract supplementation on lipid peroxidation, antioxidant capacity, PGC-1alpha content and endurance exercise performance in rats. J Int Soc Sports Nutr. 2017;14:11.

584. Vasileva LV, Savova MS, Tews D, Wabitsch M, Georgiev MI. Rosmarinic acid attenuates obesity and obesity-related inflammation in human adipocytes. Food Chem Toxicol. 2021;149:112002.
585. Kim NY, Thomas SS, Hwang DI, Lee JH, Kim KA, Cha YS. Anti-Obesity Effects of Morus alba L. and Aronia melanocarpa in a High-Fat Diet-Induced Obese C57BL/6J Mouse Model. Foods. 2021;10(8).
586. Fabbrini E, Sullivan S, Klein S. Obesity and nonalcoholic fatty liver disease: biochemical, metabolic, and clinical implications. Hepatology. 2010;51(2):679-89.
587. Santoro A, McGraw TE, Kahn BB. Insulin action in adipocytes, adipose remodeling, and systemic effects. Cell Metab. 2021;33(4):748-57.
588. Kahn SE, Hull RL, Utzschneider KM. Mechanisms linking obesity to insulin resistance and type 2 diabetes. Nature. 2006;444(7121):840-6.
589. Su KZ, Li YR, Zhang D, Yuan JH, Zhang CS, Liu Y, et al. Relation of Circulating Resistin to Insulin Resistance in Type 2 Diabetes and Obesity: A Systematic Review and Meta-Analysis. Front Physiol. 2019;10:1399.
590. Wondmkun YT. Obesity, Insulin Resistance, and Type 2 Diabetes: Associations and Therapeutic Implications. Diabetes Metab Syndr Obes. 2020;13:3611-6.
591. Ye J. Mechanisms of insulin resistance in obesity. Front Med. 2013;7(1):14-24.
592. Matthews DR, Hosker JP, Rudenski AS, Naylor BA, Treacher DF, Turner RC. Homeostasis model assessment: insulin resistance and beta-cell function from fasting plasma glucose and insulin concentrations in man. Diabetologia. 1985;28(7):412-9.
593. Huang X, Liu G, Guo J, Su Z. The PI3K/AKT pathway in obesity and type 2 diabetes. Int J Biol Sci. 2018;14(11):1483-96.
594. Acosta-Martinez M, Cabail MZ. The PI3K/Akt Pathway in Meta-Inflammation. Int J Mol Sci. 2022;23(23).
595. Long YC, Zierath JR. AMP-activated protein kinase signaling in metabolic regulation. J Clin Invest. 2006;116(7):1776-83.
596. Mills EL, Harmon C, Jedrychowski MP, Xiao H, Gruszczyk AV, Bradshaw GA, et al. Cysteine 253 of UCP1 regulates energy expenditure and sex-dependent adipose tissue inflammation. Cell Metab. 2022;34(1):140-57 e8.
597. Schneider K, Valdez J, Nguyen J, Vawter M, Galke B, Kurtz TW, et al. Increased Energy Expenditure, Ucp1 Expression, and Resistance to Diet-induced Obesity in Mice Lacking Nuclear Factor-Erythroid-2-related Transcription Factor-2 (Nrf2). J Biol Chem. 2016;291(14):7754-66.
598. Qiu Y, Yang Y, Wei Y, Liu X, Feng Z, Zeng X, et al. Glyburide Regulates UCP1 Expression in Adipocytes Independent of K(ATP) Channel Blockade. iScience. 2020;23(9):101446.
599. Brusq JM, Ancellin N, Grondin P, Guillard R, Martin S, Saintillan Y, et al. Inhibition of lipid synthesis through activation of AMP kinase: an additional mechanism for the hypolipidemic effects of berberine. J Lipid Res. 2006;47(6):1281-8.
600. Xiang HC, Lin LX, Hu XF, Zhu H, Li HP, Zhang RY, et al. AMPK activation attenuates inflammatory pain through inhibiting NF-kappaB activation and IL-1beta expression. J Neuroinflammation. 2019;16(1):34.

601. Mancini SJ, White AD, Bijland S, Rutherford C, Graham D, Richter EA, et al. Activation of AMP-activated protein kinase rapidly suppresses multiple pro-inflammatory pathways in adipocytes including IL-1 receptor-associated kinase-4 phosphorylation. Mol Cell Endocrinol. 2017;440:44-56.
602. Chan PC, Liao MT, Hsieh PS. The Dualistic Effect of COX-2-Mediated Signaling in Obesity and Insulin Resistance. Int J Mol Sci. 2019;20(13).
603. Molina-Tijeras JA, Diez-Echave P, Vezza T, Hidalgo-Garcia L, Ruiz-Malagon AJ, Rodriguez-Sojo MJ, et al. Lactobacillus fermentum CECT5716 ameliorates high fat diet-induced obesity in mice through modulation of gut microbiota dysbiosis. Pharmacol Res. 2021;167:105471.
604. Breton J, Galmiche M, Dechelotte P. Dysbiotic Gut Bacteria in Obesity: An Overview of the Metabolic Mechanisms and Therapeutic Perspectives of Next-Generation Probiotics. Microorganisms. 2022;10(2).
605. Dai YJ, Liu WB, Abasubong KP, Zhang DD, Li XF, Xiao K, et al. The Mechanism of Lipopolysaccharide Escaping the Intestinal Barrier in Megalobrama amblycephala Fed a High-Fat Diet. Front Nutr. 2022;9:853409.
606. Reitmeier S, Hitch TCA, Treichel N, Fikas N, Hausmann B, Ramer-Tait AE, et al. Handling of spurious sequences affects the outcome of high-throughput 16S rRNA gene amplicon profiling. ISME Communications. 2021;1(1).
607. Zheng J, Zhang J, Guo Y, Cui H, Lin A, Hu B, et al. Improvement on metabolic syndrome in high fat diet-induced obese mice through modulation of gut microbiota by sangguayin decoction. Journal of Ethnopharmacology. 2020;246.
608. Mu H, Zhou Q, Yang R, Zeng J, Li X, Zhang R, et al. Naringin Attenuates High Fat Diet Induced Non-alcoholic Fatty Liver Disease and Gut Bacterial Dysbiosis in Mice. Frontiers in Microbiology. 2020;11.
609. Jiang H, Ling Z, Zhang Y, Mao H, Ma Z, Yin Y, et al. Altered fecal microbiota composition in patients with major depressive disorder. Brain, Behavior, and Immunity. 2015;48:186-94.
610. Parada Venegas D, De la Fuente MK, Landskron G, González MJ, Quera R, Dijkstra G, et al. Short Chain Fatty Acids (SCFAs)-Mediated Gut Epithelial and Immune Regulation and Its Relevance for Inflammatory Bowel Diseases. Frontiers in Immunology. 2019;10.
611. Gaudier E, Jarry A, Blottière HM, de Coppet P, Buisine MP, Aubert JP, et al. Butyrate specifically modulatesMUCgene expression in intestinal epithelial goblet cells deprived of glucose. American Journal of Physiology-Gastrointestinal and Liver Physiology. 2004;287(6):G1168-G74.
612. Chakraborti CK. New-found link between microbiota and obesity. World Journal of Gastrointestinal Pathophysiology. 2015;6(4).
613. Chen J, Vitetta L. The Role of Butyrate in Attenuating Pathobiont-Induced Hyperinflammation. Immune Network. 2020;20(2).
614. Tian X, Hellman J, Horswill AR, Crosby HA, Francis KP, Prakash A. Elevated Gut Microbiome-Derived Propionate Levels Are Associated With Reduced Sterile Lung Inflammation and Bacterial Immunity in Mice. Frontiers in Microbiology. 2019;10.
615. Gao Z, Yin J, Zhang J, Ward RE, Martin RJ, Lefevre M, et al. Butyrate Improves Insulin Sensitivity and Increases Energy Expenditure in Mice. Diabetes. 2009;58(7):1509-17.

616. Parker BJ, Wearsch PA, Veloo ACM, Rodriguez-Palacios A. The Genus Alistipes: Gut Bacteria With Emerging Implications to Inflammation, Cancer, and Mental Health. Front Immunol. 2020;11:906.
617. Lim S, Chang D-H, Ahn S, Kim B-C. Whole genome sequencing of “Faecalibaculum rodentium” ALO17, isolated from C57BL/6J laboratory mouse feces. Gut Pathogens. 2016;8(1):3.
618. Drummond GR, Sobey CG. Endothelial NADPH oxidases: which NOX to target in vascular disease? Trends in Endocrinology & Metabolism. 2014;25(9):452-63.
619. Kozłowska A, Szostak-Węgierek D. Targeting Cardiovascular Diseases by Flavonols: An Update. Nutrients. 2022;14(7).
620. Nyandwi J-B, Ko YS, Jin H, Yun SP, Park SW, Kim HJ. Rosmarinic Acid Increases Macrophage Cholesterol Efflux through Regulation of ABCA1 and ABCG1 in Different Mechanisms. International Journal of Molecular Sciences. 2021;22(16).
621. Biller LH, Schrag D. Diagnosis and Treatment of Metastatic Colorectal Cancer. Jama. 2021;325(7).
622. Hervieu C, Christou N, Battu S, Mathonnet M. The Role of Cancer Stem Cells in Colorectal Cancer: From the Basics to Novel Clinical Trials. Cancers. 2021;13(5).
623. Cole AJ, Fayomi AP, Anyaeche VI, Bai S, Buckanovich RJ. An evolving paradigm of cancer stem cell hierarchies: therapeutic implications. Theranostics. 2020;10(7):3083-98.
624. Baghban R, Roshangar L, Jahanban-Esfahlan R, Seidi K, Ebrahimi-Kalan A, Jaymand M, et al. Tumor microenvironment complexity and therapeutic implications at a glance. Cell Communication and Signaling. 2020;18(1).
625. Cao Y, Oh J, Xue M, Huh WJ, Wang J, Gonzalez-Hernandez JA, et al. Commensal microbiota from patients with inflammatory bowel disease produce genotoxic metabolites. Science. 2022;378(6618).
626. Kosumi K, Mima K, Baba H, Ogino S. Dysbiosis of the gut microbiota and colorectal cancer: the key target of molecular pathological epidemiology. Journal of Laboratory and Precision Medicine. 2018;3:76-.
627. Fong W, Li Q, Yu J. Gut microbiota modulation: a novel strategy for prevention and treatment of colorectal cancer. Oncogene. 2020;39(26):4925-43.
628. Sugimura N, Li Q, Chu ESH, Lau HCH, Fong W, Liu W, et al. Lactobacillus gallinarum modulates the gut microbiota and produces anti-cancer metabolites to protect against colorectal tumourigenesis. Gut. 2022;71(10):2011-21.
629. Bar-Shalom R, Bergman M, Grossman S, Azzam N, Sharvit L, Fares F. Inula Viscosa Extract Inhibits Growth of Colorectal Cancer Cells in vitro and in vivo Through Induction of Apoptosis. Frontiers in Oncology. 2019;9.
630. Qu H, Wang Y, Yang F, Wang G, Gao L, Li K. A randomized, controlled trial of intense pulsed light in combination with minocycline hydrochloride for the treatment of inflammatory acne vulgaris. Journal of Cosmetic Dermatology. 2022;21(8):3386-92.
631. Bland PS, Goodson JM, Gunsolley JC, Grossi SG, Otomo-Corgel J, Doherty F, et al. Association of antimicrobial and clinical efficacy: periodontitis

therapy with minocycline microspheres. Journal of the International Academy of Periodontology. 2010;12(1):11-9.
632. Cohen AL, Anker CJ, Johnson B, Burt LM, Shrieve DC, Salzman K, et al. Repeat radiation with bevacizumab and minocycline in bevacizumab-refractory high grade gliomas: a prospective phase 1 trial. Journal of Neuro-Oncology. 2020;148(3):577-85.
633. Dong Z, Abbas MN, Kausar S, Yang J, Li L, Tan L, et al. Biological Functions and Molecular Mechanisms of Antibiotic Tigecycline in the Treatment of Cancers. International Journal of Molecular Sciences. 2019;20(14).
634. Li H, Jiao S, Li X, Banu H, Hamal S, Wang X. Therapeutic effects of antibiotic drug tigecycline against cervical squamous cell carcinoma by inhibiting Wnt/β-catenin signaling. Biochemical and Biophysical Research Communications. 2015;467(1):14-20.
635. Tenbaum SP, Ordóñez-Morán P, Puig I, Chicote I, Arqués O, Landolfi S, et al. β-catenin confers resistance to PI3K and AKT inhibitors and subverts FOXO3a to promote metastasis in colon cancer. Nature Medicine. 2012;18(6):892-901.
636. Xiong H, Zhang Z-G, Tian X-Q, Sun D-F, Liang Q-C, Zhang Y-J, et al. Inhibition of JAK1, 2/STAT3 Signaling Induces Apoptosis, Cell Cycle Arrest, and Reduces Tumor Cell Invasion in Colorectal Cancer Cells. Neoplasia. 2008;10(3):287-97.
637. Lu R, Zhang Y-g, Sun J. STAT3 activation in infection and infection-associated cancer. Molecular and Cellular Endocrinology. 2017;451:80-7.
638. Desjarlais M, Pratt J, Lounis A, Mounier C, Haidara K, Annabi B. Tetracycline Derivative Minocycline Inhibits Autophagy and Inflammation in Concanavalin-A-Activated Human Hepatoma Cells. Gene Regulation and Systems Biology. 2014;8.
639. Anto RJ, Yang B, Lu Y, Zhang A, Zhou A, Zhang L, et al. Doxycycline Induces Apoptosis and Inhibits Proliferation and Invasion of Human Cervical Carcinoma Stem Cells. Plos One. 2015;10(6).
640. Tan J, Song M, Zhou M, Hu Y. Antibiotic tigecycline enhances cisplatin activity against human hepatocellular carcinoma through inducing mitochondrial dysfunction and oxidative damage. Biochemical and Biophysical Research Communications. 2017;483(1):17-23.
641. Liu WT, Huang CY, Lu IC, Gean PW. Inhibition of glioma growth by minocycline is mediated through endoplasmic reticulum stress-induced apoptosis and autophagic cell death. Neuro-Oncology. 2013;15(9):1127-41.
642. Hu B, Guo Y. Inhibition of mitochondrial translation as a therapeutic strategy for human ovarian cancer to overcome chemoresistance. Biochemical and Biophysical Research Communications. 2019;509(2):373-8.
643. Kaufmann SH, Desnoyers S, Ottaviano Y, Davidson NE, Poirier GG. Specific proteolytic cleavage of poly(ADP-ribose) polymerase: an early marker of chemotherapy-induced apoptosis. Cancer Res. 1993;53(17):3976-85.
644. Waetzig V, Herdegen T. A Single c-Jun N-terminal Kinase Isoform (JNK3-p54) Is an Effector in Both Neuronal Differentiation and Cell Death. Journal of Biological Chemistry. 2003;278(1):567-72.
645. Yeung TM, Gandhi SC, Wilding JL, Muschel R, Bodmer WF. Cancer stem cells from colorectal cancer-derived cell lines. 2010;107(8):3722-7.

646. Zhang L, Xu L, Zhang F, Vlashi E. Doxycycline inhibits the cancer stem cell phenotype and epithelial-to-mesenchymal transition in breast cancer. Cell Cycle. 2017;16(8):737-45.
647. Liu H, Tao H, Wang H, Yang Y, Yang R, Dai X, et al. Doxycycline Inhibits Cancer Stem Cell-Like Properties via PAR1/FAK/PI3K/AKT Pathway in Pancreatic Cancer. Frontiers in Oncology. 2021;10.
648. Al-Hajj M, Clarke MF. Self-renewal and solid tumor stem cells. Oncogene. 2004;23(43):7274-82.
649. Scatena C, Roncella M, Di Paolo A, Aretini P, Menicagli M, Fanelli G, et al. Doxycycline, an Inhibitor of Mitochondrial Biogenesis, Effectively Reduces Cancer Stem Cells (CSCs) in Early Breast Cancer Patients: A Clinical Pilot Study. Frontiers in Oncology. 2018;8.
650. Qin Y, Zhang Q, Lee S, Zhong W-l, Liu Y-r, Liu H-j, et al. Doxycycline reverses epithelial-to-mesenchymal transition and suppresses the proliferation and metastasis of lung cancer cells. 2015;6(38).
651. Villarejo A, Cortés-Cabrera Á, Molina-Ortíz P, Portillo F, Cano A. Differential Role of Snail1 and Snail2 Zinc Fingers in E-cadherin Repression and Epithelial to Mesenchymal Transition. Journal of Biological Chemistry. 2014;289(2):930-41.
652. de Sousa e Melo F, Vermeulen L. Wnt Signaling in Cancer Stem Cell Biology. Cancers. 2016;8(7).
653. Su YJ, Chang YW, Lin WH, Liang CL, Lee JL. An aberrant nuclear localization of E-cadherin is a potent inhibitor of Wnt/β-catenin-elicited promotion of the cancer stem cell phenotype. Oncogenesis. 2015;4(6):e157-e.
654. Junttila MR, Mao W, Wang X, Wang B-E, Pham T, Flygare J, et al. Targeting LGR5⁺ cells with an antibody-drug conjugate for the treatment of colon cancer. 2015;7(314):314ra186-314ra186.
655. Kemper K, Prasetyanti PR, De Lau W, Rodermond H, Clevers H, Medema JP. Monoclonal Antibodies Against Lgr5 Identify Human Colorectal Cancer Stem Cells. Stem Cells. 2012;30(11):2378-86.
656. Li D, Yang Z-K, Bu J-Y, Xu C-Y, Sun HUI, Tang J-B, et al. OCT4B modulates OCT4A expression as ceRNA in tumor cells. Oncology Reports. 2015;33(5):2622-30.
657. Zhu Y, Huang S, Chen S, Chen J, Wang Z, Wang Y, et al. SOX2 promotes chemoresistance, cancer stem cells properties, and epithelial–mesenchymal transition by β-catenin and Beclin1/autophagy signaling in colorectal cancer. Cell Death & Disease. 2021;12(5).
658. Chen BFZaW. Dual Roles of Immune Cells and Their Factors in Cancer Development and Progression International Journal of Biological Sciences. 2011; 7:651-8.
659. Clarke WT, Feuerstein JD. Colorectal cancer surveillance in inflammatory bowel disease: Practice guidelines and recent developments. World Journal of Gastroenterology. 2019;25(30):4148-57.
660. Ling A, Lundberg IV, Eklöf V, Wikberg ML, Öberg Å, Edin S, et al. The infiltration, and prognostic importance, of Th1 lymphocytes vary in molecular subgroups of colorectal cancer. The Journal of Pathology: Clinical Research. 2015;2(1):21-31.

661. Raskov H, Orhan A, Christensen JP, Gögenur I. Cytotoxic CD8+ T cells in cancer and cancer immunotherapy. British Journal of Cancer. 2020;124(2):359-67.
662. Garrett WS. The gut microbiota and colon cancer. Science. 2019;364(6446):1133-5.
663. Ibrahim A, Hugerth LW, Hases L, Saxena A, Seifert M, Thomas Q, et al. Colitis-induced colorectal cancer and intestinal epithelial estrogen receptor beta impact gut microbiota diversity. International Journal of Cancer. 2019;144(12):3086-98.
664. Ghanem S, Kim CJ, Dutta D, Salifu M, Lim SH. Antimicrobial therapy during cancer treatment: Beyond antibacterial effects. Journal of Internal Medicine. 2021;290(1):40-56.
665. Zhai R, Xue X, Zhang L, Yang X, Zhao L, Zhang C. Strain-Specific Anti-inflammatory Properties of Two Akkermansia muciniphila Strains on Chronic Colitis in Mice. Frontiers in Cellular and Infection Microbiology. 2019;9.
666. Colombo F, Illescas O, Noci S, Minnai F, Pintarelli G, Pettinicchio A, et al. Gut microbiota composition in colorectal cancer patients is genetically regulated. Scientific Reports. 2022;12(1).
667. Hou X, Zhang P, Du H, Chu W, Sun R, Qin S, et al. Akkermansia Muciniphila Potentiates the Antitumor Efficacy of FOLFOX in Colon Cancer. Frontiers in Pharmacology. 2021;12.
668. Koh GY, Kane A, Wu X, Mason J, Crott J. Parabacteroides Distasonis Attenuates Tumorigenesis, Modulates Inflammatory Markers, and Promotes Intestinal Barrier Integrity in Azoxymethane-treated Mice (OR04-02-19). Current Developments in Nutrition. 2019;3(Supplement_1).
669. Mirzaei R, Afaghi A, Babakhani S, Sohrabi MR, Hosseini-Fard SR, Babolhavaeji K, et al. Role of microbiota-derived short-chain fatty acids in cancer development and prevention. Biomedicine & Pharmacotherapy. 2021;139.
670. Yang J, McDowell A, Kim EK, Seo H, Lee WH, Moon C-M, et al. Development of a colorectal cancer diagnostic model and dietary risk assessment through gut microbiome analysis. Experimental & Molecular Medicine. 2019;51(10):1-15.
671. Wu Y, Jiao N, Zhu R, Zhang Y, Wu D, Wang A-J, et al. Identification of microbial markers across populations in early detection of colorectal cancer. Nature Communications. 2021;12(1).
672. Dong Y, Zhou J, Zhu Y, Luo L, He T, Hu H, et al. Abdominal obesity and colorectal cancer risk: systematic review and meta-analysis of prospective studies. Biosci Rep. 2017;37(6).
673. Jarvis D, Mitchell JS, Law PJ, Palin K, Tuupanen S, Gylfe A, et al. Mendelian randomisation analysis strongly implicates adiposity with risk of developing colorectal cancer. Br J Cancer. 2016;115(2):266-72.
674. Martinez-Useros J, Garcia-Foncillas J. Obesity and colorectal cancer: molecular features of adipose tissue. Journal of Translational Medicine. 2016;14(1).
675. Vasconcelos-Dos-Santos A, Loponte HF, Mantuano NR, Oliveira IA, de Paula IF, Teixeira LK, et al. Hyperglycemia exacerbates colon cancer malignancy through hexosamine biosynthetic pathway. Oncogenesis. 2017;6(3):e306.

676. Kiunga GA, Raju J, Sabljic N, Bajaj G, Good CK, Bird RP. Elevated insulin receptor protein expression in experimentally induced colonic tumors. Cancer Letters. 2004;211(2):145-53.
677. Tran TT, Naigamwalla D, Oprescu AI, Lam L, McKeown-Eyssen G, Bruce WR, et al. Hyperinsulinemia, but not other factors associated with insulin resistance, acutely enhances colorectal epithelial proliferation in vivo. Endocrinology. 2006;147(4):1830-7.
678. Gallagher EJ, LeRoith D. The proliferating role of insulin and insulin-like growth factors in cancer. Trends Endocrinol Metab. 2010;21(10):610-8.
679. Chaudhary SC, Kurundkar D, Elmets CA, Kopelovich L, Athar M. Metformin, an antidiabetic agent reduces growth of cutaneous squamous cell carcinoma by targeting mTOR signaling pathway. Photochem Photobiol. 2012;88(5):1149-56.
680. Back JH, Rezvani HR, Zhu Y, Guyonnet-Duperat V, Athar M, Ratner D, et al. Cancer cell survival following DNA damage-mediated premature senescence is regulated by mammalian target of rapamycin (mTOR)-dependent Inhibition of sirtuin 1. J Biol Chem. 2011;286(21):19100-8.
681. Tomimoto A, Endo H, Sugiyama M, Fujisawa T, Hosono K, Takahashi H, et al. Metformin suppresses intestinal polyp growth in ApcMin/+ mice. Cancer Sci. 2008;99(11):2136-41.
682. Friedrich K, Sommer M, Strobel S, Thrum S, Bluher M, Wagner U, et al. Perturbation of the Monocyte Compartment in Human Obesity. Front Immunol. 2019;10:1874.
683. Hanai H, Iida T, Takeuchi K, Watanabe F, Yamada M, Kikuyama M, et al. Adsorptive depletion of elevated proinflammatory CD14+CD16+DR++ monocytes in patients with inflammatory bowel disease. Am J Gastroenterol. 2008;103(5):1210-6.
684. Mantovani A, Allavena P, Sica A, Balkwill F. Cancer-related inflammation. Nature. 2008;454(7203):436-44.
685. Caer C, Wick MJ. Human Intestinal Mononuclear Phagocytes in Health and Inflammatory Bowel Disease. Front Immunol. 2020;11:410.
686. Frigerio S, Lartey DA, D'Haens GR, Grootjans J. The Role of the Immune System in IBD-Associated Colorectal Cancer: From Pro to Anti-Tumorigenic Mechanisms. Int J Mol Sci. 2021;22(23).
687. Chan IH, Jain R, Tessmer MS, Gorman D, Mangadu R, Sathe M, et al. Interleukin-23 is sufficient to induce rapid de novo gut tumorigenesis, independent of carcinogens, through activation of innate lymphoid cells. Mucosal Immunol. 2014;7(4):842-56.
688. Crusz SM, Balkwill FR. Inflammation and cancer: advances and new agents. Nat Rev Clin Oncol. 2015;12(10):584-96.
689. Johnson DE, O'Keefe RA, Grandis JR. Targeting the IL-6/JAK/STAT3 signalling axis in cancer. Nat Rev Clin Oncol. 2018;15(4):234-48.
690. Sharma C, Pradeep A, Wong L, Rana A, Rana B. Peroxisome proliferator-activated receptor gamma activation can regulate beta-catenin levels via a proteasome-mediated and adenomatous polyposis coli-independent pathway. J Biol Chem. 2004;279(34):35583-94.
691. Fujisawa T, Nakajima A, Fujisawa N, Takahashi H, Ikeda I, Tomimoto A, et al. Peroxisome proliferator-activated receptor gamma (PPARgamma)

suppresses colonic epithelial cell turnover and colon carcinogenesis through inhibition of the beta-catenin/T cell factor (TCF) pathway. J Pharmacol Sci. 2008;106(4):627-38.
692. Yasui Y, Hosokawa M, Sahara T, Suzuki R, Ohgiya S, Kohno H, et al. Bitter gourd seed fatty acid rich in 9c,11t,13t-conjugated linolenic acid induces apoptosis and up-regulates the GADD45, p53 and PPARgamma in human colon cancer Caco-2 cells. Prostaglandins Leukot Essent Fatty Acids. 2005;73(2):113-9.
693. Lei P, Abdelrahim M, Cho SD, Liu S, Chintharlapalli S, Safe S. 1,1-Bis(3'-indolyl)-1-(p-substituted phenyl)methanes inhibit colon cancer cell and tumor growth through activation of c-jun N-terminal kinase. Carcinogenesis. 2008;29(6):1139-47.
694. Kulke MH, Demetri GD, Sharpless NE, Ryan DP, Shivdasani R, Clark JS, et al. A phase II study of troglitazone, an activator of the PPARgamma receptor, in patients with chemotherapy-resistant metastatic colorectal cancer. Cancer journal (Sudbury, Mass). 2002;8(5):395-9.
695. Mueller E, Smith M, Sarraf P, Kroll T, Aiyer A, Kaufman DS, et al. Effects of ligand activation of peroxisome proliferator-activated receptor gamma in human prostate cancer. Proceedings of the National Academy of Sciences of the United States of America. 2000;97(20):10990-5.
696. Berger J, Bailey P, Biswas C, Cullinan CA, Doebber TW, Hayes NS, et al. Thiazolidinediones produce a conformational change in peroxisomal proliferator-activated receptor-gamma: binding and activation correlate with antidiabetic actions in db/db mice. Endocrinology. 1996;137(10):4189-95.
697. Cerdá C, Sánchez C, Climent B, Vázquez A, Iradi A, El Amrani F, et al. Oxidative Stress and DNA Damage in Obesity-Related Tumorigenesis. In: Camps J, editor. Oxidative Stress and Inflammation in Non-communicable Diseases - Molecular Mechanisms and Perspectives in Therapeutics. Cham: Springer International Publishing; 2014. p. 5-17.
698. Kompella P, Vasquez KM. Obesity and cancer: A mechanistic overview of metabolic changes in obesity that impact genetic instability. Mol Carcinog. 2019;58(9):1531-50.
699. Wang Y, Li H. Gut microbiota modulation: a tool for the management of colorectal cancer. J Transl Med. 2022;20(1):178.
700. Shan L, Tyagi A, Shabbir U, Chen X, Vijayalakshmi S, Yan P, et al. The Role of Gut Microbiota Modulation Strategies in Obesity: The Applications and Mechanisms. Fermentation. 2022;8(8).
701. Liu T, Guo Z, Song X, Liu L, Dong W, Wang S, et al. High-fat diet-induced dysbiosis mediates MCP-1/CCR2 axis-dependent M2 macrophage polarization and promotes intestinal adenoma-adenocarcinoma sequence. J Cell Mol Med. 2020;24(4):2648-62.
702. Koh GY, Kane AV, Wu X, Crott JW. Parabacteroides distasonis attenuates tumorigenesis, modulates inflammatory markers and promotes intestinal barrier integrity in azoxymethane-treated A/J mice. Carcinogenesis. 2020;41(7):909-17.
703. Ji Y, Tao T, Zhang J, Su A, Zhao L, Chen H, et al. Comparison of effects on colitis-associated tumorigenesis and gut microbiota in mice between

Ophiocordyceps sinensis and Cordyceps militaris. Phytomedicine. 2021;90:153653.
704. Liu J, Dong W, Zhao J, Wu J, Xia J, Xie S, et al. Gut microbiota profiling variated during colorectal cancer development in mouse. BMC Genomics. 2022;23(Suppl 4):848.
705. Obanda D, Page R, Guice J, Raggio AM, Husseneder C, Marx B, et al. CD Obesity-Prone Rats, but not Obesity-Resistant Rats, Robustly Ferment Resistant Starch Without Increased Weight or Fat Accretion. Obesity (Silver Spring). 2018;26(3):570-7.
706. Barouei J, Bendiks Z, Martinic A, Mishchuk D, Heeney D, Hsieh YH, et al. Microbiota, metabolome, and immune alterations in obese mice fed a high-fat diet containing type 2 resistant starch. Mol Nutr Food Res. 2017;61(11).
707. Jain T, Sharma P, Are AC, Vickers SM, Dudeja V. New Insights Into the Cancer-Microbiome-Immune Axis: Decrypting a Decade of Discoveries. Front Immunol. 2021;12:622064.
708. Yu LC, Wei SC, Li YH, Lin PY, Chang XY, Weng JP, et al. Invasive Pathobionts Contribute to Colon Cancer Initiation by Counterbalancing Epithelial Antimicrobial Responses. Cell Mol Gastroenterol Hepatol. 2022;13(1):57-79.
709. Ridlon JM, Wolf PG, Gaskins HR. Taurocholic acid metabolism by gut microbes and colon cancer. Gut Microbes. 2016;7(3):201-15.
710. Wang Q, Wang K, Wu W, Lv L, Bian X, Yang L, et al. Administration of Bifidobacterium bifidum CGMCC 15068 modulates gut microbiota and metabolome in azoxymethane (AOM)/dextran sulphate sodium (DSS)-induced colitis-associated colon cancer (CAC) in mice. Appl Microbiol Biotechnol. 2020;104(13):5915-28.
711. Busi SB, Leon KBD, Wall JD, Amos-Landgraf JM. Abstract 4987: Biofilm-producing sulfate-reducing bacteria suppress tumor burden in a rat model of colon cancer. Cancer Research. 2018;78(13_Supplement):4987-.
712. Nova E, Gomez-Martinez S, Gonzalez-Soltero R. The Influence of Dietary Factors on the Gut Microbiota. Microorganisms. 2022;10(7).
713. Zhang C, Zhang M, Pang X, Zhao Y, Wang L, Zhao L. Structural resilience of the gut microbiota in adult mice under high-fat dietary perturbations. ISME J. 2012;6(10):1848-57.

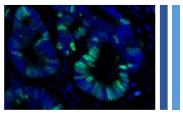

ABBREVIATIONS

ABBREVIATIONS

A

ABCB1: ATP binding cassette subfamily B 1

ABCG1: ATP binding cassette subfamily G 1

ADSCs: adipose tissue-derived stem cells

AIF: apoptosis inducing factor

ALDH1: aldehyde dehydrogenase 1

AMPK: AMP-activated protein kinase

ANGPT: angiopoietin

ANXV: Annexin V

AOM: azoxymethane

APAF-1: apoptosis protease-activating factor-1

APC: *Adenomatous polyposis coli*

ASVs: amplicon sequence variants

ATF: activating transcription factor

AUC: area under the curve

B

BAK: BCL-2 antagonist killer

BAT: brown adipose tissue

BAX: BCL-2-associated x protein

BCA: bicinchoninic acid

Bcl: B cell lymphoma

Bcl-xL: Bcl-extra large

BID: BH3 Interacting Domain Death Agonist

BIP: immunoglobulin-binding protein

BSA: bovine serum albumin

BSH: bile salt hydrolase

C

C/EBPα: CCAT/enhancer binding protein

CAC: colitis-associated CRC

CAD: caspase-activated DNAse

CASPs: caspases

CCL-20: CC-chemokine-ligand-20

CDH1: E-cadherin 1

cDNA: complementary DNA

CHOP: C/EBP homologous protein (DDIT3)

CIMP: CpG island methylator phenotype

CK1: casein kinase 1

CM: conditioned medium

CMS: consensus Molecular Subtypes

COX-2: cyclooxigease-2

CRC: colorectal cancer

CRE: ATF/cAMP response elements

CSC: cancer stem cell

CSK-3: glycogen synthase kinase 3

CTLs: cytotoxic T lymphocytes

CTNNB1: β-catenin

D

DAI: Disease Activity Index

DEAB: N,N-diethylaminobenzaldehyde, ALDH inhibitor

DIABLO: direct IAP-binding protein with low PI

DISC: death inducing signaling complex

DMEM: Dulbecco's modified Eagle's medium

DMSO: Dimethyl sulfoxide

DPPH: 1,1-diphenyl-2-picrylhydrazyl

DR5*:* death-receptor 5

DSS: dextran sulfate sodium

DTT: Dithiothreitol

E

4E-BP1: 4E-binding protein 1

EB1: end-binding 1

EDTA: Ethylenediamine tetraacetic acid

EGF: epidermal growth factor

EGFR: epidermal growth factor receptor

EGTA: ethylene glycol-bis(β-aminoethyl ether)-N,N,N′,N′-tetraacetic acid

EMT: epithelial-mesenchymal transition

ER: endoplasmic reticulum

ERK: extracellular-signal-regulated kinase

F

5-FU: 5-fluorouracil

F/B: *Firmicutes*/*Bacteroidetes*

FABP4: fatty acid binding protein 4

FAP: familial adenomatous polyposis

FasL: Fas ligand

FasR: Fas receptor

FBS: fetal bovine serum

FDA: Food and Drug Administration

FGF: fibroblast growth factor

FLOX: 5-FU + leucovorin

FMT: fecal microbiota transplantation

FOLFIRI: irinotecan + 5-FU + leucovorin

FOLFOX: 5-FU + oxaliplatin

G

GLUT2: Glucose transporter type 2

GRP78: glucose-regulated protein 78

GTT: glucose tolerance test

H

4-HNE: 4-hydroxy-2-nonenal

HAT: histone acetyltransferases

HCAM: homing cell adhesion molecule

HDACs: histone deacetylase

HDL: high-density lipoprotein

HDLG: human disc large

HEPES: 4-(2-hydroxyethyl)-1-piperazineethanesulfonic acid

HER1: human growth factor 1

HFD: high fat diet

HIF1α: hypoxia-inducible factor-1α

HOMA-IR: Homeostasis Model Assessment - Insulin Resistance

I

IAPs: inhibitor of apoptosis proteins

IBD: inflammatory bowel disease.

IBS: irritable bowel syndrome

IC50: half maximal inhibitory concentration

IFNγ: interferon gamma

IGF2: insulin-like growth factor 2

IL-6R: IL-6 receptor

IMIDA: Instituto Murciano de Investigación y Desarrollo Agrario y Alimentario

iNOS: inducible NO synthase

IP3Rs: inositol 1,4,5-trisphosphate receptors

IRE1: inositol-requiring enzyme 1

ISAPP: International Scientific association of Probiotics and Prebiotics

J

JAK: Janus kinase

JNK: c-Jun N-terminal kinase

L

LDA: linear discriminant analysis

LDL: low-density lipoprotein

LGR5: Leucine-rich repeat-containing G-protein coupled receptor 5

LPS: lipopolysaccharide

M

M1 or **M2**: macrophage type 1 or 2

MAE: *Morus alba* extract

MAPK: mitogen-activated protein kinase

MDA: malondialdehyde

MET: metformin

MFI: Mean Fluorescence Intensity

miRNAs: micro-RNAs or small non-coding RNAs

MLN: mesenteric lymph nodes

MMPs: metalloproteinases

mTORC: mammalian target of rapamycin complex

MTS: 5-(3-carboxymethoxyphenyl)-2-(4,5-dimethylthiazoly)-3-(4-sulfophenyl)tetrazolium- inner salt

Muc: Mucin

N

NADPH: nicotinamide adenine dinucleotide phosphate

NAFLD: non-alcoholic fatty liver disease

NANOG: Nanog homeobox

NF-κB: nuclear factor-kappaB

NLRP3: NOD-like receptor family pyrin domain containing 3

NO: nitric oxide

NOXA: also called PMAIP1 (Phorbol-12-myristate-13-acetate-induced protein 1)

NSAIDs: non-steroidal anti-inflammatory drugs

NSG mice: NOD scid gamma mouse (extremely immunodeficient mouse)

O

OTU: operational taxonomic unit

P

PARP: poly (ADP-ribose) polymerase

PBS: phosphate buffered saline

PCoA: Principal Coordinate Analysis

PERK: protein kinase RNA-like ER kinase

PFA: paraformaldehyde

PGE2: prostaglandin E2

PI: propidium iodide

PI3K: phosphoinositide-3-kinase

PIAS3: E3 SUMO-protein ligase

PIP_2: phosphorylates phosphatidylinositol 4,5 biphosphate

PIP_3: phosphatidylinositol 3,4,5 triphosphate

PKB: protein kinase B

PMSF: phenylmethylsulfonyl fluoride

POU5F1: POU Class 5 Homeobox 1, also called OCT4

PPI: Proton-Pump inhibitors

PP2A: protein phosphatase 2A

PUMA: p53 upregulated modulator of apoptosis

R

RDP: Ribosomal Database Project

RHEB: Ras homolog enriched in brain

ROS: reactive oxygen species

rRNA: ribosomal RNA

RSA: radical DPPH scavenging activity

RyRs: ryanodine receptors

S

S6K: S6 kinase

SAPK: stress-activated protein kinase

SCFA: short-chain fatty acids

SCID: severe combined immune-deficient

SD: standard diet

Ser/THr kinase: serine/threonine protein kinase

SERCA: sarco/endoplasmic-reticulum Ca^{2+}-ATPase

SFE: Sphere forming efficiency

SFE: sphere-forming efficiency

SLUG: also called SNAI2

SMAC: second mitochondria-derived activator of caspase

SNAI1: Snail Family Transcriptional Repressor 1

SOCS3: suppressor of cytokine signaling 3

SOX2: SRY-box transcription factor 2

SREBP1: sterol regulatory element-binding protein-1

STAT: signal transducer and activator of transcription

T

T25: tigecycline 25 µM (*in vitro* studies) / 25 mg/Kg/day (*in vivo* studies)

T50: tigecycline 50 µM (*in vitro* studies) / 50 mg/Kg/day (*in vivo* studies)

TAMs: tumor-associated macrophages

TBA: thiobarbituric acid

TBARS: thiobarbituric acid reactive substances

tBID: truncation of BID

Tc1: cytotoxic T cell type 1

Tcf/Lef1: T-cell factor/Lymphoid enhancer factor 1

TGF-β: transforming growth factor-β

Th: T-helper

TLR: Toll-like receptor

TMAO: trimethylamine N-oxide

TNF: tumor necrosis factor

TNFR1: tumor necrosis factor receptor 1

TNM: Tumor/Nodes/Metastasis

***TP53*:** tumor protein 53

Treg: regulatory T

TSC2: tuberous sclerosis complex 2

TUNEL: Terminal deoxynucleotidyl transferase dUTP nick end labeling

TWISTs: twist family helix-loop-helix transcription factors

Tyk2: Tyrosine kinase 2

U

UCP1: uncoupling protein-1

ULK1: Unc-51-like kinase 1

UPR: unfolded protein response

V

VEGF: vascular endothelial growth factor

VIM: vimentin

W

W/L: weight/length

WAT: white adipose tissue

WHO: World Health Organization

X

XELOX: capecitabine + oxaliplatin

Z

ZEBs: zinc-finger E-box-binding homeobox family proteins

Zo-1: zonula occludens 1

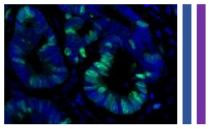

ANNEX

ANNEX

Antonio Jesus Ruiz Malagón is a predoctoral fellow within the "Formación de Profesorado Universitario" programme (FPU-Ministry of Science, Innovation and Universities, Spanish Government (FPU17/04689)). During his training, he has worked within the research group "Pharmacology of natural products". Here, he has participated in different projects and consequently several studies have been published in international scientific journals with high impact factor. Moreover, the PhD student has completed different courses, attended at national and international congresses, and he has participated in international predoctoral stays.

Scientific production: Publications and scientific documents.

1. García-Nicolás M, Pastor-Belda M, Campillo N, Rodríguez-Sojo MJ, **Ruiz-Malagón AJ**, Hidalgo-García L, Abad P, de la Torre JM, Guillamón E, Baños A, Gálvez J, Viñas P, Arroyo-Manzanares N. Analytical Platform for the Study of Metabolic Pathway of Propyl Propane Thiosulfonate (PTSO) from Allium spp. Foods. 2023; 12(4):823. https://doi.org/10.3390/foods12040823.

2. Rodríguez-Sojo MJ, Garcia-Garcia J, **Ruiz-Malagón AJ**, Diez-Echave P, Hidalgo-García L, Molina-Tijeras JA, González-Lozano E, López-Escanez L, Rodríguez-Cabezas ME, Rodríguez-Sánchez MJ, Rodríguez-Nogales A, Mediavilla C, Galvez J. Beneficial Effects of *Limosilactobacillus fermentum* in the DCA Experimental Model of Irritable Bowel Syndrome in Rats. Nutrients. 2022; 15(1):24. doi: 10.3390/nu15010024.

3. **Ruiz-Malagón AJ,** Rodríguez-Sojo MJ, Rodríguez-Cabezas ME, Gálvez J, Rodríguez-Nogales A. *Limosilactobacillus fermentum* CECT5716: Mechanisms and Therapeutic Insights. Nutrients. 2021; 13(3):1016. doi:10.3390/nu13031016.

4. **Ruiz-Malagón AJ**, Rodríguez-Sanchez MJ, Rodríguez-Sojo MJ, Vezza T, Pischel I, Algieri F, Rodríguez-Cabezas ME, Rodríguez-Nogales A, Gálvez J. Intestinal anti-inflammatory and visceral analgesic effects of a *Serpylli herba*

extract in an experimental model of irritable bowel syndrome in rats. Front Pharmacol. 2022;13:967644. doi: 10.3389/fphar.2022.967644

5. Diez-Echave P, Vezza T, Algieri F, **Ruiz-Malagón AJ**, Hidalgo-García L, García F, Morón R, Sánchez M, Toral M, Romero M, Duarte J, Garrido-Mesa J, Rodríguez-Cabezas ME, Rodríguez-Nogales A, Gálvez J. The melatonergic agonist agomelatine ameliorates high fat diet-induced obesity in mice through the modulation of the gut microbiome. Biomed Pharmacother. 2022; 153:113445. doi:10.1016/j.biopha.2022.113445.

6. **Ruiz-Malagón AJ**, Rodríguez-Sojo MJ, Hidalgo-García L, Molina-Tijeras JA, García F, Pischel I, Romero M, Duarte J, Diez-Echave P, Rodríguez-Cabezas ME, Rodríguez-Nogales A, Gálvez J. The Antioxidant Activity of *Thymus serpyllum* Extract Protects against the Inflammatory State and Modulates Gut Dysbiosis in Diet-Induced Obesity in Mice. Antioxidants (Basel). 2022;11(6):1073. doi: 10.3390/antiox11061073.

7. Tijani RO, Molina-Tijeras JA, Vezza T, **Ruiz-Malagón AJ**, Cádiz-Gurrea ML, Segura-Carretero A, Abiodun OO, Galvez J. Myrianthus arboreus P. Beauv improves insulin sensitivity in high fat diet-induced obese mice by reducing inflammatory pathways activation. J Ethnopharmacol. 2022 Jan 10;282:114651. doi: 10.1016/j.jep.2021.114651. Epub 2021 Sep 16. PMID: 34537282.

8. Vezza T, Garrido-Mesa J, Diez-Echave P, Hidalgo-García L, **Ruiz-Malagón AJ**, García F, Sánchez M, Toral M, Romero M, Duarte J, Guillamón E, Baños Arjona A, Moron R, Galvez J, Rodríguez-Nogales A, Rodríguez-Cabezas ME. *Allium*-Derived Compound Propyl Propane Thiosulfonate (PTSO) Attenuates Metabolic Alterations in Mice Fed a High-Fat Diet through Its Anti-Inflammatory and Prebiotic Properties. Nutrients. 2021;13(8):2595. doi: 10.3390/nu13082595.

9. **Ruiz-Malagón AJ**, Diez-Echave P, Molina-Tijeras JA, Hidalgo-García L, Vezza T, Cenis-Cifuentes L, Rodríguez-Sojo MJ, Cenis JL, Rodríguez-Cabezas ME, Rodríguez-Nogales A, Gálvez J, Lozano-Pérez AA. Silk fibroin nanoparticles enhance quercetin immunomodulatory properties in DSS-induced mouse colitis. Int J Pharm. 2021; 606:120935. doi: 10.1016/j.ijpharm.2021.120935.

10. Diez-Echave P, Vezza T, Rodríguez-Nogales A, Hidalgo-Garcia L, Garrido-Mesa J, **Ruiz-Malagon AJ**, Molina-Tijeras JA, Romero M, Robles-Vera I, Leyva-Jiménez FJ, Lozano-Sanchez J, Arráez-Román D, Segura-Carretero A, Micol V, García F, Morón R, Duarte J, Rodríguez-Cabezas ME, Gálvez J. The Beneficial Effects of Lippia Citriodora Extract on Diet-Induced Obesity in Mice Are Associated with Modulation in the Gut Microbiota Composition. Mol Nutr Food Res. 2020;64(13):e2000005. doi: 10.1002/mnfr.202000005.

11. Hidalgo-Garcia L, Molina-Tijeras JA, Huertas-Peña F, **Ruiz-Malagón AJ**, Diez-Echave P, Vezza T, Rodríguez-Sojo MJ, Morón R, Becerra-Massare P, Rodríguez-Nogales A, Gálvez J, Rodríguez-Cabezas ME, Anderson P. Intestinal mesenchymal cells regulate immune responses and promote epithelial regeneration in vitro and in dextran sulfate sodium-induced experimental colitis in mice. Acta Physiol (Oxf). 2021;233(2):e13699. doi: 10.1111/apha.13699.

12. Molina-Tijeras JA, Diez-Echave P, Vezza T, Hidalgo-García L, **Ruiz-Malagón AJ**, Rodríguez-Sojo MJ, Romero M, Robles-Vera I, García F, Plaza-Diaz J, Olivares M, Duarte J, Rodríguez-Cabezas ME, Rodríguez-Nogales A, Gálvez J. *Lactobacillus fermentum* CECT5716 ameliorates high fat diet-induced obesity in mice through modulation of gut microbiota dysbiosis. Pharmacol Res. 2021;167:105471. doi: 10.1016/j.phrs.2021.105471.

13. Diez-Echave P, Vezza T, Rodríguez-Nogales A, **Ruiz-Malagón AJ**, Hidalgo-García L, Garrido-Mesa J, Molina-Tijeras JA, Romero M, Robles-Vera I, Pimentel-Moral S, Borras-Linares I, Arráez-Román D, Segura-Carretero A, Micol V, García F, Duarte J, Rodríguez-Cabezas ME, Gálvez J. The prebiotic properties of Hibiscus sabdariffa extract contribute to the beneficial effects in diet-induced obesity in mice. Food Res Int. 2020;127:108722. doi: 10.1016/j.foodres.2019.108722.

14. **Ruiz-Malagón AJ**, Leyva-Jiménez FJ, Molina-Tijeras JA, Diez-Echave P, Vezza T, Hidalgo-García L, Lozano-Sánchez J, Arráez-Román D, Cenis JL, Lozano-Pérez AA, Rodríguez-Nogales A, Segura-Carretero A, Gálvez J. Comparative Study of the Antioxidant and Anti-Inflammatory Effects of Leaf Extracts from Four

Different *Morus alba* Genotypes in High Fat Diet-Induced Obesity in Mice. Antioxidants (Basel). 2020;9(8):733. doi: 10.3390/antiox9080733.

Works submitted to national or international conferences.

1. Evaluación del efecto antitumoral de la tigeciclina en un modelo experimental de cáncer colorrectal asociado a colitis: impacto en la composición de la microbiota intestinal. III Jornadas de Jóvenes Investigadores. Granada, Spain, 2022. Authors: Antonio Jesús Ruiz Malagón; Laura Hidalgo García; María Jesús Rodríguez Sojo; Jose Alberto Molina Tijeras; Federico García; Patricia Díez Echave; Teresa Vezza; Patricia Becerra; Juan Antonio Marchal; Eduardo Redondo Cerezo; Martin Hausmann; Gerhard Rogler; José Garrido Mesa; María Elena Rodríguez Cabezas; Alba Rodríguez Nogales; Julio Gálvez. Type of participation: oral communication.

2. Actividad antitumoral del Limosilactobacillus fermentum CECT5716 en un modelo experimental de cáncer colorrectal asociado a colitis: impacto sobre la composición del microbioma intestinal. XIII Workshop Sociedad Española de Microbiota, Probióticos y Prebióticos (SEMiPyP 2021). Valencia, Spain, 2022. Authors: Molina-Tijeras JA; Ruiz-Malagón AJ; Hidalgo-García L; Díez-Echave P; Rodríguez-Sojo MJ; Vezza T; Bañuelos-O; Olivares M; Rodríguez Cabezas M.E.; Rodríguez Nogales A.; Gálvez J. Type of participation: poster.

3. El extracto Serpilly herba mejora la inflamación, esteatosis hepática y disbiosis intestinal asociados a obesidad. XIII Workshop Sociedad Española de Microbiota, Probióticos y Prebióticos (SEMiPyP 2021). Valencia, Spain, 2022. Authors: Rodríguez-Sojo MJ; Ruiz-Malagón AJ; Hidalgo-García L; Molina-Tijeras JA; García F; Ivo P; Romero M; Duarte J; Díez-Echave P; Rodríguez Cabezas M.E.; Rodríguez Nogales A.; Gálvez J. Type of participation: poster.

4. Evaluación de la capacidad inmunomoduladora de vesículas extracelulares del probiótico Limosilactobacillus fermentum CECT5716. XIII Workshop Sociedad Española de Microbiota, Probióticos y Prebióticos (SEMiPyP 2021). Valencia, Spain, 2022. Authors: López-Escánez L; Rodríguez-Sojo MJ; Molina-Tijeras JA;

Ruiz-Malagón AJ; Hidalgo-García L; Díez-Echave P; Rodríguez Cabezas M.E.; Gálvez J; Rodríguez Nogales A. Type of participation: poster.

5. La disbiosis producida en la obesidad incrementa la inflamación y tumorigénesis del cáncer colorrectal. XIII Workshop Sociedad Española de Microbiota, Probióticos y Prebióticos (SEMiPyP 2021). Valencia, Spain, 2022. Authors: Ruiz-Malagón AJ; Molina-Tijeras JA; Rodríguez-Sojo MJ; Hidalgo-García L; Díez-Echave P; Vezza T; Rodríguez Cabezas M.E.; Rodríguez Nogales A.; Marchal J.A.; Gálvez J. Type of participation: oral communication.

6. Las células mesenquimales intestinales modulan la microbiota intestinal en un modelo preclínico de cáncer colorrectal. XIII Workshop Sociedad Española de Microbiota, Probióticos y Prebióticos (SEMiPyP 2021). Valencia, Spain, 2022. Authors: Hidalgo-García L; Ruiz-Malagón AJ; Huertas-Peña F; Mirón-Pozo B; Molina-Tijeras JA; Rodríguez-Sojo MJ; Díez-Echave P; Vezza T; López-Escánez L; Morón R; Becerra-Massare P; Rodríguez Nogales A.; Gálvez J; Rodríguez Cabezas M.E.; Anderson P. Type of participation: oral poster.

7. Efecto de Limosilactobacillus fermentum CECT5716 en un modelo experimental de cáncer colorrectal asociado a colitis: impacto en la modulación del sistema inmune. XII Reunión de Jóvenes Farmacólogos de Andalucía. Sevilla, Spain, 2022. Authors: Molina-Tijeras JA; Ruiz-Malagón AJ; Hidalgo-García L; Díez-Echave P; Rodríguez-Sojo MJ; Vezza T; Bañuelos O; Olivares M; Rodríguez Cabezas M.E.; Rodríguez Nogales A.; Gálvez J. Type of participation: oral communication.

8. Estudio del impacto de la disbiosis intestinal producida en la obesidad y la modulación de esta mediante trasplante de microbiota fecal en el cáncer colorrectal asociado a colitis. XII Reunión de Jóvenes Farmacólogos de Andalucía. Sevilla, Spain, 2022. Authors: Ruiz-Malagón AJ; Molina-Tijeras JA; Rodríguez-Sojo MJ; Hidalgo-García L; Díez-Echave P; Vezza T; Rodríguez Cabezas M.E.; Rodríguez Nogales A.; Marchal J.A.; Gálvez J. Type of participation: oral communication.

9. Impacto del tratamiento oral de diferentes extractos de Morus alba en un modelo experimental de obesidad. XII Reunión de Jóvenes Farmacólogos de Andalucía.

Sevilla, Spain, 2022. Authors: Rodríguez-Sojo MJ; Ruiz-Malagón AJ; Hidalgo-García L; Díez-Echave P; Molina-Tijeras JA; Romero M; Duarte J; Rodríguez Cabezas M.E.; Rodríguez Nogales A.; Gálvez J. Type of participation: oral communication.

10. Intestinal mesenchymal cells modulate inflammation and gut microbiota composition in a mouse model of inflammation-induced colorectal cancer. XII Reunión de Jóvenes Farmacólogos de Andalucía. Sevilla, Spain, 2022. Authors: Hidalgo-García L; Ruiz-Malagón AJ; Huertas-Peña F; Mirón-Pozo B; Molina-Tijeras JA; Rodríguez-Sojo MJ; Díez-Echave P; Vezza T; López-Escánez L; Rodríguez Nogales A.; Gálvez J; Rodríguez Cabezas M.E.; Anderson P. Type of participation: oral communication.

11. Marcadores ómicos en pacientes con COVID-19 como predictores de la evolución de la enfermedad. XII Reunión de Jóvenes Farmacólogos de Andalucía. Sevilla, Spain, 2022. Authors: Díez-Echave P; Hidalgo-García L; Ruiz-Malagón AJ; Molina-Tijeras JA; Rodríguez-Sojo MJ; López-Pérez D; Redruello-Romero A; Martín-Castaño B; Martínez-Zaldívar M; Mota E; Cobo F; Álvarez-Estevez M; García F; Morales-García C; Merlos S; García-Flores P; Colmenero-Ruiz M; Pérez del Palacio J; López-Cobo A; Vicente F; Hernández Quero J; Nuñez M; Rodríguez Cabezas M.E.; Carazo A; Martín J; Rodríguez Nogales A.; Morón R; Gálvez J. Type of participation: oral communication.

12. Evaluación del efecto antitumoral de la tigeciclina en un modelo experimental de cáncer colorrectal asociado a colitis: impacto en la composición de la microbiota intestinal. II Congreso Investigación PTS. Granada, Spain, 2022. Authors: Antonio Jesus Ruiz Malagón; Laura Hidalgo García; Maria Jesús Rodríguez Sojo; Jose Alberto Molina Tijeras; Patricia Diez Echave; Teresa Vezza; Jose Garrido Mesa; Maria Elena Rodríguez Cabezas; Alba Rodríguez Nogales; Juan Marchal; Julio Gálvez. Type of participation: oral communication.

13. Impacto del probiótico Limosilactobacillus fermentum CECT5716 en un modelo experimental de cáncer asociado a colitis: evaluación del efecto antitumoral antiinflamatorio. II Congreso Investigación PTS. Granada, Spain, 2022. Authors: Jose Alberto Molina Tijeras; Antonio Jesus Ruiz Malagón; Laura Hidalgo García; Patricia Diez Echave; Maria Jesús Rodríguez Sojo; Teresa Vezza; Bañuelos O;

Mónica Olivares; Maria Elena Rodríguez Cabezas; Alba Rodríguez Nogales; Julio Gálvez. Type of participation: Poster.

14. La modulación de la inflamación intestinal mediada por células mesenquimales estromales del intestino humano reduce el cáncer colorectal asociado a colitis. II Congreso Investigación PTS. Granada, Spain, 2022. Auhtors: Laura Hidalgo García; Antonio Jesus Ruiz Malagón; Francisco Huertas Peña; Mirón-Pozo B; Jose Alberto Molina Tijeras; Maria Jesús Rodríguez Sojo; Patricia Diez Echave; Teresa Vezza; Rocío Moron; Patricia Becerra Massare; Alba Rodríguez Nogales; Julio Gálvez; Maria Elena Rodríguez Cabezas; Per Anderson. Type of participation: oral communication.

15. Marcaodres ómicos en pacientes con COVID como predictores de la evolución de la enfermedad-19II Congreso Investigación PTS. Granada, Spain, 2022. Auhtors: Díez-Echave P; Hidalgo-García L; Ruiz-Malagón AJ; Molina-Tijeras JA; Rodríguez-Sojo MJ; López-Pérez D; Redruello-Romero A; Martín-Castaño B; Martínez-Zaldívar M; Mota E; Cobo F; Álvarez-Estevez M; García F; Morales-García C; Merlos S; García-Flores P; Colmenero-Ruiz M; Pérez del Palacio J; López-Cobo A; Vicente F; Hernández Quero J; Nuñez M; Rodríguez Cabezas M.E.; Carazo A; Martín J; Rodríguez Nogales A.; Morón R; Gálvez J. Type of participation: oral communication.

16. Antitumor effect of tigecycline in a colitis-associated colorectal cancer murine model: impact on gut microbiota composition. XII Workshop Sociedad Española de Microbiota, Probióticos y Prebióticos (SEMiPyP 2021). Madrid, Spain, 2021. Authors: Ruiz-Malagón AJ; Hidalgo-García L; Rodríguez-Sojo MJ; Molina-Tijeras JA; Díez-Echave P; Vezza T; Garrido Mesa J.; Rodríguez Cabezas M.E.; Rodríguez Nogales A.; Marchal J.A.; Gálvez J. Type of participation: oral communication.

17. Evaluación del efecto antitumoral del probiótico Limosilactobacillus fermentum CECT5716 en un modelo experimental de cáncer colorrectal. XII Workshop Sociedad Española de Microbiota, Probióticos y Prebióticos (SEMiPyP 2021). Madrid, Spain, 2021. Authors: Molina-Tijeras JA; Ruiz-Malagón AJ; Hidalgo-García L; Díez-Echave P; Rodríguez-Sojo MJ; Vezza T; Bañuelos Ó; Olivares

M; Rodríguez Cabezas ME; Rodríguez Nogales A; Gálvez J. Type of participation: poster.

18. Intestinal mesenchymal cells modulate gut microbiota composition in DSS-induced colitis in mice. XII Workshop Sociedad Española de Microbiota, Probióticos y Prebióticos (SEMiPyP 2021). Madrid, Spain, 2021. Authors: Hidalgo-García L; Molina-Tijeras JA; Huertas-Peña F; Ruiz-Malagón AJ; Díez-Echave P; Vezza T; Rodríguez-Sojo MJ; Morón R; Becerra-Massare P; Rodríguez Nogales A.; Gálvez J; Rodríguez Cabezas ME; Anderson P. Type of participation: oral communication.

19. Metabolic and anti-inflammatory effects of an olive leaf extract (OLE) in a fecal microbiota transplant model (FMT) in obese mice. XII Workshop Sociedad Española de Microbiota, Probióticos y Prebióticos (SEMiPyP 2021). Madrid, Spain, 2021. Authors: Vezza T; Molina-Tijeras JA; Díez-Echave P; Ruiz-Malagón AJ; Hidalgo-García L; Rodríguez-Sojo MJ; Rodríguez-Nogales A; Romero M; Robles Vera I; Martín-García B; Gómez-Caravaca AM; Arráez-Román D; Segura-Carretero A; Duarte J; Rodríguez-Cabezas ME; Gálvez J. Type of participation: oral communication.

20. Antitumor effect of tigecycline in a colitis-associated colorectal cancer murine model. LXXX Congreso de la Sociedad Española de Patología Digestiva. Madrid, Spain, 2021. Authors: Antonio Jesús Ruiz Malagón; Laura Hidalgo García; María Jesús Rodríguez Sojo; Jose Alberto Molina Tijeras; Patricia Diez Echave; Teresa Vezza; Alba Rodríguez Nogales; María Elena Rodríguez Cabezas; Juan Antonio Marchal Corrales; Julio Gálvez Peralta. Type of participation: oral communication.

21. Intestinal mesenchymal cells regulate immune resonses and promote epithelial regeneration in-vitro and in DSS-induced experimental colitis. LXXX Congreso de la Sociedad Española de Patología Digestiva. Madrid, Spain, 2021. Authors: Laura Hidalgo García; José Alberto Molina Tijeras; Francisco Huertas Peña; Antonio Jesus Ruíz Malagón; Patricia Diez Echave; Teresa Vezza; Maria Jesus Rodríguez Sojo; Rocío Morón Romero; Patricia Becerra Massare; Alba

Rodríguez Nogales; Julio Juan Gálvez Peralta; Maria Elena Rodríguez Cabezas; Per Anderson. Type of participation: oral communication.

22. Lactobaccillus fermentum CECT5716 Exerts beneficial effects in an experimental model of irritable bowel syndrome induced by DCA in Rats. LXXX Congreso de la Sociedad Española de Patología Digestiva. Madrid, Spain, 2021. Authors: Maria Jesus Rodríguez Sojo; Patricia Diez Echave; Antonio Jesus Ruíz Malagón; José Alberto Molina Tijeras; Laura Hidalgo García; Maria Elena Rodríguez Cabezas; Julio Juan Gálvez Peralta; Alba Rodríguez Nogales. Type of participation: oral communication.

23. Silk fibroin nanoparticles enhance quercetin immunomodulatoroy properties in DSS-induced mouse colitis. LXXX Congreso de la Sociedad Española de Patología Digestiva. Madrid, Spain, 2021. Authors: Patricia Diez Echave; Antonio Jesus Ruíz Malagón; José Alberto Molina Tijeras; Laura Hidalgo García; Teresa Vezza; Luis Cenis Cifuentes; Maria Jesus Rodríguez Sojo; Maria Elena Rodríguez Cabezas; Alba Rodríguez Nogales; Julio Juan Gálvez Peralta; Abel Lozano Pérez. Type of participation: poster.

24. The intestinal antiinflammatory effects of minocycline in DSS-induced colitis are associated with an amelioration in the inflammation-associated visceral pain. LXXX Congreso de la Sociedad Española de Patología Digestiva. Madrid, Spain, 2021. Authors: José Alberto Molina Tijeras; Teresa Vezza; Patricia Diez Echave; Laura Hidalgo García; Antonio Jesus Ruíz Malagón; Maria Jesus Rodríguez Sojo; R González Cano; Maria Elena Rodríguez Cabezas; Alba Rodríguez Nogales; Enrique J Cobos; Julio Juan Gálvez Peralta. Type of participation: oral communication.

25. Antiproliferative effect of Tigecycline on HCT-116 xenograft tumor in mice. IV National Congress for Young Researchers in Biomedicine. Granada, Spain, 2020. Authors: Antonio Jesús Ruiz Malagón; Carmen Griñán Lisón; María Jesús Rodríguez Sojo; Teresa Vezza; Laura Hidalgo García; Jose Alberto Molina Tijeras; Patricia Diez Echave; Alba Rodríguez Nogales; María Elena Rodríguez Cabezas; Juan Antonio Marchal Corrales; Julio Gálvez Peralta. Type of participation: oral communication.

26. Effects of quercetin loaded silk fibroin nanoparticles in DSS experimental colitis in mice. IV National Congress for Young Researchers in Biomedicine. Granada, Spain, 2020. Authors: Díez-Echave P; Vezza T; Ruiz-Malagón AJ; Molina-Tijeras JA; Hidalgo-García L; Rodríguez-Cabezas ME; Lozano-Pérez A.; Cenis JL; Gálvez J. Type of participation: poster.

27. Immunomodulatory properties of human intestinal mesenchymal cells on peripheral blood mononuclear cells, macrophages and epithelial cells. IV National Congress for Young Researchers in Biomedicine. Granada, Spain, 2020. Authors: Hidalgo-García L; Molina-Tijeras JA; Huertas-Peña F; Ruiz-Malagón AJ; Díez-Echave P; Vezza T; Rodríguez-Sojo MJ; Morón R; Becerra Massare; Rodríguez-Nogales A; Gálvez J; Rodríguez-Cabezas ME; Anderson P. Type of participation: poster.

28. Lactobacillus fermentum CECT5716 ameliorates high fat diet-induced obesity in mice through modulation of gut microbiota dysbiosis. IV National Congress for Young Researchers in Biomedicine. Granada, Spain, 2020. Authors: Molina-Tijeras JA; Díez-Echave P; Hidalgo-García L; Ruiz-Malagón AJ; Rodríguez-Sojo MJ; Romero M; Robles-Vera I; García F; Rodríguez-Cabezas ME; Plaza-Diaz J; Olivares M; Duarte J; Rodríguez-Cabezas ME; Rodríguez-Nogales A; Gálvez J. Type of participation: oral communication.

29. Efecto antiinflamatorio de un extracto de hoja de olivo en un modelo de trasplante de microbiota fecal (FMT) en ratones obesos. XI Workshop Sociedad Española de Microbiota, Probióticos y Prebióticos (SEMiPyP 2020). Granada, Spain, 2020. Authors: Vezza T; Molina-Tijeras JA; Ruiz-Malagón AJ; Hidalgo-García L; Díez-Echave P; Rodríguez-Sojo MJ; Rodríguez-Nogales A; Romero M; Robles Vera I; Martín-García B; Gómez-Caravaca AM; Arráez-Román D; Segura-Carretero A; Duarte J; Rodríguez-Cabezas ME; Gálvez J. Type of participation: poster.

30. Impacto del probiótico Lactobacillus fermentum CECT5716 sobre el proceso inflamatorio asociado a la obesidad experimental en ratones. XI Workshop Sociedad Española de Microbiota, Probióticos y Prebióticos (SEMiPyP 2020). Granada, Spain, 2020. Authors: Jose Alberto Molina Tijeras; Teresa Vezza; Patricia Diez Echave; Laura Hidalgo García; Antonio Jesus Ruíz Malagón; Maria

Jesus Rodríguez Sojo; Bañuelos O; Mónica Olivares; Maria Elena Rodríguez Cabezas; Julio Gálvez. Type of participation: oral communication.

31. La microbiota de ratones obesos incrementa el proceso tumoral e inflamatorio en cáncer colorrectal. XI Workshop Sociedad Española de Microbiota, Probióticos y Prebióticos (SEMiPyP 2020). Granada, Spain, 2020. Authors: Antonio Jesús Ruiz Malagón; Teresa Vezza; Laura Hidalgo García; Patricia Diez Echave; Jose Alberto Molina Tijeras; María Jesús Rodríguez Sojo; María Elena Rodríguez Cabezas; Juan Antonio Marchal; Julio Gálvez. Type of participation: poster.

32. La microbiota de ratones obesos incrementa el proceso tumoral e inflamatorio en cáncer colorrectal. II Jornadas de Jóvenes Investigadores de la Facultad de Farmacia de la UGR. Granada, Spain, 2020. Authors: Antonio Jesús Ruiz Malagón; Teresa Vezza; Laura Hidalgo García; Patricia Diez Echave; Jose Alberto Molina Tijeras; María Jesús Rodríguez Sojo; María Elena Rodríguez Cabezas; Juan Antonio Marchal; Julio Gálvez. Type of participation: poster.

33. Effect of a Morus alba leaf extract in an experimental model of obesity: impact on liver steatosis and inflammation. I Symposium de Medicina de Precisión. Granada, Spain, 2019. Authors: Antonio Jesús Ruiz Malagón; Jose Alberto Molina Tijeras; Patricia Díez Echave; Laura Hidalgo García; Teresa Vezza; María Jesús Rodríguez Sojo; María Elena Rodríguez Cabezas; Abel Lozano Pérez; Jose Luis Cenis; Julio Juan Gálvez Peralta. Type of participation: poster.

34. Beneficial effects of agomelatine on liver inflammation in obese mice. XI Reunión de Jóvenes Farmacólogos de Andalucía. Málaga, Spain, 2019. Authors: María Jesús Rodríguez Sojo; Teresa Vezza; Patricia Díez Echave; Laura Hidalgo García; Antonio Jesús Ruiz Malagón; Jose Alberto Molina Tijeras; María Elena Rodríguez Cabezas; Julio Gálvez. Type of participation: oral communication.

35. The probiotic Lactobacillus fermentum CECT5716 shows anti-obesity properties in diet-induced obesity mice. XI Reunión de Jóvenes Farmacólogos de Andalucía. Málaga, Spain, 2019. Authors: Jose Alberto Molina Tijeras; Teresa Vezza; Patricia Díez Echave; Laura Hidalgo García; Antonio Jesús Ruiz Malagón; María Jesús Rodríguez Sojo; Oscar Bañuelos; Mónica Olivares; María

Elena Rodríguez Cabezas; Julio Gálvez. Type of participation: oral communication.

36. Análisis de la inmunomodulación de Células Estromales Mesenquimales de distintos tejidos mediante el uso de agonistas de TLRs y el probiótico Lactobacillus fermentum CECT5716. XI Reunión de Jóvenes Farmacólogos de Andalucía. Málaga, Spain, 2019. Authors: Jose Alberto Molina Tijeras; Teresa Vezza; Patricia Díez Echave; Laura Hidalgo García; Antonio Jesús Ruiz Malagón; María Jesús Rodríguez Sojo; Oscar Bañuelos; Mónica Olivares; María Elena Rodríguez Cabezas; Julio Gálvez. Type of participation: oral communication.

37. The immunomodulatory properties of PTSO contribute to its beneficial effects in diet-induced obesity in mice. XI Reunión de Jóvenes Farmacólogos de Andalucía. Málaga, Spain, 2019. Authors: Antonio Jesús Ruiz Malagón; Teresa Vezza; Patricia Díez Echave; Laura Hidalgo García; Jose Alberto Molina Tijeras; María Jesús Rodríguez Sojo; Alberto Baños; María Elena Rodríguez Cabezas; Julio Gálvez. Type of participation: oral communication.

38. The metabolic protective effects of Olive (Olea europaea L.) leaf extract in diet-induced obesity in mice is related to the restoration of gut microbiota dysbiosis and to its immunomodulatory properties. XI Reunión de Jóvenes Farmacólogos de Andalucía. Málaga, Spain, 2019. Authors: Teresa Vezza; Alba Rodríguez Nogales; Francesca Algieri; José Garrido Mesa; Jose Alberto Molina Tijeras; Laura Hidalgo García; María Jesús Rodríguez Sojo; Antonio Jesús Ruiz Malagón; Patricia Díez Echave; Miguel Romero; Manuel Sánchez; Marta Toral; F García; María Pilar Utrilla Navarro; Juan Duarte; María Elena Rodríguez Cabezas; Julio Gálvez. Type of participation: oral communication.

39. Effect of a Morus alba leaf extract in an experimental model of obesity: impact on liver steatosis and inflammation. I Congreso de Investigadores del PTS. Granada, Spain, 2019. Authors: Antonio Jesús Ruiz Malagón; Jose Alberto Molina Tijeras; Patricia Díez Echave; Laura Hidalgo García; Teresa Vezza; María Elena Rodríguez Cabezas; Abel Lozano Pérez; Jose Luis Cenis; Julio Juan Gálvez Peralta. Type of participation: poster.

40. Effect of quercetin loaded silk fibroin nanoparticles in DSS experimental colitis in mice. Falk Symposium 212 2018. Kyoto, Japan, 2018. Authors: Lorente M.D.; Diez-Echave P.; Vezza T.; Ruiz-Malagon A.; Molina-Tijeras J.A.; Hidalgo-Garcia L.; Rodriguez-Cabezas M.E.; Lozano-Perez A.; Cenis J.L.; Galvez J. Type of participation: poster.

41. Anti-inflammatory properties of oligosaccharides derived from Cynara scolymus in DSS-induced colitis in mice. Falk Symposium 212 2018. Kyoto, Japan, 2018. Authors: Jose Alberto Molina Tijeras; Laura Hidalgo García; Patricia Díez Echave; Antonio Jesús Ruiz Malagón; Teresa Vezza; N. Muñoz-Almagro; C. Sabater; María Elena Rodríguez Cabezas; Julio Juan Gálvez Peralta; María Pilar Utrilla Navarro. Type of participation: poster.

42. Effect of a Morus alba leaf extract in an experimental model of obesity: impact on liver steatosis and inflammation. Falk Symposium 212 2018. Kyoto, Japan, 2018. Authors: Antonio Jesús Ruiz Malagón; Jose Alberto Molina Tijeras; Patricia Díez Echave; Laura Hidalgo García; Teresa Vezza; María Elena Rodríguez Cabezas; Abel Lozano Pérez; Jose Luis Cenis; Julio Juan Gálvez Peralta. Type of participation: poster.

43. Effects of quercetin loaded silk fibroin nanoparticles in DSS experimental colitis in mice. Falk Symposium 212 2018. Kyoto, Japan, 2018. Authors: Antonio Jesús Ruiz Malagón; María Dolores Lorente; Patricia Díez Echave; Teresa Vezza; Antonio Jesús Ruiz Malagón; Jose Alberto Molina Tijeras; Laura Hidalgo García; María Elena Rodríguez Cabezas; Abel Lozano Pérez; Jose Luis Cenis; Julio Juan Gálvez Peralta. Type of participation: poster.

44. Intestinal anti-inflammatory effects of Kalanchoe brasilensis and Kalanchoe pinnata extracts exert intestinal anti-inflammatory effects in experimental colitis. Falk Symposium 212 2018. Kyoto, Japan, 2018. Authors: Laura Hidalgo García; Jose Alberto Molina Tijeras; Patricia Díez Echave; Antonio Jesús Ruiz Malagón; Anderson Lopes; S.M. Zucolotto; G. Coelho; María Elena Rodríguez Cabezas; Julio Juan Gálvez Peralta. Type of participation: poster.

45. TNF-alpha and IFN-gamma induce an anti-inflammatory phenotype in intestinal mesenchymal stromal cells. Falk Symposium 212 2018. Kyoto, Japan, 2018. Authors: Laura Hidalgo García; María Elena Rodríguez Cabezas; Jose Alberto Molina Tijeras; Teresa Vezza; Patricia Díez Echave; Antonio Jesús Ruiz Malagón; Francisco Huertas; P. Becerra-Massare; Julio Juan Gálvez Peralta; Per Anderson. Type of participation: poster.

46. Antiinflammatory properties of oligosaccharides derived from Cynara Scolymus in DSS.induced colitis in mice. X Reunion de Jovenes Farmacologos. Granada, Spain, 2018. Authors: Molina-Tijeras J.A.; Hidalgo-Garcia L.; Diez-Echave P.; Ruiz-Malagon A.; Vezza T.; Muñoz-Almagro N.; Sabater C.; Rodríguez-Cabezas ME.; Gálvez J.; Utrilla M.P. Type of participation: oral communication.

47. Effect of a Morus alba leaf extract in an experimental model of obesity: impact on liver steatosis and inflammation. X Reunion de Jovenes Farmacologos. Granada, Spain, 2018. Authors: Antonio Jesús Ruiz Malagón; Jose Alberto Molina Tijeras; Patricia Díez Echave; Laura Hidalgo García; Teresa Vezza; María Elena Rodríguez Cabezas; Abel Lozano Pérez; Jose Luis Cenis; Julio Juan Gálvez Peralta. Type of participation: oral communication.

48. Immunomodulatory effects of the probiotic Lactobacillus paracasei INIA P272 in DSS-colitis: Impact on immune cells populations. IX GASTRO-CONFERENCE (Part II) IBD 2017- Therapeutic and Biological Barriers. Berlin, Germany, 2017. Authors: Antonio Jesús Ruiz Malagón; Patricia Díez Echave; José Garrido Mesa; Teresa Vezza; Alba Rodríguez Nogales; Francesca Algieri; María Pilar Utrilla Navarro; Eva Rodríguez; Susana Langa; Juan Luis Arques; María Elena Rodríguez Cabezas; Julio Juan Gálvez Peralta. Type of participation: poster.

Prizes, mentions and distinctions

1. Premio a la mejor comunicación oral en el XII Workshop de la Sociedad Española de Microbiota, Probióticos y Prebióticos. Awarding entity: LABORATORIOS GRIFOLS, S.A. Conferral date: 18/09/202. Recognition linked: Primer autor del trabajo premiado.

2. Premio Arias Vallejo Awarding entity: Sociedad Española de Patología Digestiva. Conferral date: 07/05/2021. Recognition linked: Co-autor de la comunicación premiada.

3. Premio a las tres mejores comunicaciones orales breves. Awarding entity: Sociedad Española de Patología Digestiva. Conferral date: 07/05/2021. Recognition linked: Co-autor de la comunicación premiada.

4. Premio a la mejor comunicación oral en la "XI reunión de Jóvenes Farmacólogos de Andalucía". Awarding entity: Universidad de Málaga City. Conferral date: 31/05/2019 Recognition linked: Co-autor del trabajo premiado.